2013

Seasonal Particle and Carbon Dynamics in the Eastern Bering Sea

Matthew S. Baumann
University of Rhode Island, mbaumann11985@gmail.com

SEASONAL PARTICLE AND CARBON DYNAMICS IN THE EASTERN BERING SEA

BY

MATTHEW S. BAUMANN

A DISSERTATION SUBMITTED IN PARTIAL FULFILLMENT OF THE REQUIREMENTS FOR THE DEGREE OF

DOCTOR OF PHILOSOPHY

IN

OCEANOGRAPHY

UNIVERSITY OF RHODE ISLAND

2013

DOCTOR OF PHILOSOPHY DISSERTATION

OF

MATTHEW S. BAUMANN

APPROVED:

Dissertation Committee:

Major Professor S. Bradley Moran

Edward Durbin

Dawn Cardace

Nasser H. Zawia
DEAN OF THE GRADUATE SCHOOL

UNIVERSITY OF RHODE ISLAND
2013

ABSTRACT

The ocean margins of high-latitude seas, such as the eastern Bering Sea, are recognized as important areas for the enhanced scavenging removal of particle reactive chemicals and for the potential to sequester atmospheric carbon dioxide via photosynthetic conversion to biogenic particles and subsequent downward particle transport to deeper waters. This region is expected to warm in the future, and with the warming will come a reduction in the extent and duration of seasonal sea-ice. This physical process exerts an important control on the timing, location, and magnitude of the spring primary production bloom. Within the context that 2008-2010 are characterized as cold years in the eastern Bering Sea, establishing the mechanistic link between primary production and the seasonal progression in particle export represents a significant challenge because these processes exert a control on organic matter transport from the surface ocean and on the success of economically and culturally important animals.

During spring and summer cruises in 2009 and 2010, distributions of ^{234}Th ($t_{1/2}$ = 24.1 days) in the water column and sediments were measured at ~60 stations over the middle and outer regions of the shelf and at the shelf break. The inventory of excess ^{234}Th (^{234}Th which is not produced in the sediments) in shelf sediments was ~1/3 of the total deficit of ^{234}Th (^{234}Th scavenged by sinking particles) in the overlying water column leading to an average focusing factor of 0.34 ± 0.23. Further, ^{234}Th export from the shelf was determined to ~30% of the total production of this radionuclide by ^{238}U decay based on a ^{234}Th budget. These results, taken together with elevated focusing factors in the off-shelf region, suggest that the shelf sediments and lateral transport of particles from the shelf represent significant sinks for biogenic particles produced over the shelf in the spring and summer.

The elevated focusing factors at the shelf break are attributed to enhanced particle flux from blooms of primary production in this region, an area commonly referred to as the 'Green Belt' for its exceptionally high rates of primary production. Thus, seasonal export of particles from elevated rates of primary production at the shelf break may transfer a significant amount of particulate organic carbon (POC) from the surface waters. POC export in this region demonstrates a clear seasonal progression with low fluxes in the early spring that increase by late spring and early summer. Rates of net primary production (NPP) were high and export fluxes relatively low near the ice-edge in spring, leading to export ratios (*e*-ratio = POC export/NPP) <0.25. In early summer, POC export exceeded NPP individual stations leading e-ratios >1, which is attributed to a temporal lag, or offset, between the high rates of primary production in spring and export as POC during the early summer. Using a water column-sediment ^{234}Th budget, the export of POC from the outer shelf to slope water was estimated to be 24±35 mmol C m^{-2} d^{-1}, which represents an off-shelf *e*-ratio of 0.07-0.52 for contemporaneous seasonally averaged and historical monthly averaged daily rates of NPP. In addition to the vertical POC fluxes measured at the shelf break, the imputed off-shelf export flux and *e*-ratios further suggests that there may be a significant transfer of shelf-derived particles to the slope waters.

The high *e*-ratios and particles fluxes determined at the shelf may be a result of the biological response to the timing of physical processes in spring and summer of cold years. In spring, total chlorophyll a concentrations are generally low; however, localized phytoplankton blooms near the marginal ice zone (MIZ) lead to elevated spring average chlorophyll *a* concentrations, relative to summer, over the shelf and at the shelf break.

Diatoms represent the greatest contribution to total chlorophyll *a* in spring and summer of cold years. This algal class also represents the majority of total chlorophyll *a* in particles sinking through the water column. Further, the relatively high proportion of pheophorbide *a* in sediment trap material indicates that sinking of zooplankton fecal pellets facilitates the export of particles through the water column. In cold years, the emergence of large diatom blooms in the spring MIZ supports the production of abundant large zooplankton. Large zooplankton are a primary food source for juvenile pelagic fishes of economically important species. Therefore, these cold year specific processes may be essential for the transfer of POC from the surface waters and the success of the economically important pelagic fishery. A consequence of a warmer Bering Sea in the coming decades is a reduction in seasonal sea-ice extent and duration. A change in sea-ice cover may alter the timing and magnitude of spring primary production and the flow of energy through the lower trophic levels.

ACKNOWLEDGMENTS

I compiled a pretty large list of people and experiences worth acknowledging over the past half decade. I should have written them down or something because I'm sure I'll forget some.

I'll start off by thanking my advisor, Dr. Bradley Moran. He gave me an opportunity to succeed in this field. The Ph.D. process is rough and seemingly unending, but years ago Brad mentioned to me that all of the small processes, such as rotating samples on a nightly basis and keeping up with data reduction, will pay off. His pragmatic approach to science led me to an early start on the writing process. For this I'm thankful; I was a terrible writer early on. He's also provided me with, as my predecessor, Scott Stachelhaus, eloquently stated – 'food and shelter' and 'gainful employment'. Brad allows for all of his students to have a life outside of the lab and office and to work independently. The Ph.D. process is stressful from time to time, and I'm grateful for the freedom to have a life outside of science.

I need to thank Dr. Mike Lomas, my co-advisor, for his guidance over the years, especially in the areas of biology and working at sea. He's a model of tireless hard work, persistence, and productivity. Those are traits I hope to carry with me.

Thank you to my committee members, Dr. Ted Durbin and Dr. Dawn Cardace. I'm appreciative for their help with comps and for their comments and suggestions that have improved the following manuscripts.

And now for Pat Kelly; without his help, this dissertation would not have been possible. I feel like I'm repeating acknowledgements in past theses from this lab, but his guidance and technical knowledge are the foundation for these manuscripts. His stern

approach and sound execution while working at sea provided me with a great data set, and for that I cannot be more grateful.

I've had teachers along the way that have shown me the meaning of hard work and to take my passions and run with them. The list of those people is long and I know I will forget to mention some, but there a few that need to be mentioned. From my time at Carthage College, Drs. Christine Blaine and Doug Arion have had more of a positive impact on my education than I can describe here. Dr. Blaine convinced me to apply for the REU fellowship at the UW-Milwaukee [then named] Great Lakes WATER Institute. While there I worked in Dr. Val Klump's lab and met Dr. James Waples. My interaction with these outstanding researchers inspired me to pursue a Ph.D. in aquatic sciences. Here at GSO, Drs. Pilson and Oviatt provided a wealth of fundamental knowledge about oceanography. My background had little to do with this field, and I'm extremely thankful for what they have shared.

The 'front office' of David Smith, April Pariseault, and Meredith Clark have helped me countless times with paperwork, book keeping, and all other things administrative. David also threatened to not graduate me if the Chicago Blackhawks won the 2013 Stanley Cup Finals. I'm thankful that he didn't follow through.

Thank you to my office mates Scott Stachelhaus and Brendan Mackinson; both of whom are fans of Boston sports in some respect. I cherish our many disagreements.

I need to thank my parents, girlfriend, and friends for their support over the years. My sanity depended on it. There have been many who have lent an ear over the years, and I cannot thank them enough.

I'll admit I've learned an awful lot over the past 10 or so years of school. One of the most important principles I've gained in going through the Ph.D. process in particular is that there is still way (!) more that I don't know. It's quite humbling to come to grips with that reality actually, and hopefully the tools I've picked up here will allow me to balance the known/unknown out some. That's really all we can ask for, right? Keep moving in a forward direction. The Ph.D. thing is a long, trying, and ultimately less glorious process than I had imagined years ago. That being said, this has been an incredible experience, and I'm thankful for the set of circumstances that moved me along the path to this point.

PREFACE

The eastern Bering Sea supports nearly half of the US fishing industry in terms of fish catch revenue (National Marine Fisheries Service) and provides sustenance harvesting for the thousands of natives residing on the islands and Alaskan shore. This region is predicted to warm in the future. A warmer climate will alter the timing of annual physical processes, such as sea-ice advance in the fall and retreat in the spring. These physical processes are the most important control on the structure of the ecosystem, in particular, at the lowest trophic levels (phytoplankton and zooplankton). The magnitude and composition of the lowest trophic levels, in turn, have a direct impact on the success of economically important animals. The three years (2008-2010) of the field study, from which the three following manuscripts are derived, are considered cold years in this region characterized by extensive sea-ice cover that persists late into spring. This dissertation is an investigation of the seasonality of particle dynamics in this region, and results are discussed within the context that these observations are from cold years. The following section provides a brief overview of the objectives of this thesis and the approaches employed to achieve those goals.

The radiochemical balance of ^{234}Th ($t_{1/2}$ = 24.1 days) over the eastern Bering Sea shelf is used to estimate (a) the fraction of particles produced in the water column that are retained in shelf sediments and (b) the net flux of particles, defined here as particulate organic carbon (POC), from the shelf to the slope waters over a seasonal time-scale. Uranium-series radionuclides are proven tracers of particle transport process in aquatic environments. Previous studies; however, have utilized long-lived tracers, such as ^{210}Pb ($t_{1/2}$ = 22.3 years), ^{230}Th ($t_{1/2}$ = 75, 200 years), and ^{231}Pa ($t_{1/2}$ = 32, 500 years) to

investigate processes over decadal and longer time-scales (Anderson *et al.*, 1994; Bacon *et al.*, 1994; Nozaki *et al.*, 1997; Roy-Barman, 2009). The relatively short half-life, particle reactive nature, and known rate of production of ^{234}Th suit this radionuclide as a tracer of particle transport over seasonal time-scales, a method which has not be used before. Following the approach described by Bacon *et al.* (1994) and assuming a steady-state of several months for ^{234}Th, the radiochemical balance over the shelf is defined as:

$$\lambda A_U + V * \Delta Th_{CS} = \lambda A_{Th} + T * \Delta Th_{AS} + J_{sed} + J_{exp} \quad \text{(i.1)}$$

This equation represents the balance between the supply of ^{234}Th via *in situ* production from ^{238}U decay, λA_U (^{234}Th decay constant; λ = 0.0288 d^{-1}), and the net flux of ^{234}Th from the Oceanic to the Outer shelf waters, $V^{*}\Delta Th_{CS}$ (dpm cm^{-2} d^{-1}), where V (m^2 s^{-1}) is the horizontal cross-front exchange rate and ΔTh_{CS} (dpm m^{-4}) represents the cross-shelf ^{234}Th activity gradient between the Oceanic and Outer domains (ΔTh_{CS} can be represented by dTh/dy, where y represents the cross-shelf direction). The removal terms include the *in situ* decay of ^{234}Th, λA_{Th}, and the along-shelf transport of ^{234}Th, $T^{*}\Delta Th_{AS}$ (dpm cm^{-2} d^{-1}), where T (m s^{-1}) represents the along-shelf water volume transport and ΔTh_{AS} (dpm m^{-3}) is defined as ^{234}Th activity difference between the northern and southern regions. The term J_{sed} represents the net flux of ^{234}Th to the sediments, and J_{exp} is the net ^{234}Th export from the shelf to the ocean interior.

Sub-tidal flow fields and cross-front exchange rates are small over the mean life of ^{234}Th (35 days), therefore the terms $V^{*}\Delta Th_{CS}$ and $T^{*}\Delta Th_{AS}$ are negligible in the overall ^{234}Th balance. Thus, Eq. (i.1) is simplified:

$$\lambda A_U = \lambda A_{Th} + J_{sed} + J_{exp} \quad \text{(i.2)}$$

The production and decay terms are evaluated using spatially averaged, depth integrated activities of ^{234}Th and ^{238}U. The difference between the production and decay rates of ^{234}Th ($\lambda(A_U - A_{Th})$) is equal to the total particle removal flux ($J_{sed} + J_{exp}$). Once again, assuming a steady-state, the flux of ^{234}Th into sediments must be balanced by the decay in the sediment column. Therefore, J_{sed} is quantified as the product of the average excess sediment inventory of ^{234}Th and the ^{234}Th decay constant (Bacon *et al.*, 1994):

$$J_{sed} = \lambda \int_0^z 234_{Th_{xs}}\, dz \qquad \text{(i.3)}$$

The remainder of Eq. (i.2) is the daily flux of ^{234}Th from the shelf to the slope waters (J_{exp}) over seasonal-time scales. Multiplying a POC/^{234}Th by J_{exp} converts the off-shelf ^{234}Th flux to a daily POC flux to off-shelf waters. In this region, the majority of the annual carbon fixation occurs during the spring bloom. Because of the seasonality in this system, constraining the fraction of POC production from the spring bloom event exported from the shelf and, more generally, from the surface ocean has implications in regional carbon budgets.

The shelf break of the eastern Bering Sea is well known for its rich levels of spring primary production (Springer *et al.*, 1996). An accurate assessment of the seasonal progression of primary production and subsequent POC export in relation to seasonal sea-ice is necessary for the development of carbon budgets and understanding how carbon flows through the lowest trophic levels. Further, an improved understanding of the seasonality and magnitudes of primary and export production in cold years will provide a framework from which future observations from a warmer eastern Bering Sea may be interpreted.

There is no truly unbiased method to estimate POC export from the upper ocean. A combination of the ^{234}Th approach and sediment traps are used to provide a range in estimates of POC export. The use of ^{234}Th to constrain the vertical flux of POC from the upper ocean is a more traditional application of this radionuclide. It has been increasingly utilized in high-latitude system over the past few decades (Amiel and Cochran, 2008; Amiel *et al.*, 2002; Cai *et al.*, 2010; Gustafsson and Andersson, 2012; Lalande *et al.*, 2007; Lalande *et al.*, 2008; Moran *et al.*, 1997; Moran and Smith, 2000); however, a multi-year study of the eastern Bering Sea has yet to be presented.

A one-box model is typically used for the calculation of the ^{234}Th flux through the upper ocean water column (Savoye *et al.*, 2006):

$$\frac{dA_{Th}}{dt} = A_U\,\lambda - A_{Th}\lambda - P_{Th} + V_{Th} \quad \text{(i.4)}$$

where the change in ^{234}Th activity over time (dA_{Th}/dt) is equal to production (λA_U) and decay (λA_{Th}) of the radionuclide in the water column, vertical flux of particulate ^{234}Th from the upper water column (P_{Th}), and net transport of ^{234}Th by advection and diffusion (V_{Th}). A lack of time-series measurements necessitates the assumption of one-dimensional (V_{Th}=0) and steady-state (SS; dA_{Th}/dt=0) conditions, which simplifies Eq. (i.4):

$$P_{Th} = \lambda(A_U - A_{Th}) \quad \text{(i.5)}$$

Trapezoidal integration of Eq (i.5) yields the flux of particle flux of ^{234}Th through a specified depth horizon:

$$P_{Th} = \lambda \int_0^z (A_U - A_{Th})dz \quad \text{(i.6)}$$

The ^{234}Th-derived POC flux (P_{POC}) is then calculated as the product of P_{Th} and POC/^{234}Th ratio $(POC/^{234}Th_{trap})$ on sinking particles determined from sediment traps

$$P_{POC} = \left(\frac{POC}{^{234}Th}\right)_{trap} x\ P_{Th} \quad \text{(i.7)}$$

At individual stations, the fraction of net primary production exported from the photic zone is traditionally represented as the export ratio (*e*-ratio):

$$e - ratio = \frac{POC\ export}{NPP} \quad \text{(i.8)}$$

where POC export is either the sediment trap derived or the ^{234}Th-derived POC flux. Each *e*-ratio calculated at the shelf break represents a single observation or 'snapshot' on the day the measurements were made. Compiling *e*-ratios over time and space can be used to infer the seasonality in the pulse of primary production in the photic zone and export of particles from the surface waters. More specifically, the seasonal succession of the *e*-ratio, coupled with proximity to the retreating sea-ice edge and data on the seasonal emergence of zooplankton stocks, provides the basis to interpret carbon cycling within the sunlit upper ocean, the magnitude of particle export from this layer, and perhaps the fraction of carbon available for transfer to higher trophic level, economically important animals.

The composition of the autotrophic community and seasonal emergence of zooplankton may control the seasonal fluxes of POC from the surface ocean in cold years as described above. Algal classes, such as diatoms or prymnesiophytes, produce specific accessory pigments. For example, the pigment fucoxanthin is found in the chloroplasts of brown algae. The primary brown algae in the eastern Bering Sea are diatoms and, to a

lesser extent, chrysophytes (silicoflagellates). A more complete description of the specific accessory pigments associated with various algal classes is presented in Mackey *et al*. (1996). The CHEMTAX program (also described in Mackey *et al.*, 1996) uses the ratio of these indicator pigments to total chlorophyll *a* from water column samples to calculate the relative contribution of the algal classes to total chlorophyll *a*. The approach is used to interpret the seasonal evolution of the autotrophic community in spring and summer over shelf and shelf break. The same program is used to evaluate the composition of phytoplankton sinking through the water column. In addition, the pheopigment signature in settling material is used a proxy for the influence that sinking zooplankton fecal pellets exert on the flux of particulate organic matter (POM) from the photic zone.

In the following dissertation, the above approaches are utilized to improve the understanding of carbon cycling in the Bering Sea within the context that these studies are conducted over a multi-year cold period in this region. In Manuscript I, titled "^{234}Th balance and implications for seasonal particle retention in the eastern Bering Sea," the radiochemical balance (Eq. i.1) is used to provide estimates of the off-shelf ^{234}Th flux over seasonal time-scales. Further, retention of water column produced particles in the underlying sediments is evaluated on a station by station basis using the ratio of the excess ^{234}Th in the sediment to the ^{234}Th deficit in the water column. These ratios, known as focusing factors (FF_{Th}s), are used as a means to determine whether local areas serve as regions of net sediment gain or loss by lateral transport. This manuscript was published in *Deep Sea Research Part II: Topical Studies in Oceanography* (October, 2013) in the second special issue on results from BEST-BSIERP (Bering Sea Project). In

Manuscript II, titled "Seasonal decoupling of particulate organic carbon export and net primary production in relation to sea-ice at the shelf break of the eastern Bering Sea: implications for off-shelf carbon export," the vertical flux of POC from the photic zone at the shelf break is investigated using Eqs. (i.2-i.8). The seasonal progression in the flux of POC from the photic zone and *e*-ratio is compared with the results of the first manuscript and a concurrent integrated assessment of the carbon budget of the eastern Bering Sea (J.N. Cross et al., submitted manuscript). Manuscript II was published in *Journal of Geophysical Research-Oceans* in the fall of 2013. In Manuscript III, titled "Diatom control of the autotrophic community and particle export in the eastern Bering Sea during the recent cold years (2008-2010)," we use the concentrations of autotrophic pigments and particle nutrients in suspended and settling particles to infer the biological controls that the lowest trophic levels exert on carbon and particle cycling. Here, we determine the seasonal structure of the autotrophic community and composition of particles sinking from the photic zone. The composition of sinking particles is used to assess the influence of phytoplankton and zooplankton fecal pellets on the vertical flux of POM. The results of Manuscript III provide the lowest trophic level controls on the particle fluxes presented in the first two manuscripts during the cold years of this field program. This manuscript will be submitted to *Journal of Marine Research* in December 2013. This dissertation is presented in manuscript format in accordance with the guidelines of the Graduate School of the University of Rhode Island. The bibliographic format follows that required for submission to *Deep Sea Research*.

References

Amiel, D. and Cochran, J. K. 2008. Terrestrial and marine POC fluxes derived from ^{234}Th distributions and δ^{13}C measurements on the Mackenzie Shelf. J. Geophys. Res. 113(C3), DOI: 10.1029/2007JC004260.

Amiel, D., Cochran, J. K., Hirschberg, D. J. 2002. ^{234}Th/^{238}U disequilibrium as an indicator of the seasonal export flux of particulate organic carbon in the North Water. Deep-Sea Res. Pt. II. 49, 5191-5209.

Anderson, R. F., Fleisher, M. Q., Biscaye, P. E., Kumar, N., Ditrich, B., Kubik, P., Suter, M. 1994. Anomalous boundary scavenging in the Middle Atlantic Bight: evidence from Th-230, Pa-231, Be-1O and Pb-210. Deep-Sea Res. Pt. II. 41(2-3), 537-561.

Bacon, M. P., Belastock, R. A., Bothner, M. H. 1994. Pb-210 balance and implications for particle-transport on the continental-shelf, US Middle Atlantic Bight. Deep-Sea Res. Pt. II. 41(2-3), 511-535.

Cai, P., Rutgers van der Loeff, M., Stimac, I., Nöthig, E. M., Lepore, K., Moran, S. B. 2010. Low export flux of particulate organic carbon in the central Arctic Ocean as revealed by 234Th:238U disequilibrium. J. Geophys. Res. 115(C10), C10037, 10.1029/2009jc005595.

Gustafsson, Ö. and Andersson, P. S. 2012. ^{234}Th-derived surface export fluxes of POC from the Northern Barents Sea and the Eurasian sector of the Central Arctic Ocean. Deep-Sea Res. Pt. I. 68(0), 1-11.

Lalande, C., Lepore, K., Cooper, L. W., Grebmeier, J. M., Moran, S. B. 2007. Export fluxes of particulate organic carbon in the Chukchi Sea: A comparative study using ^{234}Th/^{238}U disequilibria and drifting sediment traps. Mar. Chem. 103, 185-196.

Lalande, C., Moran, S. B., Wassmann, P., Grebmeier, J. M., Cooper, L. W. 2008. ^{234}Th-derived particulate organic carbon fluxes in the northern Barents Sea with comparison to drifting sediment trap fluxes. J. Mar. Syst. 73(1–2), 103-113.

Mackey, M. D., Mackey, D. J., Higgins, H. W., Wright, S. W. 1996. CHEMTAX - A program for estimating class abundances from chemical markers: Application to HPLC measurements of phytoplankton. Mar. Ecol. Prog. Ser. 144(1-3), 265-283.

Moran, S. B., Ellis, K. M., Smith, J. N. 1997. Th-234/U-238 disequilibrium in the central Arctic Ocean: implications for particulate organic carbon export. Deep-Sea Res. Pt. II. 44(8), 1593-1606.

Moran, S. B. and Smith, J. N. 2000. ^{234}Th as a tracer of scavenging and particle export in the Beaufort Sea. Cont. Shelf Res. 20(2), 153-167.

Nozaki, Y., Zhang, J., Takeda, A. 1997. Pb-210 and Po-210 in the equatorial Pacific and the Bering Sea: the effects of biological productivity and boundary scavenging. Deep-Sea Res. Pt. II. 44(9-10), 2203-2220.

Roy-Barman, M. 2009. Modelling the effect of boundary scavenging on thorium and protactinium profiles in the ocean. Biogeosciences. 6(12), 3091-3107.

Savoye, N., Benitez-Nelson, C., Burd, A. B., Cochran, J. K., Charette, M., Buesseler, K. O., Jackson, G. A., Roy-Barman, M., Schmidt, S., Elskens, M. 2006. ^{234}Th sorption and export models in the water column: A review. Mar. Chem. 100, 234-249.

Springer, A. M., McRoy, C. P., Flint, M. V. 1996. The Bering Sea Green Belt: Shelf-edge processes and ecosystem production. Fish. Oceanogr. 5(3-4), 205-223.

TABLE OF CONTENTS

Abstract……iii

Acknowledgments……vi

Preface……ix

References……xvi

Table of Contents……xix

List of Tables……xxiii

List of Figures……xxvi

Publication Status……1

Manuscript I: ^{234}Th balance and implications for seasonal particle retention in the eastern Bering Sea……2

Abstract……2

1.1. Introduction……2

a. Study area……4

1.2. Methods……5

a. Water column ^{234}Th sampling and analysis……5

b. Sediment core ^{234}Th sampling and analysis……7

1.3. Results……8

a. Water column ^{234}Th- ^{238}U disequilibrium……8

b. Sediment excess ^{234}Th……8

c. Water column deficits of ^{234}Th……9

d. Sediment inventories of excess ^{234}Th……10

1.4. Discussion……11

a. ^{234}Th balance over the eastern Bering Sea shelf……11

a.1. Diffusive and advective fluxes of ^{234}Th……12

a.2. Production, decay, and sediment flux of ^{234}Th over the shelf ……14

a.3. Off-shelf export of ^{234}Th……...……..16

b. Residence time of ^{234}Th in the water column……17

c. ^{234}Th focusing factors…… 18

d. Implications for particle transport and retention……20

1.5. Conclusions……21

Acknowledgments……..23

References……..24

Tables……..30

Figures……38

Publication Status……...50

Manuscript II: Seasonal decoupling of particulate organic carbon export and net primary production in relation to sea-ice at the shelf break of the eastern Bering Sea: implications for off-shelf carbon export……51

Abstract……..51

2.1. Introduction……52

2.2. Methods……...55

a. Study area……...55

b. Sediment trap sampling……..56

c. Water column sampling……56

d. ^{234}Th and ^{238}U analysis……...57

e. Analysis of POC……58

2.3. Results……58

a. Hydrographic characteristics of the southeastern Bering Sea Outer shelf and shelf break……...58

b. Sediment trap POC and ^{234}Th fluxes…….60

c. ^{234}Th fluxes from ^{234}Th-^{238}U disequilibrium and ^{234}Th-derived POC fluxes……..61

d. Non-steady state ^{234}Th fluxes…….64

2.4. Discussion……...……66

a. Seasonal succession of NPP, POC export, and the export ratio…….66

b. Significance of carbon export from the Outer shelf to the deep ocean ……72

2.5. Conclusions…….74

Acknowledgments……..76

References……..77

Tables…….88

Figures……97

Publication Status…….109

Manuscript III: Diatom control of the autotrophic community and particle export in the eastern Bering Sea during the recent cold years (2008-2010)…….110

Abstract……110

3.1. Introduction……...111

3.2. Methods…….114

a. Upper water column POC, PON, POP, bSi, and autotrophic pigments ……114

b. Sediment trap sampling……....115

c. Analysis of POC, PON, POP, and bSi……115

d. Pigment analysis by HPLC……..116

e. Pigment analysis by CHEMTAX……117

3.3. Results……...118

a. Mixed layer hydrography……118

b. Water column pigment and POM concentrations……119

c. Pigment and particulate organic matter fluxes……120

3.4. Discussion……122

a. Characterization of the autotrophic community and vertical export ……..122

b. Elemental composition of phytoplankton and zooplankton controlled export……...127

3.5. Conclusions……...132

Acknowledgments……133

References……....134

Tables……...145

Figures……..162

Appendix A: Supporting tables for the CHEMTAX analysis presented in Manuscript III ……..171

Tables……...172

Bibliography…….……...174

LIST OF TABLES

TABLE PAGE

Table 1.1. Sampling dates during the 2009 and 2010 BEST-BSIERP field program. ……30

Table 1.2. Water column ^{234}Th *deficit*, sediment excess inventory ($^{234}Th_{xs}$), focusing factor (FF_{Th}), and residence time of total ^{234}Th (τ_t) for the eastern Bering Sea during 2009 and 2010. ……..31

Table 1.3. Seasonal ^{234}Th budget for the middle and outer domains of the eastern Bering Sea shelf (all units in dpm cm^{-2} d^{-1}). ……35

Table 1.4. Shelf averages (Middle and Outer domains) of the water column ^{234}Th *deficit* and sediment $^{234}Th_{xs}$ inventory. FF_{Th}s were calculated from average deficits and inventories. ……37

Table 2.1. Spring and summer cruises during the 2008-2010 NSF-NPRB BEST-BSIERP field program. ……88

Table 2.2. Sediment trap deployments from 2008-2010. ……89

Table 2.3. ^{234}Th fluxes ($^{234}Th_{trap}$ Flux), POC fluxes (POC_{trap} Flux) and POC/^{234}Th ratios (POC/$^{234}Th_{trap}$) determined using sediment traps together with ^{234}Th fluxes from ^{234}Th-^{238}U disequilibrium ($^{234}Th_{sv}$ Flux), ^{234}Th-derived POC fluxes (P_{POC}) and P_{POC}/POC_{trap}. ……90

Table 2.4. Comparison of steady state (SS) and non-steady state (NSS) ^{234}Th fluxes (dpm m^{-2} d^{-1}) at BL (a in Fig. 8) and MN19 (b) for the upper 75 m. ……93

Table 2.5. Export ratios determined from ^{14}C-derived NPP (mmol C m^{-2} d^{-1}) and ^{234}Th-

derived (*ThE*) and sediment trap (*e*-ratio) POC fluxes. Rates of NPP are from Lomas *et al.* (2012). ……..94

Table 2.6. Summary of POC export and export ratios in high latitude systems. ……95

Table 3.1. List of cruises and number of sampling profiles collected during the 2008-2010 NSF-NPRB BEST-BSIERP field program. ……...145

Table 3.2. BSIERP domains grouped into 7 larger geographic regions as illustrated in Fig. 3.1. ……...146

Table 3.3. Regional averages of mixed layer depth (MLD, m), depth of the photic zone (1% PAR, m), and percent ice at stations within each region (% Ice Cover) together with MLD averages of temperature (°C), salinity (‰), density (σ_t, Density – 1000 kg m^{-3}), dissolved oxygen (DO, µmol kg^{-1}), and dissolved oxygen saturation from equilibrium (ΔDO Saturation, µmol kg^{-1}). ……....147

Table 3.4. Regional averages of primary pigment concentrations (µg L^{-1}) in the upper water column: total chlorophyll *a* (TChl *a*), fucoxanthin, total chlorophyll *b* (TChl *b*), 19'-Hexanoyloxyfucoxanthin, (19'-Hex), Pheophytin *a*, and Pheophorbide *a*. ……..149

Table 3.5. Station averages of upper water column particulate organic carbon (POC), particulate organic nitrogen (PON), particulate organic phosphorus (POP), and biogenic silica (bSi). All units in µmol L^{-1}. ……...151

Table 3.6. Sediment trap profiles of primary pigment (mg m^{-2} d^{-1}) and particulate fluxes (mmol m^{-2} d^{-1}): total chlorophyll *a* (TChl *a*), fucoxanthin , Pheophytin *a*, Pheophorbide *a*, particulate organic carbon (POC), particulate organic nitrogen (PON), particulate organic phosphorus (POP), and biogenic silica (bSi). ……..153

Table 3.7. Regional averages of percent contribution by algal group to total chlorophyll *a*. ……..156

Table 3.8. Algal group percent contribution to the flux of total chlorophyll *a* through the water column. ……..158

Table 3.9. Photic zone stock of particulate organic carbon (POC, mmol m^{-2}), total chlorophyll *a* (TChl *a*, mg m^{-2}), pheopigment sum (Σpheopigment, Pheophytin *a* + Pheophorbide *a*, mg m^{-2}), and fucoxanthin (mg m^{-2}) together with daily loss rates and fraction of total POC flux associated with TChl *a* (F Chl *a* (C)) and pheopigments (F pheo (C)). ……160

Table A.1. Final matrices in the CHEMTAX analysis of the water column samples using fucoxanthin:chlorophyl a ratios of 0.75 (a), 0.35 (b), and 1.1 (c)……172

Table A.2. Initial pigment:chlorophyl a matrix (a) used for the CHEMTAX analysis together with final matrices for the water column (b) and sediment trap (c) analyses. ……..173

LIST OF FIGURES

FIGURE PAGE

Figure 1.1. Map of the eastern Bering Sea identifying the major transects during the BEST-BSIERP field program and station locations where water column and sediment samples were collected. …….....38

Figure 1.2. Temperature (°C), salinity (PSU), and density anomaly (kg m^{-3}) sections along the MN line for spring and summer 2009-10. …….39

Figure 1.3. Depth profiles of ^{234}Th-^{238}U activity ratios according to season and domain. Slope-Oceanic Domain profiles plotted to a maximum depth of 500 m. Middle and Outer domains profiles plotted to sea floor. ……...40

Figure 1.4. Seasonal variability in ^{234}Th-^{238}U activity ratio (AR) along the MN Line. ……....41

Figure 1.5. Depth profiles of sediment $^{234}Th_{xs}$ (dpm g^{-1}). Profiles are plotted to a maximum depth of 1.5 cm (1.25 cm mid-point), which correlates with integration depth. …….42

Figure 1.6. Maps of water column ^{234}Th *deficit* and sediment $^{234}Th_{xs}$ inventory. Note that two Oceanic sediment $^{234}Th_{xs}$ inventories for summer 2010 are off-scale and indicated by lightly shaded symbols. ……43

Figure 1.7. Illustration of the supply and removal terms responsible for the radiochemical balance of ^{234}Th over the eastern Bering Sea shelf. Terms defined in Table 1.3. ……..44

Figure 1.8. Seasonally averaged supply (white bar), removal (black bars), and off-shelf

export (gray bar) of ^{234}Th over the eastern Bering Sea shelf. ……...45

Figure 1.9. Distributions of total ^{234}Th residence time (τ_t, d) in the eastern Bering Sea. ……46

Figure 1.10. Plot of sediment $^{234}Th_{xs}$ inventory against water column deficit of ^{234}Th for the eastern Bering Sea shelf. Data plotted only for the Middle and Outer shelf regions. ……..47

Figure 1.11. ^{234}Th focusing factors (FF_{Th}) determined in the eastern Bering Sea. ……..48

Figure 1.12. Average FF_{Th} calculated according to season and domain. Uncertainties represent 1 σ. ……49

Figure 2.1. Map of the eastern Bering Sea study area. The black circles indicate the stations where drifting sediment traps were deployed. Several locations are stations in which multiple deployments occurred throughout the field program. Solid and dashed lines represent the maximum and minimum ice-edge extent, respectively, during spring sampling periods. Colors: red (2008), blue (2009) and green (2010). Specific dates are listed on the figure. ……...97

Figure 2.2. Temperature (°C) – salinity (psu) plots at sediment traps stations. Points are 1 m averaged values from the CTD for the upper 150 m (or surface to bottom if shallower than 150 m) of the water column. Panels: spring 2008 (a), summer 2008 (b), spring 2009 (c), summer 2009 (d), spring 20010 (e) and summer 2010 (f). Data from UCAR EOL archive: http://catalog.eol.ucar.edu/best/. ……98

Figure 2.3. Depth profiles of sediment trap ^{234}Th fluxes ($^{234}Th_{trap}$ *Flux*; dpm m^{-2} d^{-1}),

POC fluxes (POC_{trap} *Flux*; mmol C m^{-2} d^{-1}), $POC/^{234}Th$ ratios ($POC/^{234}Th_{trap}$; µmol dpm^{-1}), ^{234}Th fluxes calculated from ^{234}Th-^{238}U disequilibrium (P_{Th}), and ^{234}Th-derived POC export (P_{POC}) for spring (top) and summer (bottom) of 2008. ……99

Figure 2.4. Depth profiles of sediment trap ^{234}Th flux ($^{234}Th_{trap}$ *Flux*; dpm m^{-2} d^{-1}), POC flux (POC_{trap} *Flux*; mmol C m^{-2} d^{-1}), $POC/^{234}Th$ ratios ($POC/^{234}Th_{trap}$; µmol dpm^{-1}), ^{234}Th fluxes calculated from ^{234}Th-^{238}U disequilibrium (P_{Th}), and ^{234}Th-derived POC export (P_{POC}) for spring (top) and summer (bottom) of 2009. ……..100

Figure 2.5. Depth profiles of sediment trap ^{234}Th flux ($^{234}Th_{trap}$ *Flux*; dpm m^{-2} d^{-1}), POC flux (POC_{trap} *Flux*; mmol C m^{-2} d^{-1}), $POC/^{234}Th$ ratios ($POC/^{234}Th_{trap}$; µmol dpm^{-1}), and ^{234}Th fluxes calculated from ^{234}Th-^{238}U disequilibrium (P_{Th}), and ^{234}Th-derived POC export (P_{POC}) for spring (top) and summer (bottom) of 2010. ……101

Figure 2.6. Seasonal comparison of ^{234}Th fluxes (dpm m^{-2} d^{-1}) at sediment trap stations determined by ^{234}Th-^{238}U disequilibrium (P_{Th}) and by sinking particles collected in sediment traps ($^{234}Th_{trap}$ *Flux*). Water column profiles integrated to depth of corresponding sediment traps (25, 40, 50, 60 and 100 m). Panels: spring 2008 (a), summer 2008 (b), spring 2009 (c), summer 2009 (d), spring 20010 (e) and summer 2010 (f). Note that the scale varies from season to season. Two points from spring 2009 (c) are off-scale (listed in Table 1.3). ……102

Figure 2.7. Seasonal comparison of POC export (mmol C m^{-2} d^{-1}) determined by the ^{234}Th method (P_{POC}) and sediment traps (POC_{trap} *Flux*). Panels: spring 2008 (a), summer 2008 (b), spring 2009 (c), summer 2009 (d), spring 20010 (e) and

summer 2010 (f). Note that the scale varies from season to season. One point from spring 2009 (c) is off scale (listed in Table 1.3). ……...103

Figure 2.8. Comparison of steady state (SS; $\partial A_{Th}/\partial t = 0$) and non-steady state (NSS; $\partial A_{Th}/\partial t \neq 0$) ^{234}Th fluxes at two locations: Bloom station (BL) in 2009 (a) and MN19 in 2010 (b). Profiles were integrated to 75 m in both cases. Water column depths were ~125 and ~160 m at BL and MN19, respectively. ……..104

Figure 2.9. Photic zone integrated rate of net primary production (NPP; mmol C m^{-2} d^{-1}) from ^{14}C incubations versus POC fluxes derived from the ^{234}Th approach (a; *ThE*) and sediment traps (b; *e*-ratio). ^{234}Th integrations extend to the base of the photic zone and sediment trap POC fluxes and $POC/^{234}Th$ are from the nearest in depth array. Lines of 50, 25 and 10% have been drawn for comparison of the data. ……..…105

Figure 2.10. (a) Average POC fluxes from 40–100 m for individual sediment trap deployments in relation to the distance from the ice-edge (<8/10ths ice cover). The break separates near-ice stations from open water stations, which are grouped together. Dark/open circles and squares represent spring/summer POC_{trap} and P_{POC} average fluxes (± 1σ), respectively. (b) Same as (a) but for export ratios calculated according to Eq. (2.7). Dark/open circles and squares represent spring/summer *e*-ratio and *ThE*, respectively. ……..…106

Figure 2.11. (a) POC fluxes below 40 m average by cruise and plotted at the ~mid-point

of the expedition. Dark/open circles and squares represent spring/summer POC_{trap} and P_{POC} average fluxes (± 1σ), respectively. (b) Individual export ratios plotted by cruise at the ~mid-point of the expedition. Dark/open circles and squares represent spring/summer *e*-ratio and *ThE*, respectively. ……107

Figure 2.12.Average spring-summer POC export based on a ^{234}Th budget for the Outer Domain of the eastern Bering Sea adapted from Baumann et al. (2013) The off-shelf export flux of ^{234}Th was converted to POC using a $POC/^{234}Th$ ratio of 11 ± 9 µmol dpm^{-1}. POC export units are mmol C m^{-2} d^{-1}. The vertical arrow represents minimum and maximum averages of P_{POC} for late spring and early summer. Primary production values are from Rho and Whitledge (2007). ……...108

Figure 3.1. Map of the eastern Bering Sea study area. Thin lines delineate the regions designated during the BEST-BSIERP program. Bold lines represent the seven larger geographic regions used for data interpretation in this study. Listed in Table 2 are the BEST-BSIERP regions grouped in this study. White (spring) and black (summer) symbols represent water column sampling locations during the field study (see Table 1 for cruise information). Cross symbols are sediment trap deployment locations. ……162

Figure 3.2. Depth profiles of total chlorophyll *a* and fucoxanthin (µg L^{-1}). Open (spring) and shaded (summer) symbols correspond to specific cruises listed on the figure. ……..163

Figure 3.3. Relationship between water column concentrations (a) and sediment trap fluxes (b) of total chlorophyll *a* and fucoxanthin (a: µg L^{-1}, b: mg m^{-2} d^{-1}). …..164

Figure 3.4. Percent contribution to total ambient chlorophyll *a* (a-c) and total chlorophyll

a flux (d-f) for diatoms (a and d), chlorophytes (b and e), and prymnesiophytes (c and f). ……..165

Figure 3.5. Chlorophyte and prymnesiophyte contribution versus diatom contribution to total chlorophyll *a* (a: chlorophytes, b: prymnesiophytes) and total chlorophyll a flux (d: chlorophytes, e: prymnesiophytes). Prymnesiophyte contribution versus chlorophyte contribution for water column total chlorophyll *a* (c) and total chlorophyll *a* flux (f). ……..166

Figure 3.6. Average algal class contribution to autotrophic community (%) by region for spring (a) and summer (b). Thin bars represent average total chlorophyll a (black) and fucoxanthin (grey) concentrations, and correspond to the right vertical axes. ……..167

Figure 3.7. Phytoplankton composition (%) of the vertical flux of POM by cruise. Thin bars represent average total chlorophyll a (black), fucoxanthin (grey), and Σpheopigments, and correspond to the right vertical axes. …….168

Figure 3.8. N:P (a and b) and C:P (c and d) of suspended POM plotted against fucoxanthin concentration (µg L^{-1}; a and c) and the ratio of fucoxanthin to total chlorophyll *a* (b and d). Reference lines of 16:1 and 106:1 are drawn for N:P and C:P, respectively, for comparison of the data. ……169

Figure 3.9. N:P (a and b) and C:P (c and d) of the vertical flux of POM plotted against fucoxanthin flux (mg m^{-2} d^{-1}; a and c) and the flux ratio of fucoxanthin to total chlorophyll *a* (b and d). Reference lines of 16:1 and 106:1 are drawn for N:P and C:P, respectively, for comparison of the data. ……...….17

Publication Status

Manuscript I, titled "^{234}Th balance and implications for seasonal particle retention in the eastern Bering Sea" was published in *Deep Sea Research Part II: Topical Studies in Oceanography* in the second special issue on results from BEST-BSIERP (Bering Sea Project). This article was published in October 2013. The co-authors of this manuscript are S. B Moran, R. P. Kelly, M. W. Lomas, and D. H. Shull.

MANUSCRIPT I

^{234}TH BALANCE AND IMPLICATIONS FOR SEASONAL PARTICLE RETENTION IN THE EASTERN BERING SEA

Abstract

As part of the Bering Ecosystem Study-Bering Sea Integrated Ecosystem Research Program (BEST-BSIERP), distributions of ^{234}Th in the water column and sediments were measured at approximately 60 stations over the shelf and slope/oceanic regions of the eastern Bering Sea during spring and summer of 2009 and 2010. During this study period, the inventory of sediment excess ^{234}Th ($^{234}Th_{xs}$) on the shelf was determined to be ~1/3 of the total ^{234}Th *deficit* in the overlying water column; the average focusing factor (FF_{Th} = sediment $^{234}Th_{xs}$/ water column ^{234}Th *deficit*) was 0.34±0.23. In addition, the export flux of ^{234}Th from the shelf to the slope/oceanic region was determined to be on average ~30% of the total production of ^{234}Th over the shelf. Taken together, these results indicate that ^{234}Th and associated particles are largely retained on the shelf, and that shelf sediments represent a sink for particles. In contrast, the FF_{Th} in the slope/oceanic region was higher, averaging 1.52±1.34. The higher FF_{Th} at the slope is attributed primarily to enhanced scavenging removal and sediment deposition of ^{234}Th associated with periods of high biogenic particle flux at the marginal ice zone during the spring sea-ice retreat. A more general conclusion is that the ocean margin of the eastern Bering Sea may serve as an accumulation area for particles and associated reactive chemicals.

1.1. Introduction

Continental shelves represent only 10% of the world ocean, yet these regions account for ~20% of global primary production (Walsh, 1988). Ocean margins are recognized to be effective areas for the enhanced removal of reactive chemicals via particle scavenging and for the transfer of organic matter from continental shelves to the deep ocean. These processes are thought to play an important role in shelf-basin exchange of organic carbon and the sediment accumulation of particle-reactive pollutants on a global basis. A significant challenge is quantifying the rates and mechanisms of particle transport in shelf/slope systems.

Uranium-series radionuclides are proven tracers of particle transport processes in aquatic environments. In particular, previous studies have utilized long-lived radionuclides, such as ^{210}Pb ($t_{1/2}$ = 22.3 y), ^{230}Th ($t_{1/2}$ = 75, 200 y), and ^{231}Pa ($t_{1/2}$ = 32, 500 y) to investigate particle transport in shelf regions on decadal and longer time-scales (e.g., Anderson *et al.*, 1994; Bacon *et al.*, 1994; Nozaki *et al.*, 1997; Roy-Barman, 2009; Smith *et al.*, 2003). Over the past several decades, the short-lived, particle-reactive radionuclide ^{234}Th ($t_{1/2}$ = 24.1 d) has been increasingly used as a tracer of POC export from the upper ocean (e.g., Buesseler, 1998; Buesseler *et al.*, 1998; Charette *et al.*, 2001; Lalande *et al.*, 2007; Moran and Buesseler, 1993; Moran *et al.*, 2003; Savoye *et al.*, 2004). In addition to its utility in quantifying POC export from the upper water column, the disequilibrium between ^{234}Th and its soluble parent ^{238}U in seawater and sediments has significant potential in quantifying seasonal particle transport and retention in shelf systems; for example, in a manner similar to that described for ^{210}Pb (e.g., Bacon *et al.*, 1994).

As part of the Bering Ecosystem Study-Bering Sea Integrated Ecosystem Research Program (BEST-BSIERP), measurements of the water column deficit of ^{234}Th

and sediment excess inventory ($^{234}Th_{xs}$) are presented from 2009 and 2010 over the eastern Bering Sea shelf and slope (Fig. 1.1). These data have been used to investigate several aspects of particle transport, including: seasonal particle retention over the shelf, export of POC, and enhanced particle export and deposition associated with the marginal ice zone (MIZ). Results indicate that ~30% of ^{234}Th produced over the shelf is exported to the ocean interior, implying that ^{234}Th and, by inference, associated particles in this system are largely retained over the shelf on a seasonal basis. In addition, relatively large inventories of $^{234}Th_{xs}$ observed in the slope and deep ocean sediments during summer are suggested to result from enhanced scavenging removal and deposition of ^{234}Th associated with the MIZ during the spring sea-ice retreat, and possibly augmented by boundary scavenging removal of ^{234}Th at the ocean margin.

a. Study area

The broad (~500 km) and extensive (>500,000 km^2) seasonally ice-free eastern Bering Sea shelf is bordered on the south by the Alaska Peninsula and to the east by the Alaska mainland (Fig. 1.1). The shelf break, located approximately at the 170 m isobath, extends northwestward from Unimak Pass and encompasses the Pribilof Islands, St. Matthew Island, Nunivak Island, and St. Lawrence Island. During the ice-free months, the shelf waters may be subdivided into three cross-shelf domains, separated by three fronts (Coachman, 1986; McRoy *et al.*, 1986). The Inner Front, located near the 50 m isobath, separates the shallow, well-mixed Coastal Domain (0-50 m) from the two-layered Middle Domain (50-100 m) (Kachel *et al.*, 2002; McRoy *et al.*, 1986). The Coastal Domain is well-mixed because the wind and tidally mixed layers overlap. The Middle Domain, characterized by the strongest stratification and the presence of a

summer cold pool (Fig. 1.2; summer temperature section), is isolated from the Outer Domain by the Middle Front, which overlies the 100 m isobath. Recent observations (Stabeno *et al.*, 2002) have indicated north-south variability within the Middle Domain, though these trends are less pronounced than cross-shelf variability. The Outer Domain (100 m-shelf break) is characterized by surface and bottom mixed layers, though is separated by a structured middle layer (Stabeno *et al.*, 1999). The Shelf Break Front separates the Outer Domain from the Oceanic Domain. These fronts affect lateral advection and diffusion, property exchange rates, and mixing between the water masses.

1.2. Methods

Water column and sediment core samples were collected in the eastern Bering Sea during spring and summer cruises as part of the 2009 and 2010 BEST-BSIERP field program (Fig. 1.1). A series of transects were completed during each cruise aboard *USCGC Healy* (March 31 to May 12, 2009), *R/V Knorr* (June 14-July 13, 2009), and *R/V Thomas G. Thompson* (May 9-June 14, 2010 and June 16-July 13, 2010) (Table 1.1). Because the 2010 spring cruise was delayed until May and early June it is referred to as 'late' spring compared to 2009. Major transects from south to north are as follows: CN (Cape Newenham), NP (Nunivak Island-St. Paul Island), MN (St. Matthew Island-Nunivak Island), SL (St. Lawrence Island) and the 70 m isobath line running from CN northward to SL (Fig. 1.1).

a. Water column ^{234}Th sampling and analysis

^{234}Th water column profiles were obtained via small volume (4 L) water samples collected from CTD-rosette casts (n = 27 and 29 profiles collected in 2009 and n = 29

and 19 profiles collected in 2010, during spring and summer, respectively). Samples were analyzed for total (dissolved + particulate) ^{234}Th at high vertical resolution (~10 m) throughout the upper water column to encompass the entire photic zone. On the shelf, the entire water column was sampled. In the slope/oceanic region, profiles extend to a depth of ~500 m. ^{234}Th was extracted via co-precipitation with MnO_2 (Benitez-Nelson *et al.*, 2001; Buesseler *et al.*, 2001). Briefly, the pH of the sample was raised by the drop-wise addition of concentrated ammonium hydroxide followed by the addition of 0.2 M $KMnO_4$ (25 µL) and 1.0 M $MnCl_2$ (11.5 µL) to generate the MnO_2 precipitate. After one hour of equilibration, each sample was vacuum filtered onto a 25 mm diameter 1 µm pore size glass microfiber filter (GM/F). Deep samples (>1000 m) were collected as a check for detector efficiency. Samples were spiked with a known ^{230}Th activity as an internal standard of ^{234}Th scavenging efficiency (n = 52). After ^{234}Th analysis (described below), Th was radiochemically purified and ^{230}Th was measured by alpha particle emission (Lepore *et al*., 2007). Scavenging efficiencies for the small volume ^{234}Th method were determined to be 91±4.5% (1 σ).

Total ^{234}Th in water column samples was quantified by measurement of the beta emission of ^{234m}Pa (E_{max} = 2.19 MeV; $t_{1/2}$ = 1.2 min) using a low-background beta detector (RISØ National Laboratory, Roskilde, Denmark), with an average detector efficiency of 44±3% determined at sea. Prior to analysis, each sample was mounted on an acrylic planchet and covered with clear plastic wrap and aluminum foil to shield low-level beta and alpha emitters. Samples were counted several times over the first six half-lives of ^{234}Th, with the first count at least three days after collection to allow for the decay of short lived isotopes. After 144 days (six half-lives of ^{234}Th), the activity of

^{234}Th decayed below detection limit and samples were counted to establish background levels. Data were fitted to the ^{234}Th decay curve and corrected to yield ^{234}Th activity at the time of collection.

^{238}U activities were calculated from salinity according to ^{238}U = 0.07081 x S (‰) (Chen *et al.*, 1986).

b. Sediment core ^{234}Th sampling and analysis

Sediment cores were collected during each cruise in 2009 and 2010 (n = 19 and 19 profiles collected in 2009 and n = 21 and 17 profiles collected in 2010, during spring and summer, respectively) using an Oceans Instruments MC-800 eight-tube multicorer. Cores were sectioned into 0.5 cm increments in the upper two cm, and into one cm increments for depths of 2 to 5 cm. Sediment samples were dried at 60°C in 125 mL jars, ground, and homogenized prior to analysis. The sediment density ($\rho = \rho_D (1 - \varphi)$) of each sample analyzed was calculated using an assumed solid particle density (ρ_D) of 2.65 g cm^{-3} (Burdige, 2006) and sediment porosities (φ) determined in the laboratory from measurements of wet and dry sediment weight.

Samples were analyzed for ^{234}Th using a sea-going Canberra pure Ge planar type detector (GCW3023, 2000 mm^2) or on a shore-based Canberra pure Ge well type detector (GL20203, 150 cm^3) calibrated for the specific sample geometry. Sample activities were determined by gamma emission at 63.3 keV and decay corrected to the mid-point of collection. Supported levels of ^{234}Th (^{234}Th produced in the sediment column) were measured after 144 days and subtracted from the total ^{234}Th activity. Self-absorption corrections were applied according to the method described by Cutshall *et al.*, (1983).

Detector efficiencies were determined to be 10.8±0.3% and 52.1±1.0% for ^{234}Th at 63.3 keV for the planar and well type detectors, respectively.

1.3. Results

a. Water column ^{234}Th- ^{238}U disequilibrium

The ^{234}Th-^{238}U activity ratio (AR) provides a quantitative measure of the removal of ^{234}Th relative to ^{238}U from the water column via particle scavenging and export. During spring 2009, activity ratios ranged from ~0.4 to 0.8 on the shelf, whereas secular equilibrium (AR = 1) was observed in the slope/oceanic water column (Fig. 1.3). In summer 2009, AR's measured in the shelf domains indicate a similar degree of ^{234}Th-^{238}U disequilibrium (AR < 1) compared to spring. Unlike spring, however, ^{234}Th-^{238}U disequilibrium was observed during summer in the upper water column of the Oceanic Domain. In 2010, AR's on the shelf indicate a deficiency of ^{234}Th in the water column consistent with 2009 (Fig. 1.3). In contrast to the previous spring, disequilibrium was observed in the water column of the Oceanic Domain during late spring 2010 down to depths of ~200 m. Cross-shelf ^{234}Th-^{238}U activity ratios along the MN Line (Fig. 1.4) indicate that disequilibrium is also similar between late spring and summer over the shelf and at the shelf break. The difference in water column AR's between spring 2009 and spring 2010 may be attributed to the temporal offset in sampling dates.

b. Sediment excess ^{234}Th

Sediment excess ^{234}Th ($^{234}Th_{xs}$) is defined as ^{234}Th unsupported by the decay of parent ^{238}U, and which is supplied by particle scavenging of ^{234}Th from the overlying water column to the sediments:

$$234_{Th_{xs}} = 234_{Th_{tot}} - 234_{Th_{supp}} \quad (1.1)$$

$^{234}Th_{xs}$ was observed in nearly all sediment cores, typically confined to the upper 1.5 cm (Fig. 1.5). Sediment cores were not obtained for the Coastal Domain because coring was not possible due to sandy sediment. Sediment excess ^{234}Th activities measured in shelf sediments indicate high spatial variability; though do not exceed ~40 dpm g^{-1} at the surface of the sediment column. The highest $^{234}Th_{xs}$ activities were observed during summer in the slope/oceanic region sediments, where activities of up to 135 dpm g^{-1} were measured.

c. Water column deficits of ^{234}Th

^{234}Th deficits in the water column are calculated by difference of depth integrated ^{234}Th and ^{238}U activity profiles:

$$^{234}Th\ deficit = \int_0^z (A_U - A_{Th})dz \quad (1.2)$$

where A_U is the activity of, A_{Th} is the activity of ^{234}Th and z is the depth of the water column. For the shelf regions (z<200 m), ^{234}Th and ^{238}U activities were integrated over the entire water column. For the slope/oceanic regions, the water column was integrated to the depth where ^{234}Th and ^{238}U reached secular equilibrium (~200 to 400 m).

For spring 2009, average *^{234}Th deficits* over the Middle and Outer shelf were 7.3±0.7 and 9.4±1.9 dpm cm^{-2} (1 σ), respectively. The Oceanic Domain yielded an average *^{234}Th deficit* of 3.1±3.6 dpm cm^{-2} (Fig. 1.6; Table 1.2). ^{234}Th deficits over the eastern Bering Sea during summer 2009 were 6.2±1.1 in the Middle, 10.0±1.7 dpm cm^{-2} in the Outer, and 10.7±5.2 dpm cm^{-2} in the Oceanic domains, respectively. During late

spring 2010, average deficits of ^{234}Th over the Middle and Outer shelf increased to 8.8±1.7 and 11.5±1.4 dpm cm^{-2}, respectively, though large standard error within the data sets prevent statistical differentiation between seasons. Furthermore, the late spring 2010 average deficit in the oceanic water column was 16.9±3.6 dpm cm^{-2}, which is an approximate five-fold increase from earlier in spring of 2009. Average water column deficits in the summer of 2010 were 7.2±1.3 in the Middle, 14.7±3.3 in the Outer, and 13.0±2.2 dpm cm^{-2} in the Oceanic domains, respectively (Fig. 1.6; Table 1.2).

d. Sediment inventories of excess ^{234}Th

Because $^{234}Th_{xs}$ is typically observed in the upper 1.5 cm of the sediment core, sediment profiles are integrated to this depth to yield the excess ^{234}Th inventory:

$$Excess\ ^{234}Th\ inventory = \int_0^z \left(234_{Th_{tot}} - 234_{Th_{supp}}\right) dz = \int_0^z 234_{Th_{xs}} dz \quad (1.3)$$

In spring 2009, average $^{234}Th_{xs}$ inventories were 2.8±1.1 (Middle Domain), 4.1±2.7 (Outer Domain), and 2.3±1.0 dpm cm^{-2} (Oceanic Domain) (Fig. 1.6; Table 1.2). For summer 2009, average excess inventories were 2.7±2.0, 2.3±1.0, and 3.6±1.8 dpm cm^{-2} for the Middle, Outer, and Oceanic domains, respectively. Average $^{234}Th_{xs}$ inventories in late spring 2010 are not differentiable from either season in 2009: 2.1±1.0 (Middle Domain), 3.2±1.7 (Outer Domain), and 4.0±1.2 (Oceanic Domain) dpm cm^{-2}. In summer 2010, the highest inventories were observed in the summer Oceanic Domain, while this relative increase is not observed over the shelf: 3.3±1.8 in the Middle, 3.9±3.4 in the Outer, and 30.6±18.8 dpm cm^{-2} in the Oceanic domains, respectively.

1.4. Discussion

a. ^{234}Th balance over the eastern Bering Sea shelf

The radiochemical balance of ^{234}Th over the eastern Bering Sea shelf can be used to provide insight into particle transport, including the seasonal retention of particles in shelf sediments. Specifically, particle retention can be evaluated by establishing the balance between the export flux of ^{234}Th from the water column and the flux of ^{234}Th into the sediments. This approach follows that described by Bacon *et al.* (1994), who used ^{210}Pb to evaluate the transport of particles on a decadal time-scale in the Middle Atlantic Bight (MAB). Figure 1.7 illustrates the balance between the supply and removal of ^{234}Th over the eastern Bering Sea shelf. Assuming a steady-state, the radiochemical balance of ^{234}Th over the shelf is defined as:

$$\lambda A_U + V * \Delta Th_{CS} = \lambda A_{Th} + T * \Delta Th_{AS} + J_{sed} + J_{exp} \qquad (1.4)$$

Eq. (1.4) represents the balance between the supply of ^{234}Th via *in situ* production from ^{238}U decay, λA_U (^{234}Th decay constant; λ = 0.0288 d^{-1}), and the net flux of ^{234}Th from the Oceanic to the Outer shelf waters, $V^{*}\Delta Th_{CS}$ (dpm cm^{-2} d^{-1}), where V (m^2 s^{-1}) is the horizontal cross-front exchange rate and ΔTh_{CS} (dpm m^{-4}) represents the cross-shelf ^{234}Th activity gradient between the Oceanic and Outer domains (ΔTh_{CS} can be represented by dTh/dy, where y represents the cross-shelf direction). The removal terms include the *in situ* decay of ^{234}Th, λA_{Th}, and the along-shelf transport of ^{234}Th, $T^{*}\ \Delta Th_{AS}$ (dpm cm^{-2} d^{-1}), where T (m s^{-1}) represents the along-shelf water volume transport and ΔTh_{AS} (dpm m^{-3}) is defined as ^{234}Th activity difference between the northern and southern regions. The term J_{sed} represents the net flux of ^{234}Th to the sediments, and J_{exp} is the net ^{234}Th export from

the shelf to the ocean interior. Note that this equation does not explicitly include diffusive transport of ^{234}Th over the shelf. It is assumed that the contribution of diffusion is negligible in the radiochemical balance for ^{234}Th, which is justified below. Also, this balance neglects ^{234}Th input from rivers because ^{234}Th activities in freshwater are negligible and riverine supply to the Middle and Outer shelf regions is insignificant.

a.1. Diffusive and advective fluxes of ^{234}Th

The net exchange of ^{234}Th from the Oceanic Domain to the Outer shelf can be quantified as the product of the exchange rate (V) across the shelf break and the ^{234}Th activity gradient between the Oceanic and Outer domains (ΔTh_{CS}). A similar approach was used to examine the diffusive flux of ^{210}Pb across the MAB frontal zone to the shelf (Bacon *et al.*, 1994). In their study, strong cross-shelf gradients of ^{210}Pb and a significant correlation between ^{210}Pb activity and salinity were used to estimate the flux of ^{210}Pb from the deep ocean to the shelf. For the eastern Bering Sea, however, there is not a significant correlation between ^{234}Th and salinity for any season (r^2 = 0.01 to 0.36). The calculated cross-shelf gradient in ^{234}Th (ΔTh_{CS}) between the Oceanic and Outer domains ranged from -0.0005±0.0013 to 0.0057±0.0017 (mean: 0.0018 ± 0.0028) dpm m^{-3} per m of the approximately 100 km width of the Outer Domain. The cross-front exchange rate (V) for the shelf break was determined to be 0.46 m^2 s^{-1} based on a reported net on-shelf water mass transport rate of 14, 500 km^3 y^{-1} (Aagaard *et al.*, 2006) and a shelf length of approximately 1000 km. This value is similar to cross-front exchange rates recently reported for the Middle Front at the 100 m isobath (Danielson *et al.*, 2012). Using these values, the cross-shelf exchange of ^{234}Th from the Oceanic Domain to the Outer shelf was estimated to range from -0.0018±0.0051 to 0.0226±0.0069 (mean : 0.0069±0.0100)

dpm cm^{-2} d^{-1} spread over the approximate width of the Outer shelf (Table 1.3). These low average lateral fluxes imply that the cross-shelf exchange of ^{234}Th from the deep ocean to the Outer shelf is a minor component in the ^{234}Th balance for the eastern Bering Sea shelf (Fig. 1.8).

Because of the separation imposed by the Middle Front and the difference in water mass circulation, the along-shelf transport of ^{234}Th may vary for the Outer and Middle domains. Sub-tidal water transport over the Middle and Outer shelf is small relative to boundary currents, (Coachman, 1986) and along-shelf ^{234}Th activity differences between the northern and southern regions of the eastern Bering Sea shelf are negligible. Therefore, T is small and variable and ΔTh_{AS} is zero, implying that the along-shelf transport of ^{234}Th over the shelf is negligible in the ^{234}Th budget.

A further argument for the negligible transport of ^{234}Th by advection and diffusion lies in the length scale over which these processes are significant for the relevant spatial and temporal scales. Physical transport of water over the Middle and Outer shelf of the eastern Bering Sea is predominantly due to cross-shelf tidal currents (Coachman, 1982, 1986). The eastern Bering Sea experiences mixed semi-diurnal tides, with M_2 tidal current velocities of 15-30 cm s^{-1} and the K_1 constituent contributing 10 - 20 cm s^{-1} (Coachman, 1986). The length scale (L_a) over which advective transport of ^{234}Th is significant can be determined using (e.g., Lepore *et al.*, 2007):

$$L_a = U_h t \tag{1.5}$$

where U_h is the tidal velocity (15 cm s^{-1}) and t is the mean life of ^{234}Th (35 d). Using these values, L_a is approximately 450 km. However, because daily current velocities are

a function of both ebb and flood tides, the net daily cross-shelf water flux over the Middle and Outer shelf is small. Thus, the net advective transport of ^{234}Th by tides is a minor component in the radiochemical balance of ^{234}Th.

To examine horizontal diffusion as a mechanism for the transport of ^{234}Th, the mean diffusive path length in the absence of ^{234}Th scavenging is calculated as (e.g., Lepore *et al.*, 2007; Moran *et al.*, 1997):

$$L_d = \sqrt{2K_H t} \tag{1.6}$$

Coachman (1982) determined eddy diffusion (K_H) to range from ~1 to 5 x 10^6 cm^2 s^{-1}, depending on depth, location, and time of year for the Middle and Outer shelf areas of the eastern Bering Sea. An average K_H of 2.6 x 10^6 cm^2 s^{-1} provides an L_d of ~40 km. Over transit scales of >40 km, ingrowth of ^{234}Th would tend to obscure the scavenging signature for a particular parcel of water. Note also that, assuming a shelf length of 1000 km and average depth of 170 m, the net cross-shelf water flux to the Outer shelf averaged over the entire shelf break is 85 km y^{-1}, or 8 km over the mean-life of ^{234}Th. Therefore, because L_a, L_d, and the imported signal of ^{234}Th from the deep ocean are small compared to spatial sampling, the flux of ^{234}Th from advective transport by tidal currents, horizontal diffusion, and on-shelf transport over the mean-life of ^{234}Th are insignificant over the relevant spatial and temporal time scales of this study.

a.2. Production, decay, and sediment flux of ^{234}Th over the shelf

Because advection and diffusion of ^{234}Th has been determined to be insignificant, the radiochemical balance of ^{234}Th (Eq. 1.4) for the Middle and Outer domains of the eastern Bering Sea simplifies to an equation dependent on the *in situ* water column

production and decay of ^{234}Th, the flux of ^{234}Th into the sediments, and the net particle export flux of ^{234}Th from the shelf:

$$\lambda A_U = \lambda A_{Th} + J_{sed} + J_{exp} \quad (1.7)$$

The production and decay terms are evaluated using spatially averaged, depth integrated activities of ^{234}Th and ^{238}U. On a seasonal basis, the areal production of ^{234}Th by ^{238}U decay in the water column ranges from 0.55±0.21 to 0.64±0.30 (mean: 0.59±0.04) dpm cm^{-2} d^{-1}. The areal decay of ^{234}Th in the water column is smaller than production, ranging from 0.32±0.18 to 0.36±0.23 (mean: 0.34±0.02) dpm cm^{-2} d^{-1} (Table 1.3). The difference between the production and decay rates of ^{234}Th ($\lambda(A_U - A_{Th})$) is equal to the total particle removal flux ($J_{sed} + J_{exp}$).

At steady-state, the flux of ^{234}Th into the shelf sediments must be balanced by decay in the sediment column. Thus, J_{sed} is quantified as the product of the average excess sediment inventory of ^{234}Th and the ^{234}Th decay constant (Bacon *et al.*, 1994):

$$J_{sed} = \lambda \int_0^z 234_{Th_{xs}}\, dz \quad (1.8)$$

The seasonal decay of ^{234}Th in shelf sediments of the eastern Bering Sea ranges from 0.07±0.04 to 0.10±0.07 (mean: 0.09±0.02) dpm cm^{-2} d^{-1} (Table 1.3). By comparison, decay of excess ^{234}Th in the sediments represents 15±3% of ^{234}Th production in the water column (Table 1.3). The implication is that shelf sediments are an important sink in the scavenging removal of ^{234}Th from the overlying water column.

a.3. Off-shelf export of ^{234}Th

The radiochemical balance of ^{234}Th in the eastern Bering Sea is summarized in Table 1.3. The seasonal export flux of ^{234}Th from the shelf to the ocean interior (J_{exp}) can be calculated from the difference between the supply and removal fluxes of ^{234}Th (Eq. 1.7). For spring and summer, J_{exp} represents on average 29±2% of the total production of ^{234}Th (Fig. 1.8), implying that on a seasonal basis ^{234}Th is largely retained (i.e., ~70% of ^{234}Th production) over the eastern Bering Sea shelf. This result is consistent with a previous study conducted in the MAB using ^{210}Pb, which demonstrated that ~20% of the total ^{210}Pb supplied to that shelf is removed by particle export into the interior ocean on a time-scale of decades (Bacon *et al.*, 1994). From the present data set, however, it is not possible to define a mechanism responsible for the transport and removal of ^{234}Th and associated particles off the shelf over seasonal time-scales. It is interesting to note that Bacon *et al.* (1994) propose that particles are removed from the shelf by a deposition-bioturbation-resuspension-redeposition loop over decadal time-scales, and it is possible that such a mechanism exists for the eastern Bering Sea.

In addition, J_{exp} can be used to place an upper bound on the seasonal export flux of POC. Using the average J_{exp} value (Table 1.3; 0.17±0.35 dpm cm^{-2} d^{-1}) and an average POC/^{234}Th ratio of 11±9 µmol C dpm^{-1} at 100 m measured in sediment trap material collected in spring and summer of 2008 - 2010 (Baumann *et al.*, in press) yields a POC export flux of 18±41 mmol C m^{-2} d^{-1}. Despite the inherent uncertainty in this estimate, this POC export flux is similar to values of 10±8 mmol C m^{-2} d^{-1} determined using ^{234}Th-^{238}U disequilibrium and sediment traps in 2008 (Moran *et al.*, 2012), and 19±17 mmol C m^{-2} d^{-1} recorded in sediment traps in spring and summer of 2008-2010 (Baumann *et al.*,

in press). The estimated POC export flux should be regarded as an upper estimate, due to the uncertainty in converting J_{exp} to a POC export flux using an imputed POC/^{234}Th ratio, which can vary considerably (e.g., Moran *et al.*, 2003), and to possible preferential remineralization of POC.

b. Residence time of ^{234}Th in the water column

The residence time of total ^{234}Th (τ_t) can be used to further assess the time-scale of particle retention over the eastern Bering Sea shelf. Specifically, the residence time of total ^{234}Th provides a quantitative measure of the efficiency of scavenging and transport of ^{234}Th within the shelf and upper water column of the Oceanic region. A one-dimensional, irreversible scavenging model is used for the estimation of total water column ^{234}Th residence time, which as justified above, sets advective and diffusive transport of ^{234}Th to zero (Coale and Bruland, 1987; Wei and Murray, 1992):

$$\frac{\partial A_{Th}}{\partial t} = \lambda A_U - \lambda A_{Th} - \lambda_c A_{Th} \tag{1.9}$$

where λ_c is the first-order rate scavenging constant for ^{234}Th. Eq. (1.9) describes the balance between ^{234}Th production, decay, and particle scavenging. Assuming steady-state, Eq. (1.9) simplifies to:

$$\lambda_c = \lambda \frac{\int_0^z (A_U - A_{Th}) dz}{\int_0^z A_{Th}\, dz} \tag{1.10}$$

where z is the depth of integration. The residence time of total ^{234}Th can be estimated for the entire water column by the relationship:

$$\tau_t = \frac{1}{\lambda_c} \tag{1.11}$$

Water column ^{234}Th residence times exhibit a gradient off the shelf during spring and summer (Fig. 1.9; Table 1.2). For the Middle and Outer shelf, ^{234}Th residence times average 49±26 d, which is similar to other coastal systems, such as Dabob Bay, Washington State (4 to 70 d) (Wei and Murray, 1992) and the inner region of the Gulf of Maine (34 to 143 d) (Moran and Buesseler, 1993). In the Oceanic region, residence times increase to 5 to 6 months, which are similar to those reported for the outer reaches of the Gulf of Maine (Moran and Buesseler, 1993) and Funka Bay, Japan (Wei and Murray, 1992). By comparison, estimates of water transport onto the shelf of the eastern Bering Sea and flow through the Bering Strait were used to determine water mass residence times of ~3-7 y for the shelf region (Aagaard *et al.*, 2006). Shelf water residence times are much longer than the average τ_t, which is consistent with the largely seasonal retention of ^{234}Th and associated particles over the eastern Bering Sea shelf.

c. ^{234}Th focusing factors

To further establish the extent to which there is a net seasonal retention of particles over the shelf, the exchange of ^{234}Th between the water column and sediments can be evaluated on a station-by-station basis. The relationship between the ^{234}Th deficit in the water column and $^{234}Th_{xs}$ inventory (Table 1.2) on the eastern Bering Sea shelf is illustrated in Fig. 1.10. This comparison indicates that for ~65% of stations sampled over the shelf, $^{234}Th_{xs}$ inventories are within a factor of ~1.5-4 of the measured water column deficits of ^{234}Th. This observation is consistent with the conclusion that the flux of ^{234}Th into the sediment represents an important sink for ^{234}Th produced over the shelf.

The ^{234}Th focusing factor (FF_{Th}) can be used to further quantify the exchange of ^{234}Th between the water column and sediment. In particular, the FF_{Th} is an empirical relationship that defines the efficiency of ^{234}Th transport from the water column to the underlying sediment (Cochran *et al.*, 1990). The sediment $^{234}Th_{xs}$ inventory is related to the water column deficit by the relationship (Cochran *et al.*, 1990; Lepore *et al.*, 2007):

$$FF_{Th} = \frac{\int_0^z {}^{234}Th_{xs}\,dz}{\int_0^z (A_{^{238}U} - A_{^{234}Th})\,dz} \qquad (1.12)$$

A FF_{Th} = 1 implies that the sediment inventory is in balance with water column removal of ^{234}Th over seasonal time-scales. A FF_{Th} greater, or less, than 1 indicates the redistribution of ^{234}Th into, or away from, a specific sampling location, respectively.

Evaluation of individual FF_{Th} values over the entire geographical area of the eastern Bering Sea provides insight into the shelf-wide, seasonal retention of ^{234}Th (Fig. 1.11). For the Middle Domain, seasonally averaged FF_{Th} values range from 0.25±0.11 to 0.53±0.29 (mean = 0.38±0.11), whereas values in the Outer Domain range from 0.26±0.22 to 0.33±0.15 (mean = 0.29±0.03) (Fig. 1.12; Table 1.2). Elevated (>1) FF_{Th} values are observed to a lesser extent in the oceanic/slope areas, where seasonal averages range from 0.27±0.10 to 2.71±2.07 in both years (mean = 1.52±1.34) (Figs. 1.11, 1.12), though fewer stations were occupied in the deeper slope water stations.

The observation that FF_{Th} values range from ~0.25-0.50 implies that shelf sediments are an important sink for ^{234}Th scavenged from the water column on a seasonal time-scale (Figs. 1.10, 1.11, 1.12; Table 1.4). Based on these results, vertical processes of sedimentation must be efficient at retaining particulate ^{234}Th, thereby working against

lateral processes that would otherwise largely export ^{234}Th (J_{exp}) off the shelf into the interior ocean. As noted above, this result is consistent with a previous study using ^{210}Pb in the MAB, which indicated a net retention of particles on the shelf for up to several decades (Bacon *et al.*, 1994).

d. Implications for particle transport and retention

There are several possible qualitative interpretations that may account for the elevated FF_{Th} values observed in the slope/oceanic region (Figs. 1.11, 1.12). In particular, surface water chlorophyll (Chl *a*) distributions indicate events of high autotrophic production at the MIZ associated with retreating sea-ice at the shelf break during late spring. High levels of Chl *a* persist into early summer at the shelf break and are clearly visible from satellite aqua MODIS chlorophyll distributions in May 2009 and 2010 (http://oceancolor.gsfc.nasa.gov/). Spring blooms of primary production appear coincident with the locations of the high FF_{Th} values along the shelf break. Thus, elevated FF_{Th} values in deeper water sediments may be attributed to the scavenging removal and deposition of ^{234}Th associated with biogenic particle blooms. Furthermore, there exists a temporal lag between the upper water column deficit and the high $^{234}Th_{xs}$ observed in the sediments in late spring 2010 and summer 2010 (Table 1.2). Assuming a settling speed of 80-150 m d^{-1} (Berelson, 2002) for particles sinking through a 2000 m water column, 13-25 days would be required for particles to sink from the surface waters to the underlying sediments. This suggests that vertically exported ^{234}Th from spring autotrophic blooms near the MIZ would settle to the deeper sediments after approximately several weeks.

In addition, the spatial distribution of the elevated FF_{Th} values is consistent with removal of ^{234}Th from high activity, open ocean water to the underlying deep slope sediments. This process is commonly referred to as boundary scavenging, which has been identified as important for a number of other long-lived radiochemical tracers, including ^{210}Pb, ^{230}Th, and ^{231}Pa (e.g., Anderson *et al.*, 1994; Roy-Barman, 2009). In particular, because FF_{Th} values are >1 in summer at several stations located seaward of the Shelf Break Front, and ^{234}Th export from the shelf is relatively small, the elevated FF_{Th} values are consistent with boundary scavenging removal of ^{234}Th. The source of ^{234}Th that results in the elevated sediment $^{234}Th_{xs}$ and hence high FF_{Th} values in the slope/oceanic sediments may be attributed to ^{234}Th-rich off-shore water that is transported to areas of high particle flux, such as near MIZ blooms. Therefore, boundary scavenging provides an additional explanation for the observation of large FF_{Th} values in the slope/oceanic region of the eastern Bering Sea.

Finally, post-depositional transport of surficial, shelf or slope-derived sediments could result in large FF_{Th} values in deep water sediments. Many of the deep water (>2000 m) cores were extracted from submarine canyons, such as the Pribilof and Zhemchung canyons, which may accumulate sediments from large areas of the shelf and slope.

1.5. Conclusions

The results reported in this study provide important new insights regarding our understanding of particle transport processes, water column-sediment interaction, and the magnitude of off-shelf export of particles and associated reactive chemicals in a highly

dynamic Arctic shelf environment. Prior studies in the northern Bering Sea have reported dramatic shifts in benthic productivity and water column-benthic coupling in the context of a changing climate (Grebmeier *et al.*, 2006a; Grebmeier *et al.*, 2006b). The present study utilizes a geochemical tracer method to evaluate the fate of particles over the southeastern Bering Sea shelf, which has broader applicability in quantifying particle transport processes in other complex shelf systems.

Specifically, based on comprehensive measurements of ^{234}Th in the water column and sediments, it has been determined that on a seasonal basis roughly 2/3 of the supply of ^{234}Th is balanced by decay and sediment burial over the eastern Bering Sea shelf. Furthermore, the off-shelf export flux of ^{234}Th (J_{exp}) represents ~30% of the total ^{234}Th supply, implying that ^{234}Th and associated particles are largely retained on the shelf, rather than exported to the ocean interior. While it not possible to define the mechanism(s) responsible for off-shelf export of ^{234}Th, it is suggested that this may involve a particle deposition-bioturbation-resuspension-redeposition loop, as described for the off-shelf transport of particles in the MAB (Bacon *et al.*, 1994). In addition, the results of this study have been used to provide an upper estimate of seasonal POC export from the shelf water column of 18 ± 41 mmol C m^{-2} d^{-1}. The short average residence time of ^{234}Th in the water column (49±26 d) and average FF_{Th} of 0.34±0.23 on the shelf is further indicative of the net shelf-retention of ^{234}Th in this region. Specifically, the mean residence time of total ^{234}Th is much shorter than mean water mass residence times estimated for the entire shelf, and the average FF_{Th} of ~0.3 suggests that a significant fraction of ^{234}Th removed from the water column is retained in shelf sediments. In contrast, elevated sediment $^{234}Th_{xs}$ and relatively high average FF_{Th} values of 1.52±1.34

observed in the slope/oceanic region of the eastern Bering Sea are attributed to enhanced particle scavenging associated with bloom events in the MIZ region during spring sea-ice retreat. In addition, these high $^{234}Th_{xs}$ and FF_{Th} values may also result from boundary scavenging removal of ^{234}Th supplied from high activity, open ocean water transported to areas of high particle flux at the slope, and post depositional transport of material to deeper sediments. It is concluded that ^{234}Th scavenged from the water column, and by inference particles, particulate organic carbon, and other reactive chemicals supplied to the eastern Bering Sea, are largely retained over the shelf on a seasonal time-scale.

Acknowledgments- We thank the Chief Scientists, officers, and crew of the *USCGC Healy, R/V Knorr, and R/V Thompson* for their efforts. We thank John Karavias of Walt Whitman High School (Queens, NY) and Jason Pavlich of Red Hook High School (Red Hook, NY) for their assistance as part of the ARMADA project. We thank Seth Danielson (UAF) for his input regarding physical transport processes over the eastern Bering Sea shelf. We also thank the hydrographic team from NOAA-PMEL for providing hydrographic data and assisting in sample collection, accessible through the EOL data archive supported by NSF and NOAA. Constructive reviews by three anonymous reviewers are greatly appreciated. This research was supported by awards ARC-0732680 and NPRB-B56 to SBM, ARC-0732359 to MWL, and ARC-0612380 to DHS. This is BEST-BSIERP Bering Sea Project publication number 86.

References

Aagaard, K., Weingartner, T. J., Danielson, S. L., Woodgate, R. A., Johnson, G. C., Whitledge, T. E. 2006. Some controls on flow and salinity in Bering Strait. Geophys. Res. Lett. 33(19), L19602.10.1029/2006gl026612.

Anderson, R. F., Fleisher, M. Q., Biscaye, P. E., Kumar, N., Ditrich, B., Kubik, P., Suter, M. 1994. Anomalous boundary scavenging in the Middle Atlantic Bight: evidence from Th-230, Pa-231, Be-1O and Pb-210. Deep-Sea Res. Pt. II. 41(2-3), 537-561.

Bacon, M. P., Belastock, R. A., Bothner, M. H. 1994. Pb-210 balance and implications for particle-transport on the continental-shelf, US Middle Atlantic Bight. Deep-Sea Res. Pt. II. 41(2-3), 511-535.

Baumann, M. S., Moran, S. B., Lomas, M. W., Kelly, R. P., Bell, D. W. in press. Seasonal decoupling of particulate organic carbon export and net primary production in relation to sea-ice at the shelf break of the eastern Bering Sea: implications for off-shelf carbon export Submitted to Journal of Geophysical Research Oceans.

Benitez-Nelson, C., Buesseler, K. O., Rutgers van der Loeff, M., Andrews, J., Ball, L., Crossin, G., Charette, M. 2001. Testing a new small-volume technique for determining ^{234}Th in seawater. J. Radioanal. Nucl. Ch. 248(3), 795-799.

Berelson, W. M. 2002. Particle settling rates increase with depth in the ocean. Deep-Sea Res. Pt. II. 49(1-3), 237-251.

Buesseler, K. O. 1998. The decoupling of production and particulate export in the surface ocean. Global Biogeochem. Cy. 12, 297-310.

Buesseler, K. O., Ball, L., Andrews, J., Benitez-Nelson, C., Belastock, R., Chai, F., Chao, Y. 1998. Upper ocean export of particulate organic carbon in the Arabian Sea derived from thorium-234. Deep-Sea Res. Pt. II. 45, 2461-2487.

Buesseler, K. O., Benitez-Nelson, C., Rutgers van der Loeff, M., Andrews, J., Ball, L., Crossin, G., Charette, M. A. 2001. An intercomparison of small-and large-volume technqiues for thorium-234 in seawater. Mar. Chem. 74, 15-28.

Burdige, D. J. 2006. Geochemistry of Marine Sediments, Princeton University Press Princeton, NJ,

Charette, M. A., Moran, S. B., Pike, S. M., Smith, J. N. 2001. Investigating the carbon cycle in the Gulf of Maine using the natural tracer thorium-234. J. Geophys. Res. 106, 11,553-11,579.

Chen, J. H., Edwards, R. L., Wasserburg, G. J. 1986. U-238, U-234 and Th-232 in seawater. Earth Planet. Sc. Lett. 80(3-4), 241-251.

Coachman, L. K. 1982. Flow convergence over a broad, flat continental shelf. Cont. Shelf Res. 1(1), 1-14.

Coachman, L. K. 1986. Circulation, water masses, and fluxes on the southeastern Bering Sea shelf. Cont. Shelf Res. 5(1-2), 23-108.

Coale, K. H. and Bruland, K. W. 1987. Oceanic stratified euphotic zone as elucidated by ^{234}Th:^{238}U disequilibria. Limnol. Oceanogr. 32(1), 189-200.

Cochran, J. K., Mckibbin-Vaughan, T., Dornblaser, M. M., Hirschberg, D., Livingston, H. D., Buesseler, K. O. 1990. Pb-210 scavenging in the North-Atlantic and North Pacific oceans. Earth Planet. Sc. Lett. 97(3-4), 332-352.

Cutshall, N. H., Larsen, I. L., Olsen, C. R. 1983. Direct analysis of ^{210}Pb in sediment samples: Self-absorption corrections. Nucl. Instrum. Methods. 206(1–2), 309-312.

Danielson, S., Hedstrom, K., Aagaard, K., Weingartner, T., Curchitser, E. 2012. Wind-induced reorganization of the Bering shelf circulation. Geophys. Res. Lett. 39(8), L08601, doi:10.1029/2012GL051231.

Grebmeier, J. M., Cooper, L. W., Feder, H. M., Sirenko, B. I. 2006a. Ecosystem dynamics of the Pacific-influenced northern Bering and Chukchi seas in the Amerasian Arctic. Prog. Oceanogr. 71, 331-361.

Grebmeier, J. M., Overland, J. E., Moore, S. E., Farley, E. V., Carmack, E. C., Cooper, L. W., Frey, K. E., Helle, J. H., McLaughlin, F. A., McNutt, S. L. 2006b. A major ecosystem shift in the northern Bering Sea. Science. 311, 1461-1464.

Kachel, N. B., Hunt, G. L., Salo, S. A., Schumacher, J. D., Stabeno, P. J., Whitledge, T. E. 2002. Characteristics and variability of the inner front of the southeastern Bering Sea. Deep-Sea Res. Pt. II. 49, 5889-5909.

Lalande, C., Lepore, K., Cooper, L. W., Grebmeier, J. M., Moran, S. B. 2007. Export fluxes of particulate organic carbon in the Chukchi Sea: A comparative study using $^{234}Th/^{238}U$ disequilibria and drifting sediment traps. Mar. Chem. 103, 185-196.

Lepore, K., Moran, S. B., Grebmeier, J. M., Cooper, L. W., Lalande, C., Maslowski, W., Hill, V., Bates, N. R., Hansell, D. A., Mathis, J. T., Kelly, R. P. 2007. Seasonal and interannual changes in particulate organic carbon export and deposition in the Chukchi Sea. J. Geophys. Res. 112(C10), C10024 DOI: 10.1029/2006JC003555.

McRoy, C. P., Hood, D. W., Coachman, L. K., Walsh, J. J., Goering, J. J. 1986. Processes and Resources of the Bering Sea Shelf (PROBES) - the development and accomplishments of the project. Cont. Shelf Res. 5(1-2), 5-21.

Moran, S. B. and Buesseler, K. O. 1993. Size-fractionated ^{234}Th in continental shelf waters off New England: Implications for the role of colloids in oceanic trace metal scavenging J. Mar. Res. 51, 893-922.

Moran, S. B., Ellis, K. M., Smith, J. N. 1997. Th-234/U-238 disequilibrium in the central Arctic Ocean: implications for particulate organic carbon export. Deep-Sea Res. Pt. II. 44(8), 1593-1606.

Moran, S. B., Lomas, M. W., Kelly, R. P., Gradinger, R., Iken, K., Mathis, J. T. 2012. Seasonal succession of net primary productivity, particulate organic carbon export, and autotrophic community composition in the eastern Bering Sea. Deep-Sea Res. Pt. II. 65–70, 84-97.

Moran, S. B., Weinstein, S. E., Edmonds, H. N., Smith, J. N., Kelly, R. P., Pilson, M. E. Q., Harrison, W. G. 2003. Does ^{234}Th/^{238}U disequilibrium provide an accurate record of the export flux of particulate organic carbon from the upper ocean? Limnol. Oceanogr. 48(3), 1018-1029.

Nozaki, Y., Zhang, J., Takeda, A. 1997. Pb-210 and Po-210 in the equatorial Pacific and the Bering Sea: the effects of biological productivity and boundary scavenging. Deep-Sea Res. Pt. II. 44(9-10), 2203-2220.

Roy-Barman, M. 2009. Modelling the effect of boundary scavenging on thorium and protactinium profiles in the ocean. Biogeosciences. 6(12), 3091-3107.

Savoye, N., Buesseler, K. O., Cardinal, D., Dehairs, F. 2004. ^{234}Th deficit and excess in the Southern Ocean during spring 2001: Particle export and remineralization. Geophys. Res. Lett. 31(12), L12301.

Smith, J. N., Moran, S. B., Macdonald, R. W. 2003. Shelf–basin interactions in the Arctic Ocean based on ^{210}Pb and Ra isotope tracer distributions. Deep-Sea Res Pt I. 50, 397-416.

Stabeno, P. J., Kachel, N. B., Sullivan, M., Whitledge, T. E. 2002. Variability of physical and chemical characteristics along the 70-m isobath of the southeastern Bering Sea. Deep-Sea Res. Pt. II. 49, 5931-5943.

Stabeno, P. J., Schumacher, J. D., Ohtani, K. The physical oceanography of the Bering Sea. in: A Summary of Physical, Chemical, and Biological Characteristics, and a Synopsis of Research on the Bering Sea. T. R. Loughlin and K. Ohtani (Eds.). pp 1-28. North Pacific Marine Science Organization (PICES), Univ. of Alaska Sea Grant, AK-SG-99-03. 1999.

Walsh, J. J. 1988. On the nature of continental shelves, Academic Press

Wei, C.-L. and Murray, J. W. 1992. Temporal variations of ^{234}Th activity in the water column of Dabob Bay: particle scavenging. Limnol. Oceanogr. 37(2), 296-314.

Table 1.1. Sampling dates during the 2009 and 2010 BEST-BSIERP field program.

Cruise	Vessel	Dates
HLY 0902	*USCGC Healy*	March 31 - May 12, 2009
KN195-10	*R/V Knorr*	June 14 - July 13, 2009
TN249	*R/V Thompson*	May 9 - June 14, 2010
TN 250	*R/V Thompson*	June 16 - July 13, 2010

Table 1.2. Water column ^{234}Th *deficit*, sediment excess inventory ($^{234}Th_{xs}$), focusing factor (FF_{Th}), and residence time of total ^{234}Th (τ_t) for the eastern Bering Sea during 2009 and 2010.

Station	Latitude	Longitude	Bottom Depth	^{234} *Th deficit*	^{234} Th_{xs}	FF_{Th}	τ_t
	°N	°W	m	dpm cm^{-2}	dpm cm^{-2}		d
Spring, March 31 - May 12, 2009							
Middle Domain (z=50-100 m)							
1-NP7	57.90	169.32	66	7.71 ± 0.41	nd	nd	25.9
2-NP6.5	58.04	169.23	67	8.01 ± 0.43	nd	nd	26.6
3-Ice/Process	58.23	169.12	72	nd	1.93 ± 0.35	nd	nd
9-MN4.5	59.97	169.86	55	6.32 ± 0.34	1.41 ± 0.32	0.22 ± 0.02	25.4
10-MN5	58.90	170.40	62	7.38 ± 0.39	nd	nd	25.4
14-MN8	59.91	172.18	72	7.54 ± 0.52	nd	nd	34.1
32-SL12	62.20	175.14	80	6.87 ± 0.74	3.22 ± 0.38	0.47 ± 0.06	50.3
35-SL9	61.97	173.24	62	7.26 ± 0.60	1.85 ± 0.35	0.26 ± 0.03	25.3
39-SL6	61.93	171.22	51	nd	2.96 ± 0.47	nd	nd
54-NP5	58.37	168.73	68	7.63 ± 0.66	2.76 ± 0.45	0.36 ± 0.04	28.2
58-NP9	57.45	169.75	67	7.01 ± 0.50	1.67 ± 0.29	0.24 ± 0.02	33.2
66-NP11	56.98	170.28	75	6.87 ± 0.61	nd	nd	40.3
83-ICE 3	60.81	174.39	91	nd	4.05 ± 0.45	nd	nd
92-MN-SL5	61.57	173.71	72	8.47 ± 0.52	4.79 ± 0.58	0.57 ± 0.04	28.4
93-BN1	62.25	172.51	57	6.06 ± 0.39	nd	nd	29.3
98-SL12	62.18	175.15	81	7.69 ± 0.69	3.74 ± 0.35	0.49 ± 0.05	41.1
120-70M42	60.00	172.73	64	6.62 ± 0.56	nd	nd	38.7
			Average (± 1 σ)	7.2 ± 0.7	2.8 ± 1.1	0.37 ± 0.14	32.3 ± 7.7
Outer Domain (z=100-200 m)							
17-MN11	59.90	173.99	104	nd	3.64 ± 0.44	nd	nd
19-MN13	59.86	175.22	120	10.12 ± 1.11	2.05 ± 0.31	0.20 ± 0.03	55.6
22-MN16	59.90	176.99	136	7.37 ± 1.55	nd	nd	107.6
29-MN-SL4	61.78	176.80	113	7.68 ± 1.16	nd	nd	72.8
60-ST	56.27	171.08	142	6.70 ± 1.80	nd	nd	131.7
65-NP12	56.72	170.53	109	nd	9.75 ± 0.96	nd	nd
69-BL1	59.56	175.20	133	10.30 ± 1.34	5.31 ± 0.64	0.52 ± 0.07	61.3
73-BL4	59.59	175.08	129	9.85 ± 1.35	2.62 ± 0.34	0.27 ± 0.04	63.5
90-BL20	59.55	175.15	132	12.30 ± 0.98	2.47 ± 0.34	0.20 ± 0.02	36.0
116-BL15	59.56	175.15	130	10.53 ± 1.38	2.91 ± 0.38	0.28 ± 0.04	61.0
			Average (± 1 σ)	9.4 ± 1.9	4.1 ± 2.7	0.29 ± 0.13	73.7 ± 30.9
Oceanic Domain (z= >200 m)							
25-MN19	59.89	178.90	705	1.26 ± 0.14	1.57 ± 0.23	1.25 ± 0.17	-
26-MN20	59.92	179.45	2714	0.71 ± 0.08	2.96 ± 0.51	4.17 ± 0.59	-
61-NP15	56.05	171.30	2760	7.23 ± 5.91	nd	nd	-
			Average (± 1 σ)	3.1 ± 3.6	2.3 ± 1.0	2.71 ± 2.07	-

Summer, June 14 - July 13, 2009

Middle Domain (z=50-100 m)

10-UAP3	55.96	163.14	90	7.85 ± 0.76	nd	nd	44.0
17-CN2	57.56	162.13	51	5.75 ± 0.32	1.49 ± 0.35	0.26 ± 0.03	23.4
45-NP7	57.90	169.24	70	5.97 ± 0.60	0.64 ± 0.09	0.11 ± 0.01	44.3
89-XB6	59.71	170.32	66	5.82 ± 0.56	5.34 ± 0.77	0.92 ± 0.11	40.8
100-MN6	59.90	171.00	70	7.19 ± 0.65	nd	nd	39.4
104-MN9	59.90	172.80	77	4.62 ± 0.86	nd	nd	83.2
130-XB2-4	61.00	171.76	65	nd	5.51 ± 0.45	nd	nd
137-SL6	62.20	171.89	51	5.20 ± 0.34	2.09 ± 0.33	0.40 ± 0.04	29.3
140-SL9	62.20	173.11	62	7.06 ± 0.41	3.21 ± 0.42	0.45 ± 0.03	25.8
147-SL16	62.20	175.98	95	7.73 ± 0.88	0.75 ± 0.06	0.10 ± 0.01	52.5
165-70M41	59.91	172.42	70	5.68 ± 0.75	nd	nd	61.2
181-70M25	58.05	169.65	68	5.19 ± 0.45	nd	nd	38.4
			Average (± 1 σ)	6.2 ± 1.1	2.7 ± 2.0	0.37 ± 0.30	43.8 ± 17.1

Outer Domain (z=100-200 m)

22-CN12	56.13	166.13	113	10.04 ± 0.95	2.18 ± 0.27	0.22 ± 0.02	43.1
25-CN17	55.43	168.06	203	10.61 ± 2.57	nd	nd	115.1
32-CNN6	56.80	167.87	104	10.86 ± 0.81	2.19 ± 0.41	0.20 ± 0.02	33.1
60-SB7	56.28	173.84	196	12.63 ± 2.20	1.72 ± 0.33	0.14 ± 0.03	80.5
79-XB16	57.16	172.95	121	8.14 ± 1.36	4.10 ± 0.48	0.50 ± 0.09	72.7
106-MN11	60.00	174.00	105	8.14 ± 1.07	1.12 ± 0.23	0.14 ± 0.02	58.4
109-MN14	59.90	175.80	132	11.98 ± 1.34	nd	nd	51.4
112-MN17	59.90	177.60	140	10.73 ± 1.49	nd	nd	64.3
113-MN19	59.90	178.74	152	8.29 ± 1.92	3.10 ± 0.46	0.37 ± 0.09	-
122-XB2-12	59.56	175.20	136	8.49 ± 1.57	1.94 ± 0.32	0.23 ± 0.05	84.8
			Average (± 1 σ)	10.0 ± 1.7	2.3 ± 1.0	0.26 ± 0.13	67.0 ± 24.7

Oceanic Domain (z= >200 m)

1-U1	54.25	166.56	1246	15.96 ± 2.80	4.51 ± 0.4748	0.28 ± 0.05	92.0
27-CN20	55.02	169.22	2343	15.38 ± 3.87	3.79 ± 0.4348	0.25 ± 0.07	124.2
53-NP15	56.06	171.34	2800	10.65 ± 4.34	2.99 ± 0.348	0.28 ± 0.12	193.9
66-P14-7	58.23	171.59	2090	13.29 ± 3.30	nd	nd	142.5
67-P14-10	57.50	175.24	3492	4.19 ± 0.46	1.11 ± 0.181	0.26 ± 0.04	-
115-MN20	59.89	179.37	2779	4.87 ± 3.78	6.02 ± 0.4668	1.24 ± 0.97	-
			Average (± 1 σ)	10.7 ± 5.2	3.7 ± 1.8	0.46 ± 0.43	138.1 ± 42.7

Spring, May 9 - June 14, 2010							
Middle Domain (z=50-100 m)							
15-Z6	57.90	170.65	80	10.63 ± 0.46	1.51 ± 0.27	0.14 ± 0.01	19.0
24-Z15	58.35	171.80	99	13.01 ± 0.63	3.04 ± 0.44	0.23 ± 0.02	21.6
66-NZ4.5	59.07	170.17	67	6.96 ± 0.45	0.99 ± 0.29	0.14 ± 0.02	29.3
71-HBR1	56.92	167.32	78	9.14 ± 0.51	1.76 ± 0.37	0.19 ± 0.02	24.5
80-AL2	57.18	170.87	85	nd	1.27 ± 0.24	nd	nd
81-70M26	58.17	169.91	72	8.77 ± 0.41	4.22 ± 0.60	0.48 ± 0.03	23.0
99-70M4	56.85	164.51	73	7.30 ± 0.56	1.42 ± 0.23	0.20 ± 0.02	33.6
121-70M26	58.15	169.92	71	8.74 ± 0.42	nd	nd	21.2
124-70M29	58.62	170.28	72	8.11 ± 0.51	2.05 ± 0.36	0.25 ± 0.02	28.4
147-70M52	61.41	173.74	75	7.85 ± 0.58	2.20 ± 0.35	0.28 ± 0.03	33.4
156-SL12	62.19	175.15	80	8.22 ± 0.65	2.90 ± 0.31	0.35 ± 0.03	35.9
175-MN8	59.90	172.20	73	7.72 ± 0.56	nd	nd	33.1
178-AL4	59.52	170.50	68	nd	1.66 ± 0.30	nd	nd
			Average (± 1 σ)	8.8 ± 1.7	2.1 ± 1.0	0.25 ± 0.11	27.5 ± 5.9
Outer Domain (z=100-200 m)							
2-NP14	56.28	171.05	141	8.96 ± 1.51	nd	nd	83.8
6-NP13	56.51	170.80	122	nd	1.83 ± 0.31	nd	nd
7-NP12	56.73	171.57	109	11.71 ± 0.93	nd	nd	37.7
35-ZC8	58.74	174.90	146	13.16 ± 1.40	4.62 ± 0.60	0.35 ± 0.04	49.8
39-IE1	59.33	177.61	138	12.71 ± 1.33	1.80 ± 0.31	0.14 ± 0.02	49.6
54-AL1	58.86	176.86	126	nd	1.08 ± 0.24	nd	nd
84-CN17	55.44	168.06	200	12.36 ± 2.25	nd	nd	88.0
87-CN17	55.43	168.06	204	11.24 ± 2.50	3.52 ± 0.46	0.31 ± 0.08	108.1
161-MN19	59.90	178.91	206	10.12 ± 2.61	nd	nd	125.1
169-MN14	59.90	175.81	130	12.75 ± 1.21	3.68 ± 0.50	0.29 ± 0.03	44.3
190-NP14	56.28	171.06	188	10.65 ± 1.42	5.94 ± 0.64	0.56 ± 0.08	62.5
			Average (± 1 σ)	11.5 ± 1.4	3.2 ± 1.7	0.33 ± 0.15	72.1 ± 30.7
Oceanic Domain (z= >200 m)							
49-MN19	59.90	178.91	489	13.65 ± 5.44	4.92 ± 0.72	0.36 ± 0.15	203.7
52-MN20	59.90	179.44	2699	12.55 ± 5.51	nd	nd	225.6
55-NZ11.5	58.20	174.24	381	16.41 ± 5.32	2.64 ± 0.42	0.16 ± 0.06	163.7
56-P14-3	58.00	174.85	3014	15.80 ± 5.42	nd	nd	173.0
57-NZ11.5	58.22	174.35	440	18.83 ± 5.34	nd	nd	137.8
162-MN20	59.90	179.44	2672	24.44 ± 4.79	nd	nd	99.1
163-MN19	59.89	178.90	656	16.54 ± 3.80	4.54 ± 0.55	0.27 ± 0.07	112.6
195-NP15	56.05	171.30	2740	17.28 ± 5.33	nd	nd	155.1
			Average (± 1 σ)	16.9 ± 3.6	4.0 ± 1.2	0.27 ± 0.10	158.8 ± 42.9

Summer, June 16 - July 13, 2010							
Middle Domain (z=50-100 m)							
8-UAP5	55.53	163.98	91	9.85 ± 0.69	nd	nd	31.3
15-UAP2	57.06	161.04	74	nd	1.16 ± 0.17	nd	nd
20-CN8	56.71	164.51	76	7.20 ± 0.65	2.07 ± 0.30	0.29 ± 0.03	39.8
34-CNN4	57.35	167.04	72	7.88 ± 0.52	1.15 ± 0.26	0.15 ± 0.02	29.7
47-NP9	57.44	169.82	66	6.94 ± 0.53	nd	nd	34.0
74-W7	60.00	171.06	70	nd	5.10 ± 0.66	nd	nd
91-MN10	59.90	173.40	86	7.20 ± 0.79	5.74 ± 0.76	0.80 ± 0.10	51.0
122-ML3	61.97	170.78	50	4.62 ± 0.37	3.38 ± 0.43	0.73 ± 0.07	37.1
134-SL11	62.20	173.93	64	nd	2.76 ± 0.35	nd	nd
145-BN3	62.67	173.38	66	7.30 ± 0.51	5.08 ± 0.62	0.70 ± 0.06	32.2
167-70M39	59.83	171.77	75	7.02 ± 0.62	nd	nd	40.5
197-70M9	57.26	165.75	70	7.16 ± 0.57	nd	nd	35.3
			Average (± 1 σ)	7.2 ± 1.3	3.3 ± 1.8	0.53 ± 0.29	36.8 ± 6.5
Outer Domain (z=100-200 m)							
25-CN17	55.43	168.06	198	19.28 ± 1.89	nd	nd	46.4
31-CNN7	56.35	168.29	130	nd	0.94 ± 0.15	nd	nd
53-TD2	56.25	171.11	190	11.50 ± 2.14	1.61 ± 0.23	0.14 ± 0.03	91.2
58-SB5	56.72	173.02	132	nd	7.76 ± 0.68	nd	nd
97-MN16	59.90	177.00	136	14.38 ± 1.17	7.33 ± 0.97	0.51 ± 0.05	37.4
100-TD4	59.90	178.85	225	13.43 ± 2.76	1.79 ± 0.28	0.13 ± 0.03	97.5
			Average (± 1 σ)	14.6 ± 3.3	3.9 ± 3.4	0.26 ± 0.22	68.1 ± 30.6
Oceanic Domain (z= >200 m)							
26-CN20	55.02	169.22	2332	16.52 ± 5.38	nd	nd	163.7
54-NP15	56.06	171.32	2785	12.71 ± 5.66	39.69 ± 3.77	3.12 ± 1.42	223.3
62-P14N-10	57.50	175.24	3473	13.08 ± 5.62	nd	nd	215.0
63-P14N-7	58.27	174.56	2112	12.25 ± 2.46	9.00 ± 0.74	0.73 ± 0.15	97.3
102-MN20	59.90	179.40	2705	10.62 ± 5.71	43.24 ± 4.45	4.07 ± 2.23	273.5
			Average (± 1 σ)	13.0 ± 2.2	30.6 ± 18.8	2.64 ± 1.72	194.6 ± 66.9

Table 1.3. Seasonal ^{234}Th budget for the middle and outer domains of the eastern Bering Sea shelf (all units in dpm cm^{-2} d^{-1}).

	Process	Term	Spring 2009	Summer 2009	Spring 2010	Summer 2010	Average	Fraction λU
Input	Production by *in situ* decay of ^{238}U	λU	0.55 ± 0.21	0.59 ± 0.24	0.64 ± 0.30	0.61 ± 0.32	0.59 ± 0.27	
	Cross-front exchange of ^{234}Th	$V^{*}\Delta Th_{CS}$	0.023 ± 0.007	-0.001 ± 0.006	-0.002 ± 0.005	0.008 ± 0.006	0.007 ± 0.006	0.01 ± 0.01
Output	Loss by *in situ* decay of ^{234}Th	λTh	0.32 ± 0.18	0.36 ± 0.19	0.36 ± 0.26	0.34 ± 0.23	0.34 ± 0.21	0.576 ± 0.44
	Along-shore transport	$T^{*}\Delta Th_{AS}$	0	0	0	0	0	
	Decay of ^{234}Th in sediments	J_{sed}	0.10 ± 0.06	0.07 ± 0.04	0.07 ± 0.04	0.10 ± 0.07	0.09 ± 0.05	0.146 ± 0.11
Excess	Shelf export flux of ^{234}Th	J_{exp}	0.16 ± 0.28	0.16 ± 0.31	0.21 ± 0.40	0.18 ± 0.40	0.17 ± 0.35	0.294 ± 0.60

Table 1.4. Shelf averages (Middle and Outer domains) of the water column ^{234}Th *deficit* and sediment $^{234}Th_{xs}$ inventory. FF_{Th}s were calculated from average deficits and inventories.

Season	^{234} *Th Deficit* dpm cm^{-2}	^{234} Th_{xs} dpm cm^{-2}	FF_{Th}
Spring 2009	8.01 ± 1.60	3.36 ± 1.97	0.42 ± 0.26
Summer 2009	8.00 ± 2.37	2.53 ± 1.55	0.32 ± 0.22
Spring 2010	10.01 ± 2.09	2.53 ± 1.38	0.25 ± 0.15
Summer 2010	9.52 ± 4.07	3.53 ± 2.41	0.37 ± 0.30
Average	8.79 ± 2.61	2.97 ± 1.85	0.34 ± 0.23

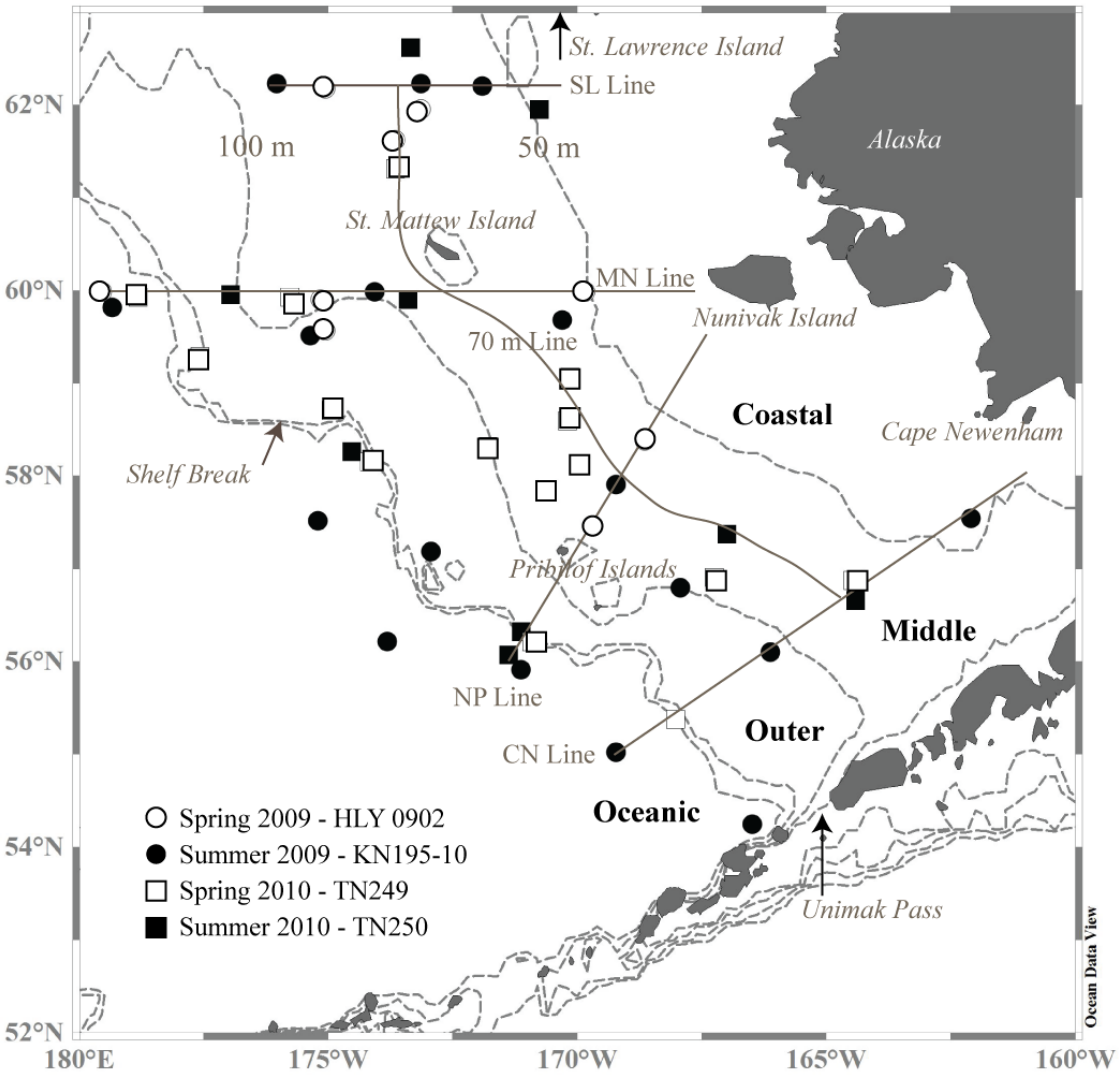

Figure 1.1. Map of the eastern Bering Sea identifying the major transects during the BEST-BSIERP field program and station locations where water column and sediment samples were collected.

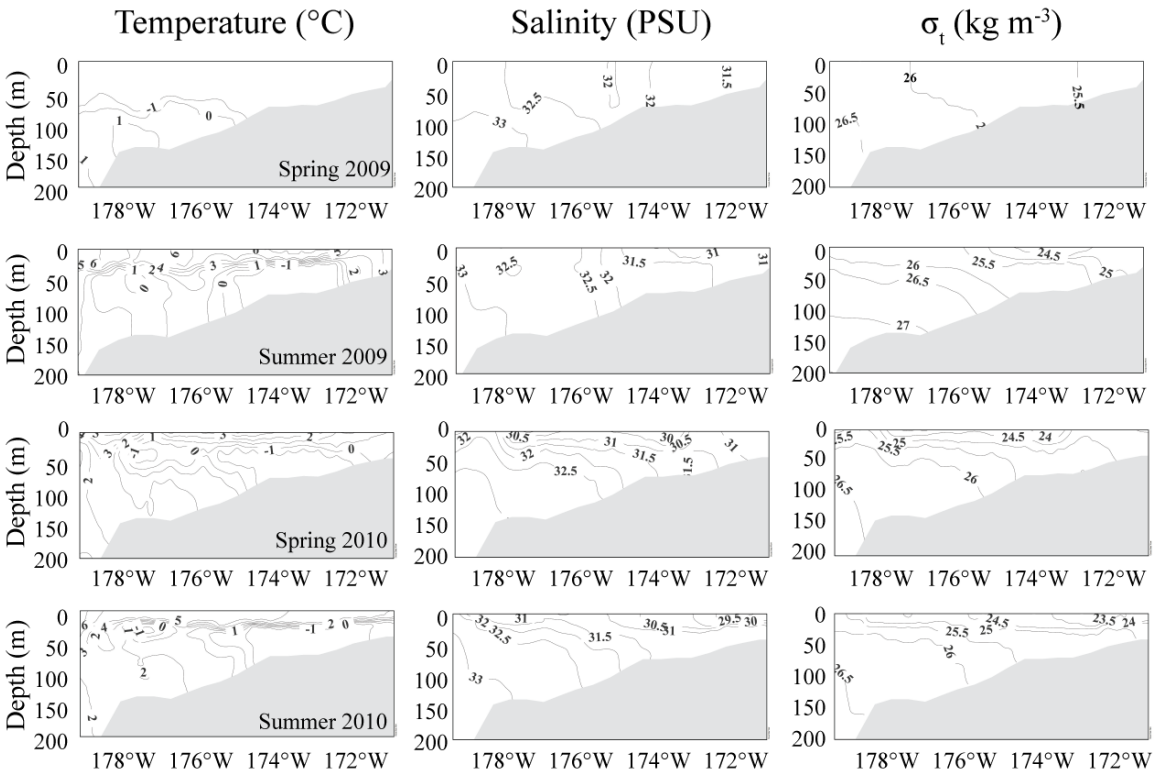

Figure 1.2. Temperature (°C), salinity (PSU), and density anomaly (kg m^{-3}) sections along the MN line for spring and summer 2009-10.

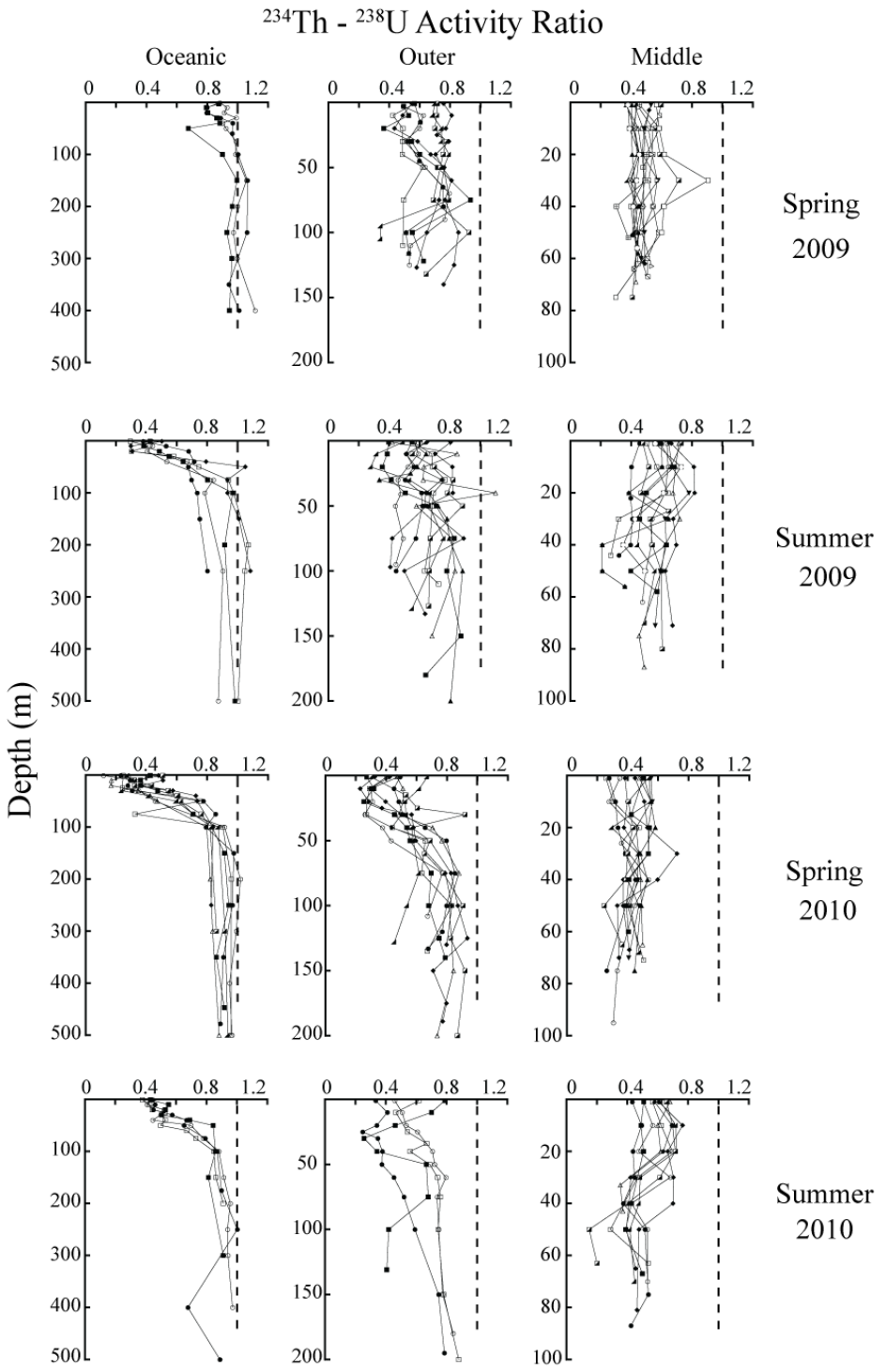

Figure 1.3. Depth profiles of ^{234}Th-^{238}U activity ratios according to season and domain. Slope-Oceanic Domain profiles plotted to a maximum depth of 500 m. Middle and Outer domains profiles plotted to sea floor.

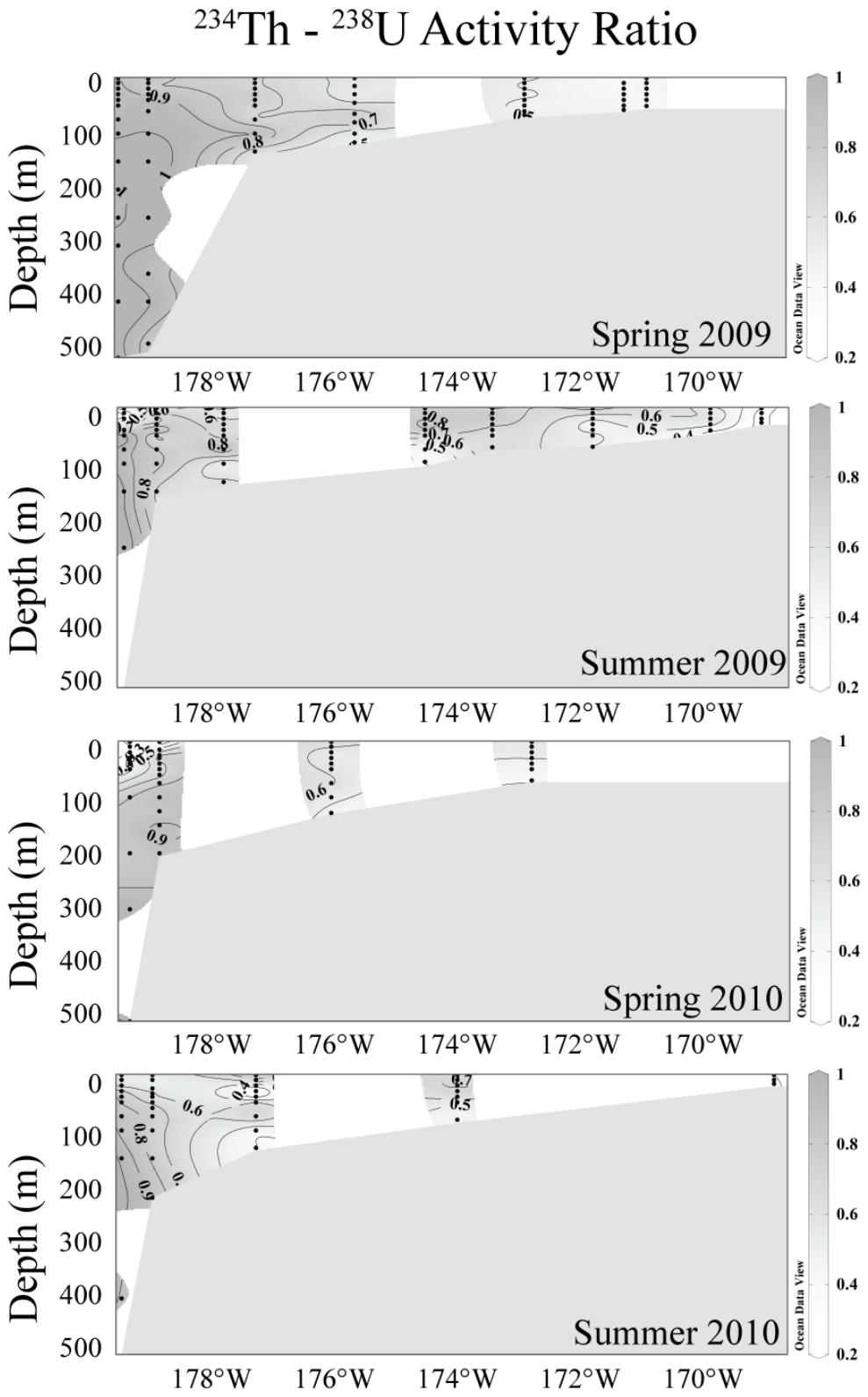

Figure 1.4. Seasonal variability in ^{234}Th-^{238}U activity ratio (AR) along the MN Line.

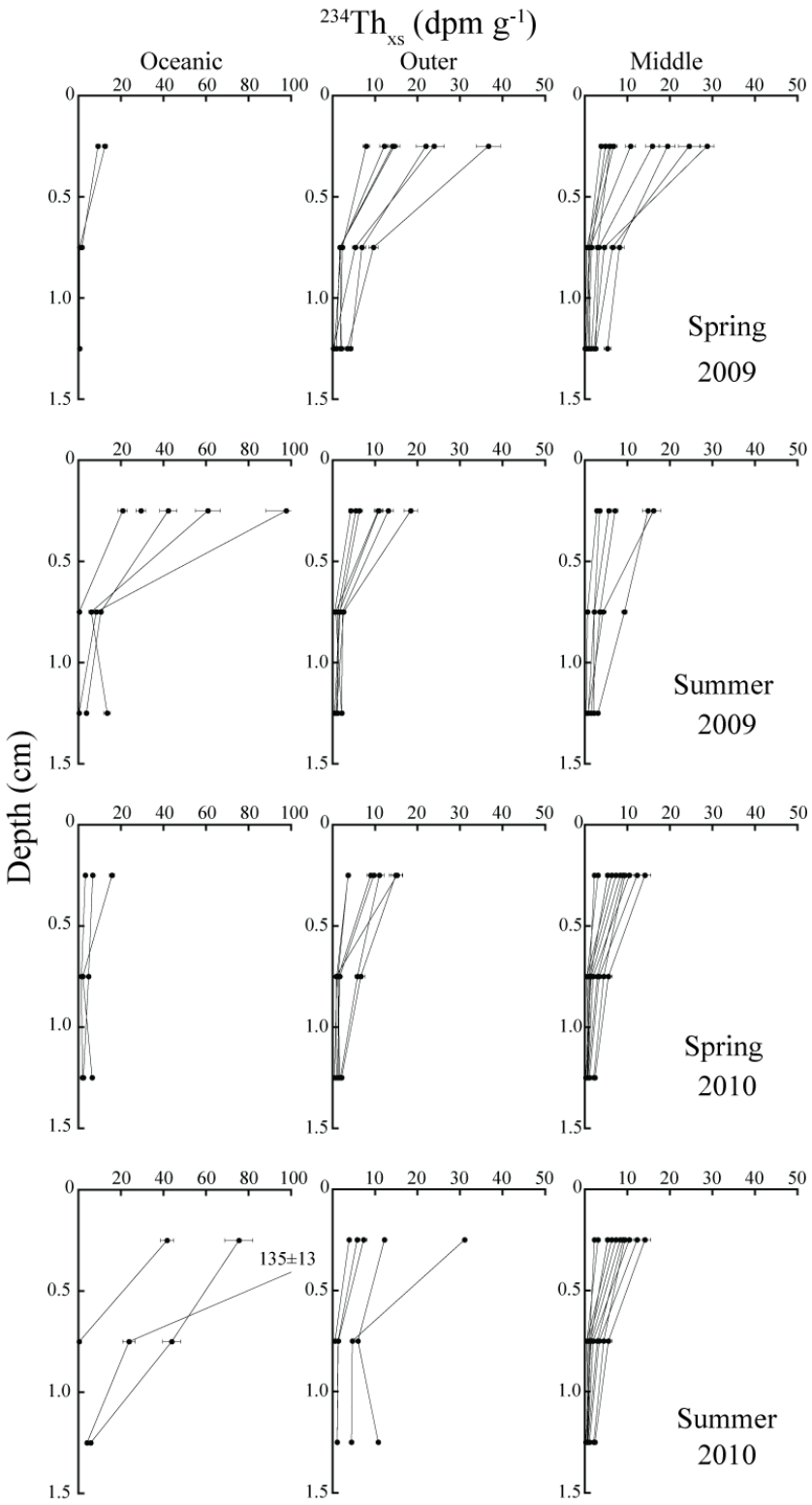

Figure 1.5. Depth profiles of sediment $^{234}Th_{xs}$ (dpm g^{-1}). Profiles are plotted to a maximum depth of 1.5 cm (1.25 cm mid-point), which correlates with integration depth.

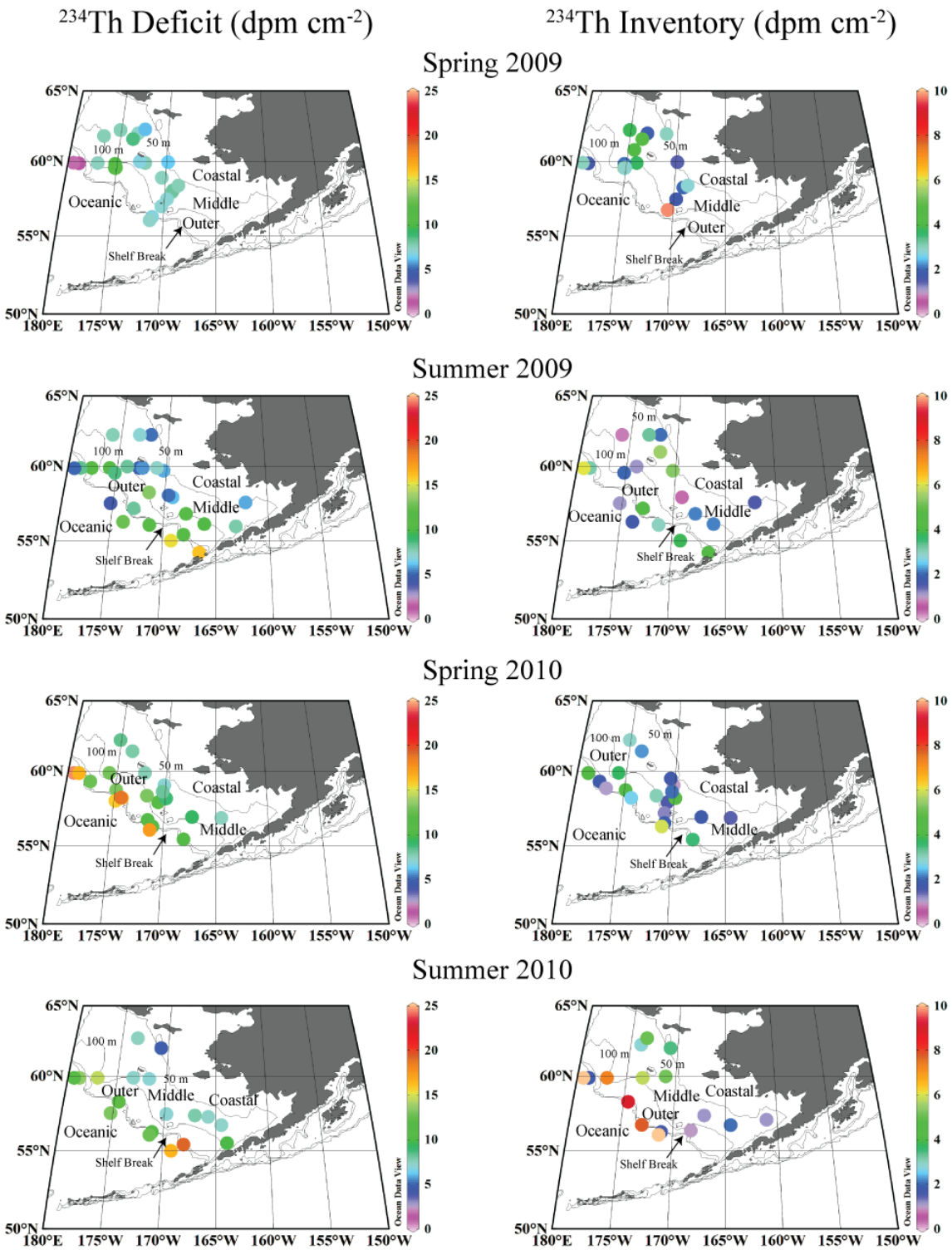

Figure 1.6. Maps of water column ^{234}Th *deficit* and sediment $^{234}Th_{xs}$ inventory. Note that two Oceanic sediment $^{234}Th_{xs}$ inventories for summer 2010 are off-scale and indicated by lightly shaded symbols.

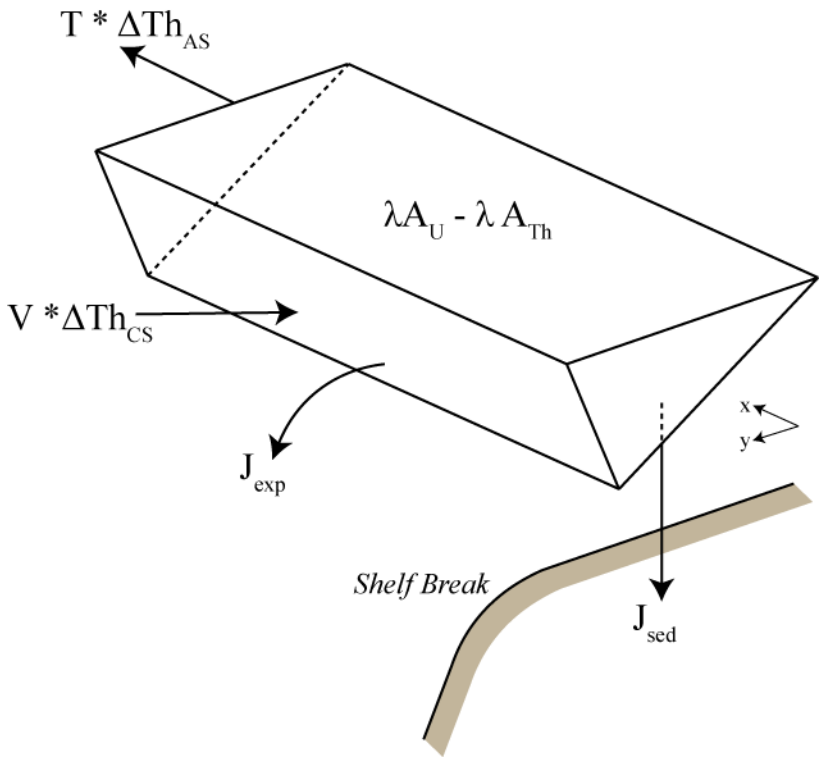

Figure 1.7. Illustration of the supply and removal terms responsible for the radiochemical balance of ^{234}Th over the eastern Bering Sea shelf. Terms defined in Table 1.3.

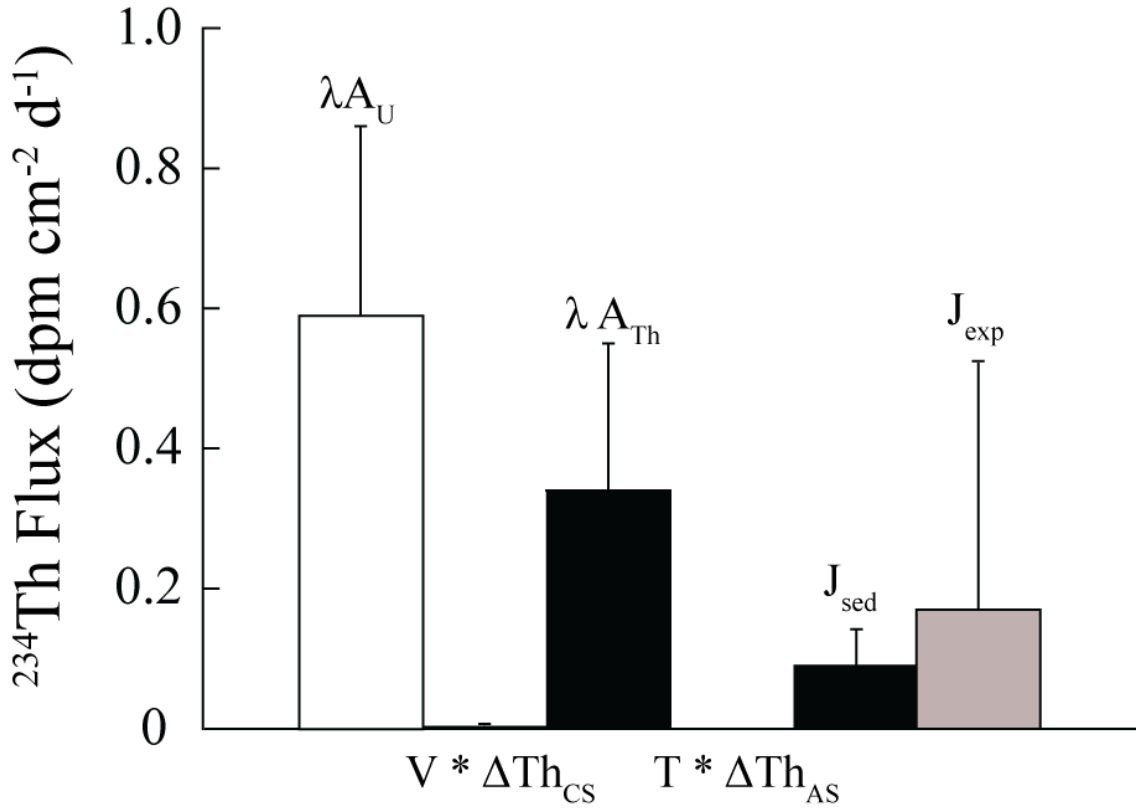

Figure 1.8. Seasonally averaged supply (white bar), removal (black bars), and off-shelf export (gray bar) of ^{234}Th over the eastern Bering Sea shelf.

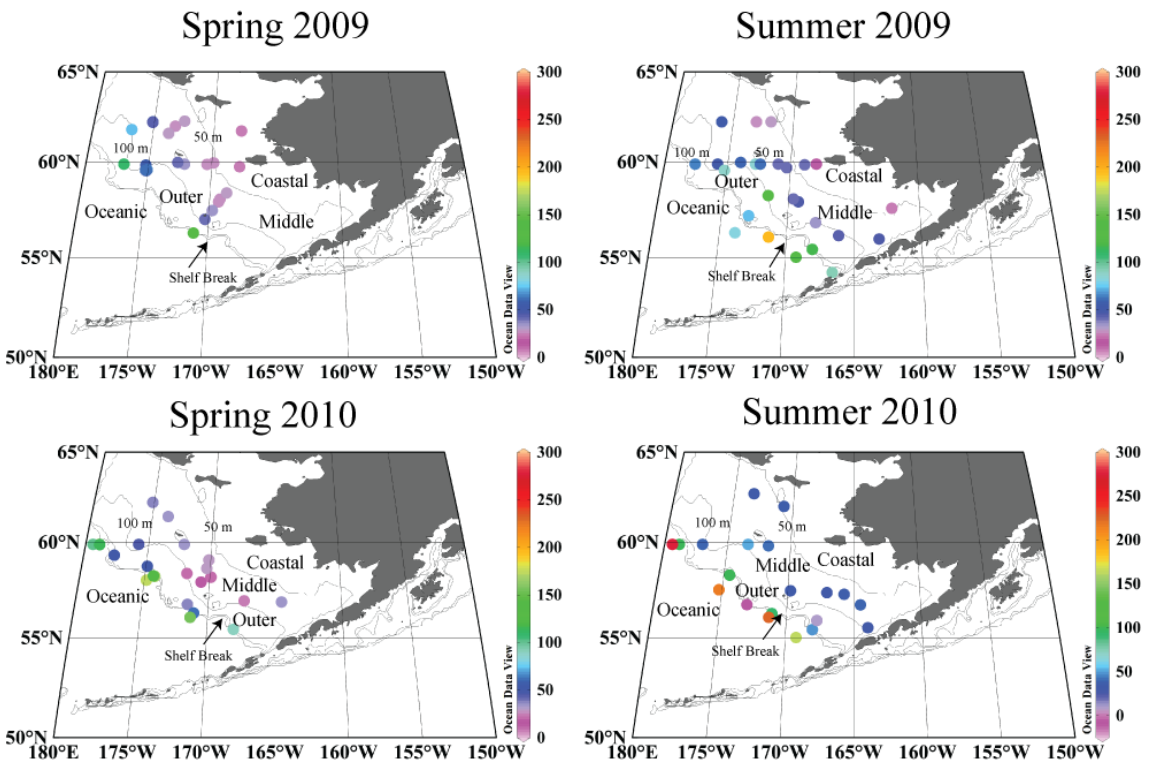

Figure 1.9. Distributions of total ^{234}Th residence time (τ_t, d) in the eastern Bering Sea.

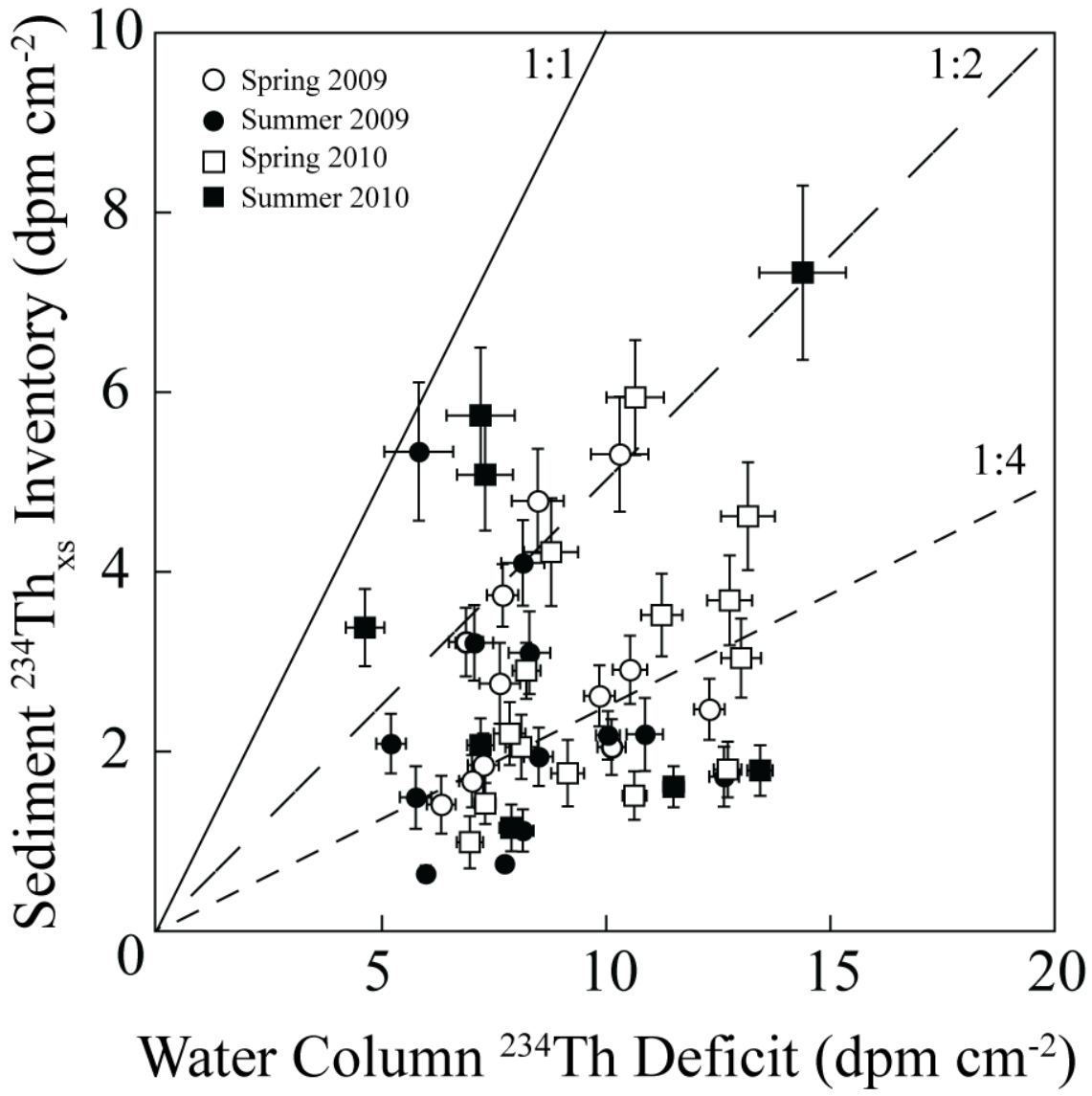

Figure 1.10. Plot of sediment $^{234}Th_{xs}$ inventory against water column deficit of ^{234}Th for the eastern Bering Sea shelf. Data plotted only for the Middle and Outer shelf regions.

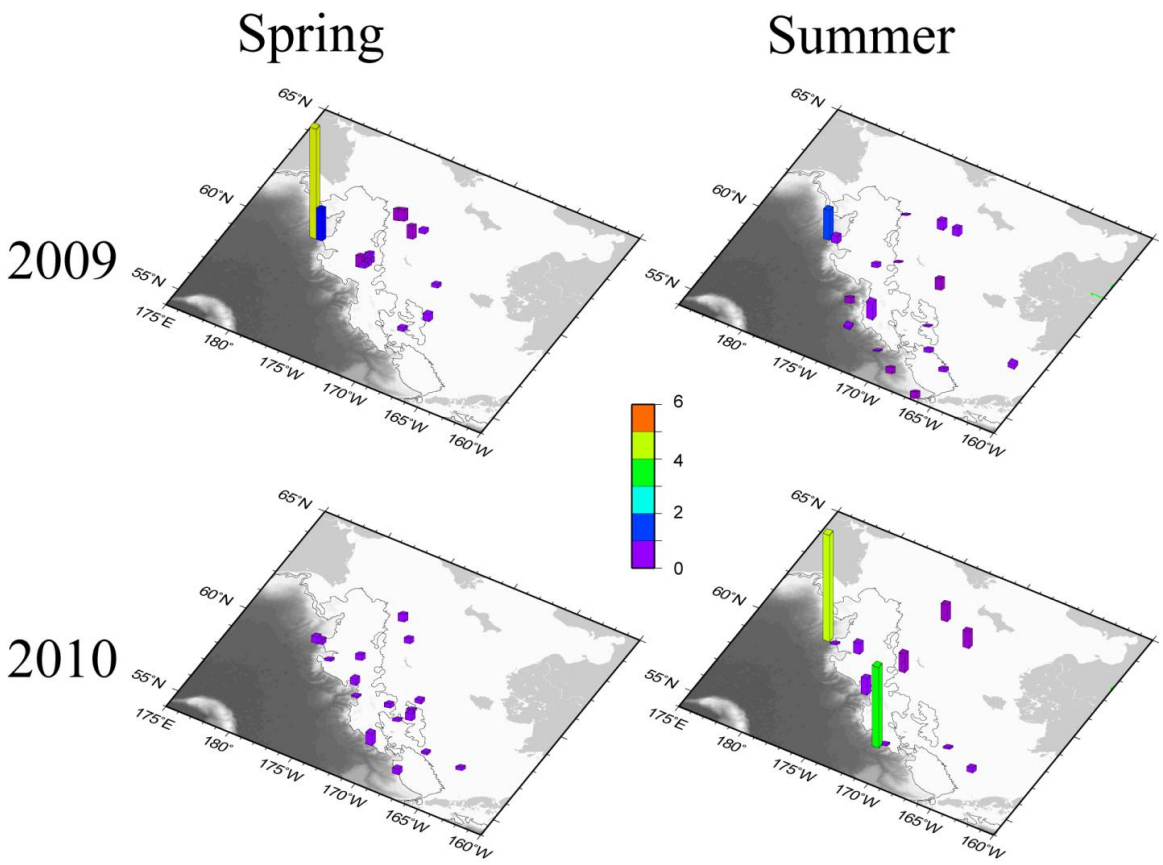

Figure 1.11. ^{234}Th focusing factors (FF_{Th}) determined in the eastern Bering Sea.

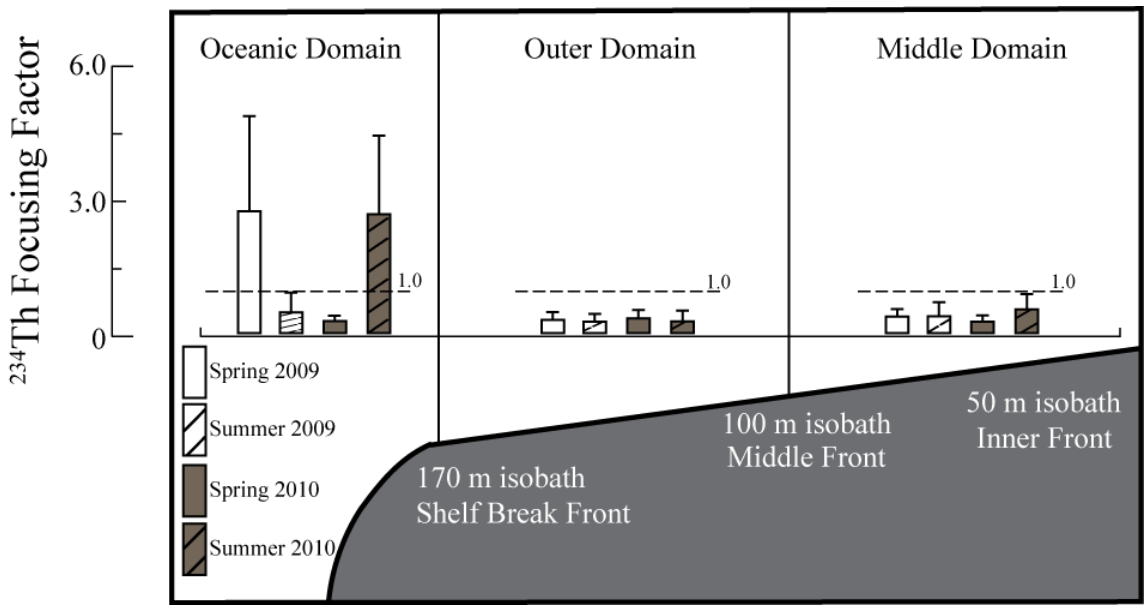

Figure 1.12. Average FF_{Th} calculated according to season and domain. Uncertainties represent 1 σ.

Publication Status

Manuscript II, titled “Seasonal decoupling of particulate organic carbon export and net primary production in relation to sea-ice at the shelf break of the eastern Bering Sea: implications for off-shelf carbon export” was published in *Journal of Geophysical Research-Ocean.* The co-authors of this manuscript are S. B Moran, M. W. Lomas, R. P. Kelly, and D. W. Bell.

MANUSCRIPT II

SEASONAL DECOUPLING OF PARTICULATE ORGANIC CARBON EXPORT AND NET PRIMARY PRODUCTION IN RELATION TO SEA-ICE AT THE SHELF BREAK OF THE EASTERN BERING SEA: IMPLICATIONS FOR OFF-SHELF CARBON EXPORT

Abstract

Particulate organic carbon (POC) export fluxes and net primary production (NPP) rates are used to assess seasonal patterns in the export ratio (*e*-ratio = POC export/NPP*)* in relation to proximity of the sea-ice edge near the shelf break of the eastern Bering Sea during 2008-2010. POC fluxes were relatively low in April (4.6±1.6, trap, and 5.7±4.3 mmol C m^{-2} d^{-1}, ^{234}Th-derived) and increased in May-early June (19.9±13.3 and 17.0±8.8 mmol C m^{-2} d^{-1}). POC export reached a maximum in mid-June-mid-July (30.0±12.6 and 48.1±17.4 in 2009; 33.1±27.6 and 57.0±68.4 mmol C m^{-2} d^{-1} in 2010) and decreased by late July (13.1±4.7 and 14.1±8.0 mmol C m^{-2} d^{-1}). NPP rates were relatively high and export fluxes low near the ice-edge in spring, leading to *e*-ratios <0.25. In early summer, POC export exceeded NPP at individual stations and resulted in *e*-ratios >1, which is attributed to a temporal decoupling, or offset, of spring NPP and export during summer. While these observations reveal a seasonal progression in POC export and the *e*-ratio, there is no direct relationship to sea-ice proximity. Furthermore, based on a water column-sediment ^{234}Th budget, the off-shelf export of POC during spring-summer is estimated to be 24±35 mmol C m^{-2} d^{-1}, which represents an off-shelf *e*-ratio of 0.07 and 0.21 for contemporaneous seasonally averaged daily rates of NPP and 0.17 and 0.52 for

historical monthly averaged daily rates of NPP. An implication is that off-shelf POC transport may represent a seasonal net sink for CO_2 in this and other polar shelf regions.

2.1. Introduction

The eastern Bering Sea shelf, as with other polar seas, influences the uptake of atmospheric CO_2 in part by the conversion of dissolved inorganic carbon into biogenic particles and subsequent vertical removal by particle export. The seasonal increase in solar irradiance, coupled with the retreat of sea-ice in spring, allows for exceptionally high rates of primary production in the nutrient rich waters of the shelf break and Outer shelf region of the eastern Bering Sea (Alexander and Niebauer, 1981; Niebauer *et al.*, 1995). The resulting pulse in primary production within the marginal ice zone (MIZ) during spring sea-ice retreat has been reported to decouple from zooplankton growth due to reduced grazing efficiency resulting in the potential for seasonally high rates of particle export in Arctic shelf systems (e.g., Wassmann *et al.*, 2004). Because of the potential for seasonally high particle export fluxes at the shelf break and Outer shelf of the eastern Bering Sea, previous studies have suggested that this region may represent a seasonal net sink for atmospheric CO_2 (Walsh *et al.*, 1981).

The recent decline in Arctic and sub-Arctic seasonal sea-ice thickness and extent may restructure energy flow through the lowest trophic levels of the ecosystem (Arrigo *et al.*, 2008; Grebmeier *et al.*, 2006; Overland and Wang, 2007), potentially impacting the export of organic carbon from the surface to deeper polar ocean waters. In particular, the seasonal timing of sea-ice retreat exerts an important control on the timing of primary production (Brown and Arrigo, 2013), but it is still unclear as to how sea-ice retreat

influences the overall magnitude of primary production in high-latitude systems. During cold years, the ice-edge can extend as far as the shelf break of the eastern Bering Sea, overlying nutrient rich water upwelled from the deep North Pacific (Alexander and Niebauer, 1981). As sea-ice retreats due to seasonal warming, the upper water column is stratified by the release of freshwater. As a result, cold years typically yield large spring blooms near the MIZ as sea-ice retreats over the shelf break. Zooplankton stocks tend not to respond as quickly to such blooms during the spring, which may allow for a more efficient particle export of primary production at the shelf break following the bloom (e.g., Sakshaug, 2004). Here, we hypothesize that such a temporal offset between the spring primary production event and subsequent export during early summer may allow for the transfer of a large fraction of POC from the surface ocean to depth, and in turn, lead to a seasonal net sink for CO_2 during cold years. Conversely, during warm years characterized by early sea-ice retreat, spring blooms tend to be delayed until the upper water column is thermally stratified and occur primarily under ice-free, open water conditions. These warmer year blooms are more tightly coupled in time with the seasonal emergence of zooplankton stocks, resulting in a greater fraction of carbon retained and recycled within the pelagic ecosystem, reduced export, and hence a reduced transfer efficiency of carbon to benthic organisms. These hypotheses form the basis of the Oscillating Control Hypothesis (OCH), which postulates that walleye pollock (*Theragra chalcogramma*) recruitment is dictated by bottom-up control during cold years and top-down control during warm years (Hunt *et al.*, 2002).

While the OCH has been recently modified (Hunt *et al.*, 2011) based on new observations obtained as part of BEST-BSIERP (Bering Ecosystem Study-Bering Sea

Integrated Ecosystem Research Project) in the relatively cold period during 2007-2011 (Stabeno *et al.*, 2012), the essential premise remains that the transfer efficiency of export production associated with the spring bloom event may be greater during cold years. However, no contemporaneous measurements of both net primary and export production exist over multiple years for the eastern Bering Sea, either during cold or warm regimes. Such information is necessary to testing not only the OCH, but also to address the notion that off-shelf export of POC may represent a seasonal net sink for CO_2 in such dynamic high-latitude shelf systems as the eastern Bering Sea.

A primary goal of this study is to assess seasonal changes in rates of POC export and the export ratio (*e*-ratio = POC export/NPP) at the shelf break and Outer shelf of the eastern Bering Sea in relation to sea-ice proximity. Because there is no ideal, truly unbiased method to quantify export production from the surface ocean, this study reports POC fluxes determined using both drifting sediment trap arrays and ^{234}Th-^{238}U disequilibria. Due to its short half life ($t_{1/2}$ = 24.1 d), particle-reactive nature, and known rate of production, ^{234}Th has been widely used as a tracer to quantify POC export from the upper ocean (Benitez-Nelson *et al.*, 2001a; Buesseler *et al.*, 1995; Buesseler *et al.*, 1998; Coale and Bruland, 1985, 1987; Moran *et al.*, 2003). The use of ^{234}Th as a flux proxy for POC export has been increasingly utilized in the Arctic (Amiel and Cochran, 2008; Amiel *et al.*, 2002; Cai *et al.*, 2010; Gustafsson and Andersson, 2012; Lalande *et al.*, 2007; Lalande *et al.*, 2008; Lepore *et al.*, 2007; Moran *et al.*, 1997; Moran *et al.*, 2005; Moran and Smith, 2000), however there is only one previous study of POC export over the eastern Bering Sea shelf, which reports data from a single year (Moran *et al.*, 2012). Within the context that 2008 - 2010 represents a multi-year cold period, sediment

trap and ^{234}Th-derived POC export, together with seasonal variability in the *e*-ratio, are compared for the eastern Bering Sea during spring and summer. In addition, an estimate of the off-shelf transport of POC is reported, based on a recent water column-sediment ^{234}Th budget for the Outer shelf (Baumann *et al.*, 2013), and the resultant implications for a net seasonal sink for atmospheric CO_2 in this region are discussed.

2.2. Methods

a. Study area

The eastern Bering Sea shelf may be subdivided into three cross-shelf domains isolated by seasonal fronts: Coastal Domain (0–50 m), Middle Domain (50–100 m), and Outer Domain (100 m – shelf break front at ~200 m) (Coachman, 1986; Kachel *et al.*, 2002; McRoy *et al.*, 1986). These three shelf domains can be further sectioned into North and South regions separated at 60°N (Mathis *et al.*, 2010). This present study is focused in the North and South Outer domains and along the shelf break/slope (off-shelf region; ~200–3500 m). For consistency, the study regions will henceforth be referred to as the Outer Domain/shelf or shelf break/off-shelf (Fig. 2.1).

Seasonal sea-ice extent and duration over the southeastern Bering Sea shelf is highly variable, with distinct temporal changes occurring on the order of less than a decade to several decades (Stabeno *et al.*, 2012). Specifically, the last three decades of the previous century were characterized by a high degree of variability in spring sea-ice cover, which was followed by a five year period (2001-2005) of reduced ice extent during the spring months. The latter period of the previous decade (2007-2010) was characterized by extensive sea-ice cover in spring and low water column temperatures.

b. Sediment trap sampling

Sediment trap and water column samples were collected along the shelf break (200–3500 m) and Outer shelf (100–200 m) of the eastern Bering Sea during spring and summer cruises from 2008-2010 as part of the BEST-BSIERP field program. Cruise information is listed in Table (2.1).

Surface tethered, drifting particle trap arrays (*KC Denmark*, Silkeborg, Denmark) were deployed near the shelf break in waters >125 m depth (Table 2.2; n = 3 and 3 for spring and summer of 2008; 5 and 4 for spring and summer of 2009 and 2010). Deployments were ~24 h in duration with trap depths of 25, 40, 50, 60, and 100 m (4x72 mm diameter traps per depth). Sediment traps were filled with non-poisoned, 0.4 µm filtered brine (S = ~85 ‰) prior to deployment to isolate swimmers and suspended particulate matter from passively sinking material. After recovery, the upper seawater layer was siphoned to the seawater-brine interface indicated by the discontinuity between the layers. Each sample was vacuum filtered onto a pre-combusted 25 mm GF/F, sub-sampled for the determination of particulate organic carbon (POC) content, dried at 60°C, and analyzed for ^{234}Th at sea.

c. Water column sampling

Total (dissolved + particulate) ^{234}Th was sampled in the water column at the locations of the sediment trap deployments. The ^{234}Th profiles are high resolution (~10 m) over the upper 100 m and also correlate with the sediment trap depths for direct comparison. Water column ^{234}Th samples were collected from CTD-rosette casts using the small volume (SV; 4 L) technique, in which ^{234}Th is extracted via co-precipitation

with manganese oxide (MnO_2) (Benitez-Nelson *et al.*, 2001b; Buesseler *et al.*, 2001). The pH of the sample was raised by the dropwise addition of concentrated ammonium hydroxide (28%) followed by the addition of 0.2 M $KMnO_4$ (25 µL) and 1.0 M $MnCl_2$ (11.5 µL) to generate the MnO_2 precipitate. After one hour of equilibration, each sample was vacuum filtered onto a 25 mm diameter 1 µm pore size glass microfiber filter (GM/F). Deep samples (>1000 m) were collected as a check for detector efficiency. In addition, replicate samples were spiked with a known ^{230}Th activity as an internal standard of ^{234}Th scavenging efficiency. Scavenging efficiencies were typically >90%.

d. ^{234}Th and ^{238}U analysis

Sediment trap and water column ^{234}Th samples were quantified by the measurement of beta emissions of ^{234m}Pa (E_{max} = 2.19 MeV; $t_{1/2}$ = 1.2 min) on a low-background beta detector (*RISØ National Laboratory*, Roskilde, Denmark; average detector efficiency: 44 ± 3%) (Charette *et al.*, 2001). Prior to analysis, each sample was mounted on an acrylic disc and covered with clear plastic wrap and aluminum foil to shield low-level beta and alpha emitters. Because of the time-sensitive nature of ^{234}Th analysis, the initial count occurred at sea. The first count for the sediment trap samples occurred immediately, while the first count for the water column samples was withheld at least three days to allow for the decay of short lived isotopes. Each sample was counted several times over the first six half-lives of ^{234}Th. After this period, each sample was counted to establish background levels. Data were fitted to the ^{234}Th decay curve and corrected to yield ^{234}Th activity at the time of collection.

Water column ^{238}U activities were calculated from salinity according to the relationship ^{238}U (dpm L^{-1}) = salinity (‰) x 0.0708 (Chen *et al.*, 1986). Salinities were obtained from CTD profiles of water column hydrography. This relationship has been previously verified by sector-ICP-MS analysis of unfiltered seawater samples from the Outer shelf and slope water of the Chukchi Sea, a similar high-latitude marginal sea to the Bering Sea (Moran *et al.*, 2005) as well as for the high salinity Mediterranean Sea, where possible nonconservative behavior of ^{238}U may be expected (Speicher *et al.*, 2006).

e. Analysis of POC

An arc-punch was used to generate a 10 mm diameter subsample from each sediment trap GF/F, which was used for the analysis of POC. It was necessary to subsample the trap GF/F by area rather than weight because of the need to analyze for ^{234}Th at sea. The POC subsample was frozen until preparation for analysis in a shore-based laboratory. The subsamples were dried at 60°C, fumed in a desiccator containing hydrochloric acid for 24 h to oxidize and remove inorganic carbon, and dried once again for 24 h at 60°C. POC was analyzed on a CE-440 Elemental Analyzer (*Exeter Analytical, Inc*., North Chelmsford, MA, USA) (Pike and Moran, 1997). Field blanks were prepared for each set of samples by filtering 200 mL of pre-filtered brine. An average blank for each cruise was subtracted from corresponding gross POC concentrations.

2.3. Results

a. Hydrographic characteristics of the southeastern Bering Sea Outer shelf and shelf break

The temporal and spatial variability of sampling during the 2008-2010 field program allowed for the characterization of the seasonal succession of primary production and subsequent export of POC during early (HLY0802 in 2008 and HLY0902 in 2009) and late (TN249 in 2010) spring as well as early (KN195-10 in 2009 and TN250 in 2010) and mid-summer (HLY0803 in 2008) under relatively persistent interannual spring sea-ice extent over the southeastern Bering Sea shelf (Fig. 2.1; Tables 2.1, 2.2). The ~sea-ice maximum (solid) and minimum (dashed) during the spring field studies are depicted on Fig. (2.1). Listed in Table (2.2) are the approximate distances from the spring sediment trap deployments to the center of the MIZ (<8/10ths ice cover) on the day of deployment. Sea-ice data were obtained from the U.S. National Ice Center (http://www.natice.noaa.gov/products/). For the HLY0802 and HLY0902 (early spring) cruises the location of sediment trap deployment ranged from 57–138 (2008) and 25–88 (2009) km from the center of the MIZ. With the exception of one TN249 (late spring 2010) sediment trap station, all other sediment trap deployments are considered open water locations as they are >150 km from the sea-ice edge.

Spring upper water column temperature, salinity, and buoyancy may provide additional, yet qualitative, insight into recent sea-ice cover and melt water release. During HLY0802, the upper water column (150 m) along the shelf break was well mixed as 0 - 40 and >40 m horizons demonstrated little variation in density (σ_t). Density of the upper 40 m ranged from 25.93 to 26.38 (mean: 26.10) and the 40-150 m ranged from 25.96 to 26.51 (mean: 26.35) kg m^{-3} at the locations of sediment trap deployments (Figs. 2.1, 2.2a; Table 2.2). Cruise HLY0902 in 2009 overlapped with spring 2008; however, substantial ship time was allocated to characterize a well-formed spring bloom (Bloom

Station; BL; Fig. 2.1; Table 2.2) over the Outer shelf (z = ~125 m). As with the shelf break, the Outer shelf water column was also well mixed in early spring. The density range in the upper 40 m was 25.69 to 26.21 (mean: 25.84) and the >40 m horizon ranged from 25.91 to 26.34 (mean: 26.26) kg m^{-3} (Fig. 2.2c). Moreover, during both early spring cruises the upper 40 m of the water column was on average 1.25°C colder and 0.46 psu (practical salinity units) less saline than the >40 m water column indicating recent melt water input from sea-ice retreat. However, during TN249 the upper water column (<40 m) of the shelf break demonstrated more stratification, which is characteristic of summer for the region. At the sediment trap stations, the upper 40 m σ_t range was 24.70 to 26.19 (mean: 25.79) kg m^{-3}, while the density structure of the deeper waters varies little between early and late spring (Fig. 2.2e).

During KN195-10 and TN250, σ_t in the <40 m horizon ranged from 25.29 to 26.22 (mean: 25.75) and 24.99 to 26.11 (mean: 25.74) kg m^{-3}, respectively (Fig. 2.2d, f). Mean density in the upper 40 m of the water column varied by only 0.04 kg m^{-3} in late spring and early summer, which indicates a similarly stratified water column between May and mid-July. During HLY0803, the σ_t range was 25.31 to 26.06 (mean: 25.57) kg m^{-3}, implying a slightly more buoyant <40 m water column than early summer (Fig. 2.2b).

b. Sediment trap POC and ^{234}Th fluxes

Along the shelf break during HLY0802, spatial and depth (40 – 100 m traps) averaged particle fluxes of ^{234}Th ($^{234}Th_{trap}$) and POC (POC_{trap}) were relatively low at 759±235 (± 1σ) dpm m^{-2} d^{-1} and 4.6±1.6 (± 1σ) mmol C m^{-2} d^{-1}, respectively (Fig. 2.3;

Table 2.3). By May and mid-June (TN249) average $^{234}Th_{trap}$ and POC_{trap} increased to 2172±803 dpm m^{-2} d^{-1} and 19.9±13.4 mmol C m^{-2} d^{-1}, respectively (Fig. 2.5). Particle fluxes of ^{234}Th during the early summer cruises (KN195-10 and TN250) were low relative to trap POC fluxes along the shelf break (Figs. 2.4, 2.5). For KN195-10, depth averaged $^{234}Th_{trap}$ and POC_{trap} were 1047±488 dpm m^{-2} d^{-1} and 30.0±12.6 mmol C m^{-2} d^{-1}, respectively. Average trap fluxes during TN250 were 1256±751 dpm m^{-2} d^{-1} for $^{234}Th_{trap}$ and 33.1±27.6 mmol C m^{-2} d^{-1} for POC_{trap} (Table 2.3). During HLY0803 in July, average $^{234}Th_{trap}$ fluxes along the shelf break were greater than the early summer, while POC_{trap} fluxes were lower averaging 1595 ± 660 dpm m^{-2} d^{-1} and 13.1±4.7 mmol C m^{-2} d^{-1}, respectively (Fig. 2.3).

At station BL during HLY0902, depth averaged $^{234}Th_{trap}$ and POC_{trap} were greater than those along the shelf break at 2000±1656 dpm m^{-2} d^{-1} and 44.6±28.1 mmol C m^{-2} d^{-1}, respectively (Fig. 2.4; Table 2.3).

c. ^{234}Th fluxes from ^{234}Th-^{238}U disequilibrium and ^{234}Th-derived POC fluxes

A one-box model is typically used for the calculation of the ^{234}Th flux through the upper ocean water column (Savoye *et al.*, 2006):

$$\frac{dA_{Th}}{dt} = A_U\,\lambda - A_{Th}\lambda - P_{Th} + V_{Th} \qquad (2.1)$$

where the change in activity of ^{234}Th over time (dA_{Th}/dt) is the balance of ^{234}Th production from ^{238}U decay ($A_U\lambda$; where λ is the ^{234}Th decay constant, = 0.0288 d^{-1}), decay of ^{234}Th ($A_{Th}\lambda$), vertical sinking flux of ^{234}Th on particles (P_{Th}), and the net transport of ^{234}Th by advection and diffusion (V_{Th}). Lepore *et al.* (2007) have shown

reasonable agreement to within a factor of 2 between one-dimensional (V_{Th}=0) and three-dimensional (which considers transport of ^{234}Th by advection and diffusion) models over the Chukchi Sea shelf; therefore, a one-dimensional model is assumed for the eastern Bering Sea. Moreover, a lack of time-series measurements at all but two locations (see below) necessitated the assumption of a steady-state (SS; dA_{Th}/dt=0) simplifying Eq. (2.1):

$$P_{Th} = \lambda(A_U - A_{Th}) \quad (2.2)$$

which implies that the vertical flux of ^{234}Th is product of ^{234}Th deficit in the water column (A_U-A_{Th}) and the ^{234}Th decay constant. Trapezoidal integration of Eq. (2.2) yields the flux of ^{234}Th at a specified depth horizon:

$$P_{Th} = \lambda \int_0^z (A_U - A_{Th})dz \quad (2.3)$$

To directly compare sediment trap and ^{234}Th-derived POC fluxes, the integration depth of the water column ^{234}Th and ^{238}U profiles correspond to the sediment trap depth.

Together with sediment trap fluxes, particle ^{234}Th fluxes determined from ^{234}Th-^{238}U disequilibrium (P_{Th}) are listed in Table 2.3. Comparing these fluxes through depth horizons that correspond with sediment trap depths ($P_{Th}/^{234}Th_{trap}$) indicates that P_{Th} generally agrees with trap ^{234}Th fluxes to within a factor of 1.5-2, which is consistent with other studies employing these methods in high-latitude, marginal seas (Lalande *et al.*, 2007; Lalande *et al.*, 2008; Moran *et al.*, 2012). Specifically, along the shelf break during early (HLY0802) and late (TN249) spring, the average $P_{Th}/^{234}Th_{trap}$ was 1.02±0.50 and 0.89±0.32, though absolute fluxes more than double during late spring (Figs. 2.3, 2.5,

2.6 a, e; Table 2.3). For KN195-10 and TN250 in 2009 and 2010, P_{Th} exceeded $^{234}Th_{trap}$ resulting in an average $P_{Th}/^{234}Th_{trap}$ of 1.87±0.88 and 1.63±0.59. These high ratios indicate a potential violation of the steady-state condition; however, the agreement between these two methods is still within a factor of 2. An average $P_{Th}/^{234}Th_{trap}$ of 0.96±0.38 was determined for HLY0803 in 2008. The average ratio close to unity determined for the mid-summer cruise suggests that the shelf break of the eastern Bering Sea may have returned close to steady-state.

P_{Th} $/^{234}Th_{trap}$ for station BL was 0.99±0.52 (Table 2.3). However, ^{234}Th water column fluxes overestimate the trap fluxes early in the bloom (BL2, BL15, BL15-1), whereas the opposite occurs during the later stages of the bloom (BL21) when water column ^{234}Th fluxes are lower than trap fluxes by up to 85%.

The ^{234}Th-derived POC flux (P_{POC}) is calculated as the product of P_{Th} and $POC/^{234}Th$ ratio $(POC/^{234}Th_{trap})$ on sinking particles determined from sediment traps (Buesseler, 1991; Moran *et al.*, 2003):

$$P_{POC} = \left(\frac{POC}{^{234}Th}\right)_{trap} x\, P_{Th} \qquad (2.5)$$

In this study, the $POC/^{234}Th$ ratio ranged widely, from 1 to 282 (25.5±37.6; avg. ± 1σ) μmol dpm^{-1} throughout the upper 100 m (Table 2.3); such variability tends to be characteristic of productive shelf waters (Amiel and Cochran, 2008; Charette *et al.*, 2001; Moran *et al.*, 2003). Higher $POC/^{234}Th$ ratios were observed during the summer and in areas with greater absolute POC flux from the photic zone (Table 3). Furthermore, during summer and in higher flux environments, $POC/^{234}Th$ ratios decreased with depth (Figs. 2.3, 2.4, 2.5), which may reflect a combination of preferential remineralization of POC,

decay of particle-bound ^{234}Th, or particle aggregation and disaggregation (Buesseler *et al.*, 1995; Burd *et al.*, 2000; Lepore and Moran, 2007).

P_{POC} fluxes were determined for each sediment trap location using depth-specific P_{Th} and $POC/^{234}Th$ as a means for comparison with sediment trap derived POC fluxes. Despite a wide range of particle flux values, $POC/^{234}Th$, and P_{Th}, P_{POC} and POC_{trap} are within a factor of ~2 for most depths and stations for all seasons (Fig. 2.7; Table 2.3). The ratios of P_{POC} and POC_{trap} (P_{POC}/POC_{trap}; Table 2.3) are nearly identical to the $P_{Th}/^{234}Th_{trap}$ ratios suggesting that the same over- or underestimation characteristics, relative to trap fluxes, are evident in the P_{POC} estimates.

P_{POC} export fluxes (corresponding with the 40-100 m trap depths) were relatively low in early spring (5.7±4.3 mmol C m^{-2} d^{-1}) and increased by May and early June (17.0±8.8 mmol C m^{-2} d^{-1}) (Table 2.3). As with trap fluxes, P_{POC} peaked in early summer (48.1±17.4 for KN195-10; 57.0±68.4 mmol C m^{-2} d^{-1} for TN250) and decreased by a factor of 2 to 3 by late July (14.1±8.0 mmol C m^{-2} d^{-1} for HLY0803) (Table 2.3).

At station BL in 2009, P_{POC} averaged 40.5±10.8 mmol C m^{-2} d^{-1} between 40 and 100 m (Table 2.3). Trap fluxes generally increased throughout the bloom period, while P_{POC} fluxes increased from BL2 to BL15 and BL15-1 then decreased by BL21. The decrease in P_{POC} during the latter stages of bloom sampling period occurs because of the apparent underestimation of P_{Th} relative to trap derived ^{234}Th fluxes at BL21.

d. Non-steady state ^{234}Th fluxes

The extended occupation of station BL during HLY0902 in 2009 and three separate occupations of MN19 during TN249 and TN250 in 2010 allowed for the

comparison of ^{234}Th fluxes calculated using non-steady state (NSS; $dA_{Th}/dt \neq 0$) and SS one-dimensional scavenging models. NSS fluxes take into account changing water column inventories of ^{234}Th over time, which is likely the case during events of elevated particle flux associated with plankton blooms (Buesseler *et al.*, 1992; Savoye *et al.*, 2006):

$$P_{Th} = \lambda \left[\frac{A_U(1-e^{-\lambda \Delta t}) + A_{Th1} e^{-\lambda \Delta t} - A_{Th2}}{1-e^{-\lambda \Delta t}} \right] \quad (2.6)$$

where Δt is the time interval between sampling, A_{Th1} and A_{Th2} are the activities of ^{234}Th for the first and second occupations, respectively, A_U is the ^{238}U activity of the first occupation, and λ is the ^{234}Th decay constant. The NSS model also assumes that the same water mass is sampled repeatedly, which is reasonable in this study due to the weak sub-tidal flow fields over the southeastern Bering Sea shelf (Schumacher and Kinder, 1983).

Here, NSS and SS 234Th fluxes through the 75 m depth horizon are compared. As described above, the SS ^{234}Th fluxes calculated during the latter stages of the bloom underestimate ^{234}Th fluxes determined from sediment traps by up to 85% (Table 2.3). The incorporation of NSS conditions into the scavenging model accounts for much of the discrepancy between SS P_{Th} and $^{234}Th_{trap}$ at station BL21. Specifically, NSS $P_{Th}/^{234}Th_{trap}$ is 1.28 and 1.04 for occupations 3 to 4 and 1 to 4, respectively, when compared with the 60 m sediment trap ^{234}Th flux at BL21 (Fig. 2.8 a; Table 2.4).

Near the shelf break, NSS and SS fluxes are in better agreement during the MN19 reoccupations (Fig. 2.8b; Table 2.4). The SS flux decreases from occupation 1 to 2 with a concomitant NSS flux smaller than either of the end-member SS fluxes, which may reflect a reduction in scavenging or supply of high ^{234}Th activity deeper water between

occupations. SS fluxes during occupation 1 and the NSS flux between occupation 1 and 2 underestimate the trap fluxes by a factor of 2-3. Trap fluxes of ^{234}Th decrease by occupations 2 and 3, relative to occupation 1, and $^{234}Th_{trap}$ and SS fluxes are good agreement (Fig. 2.8b; Table 2.4). In addition, NSS fluxes calculated between occupation 2 and 3 compare well with the SS fluxes. Overall, the results of this comparison validate the use of the SS assumption at this and other shelf break stations.

2.4. Discussion

a. Seasonal succession of NPP, POC export, and the export ratio

An overarching goal of this study is to quantify the fraction of POC production that is exported from the photic zone on a seasonal basis and in relation to sea-ice proximity. This objective is central to improving our understanding of carbon cycling and the carbon budget for this shelf region. The exported fraction of primary production from the photic zone is traditionally represented as the *e*-ratio, or *ThE*, when calculated using ^{234}Th-derived POC export (Buesseler, 1998):

$$e - ratio = \frac{POC\ export}{NPP} \quad (7)$$

where NPP is photic zone integrated rate of net primary production and POC export fluxes are determined from the nearest sediment trap below the photic zone depth or calculated at the base of the photic zone using the ^{234}Th approach. Throughout the course of this study, rates of NPP were discretely estimated by ^{14}C on-deck incubations. NPP results for 2008 and 2009 are presented elsewhere (Lomas *et al.*, 2012). During the cold years of this field program, NPP varied greatly between the Northern and Southern

regions and between spring and summer. The highest rates of primary production were typically observed in spring and in areas within the MIZ due to ice-edge blooms. Briefly, ice-edge NPP was dominated by >5 μm cells associated with diatom production (Lomas *et al.*, 2012). During the summer, the northern region was still diatom dominant, however the open water stations in the south were characterized by lower rates of primary production and the emergence of haptophytes (namely *Phaeocystis* spp.) and microflagellates as major contributors to autotrophic biomass (Moran *et al.*, 2012).

It is possible that the measured rates of NPP are underestimated in Lomas *et al.* (2012) as they are based solely on the particulate fraction and do not include passive autotrophic DOC release. Reported net community production to gross primary production (NCP/GPP) ratios over the eastern Bering Sea shelf during the concurrent field program indicate values of ~0.5 during productive bloom conditions in the MIZ and ~0.3 in post-bloom, open water conditions (M. Prokopenko *et al.*, in review) where other algal classes emerge as important contributors to autotrophic biomass. Autotrophic respiration generally consumes ~40% of GPP on a daily timescale. Thus, correcting daily rates of GPP yields rates of 'NPP' that are similar to NCP during bloom conditions, which suggests a minor contribution by passive DOC release to total NPP. However, during open water conditions, passive DOC release may represent a larger fraction of total NPP in summer. While grazing activity may also be higher, it is not possible to accurately quantify the contribution of passive DOC release to total daily NPP in this study.

The temporal and spatial variability in discrete NPP and POC export observations made during this study prevent the calculation of a statistically meaningful average

export ratio characteristic of the entire eastern Bering Sea region. However, on a station-by-station basis both the *e*-ratio and *ThE* are typically lower in spring, due mainly to elevated levels of NPP (Fig. 2.9; Table 2.5). Such low export efficiency early in the growing season in high-latitude seas has been previously observed in the Arctic (Lepore *et al.*, 2007; Moran *et al.*, 2005). In this study, spring *e*-ratio and *ThE* estimates are below ~0.25 for all but two stations (NP15 in 2008 and NZ11.5 in 2010), which had relatively low rates of NPP (Table 2.5).

As noted previously, nine spring sediment trap deployments were made within ~140 km of the ice-edge (Table 2.2). With the exception of station BL, spring stations nearer the ice pack were characterized by lower fluxes of POC from 40–100 m (Fig. 2.10a). Therefore, the relatively low export ratios in the spring are the result of a combination of higher spring NPP and lower export production (Figs. 2.9, 2.10b). As with POC export fluxes, export ratios nearer the ice-edge are low relative to the open water and summer estimates (Fig. 2.10b). Furthermore, the lowest calculated export ratios are evident for station BL (Fig. 2.10b; Table 2.5) though POC export is relatively high at this location. This is because the export ratio is more dependent on the rates of NPP, which exhibit greater variability relative to export production. These low export ratios associated with high rates of NPP are consistent with an inverse relationship between NPP and export efficiency, which has been observed in the Southern Ocean (Maiti *et al.*, 2013). There is a general increase in POC fluxes for most open water stations relative to traps near the ice-edge, though there is considerable variability between those estimates (Fig. 10a). In fact, during the summer, POC export often exceeded coincident rates of NPP along the shelf break (Figs. 2.9, 2.10b; Table 2.5).

Export ratios >1 are attributed to a temporal decoupling, or offset, between primary production in spring and subsequent export as POC early in summer.

The results of this study reveal a clear seasonal succession in both sub-photic POC export and the export ratio, though with no apparent connection between these estimates and proximity to sea-ice. Specifically, considering station BL as an anomaly, both POC export and export ratios peak in early summer (KN195-10 and TN250) based on cruise average export fluxes and individual export ratios (Fig. 2.11). Changes in the composition of exported material may provide insight into seasonal variations in export production and the *e*-ratio. Photopigment analysis of exported material reveals that diatoms are the major algal class exported during the early summer (Baumann *et al.*; Lomas *et al.*, in preparation). In addition, during the late spring (TN249) and early summer, high concentrations of degradation pigments (pheophytin *a* + pheophorbide *a*) in trap collected particles indicates the prevalence of sinking senescent cells, or cells that have been repackaged as fecal pellets produced by zooplankton grazing of spring primary production (Baumann *et al.*; Lomas *et al.*, in preparation). Therefore, export during this period in the seasonal cycle may be driven by the sinking of the enhanced spring PP typically characterized by larger cells (Lomas *et al.*, 2012; Moran *et al.*, 2012) and, perhaps, by increased zooplankton grazing of the spring primary producers. Both of these mechanisms may also contribute to the apparent temporal offset between primary and export production, leading to the elevated export ratios observed in the summer.

The observed seasonal shift in associated particle export and *e*-ratio is consistent with the revised OCH, which suggests bottom up control on age-0 walleye pollock recruitment during cold years (Hunt *et al.*, 2011). Recent evidence indicates large spring

phytoplankton blooms associated with the MIZ of sea-ice retreat during cold years favor the production of large crustacean zooplankton, such as *Calanus marshallae* and euphausiids, a common prey of juvenile and adult pollock, while the abundance of smaller copepods is independent of the type of spring bloom (Hunt *et al.*, 2011; Ohashi *et al.*, 2013). Furthermore, in cold years average energy densities in first year pollock are 33% greater in fall than during warms years, most likely attributed to abundant large zooplankton as a primary diet source (Heintz *et al.*, 2013; Ohashi *et al.*, 2013; Siddon *et al.*, 2013). In the absence of large, lipid-rich zooplankton and euphausiids during warm years, juvenile and adult pollock change their diet to age-0 pollock. Therefore, large zooplankton and euphausiids exert a control on age-0 pollock success in late summer and fall by providing an alternate food source for older pollock year classes. In addition to regulating the flow of carbon to economically important pelagic organisms, large zooplankton may facilitate the elevated flux of POC from the photic zone by generating large, rapidly sinking fecal pellets in late spring and early summer during cold years.

The difference in timing between enhanced spring primary production and the emergence of large zooplankton may be an important control on the temporal offset between primary and export production in this region. Moreover, it is possible that large copepods and euphausiids may be important in the transfer of POC to the benthos and/or off the shelf. It remains uncertain how future changes in seasonal sea-ice extent and duration will affect overall NPP, secondary production, POC export, and the export ratio in the eastern Bering Sea, which may impact the structure of the ecosystem. For example, based on historical literature, Lomas *et al.* (2012) suggests that a warmer Bering Sea may favor a regime characterized by reduced annual primary production. Conversely

Brown *et al.* (2011) and Brown and Arrigo (2013) estimate that in years with early sea-ice retreat there is 40-50% more annual primary production relative to years with late sea-ice retreat, though these two studies do not comment on autotrophic community composition or POC export.

The temporal offset of primary and export production observed in this study has been reported in other high-latitude oceanic systems. As with the eastern Bering Sea, such regions are characterized by extensive spring MIZ blooms, which are responsible for a large fraction of annual new primary production. Table (2.6) provides a summary of results from this study and prior studies relating contemporaneous measurements of primary and export production in polar systems. In particular two studies in Antarctic waters have characterized the succession of the spring bloom at the ACC Polar Front (Rutgers van der Loeff *et al.*, 1997) and over the Ross Sea shelf (Sweeney *et al.*, 2000). The spring blooms in these regions are typically comprised of diatoms, although the central Ross Sea is marked by a prevalence of haptophytes (Asper and Smith, 1999; Dunbar *et al.*, 1998; Rutgers van der Loeff *et al.*, 1997). These studies report very little export production during the onset of the spring bloom. As the bloom progressed, export fluxes increased relative to primary production and were attributed to a temporal lag between the elevated rates of production and subsequent export as POC. The enhanced export during the latter stages of the bloom may be attributed to the aggregation and sinking of cells, and a delay in the development of the grazing community. The temporal succession noted in these studies is consistent with the above proposed mechanism that results in export ratios >1 in the eastern Bering Sea (Figs. 2.9, 2.11). Similarly, recent studies conducted in the Chukchi Sea (Lepore *et al.*, 2007; Moran *et al.*, 2005) report

seasonal POC export and NPP values within the range of those measured in the eastern Bering Sea (Figs. 2.9, 2.10, 2.11; Tables 2.3, 2.5). Specifically, average spring export ratios in the Chukchi are 0.15 and 0.16 for 2002 and 2004, respectively, and increase to 0.32 and 0.22 by summer for those years along the shelf-edge and shelf break (Table 2.6). Though both years exhibited an increase in the average export ratio from spring to summer, results from 2002 showed a relative increase in summer POC export relative to NPP. Conversely, in 2004 NPP decreased from spring to summer and POC export remained the same as spring (Table 2.6).

b. Significance of carbon export from the Outer shelf to the deep ocean

Because of the apparent temporal offset between net primary and export production and the progressive increase in export efficiency of this system over the seasonal cycle, an important question concerns the magnitude of POC that may be exported off-shelf. In this regard, ^{234}Th can be used as a tracer to constrain the flux of POC from the shelf to the deep ocean during spring and summer. A water column-sediment budget of ^{234}Th based on *in-situ* production, decay, sediment burial, and off-shelf export of ^{234}Th for the Outer and Middle domains of the eastern Bering Sea shelf indicates that 29% of ^{234}Th produced in the water column (equivalent to 1740±3480 dpm m^{-2} d^{-1}) may be exported from the shelf (Baumann *et al.*, 2013). This water column-sediment ^{234}Th budget is re-evaluated here using the same data from 2009 and 2010; however, in this case only for the Outer shelf. These results yield a slightly lower estimate for off-shelf export of 24% of the total water column production of ^{234}Th (2160±2700 dpm m^{-2} d^{-1}). Using this off-shelf export flux for ^{234}Th and assuming an average $POC/^{234}Th$ ratio of 11±9 µmol dpm^{-1} (Table 2.3), an upper estimate of the off-

shelf export of POC (calculated as the product of the off-shelf ^{234}Th flux multiplied by the $POC/^{234}Th$ ratio) is 24±35 mmol C m^{-2} d^{-1}(Fig. 2.12). It must be emphasized that this is an upper estimate because it is entirely possible that some fraction of this POC is lost to grazing and/or preferential remineralization over the shelf.

By comparison, a recent carbon budget for the Outer Domain developed as part of BEST-BSIERP reports that on an annual basis, ~30% (~100 g C m^{-2} y^{-1}) of total NPP (331 g C m^{-2} y^{-1}) is lost due to lateral transport from this shelf region (J. N. Cross *et al.*, in review). Using the same analytical approach described by Cross *et al.* (in review), we extrapolate the daily flux of 24±35 mmol C m^{-2} d^{-1} to an annual off-shelf POC flux of 66±96 g C m^{-2} y^{-1} (270 d year; no winter export). Despite the relatively large uncertainties in these calculations, off-shelf POC export is within a factor of ~2 of the estimated export by lateral transport from this region and ~20% of the total NPP. An additional sink for exported POC is benthic consumption and/or burial of sinking POC over the shelf. However, the measured benthic carbon consumption and estimated sediment burial for the southern Outer Domain represents a relatively small sink for annual NPP of 7±2% (23±7 g C m^{-2} y^{-1}) and 6±3% (19±11 g C m^{-2} y^{-1}), respectively (J. N. Cross *et al.*, in review). Taken together, these results imply that the estimated spring and summer off-shelf POC flux may represent a significant fraction (~20%) of the reported annual NPP for the Outer Domain, and compares reasonably well with the annual loss of POC due to lateral transport from this region of the shelf.

Daily rates of NPP measured over the Outer shelf during this study period range from 17-541 (mean: 304±225) mmol C m^{-2} d^{-1} for spring and 47-246 (mean: 111±98) mmol C m^{-2} d^{-1} for summer (Lomas *et al.*, 2012). Using these seasonal average rates of

NPP during, an off-shelf *e*-ratio of 0.07 and 0.21 is determined for the Outer Domain during spring and summer, respectively; however, it should be noted that these average NPP estimates (Lomas *et al.*, 2012) represent only a few measurements for the Outer Domain. Rho and Whitledge (2007) report monthly mean rates of daily primary production from 1978-1981 and 1997-2001 using ^{14}C and ^{13}C incubations, respectively. For the growing season of March-June, monthly mean rates of primary production range from 45±25 (June) to 139±106 (May) mmol C m^{-2} d^{-1} for the Outer shelf, which results in an off-shelf *e*-ratio of 0.17 and 0.52 for May and June, respectively. Interestingly, these values bracket the fraction of POC production that is annually exported from the Outer shelf of 49% based on an earlier assessment of the carbon budget for the eastern Bering Sea by Walsh (1988) (Fig. 2.11). Notwithstanding the estimated uncertainties in the present data set and the historical comparison, this analysis suggests that seasonal off-shelf export of POC from the eastern Bering Sea shelf may represent a significant seasonal sink in the carbon budget, as originally postulated by Walsh et al. (1981).

2.5. Conclusions

Based on a detailed seasonal field study conducted over three consecutive years in the eastern Being Sea, we conclude that temporal decoupling exists between elevated rates of spring NPP and subsequent export as POC in early summer, as evidenced by measured *e*-ratios >1 in summer. While the measured POC export fluxes and estimates of the export ratio exhibit a seasonal cycle during 2008-2010, there is no apparent connection between these observations and proximity to sea-ice. Elevated rates of export in the summer may be attributed to sinking of the senescent spring bloom and increased fecal pellet production, the latter of which is consistent with the early summer emergence

of abundant large zooplankton and euphausiids during cold years (Hunt *et al.*, 2011). In relation to the OCH, in the absence of large zooplankton, which is a common feature during warm years, juvenile and adult pollock feed on age-0 walleye pollock and thereby threaten the success of this economically important higher trophic species. Thus, an implication of this lower trophic carbon study is that during cold years, populations of large crustacean zooplankton and euphausiids not only facilitate the transfer of carbon to higher trophic animals, but may be important drivers in the enhanced summer export flux of POC, either to the benthos or off-shelf.

A further implication of the apparent temporal offset between primary and export production is the potential for a significant off-shelf transfer of POC on a seasonal basis. Based on a ^{234}Th budget for the Outer shelf, we report an upper estimate for off-shelf POC export of 24±35 mmol C m^{-2} d^{-1} in spring and summer for this region. When extrapolated to an annual flux, off-shelf POC export may represent a significant fraction (~20%) of the total annual NPP in this region (J. N. Cross *et al.*, in review). Moreover, for the spring and summer seasons off-shelf *e*-ratios of 0.07 and 0.21 using contemporaneous NPP rates and 0.17 and 0.52 based on historical measurements of NPP are determined for the Outer shelf (Lomas *et al.*, 2012; Rho and Whitledge, 2007). The high *e*-ratios suggest that the off-shelf export of spring PP in the eastern Bering Sea, and perhaps other Arctic shelf regions, may represent an important seasonal sink for CO_2 in polar shelf carbon budgets. Because Arctic waters are predicted to warm in the coming years, the timing of physical and biological processes may further alter the carbon cycle and impact the seasonal net sink for off-shelf carbon.

Acknowledgments- We thank the Chief Scientists, officers, and crew of the *USCGC Healy*, *R/V Knorr*, and *R/V Thompson* for their efforts. We thank John Karavias of Walt Whitman High School (Queens, NY) and Jason Pavlich of Red Hook High School (Red Hook, NY) for their assistance as part of the ARMADA Project. We also thank the hydrographic team from NOAA-PMEL for providing hydrographic data and assisting in sample collection, accessible through the EOL data archive supported by NSF and NOAA. This research was supported by awards ARC-0732680 and NPRB-B56 to SBM and ARC-0732359 to MWL. This is BEST-BSIERP publication number 113.

References

Alexander, V. and Niebauer, H. J. 1981. Oceanography of the Eastern Bering Sea Ice-Edge Zone in Spring. Limnol. Oceanogr. 26(6), 1111-1125.

Amiel, D. and Cochran, J. K. 2008. Terrestrial and marine POC fluxes derived from ^{234}Th distributions and δ^{13}C measurements on the Mackenzie Shelf. J. Geophys. Res. 113(C3), DOI: 10.1029/2007JC004260.

Amiel, D., Cochran, J. K., Hirschberg, D. J. 2002. ^{234}Th/^{238}U disequilibrium as an indicator of the seasonal export flux of particulate organic carbon in the North Water. Deep-Sea Res. Pt. II. 49, 5191-5209.

Arrigo, K. R., van Dijken, G., Pabi, S. 2008. Impact of a shrinking Arctic ice cover on marine primary production. Geophys. Res. Lett. 35(19), DOI: 10.1029/2008GL035028.

Asper, V. L. and Smith, W. O., Jr. 1999. Particle fluxes during austral spring and summer in the southern Ross Sea, Antarctica. J. Geophys. Res. 104(C3), 5345-5359.

Baumann, M. S., Moran, S. B., Kelly, R. P., Lomas, M. W., Shull, D. H. 2013. ^{234}Th balance and implications for seasonal particle retention in the eastern Bering Sea. Deep-Sea Res. Pt. II. 94, 7-21.

Benitez-Nelson, C., Buesseler, K. O., Karl, D. M., Andrews, J. 2001a. A time-series study of particulate matter export in the North Pacific Subtropical Gyre based on ^{234}Th:^{238}U disequilibrium. Deep-Sea Res. Pt. I. 48(12), 2595-2611.

Benitez-Nelson, C., Buesseler, K. O., Rutgers van der Loeff, M., Andrews, J., Ball, L., Crossin, G., Charette, M. 2001b. Testing a new small-volume technique for determining ^{234}Th in seawater. J. Radioanal. Nucl. Ch. 248(3), 795-799.

Brown, Z. W. and Arrigo, K. R. 2013. Sea ice impacts on spring bloom dynamics and net primary production in the Eastern Bering Sea. Journal of Geophysical Research: Oceans. 118, 1-20, DOI: 10.1029/2012JC008034.

Brown, Z. W., van Dijken, G. L., Arrigo, K. R. 2011. A reassessment of primary production and environmental change in the Bering Sea. J Geophys Res-Oceans. 116(C8), C08014 DOI:10.1029/2010JC006766.

Buesseler, K. O. 1991. Do upper-ocean sediment traps provide an accurate record of particle-flux. Nature. 353(6343), 420-423.

Buesseler, K. O. 1998. The decoupling of production and particulate export in the surface ocean. Global Biogeochem. Cy. 12, 297-310.

Buesseler, K. O., Andrews, J. A., Hartman, M. C., Belastock, R., Chai, F. 1995. Regional estimates of the export flux of particulate organic carbon derived from thorium-234 during the JGOFS EqPac program. Deep-Sea Res. Pt. II. 42(2–3), 777-804.

Buesseler, K. O., Bacon, M. P., Cochran, J. K., Livingston, H. D. 1992. Carbon and nitrogen export during the JGOFS North Atlantic Bloom experiment estimated from ^{234}Th: ^{238}U disequilibria. Deep-Sea Res. 39(7–8), 1115-1137.

Buesseler, K. O., Ball, L., Andrews, J., Benitez-Nelson, C., Belastock, R., Chai, F., Chao, Y. 1998. Upper ocean export of particulate organic carbon in the Arabian Sea derived from thorium-234. Deep-Sea Res. Pt. II. 45, 2461-2487.

Buesseler, K. O., Benitez-Nelson, C., Rutgers van der Loeff, M., Andrews, J., Ball, L., Crossin, G., Charette, M. A. 2001. An intercomparison of small-and large-volume technqiues for thorium-234 in seawater. Mar. Chem. 74, 15-28.

Burd, A. B., Moran, S. B., Jackson, G. A. 2000. A coupled adsorption–aggregation model of the POC/234Th ratio of marine particles. Deep-Sea Res. Pt. I. 47(1), 103-120.

Cai, P., Rutgers van der Loeff, M., Stimac, I., Nöthig, E. M., Lepore, K., Moran, S. B. 2010. Low export flux of particulate organic carbon in the central Arctic Ocean as revealed by 234Th:238U disequilibrium. J. Geophys. Res. 115(C10), C10037, 10.1029/2009jc005595.

Charette, M. A., Moran, S. B., Pike, S. M., Smith, J. N. 2001. Investigating the carbon cycle in the Gulf of Maine using the natural tracer thorium-234. J. Geophys. Res. 106, 11,553-11,579.

Chen, J. H., Edwards, R. L., Wasserburg, G. J. 1986. U-238, U-234 and Th-232 in seawater. Earth Planet. Sc. Lett. 80(3-4), 241-251.

Coachman, L. K. 1986. Circulation, water masses, and fluxes on the southeastern Bering Sea shelf. Cont. Shelf Res. 5(1-2), 23-108.

Coale, K. H. and Bruland, K. W. 1985. ^{234}Th:^{238}U disequilibria within the California Current. Limnol. Oceanogr. 30(1), 22-33.

Coale, K. H. and Bruland, K. W. 1987. Oceanic stratified euphotic zone as elucidated by ^{234}Th:^{238}U disequilibria. Limnol. Oceanogr. 32(1), 189-200.

Cochran, J. K., Barnes, C., Achman, D., Hirschberg, D. J. 1995. Thorium-234/Uranium-238 disequilibrium as an indicator of scavenging rates and particulate organic carbon fluxes in the Northeast Water Polynya, Greenland. J. Geophys. Res. 100, 4399-4410.

Dunbar, R. B., Leventer, A. R., Mucciarone, D. A. 1998. Water column sediment fluxes in the Ross Sea, Antarctica: Atmospheric and sea ice forcing. J. Geophys. Res. 103(C13), 30741-30759.

Grebmeier, J. M., Overland, J. E., Moore, S. E., Farley, E. V., Carmack, E. C., Cooper, L. W., Frey, K. E., Helle, J. H., McLaughlin, F. A., McNutt, S. L. 2006. A major ecosystem shift in the northern Bering Sea. Science. 311, 1461-1464.

Gustafsson, Ö. and Andersson, P. S. 2012. ^{234}Th-derived surface export fluxes of POC from the Northern Barents Sea and the Eurasian sector of the Central Arctic Ocean. Deep-Sea Res. Pt. I. 68(0), 1-11.

Heintz, R. A., Siddon, E. C., Farley Jr, E. V., Napp, J. M. 2013. Correlation between recruitment and fall condition of age-0 pollock (Theragra chalcogramma) from the eastern Bering Sea under varying climate conditions. Deep-Sea Res. Pt. II. 94, 150-156.

Hunt, G. L., Coyle, K. O., Eisner, L. B., Farley, E. V., Heintz, R. A., Mueter, F., Napp, J. M., Overland, J. E., Ressler, P. H., Salo, S. A., Stabeno, P. J. 2011. Climate impacts on eastern Bering Sea foodwebs: a synthesis of new data and an assessment of the Oscillating Control Hypothesis. ICES Journal of Marine Science: Journal du Conseil. 68(6), 1230-1243.

Hunt, G. L., Stabeno, P., Walters, G., Sinclair, E., Brodeur, R. D., Napp, J. M., Bond, N. A. 2002. Climate change and control of the southeastern Bering Sea pelagic ecosystem. Deep-Sea Res. Pt. II. 49(26), 5821-5853.

Kachel, N. B., Hunt, G. L., Salo, S. A., Schumacher, J. D., Stabeno, P. J., Whitledge, T. E. 2002. Characteristics and variability of the inner front of the southeastern Bering Sea. Deep-Sea Res. Pt. II. 49, 5889-5909.

Klein, B., LeBlanc, B., Mei, Z.-P., Beret, R., Michaud, J., Mundy, C. J., von Quillfeldt, C. H., Garneau, M.-È., Roy, S., Gratton, Y., Cochran, J. K., Bélanger, S., Larouche, P., Pakulski, J. D., Rivkin, R. B., Legendre, L. 2002. Phytoplankton biomass, production and potential export in the North Water. Deep-Sea Res. Pt. II. 49(22–23), 4983-5002.

Lalande, C., Lepore, K., Cooper, L. W., Grebmeier, J. M., Moran, S. B. 2007. Export fluxes of particulate organic carbon in the Chukchi Sea: A comparative study using ^{234}Th/^{238}U disequilibria and drifting sediment traps. Mar. Chem. 103, 185-196.

Lalande, C., Moran, S. B., Wassmann, P., Grebmeier, J. M., Cooper, L. W. 2008. ^{234}Th-derived particulate organic carbon fluxes in the northern Barents Sea with comparison to drifting sediment trap fluxes. J. Mar. Syst. 73(1–2), 103-113.

Lepore, K. and Moran, S. B. 2007. Seasonal changes in thorium scavenging and particle aggregation in the western Arctic Ocean. Deep-Sea Res Pt I. 54(6), 919-938.

Lepore, K., Moran, S. B., Grebmeier, J. M., Cooper, L. W., Lalande, C., Maslowski, W., Hill, V., Bates, N. R., Hansell, D. A., Mathis, J. T., Kelly, R. P. 2007. Seasonal

and interannual changes in particulate organic carbon export and deposition in the Chukchi Sea. J. Geophys. Res. 112(C10), C10024 DOI: 10.1029/2006JC003555.

Lomas, M. W., Moran, S. B., Casey, J. R., Bell, D. W., Tiahlo, M., Whitefield, J., Kelly, R. P., Mathis, J. T., Cokelet, E. D. 2012. Spatial and seasonal variability of primary production on the Eastern Bering Sea shelf. Deep-Sea Res. Pt. II. 65–70(0), 126-140.

Maiti, K., Charette, M. A., Buesseler, K. O., Kahru, M. 2013. An inverse relationship between production and export efficiency in the Southern Ocean. Geophys. Res. Lett. 40(8), 1557-1561.

Mathis, J. T., Cross, J. N., Bates, N. R., Moran, S. B., Lomas, M. W., Mordy, C. W., Stabeno, P. J. 2010. Seasonal distribution of dissolved inorganic carbon and net community production on the Bering Sea shelf. Biogeosciences. 7(5), 1769-1787.

McRoy, C. P., Hood, D. W., Coachman, L. K., Walsh, J. J., Goering, J. J. 1986. Processes and Resources of the Bering Sea Shelf (PROBES) - the development and accomplishments of the project. Cont. Shelf Res. 5(1-2), 5-21.

Moran, S. B., Ellis, K. M., Smith, J. N. 1997. Th-234/U-238 disequilibrium in the central Arctic Ocean: implications for particulate organic carbon export. Deep-Sea Res. Pt. II. 44(8), 1593-1606.

Moran, S. B., Kelly, R. P., Hagstrom, K., Smith, J. N., Grebmeier, J. M., Cooper, L. W., Cota, G. F., Walsh, J. J., Bates, N. R., Hansell, D. A., Maslowski, W., Nelson, R. P., Mulsow, S. 2005. Seasonal changes in POC export flux in the Chukchi Sea and implications for water column-benthic coupling in Arctic shelves. Deep-Sea Res. Pt. II. 52(24–26), 3427-3451.

Moran, S. B., Lomas, M. W., Kelly, R. P., Gradinger, R., Iken, K., Mathis, J. T. 2012. Seasonal succession of net primary productivity, particulate organic carbon export, and autotrophic community composition in the eastern Bering Sea. Deep-Sea Res. Pt. II. 65–70, 84-97.

Moran, S. B. and Smith, J. N. 2000. ^{234}Th as a tracer of scavenging and particle export in the Beaufort Sea. Cont. Shelf Res. 20(2), 153-167.

Moran, S. B., Weinstein, S. E., Edmonds, H. N., Smith, J. N., Kelly, R. P., Pilson, M. E. Q., Harrison, W. G. 2003. Does ^{234}Th/^{238}U disequilibrium provide an accurate record of the export flux of particulate organic carbon from the upper ocean? Limnol. Oceanogr. 48(3), 1018-1029.

Niebauer, H. J., Alexander, V., Henrichs, S. M. 1995. A time-series study of the spring bloom at the Bering Sea ice edge I. Physical processes, chlorophyll and nutrient chemistry. Cont. Shelf Res. 15, 1859-1877.

Ohashi, R., Yamaguchi, A., Matsuno, K., Saito, R., Yamada, N., Iijima, A., Shiga, N., Imai, I. 2013. Interannual changes in the zooplankton community structure on the southeastern Bering Sea shelf during summers of 1994–2009. Deep-Sea Res. Pt. II. 94, 44-56.

Olli, K., Wassmann, P., Reigstad, M., Ratkova, T. N., Arashkevich, E., Pasternak, A., Matrai, P. A., Knulst, J., Tranvik, L., Klais, R., Jacobsen, A. 2007. The fate of production in the central Arctic Ocean – top–down regulation by zooplankton expatriates? Prog. Oceanogr. 72(1), 84-113.

Overland, J. E. and Wang, M. Y. 2007. Future regional Arctic sea ice declines. Geophys. Res. Lett. 34(17), L17705, doi:10.1029/2007GL030308.

Pike, S. M. and Moran, S. B. 1997. Use of Poretics® 0.7 μm pore size glass fiber filters for determination of particulate organic carbon and nitrogen in seawater and freshwater. Mar. Chem. 57(3–4), 355-360.

Rho, T. and Whitledge, T. 2007. Characteristics of seasonal and spatial variations of primary production over the southeastern Bering Sea shelf. Cont. Shelf Res. 27, 2556-2569.

Rutgers van der Loeff, M., Friedrich, J., Bathmann, U. V. 1997. Carbon export during the Spring Bloom at the Antarctic Polar Front, determined with the natural tracer Th-234. Deep-Sea Res. Pt. II. 44(1-2), 457-478.

Sakshaug, E. Primary and seconday production in the Arctic Sea. in: The Organic Carbon Cycle in the Arctic Ocean. R. Stein and R. W. MacDonald (Eds.). pp Springer. Berlin. 2004.

Savoye, N., Benitez-Nelson, C., Burd, A. B., Cochran, J. K., Charette, M., Buesseler, K. O., Jackson, G. A., Roy-Barman, M., Schmidt, S., Elskens, M. 2006. ^{234}Th sorption and export models in the water column: A review. Mar. Chem. 100, 234-249.

Schumacher, J. D. and Kinder, T. H. 1983. Low-frequency current regimes over the Bering Sea shelf. J. Phys. Oceanogr. 13, 607-623.

Siddon, E. C., Heintz, R. A., Mueter, F. J. 2013. Conceptual model of energy allocation in walleye pollock (Theragra chalcogramma) from age-0 to age-1 in the southeastern Bering Sea. Deep-Sea Res. Pt. II. 94, 140-149.

Speicher, E. A., Moran, S. B., Burd, A. B., Delfanti, R., Kaberi, H., Kelly, R. P., Papucci, C., Smith, J. N., Stavrakakis, S., Torricelli, L., Zervakis, V. 2006. Particulate organic carbon export fluxes and size-fractionated POC/^{234}Th ratios in the Ligurian, Tyrrhenian and Aegean Seas. Deep-Sea Res. Pt. I. 53(11), 1810-1830.

Stabeno, P. J., Kachel, N. B., Moore, S. E., Napp, J. M., Sigler, M. F., Yamaguchi, A., Zerbini, A. N. 2012. Comparison of warm and cold years on the southeastern

Bering Sea shelf and some implications for the ecosystem. Deep-Sea Res. Pt. II. 65–70(0), 31-45.

Sweeney, C., Smith, W. O., Hales, B., Bidigare, R. R., Carlson, C. A., Codispoti, L. A., Gordon, L. I., Hansell, D. A., Millero, F. J., Park, M. O. K., Takahashi, T. 2000. Nutrient and carbon removal ratios and fluxes in the Ross Sea, Antarctica. Deep-Sea Res. Pt. II. 47(15–16), 3395-3421.

Wallace, D. W. R., Minnett, P. J., Hopkins, T. S. 1995. Nutrients, oxygen, and inferred new production in the Northeast Water Polynya, 1992. J. Geophys. Res. 100(C3), 4323-4340.

Walsh, J. J. 1988. On the nature of continental shelves, Academic Press

Walsh, J. J., Rowe, G. T., Iverson, R. L., McRoy, C. P. 1981. Biological export of shelf carbon is a sink of the global CO2 cycle. Nature. 291(5812), 196-201.

Wassmann, P., Bauerfeind, E., Fortier, M., Fukuchi, M., Hargrave, B., Moran, S. B., Noji, T., Nöthig, E.-M., Olli, K., Peinert, R., Sasaki, H., Shevchenko, V. Particulate organic carbon flux to the Arctic Ocean sea floor. in: The Organic Carbon Cycle in the Arctic Ocean. R. Stein and R. W. MacDonald (Eds.). pp Springer. Berlin. 2004.

Table 2.1. Spring and summer cruises during the 2008-2010 NSF-NPRB BEST-BSIERP field program.

Season	Cruise	Vessel	Dates
Spring 2008	HLY 0802	*USCGC Healy*	March 29 - May 6, 2008
Summer 2008	HLY 0803	*USCGC Healy*	July 3 - July 31, 2008
Spring 2009	HLY 0902	*USCGC Healy*	March 31 - May 12, 2009
Summer 2009	KN195-10	*R/V Knorr*	June 14 - July 13, 2009
Spring 2010	TN249	*R/V Thompson*	May 9 - June 14, 2010
Summer 2010	TN 250	*R/V Thompson*	June 16 - July 13, 2010

Table 2.2. Sediment trap deployments from 2008-2010.

Trap Station	Deploy Date	Deployment		Collection		Duration	Dist. to Ice Edge
		Latitude (°N)	Longitude (°W)	Latitude (°N)	Longitude (°W)	(d)	(km)
Spring 2008							
NP15	3/31/2008	56.23	171.07	56.43	171.40	1.15	51.8
P14-4	4/22/2008	57.76	174.91	57.68	174.71	0.96	137.4
ZZ15	4/25/2008	58.59	176.62	58.59	176.60	1.10	64.5
Summer 2008							
PIT1	7/6/2008	55.29	167.94	55.22	168.04	1.00	
PIT2	7/15/2008	56.24	171.11	56.28	171.24	1.01	
PIT3	7/21/2008	58.42	174.47	58.47	174.57	1.04	
Spring 2009							
ST1	4/23/2009	56.26	171.08	56.33	171.03	0.77	88.1
BL2	4/26/2009	59.51	175.10	59.55	175.15	1.03	52.1
BL15	4/29/2009	59.55	175.16	59.56	175.28	0.44	58.4
BL15-1	4/30/2009	59.57	175.28	59.61	175.32	0.61	52.9
BL21	5/1/2009	59.44	174.22	59.44	174.22	0.23	24.7
Summer 2009							
CN17	6/19/2009	55.43	168.06	55.47	168.19	1.06	
NP15	6/23/3009	56.05	171.30	55.88	171.22	0.95	
P14-7	6/25/2009	58.23	174.57	58.27	174.56	0.99	
MN19	7/3/2009	59.90	178.79	59.99	178.80	0.95	
Spring 2010							
MN19	5/19/2010	59.90	178.91	59.98	178.90	0.93	
NZ11.5	5/21/2010	58.21	174.25	58.22	174.35	0.91	38.5
CN17	5/28/2010	55.44	168.06	55.43	168.12	0.90	
MN19-2	6/6/2010	59.89	178.90	60.61	178.67	0.91	
NP14	6/12/2010	56.26	171.11	56.30	171.15	0.70	
Summer 2010							
CN17	6/21/2010	55.43	168.06	55.54	165.40	1.02	
NP14	6/26/2010	56.26	171.12	56.34	171.47	0.85	
P14N-7	6/28/2010	58.26	174.56	58.37	174.81	0.90	
MN19	7/4/2010	59.90	178.86	59.98	178.88	0.76	

Table 2.3. ^{234}Th fluxes ($^{234}Th_{trap}$ Flux), POC fluxes (POC_{trap} Flux) and $POC/^{234}Th$ ratios ($POC/^{234}Th_{trap}$) determined using sediment traps together with ^{234}Th fluxes from ^{234}Th-^{238}U disequilibrium ($^{234}Th_{sv}$ Flux), ^{234}Th-derived POC fluxes (P_{POC}) and P_{POC}/POC_{trap}.

Trap Station	Depth	$^{234}Th_{trap}$ Flux	POC_{trap} Flux	$POC/^{234}Th_{trap}$	P_{Th}	P_{POC}	P_{POC}/POC_{trap}
	m	(dpm m^{-2} d^{-1})	(mmol m^{-2} d^{-1})	(mmol dpm^{-1})	(dpm m^{-2} d^{-1})	(mmol m^{-2} d^{-1})	
Spring 2008							
NP-15	25	1011 ± 84	1.92 ± 0.13	0.002	404 ± 77	0.76 ± 0.16	0.40 ± 0.09
	40	801 ± 69	1.67 ± 0.12	0.002	700 ± 122	1.48 ± 0.30	0.89 ± 0.19
	50	1071 ± 88	4.94 ± 0.35	0.005	915 ± 151	4.19 ± 0.79	0.85 ± 0.17
	60	1120 ± 90	2.02 ± 0.14	0.002	1069 ± 184	1.91 ± 0.38	0.95 ± 0.20
	100	1028 ± 84	4.05 ± 0.28	0.004	1440 ± 333	5.60 ± 1.40	1.38 ± 0.36
P14-4	25	378 ± 38	7.58 ± 0.53	0.020	148 ± 99	2.97 ± 2.03	0.39 ± 0.27
	40	483 ± 48	3.03 ± 0.21	0.006	229 ± 162	1.42 ± 1.02	0.47 ± 0.34
	50	535 ± 52	5.20 ± 0.36	0.010	277 ± 205	2.70 ± 2.01	0.52 ± 0.39
	60	498 ± 48	3.39 ± 0.24	0.007	320 ± 247	2.19 ± 1.71	0.65 ± 0.51
	100	457 ± 45	4.22 ± 0.30	0.009	441 ± 421	4.05 ± 3.89	0.96 ± 0.92
ZZ15	25	681 ± 85	8.91 ± 0.62	0.017	787 ± 55	13.75 ± 2.61	1.15 ± 0.23
	40	736 ± 70	7.67 ± 0.54	0.010	1163 ± 97	12.17 ± 1.66	1.59 ± 0.24
	50	698 ± 66	7.37 ± 0.52	0.011	1258 ± 134	13.33 ± 2.03	1.81 ± 0.30
	60	864 ± 80	6.21 ± 0.43	0.007	1297 ± 175	9.31 ± 1.59	1.50 ± 0.28
	100	819 ± 77	5.36 ± 0.37	0.007	1466 ± 341	9.67 ± 2.48	1.81 ± 0.48
Summer 2008							
PIT1	25	1354 ± 127	36.81 ± 2.58	0.027	801 ± 59	21.76 ± 2.81	0.64 ± 0.09
	40	1073 ± 104	22.30 ± 1.56	0.021	1184 ± 104	24.61 ± 3.45	1.19 ± 0.19
	50	1066 ± 102	16.30 ± 1.14	0.015	1301 ± 141	19.89 ± 3.04	1.32 ± 0.22
	60	887 ± 84	14.43 ± 1.01	0.016	1409 ± 181	22.87 ± 3.82	1.71 ± 0.31
	100	1075 ± 103	19.14 ± 1.34	0.018	1677 ± 351	29.80 ± 7.04	1.68 ± 0.41
PIT2	25	1461 ± 131	12.70 ± 0.89	0.009	862 ± 54	7.49 ± 0.89	0.59 ± 0.08
	40	1445 ± 129	9.00 ± 0.63	0.006	1064 ± 109	6.62 ± 0.97	0.74 ± 0.12
	50	1369 ± 123	8.09 ± 0.57	0.006	1197 ± 148	7.08 ± 1.14	0.88 ± 0.15
	60	1363 ± 121	9.57 ± 0.67	0.007	1320 ± 186	9.30 ± 1.62	0.98 ± 0.18
	100	1233 ± 114	8.17 ± 0.57	0.007	1717 ± 344	11.42 ± 2.58	1.41 ± 0.33
PIT3	25	1478 ± 130	17.43 ± 1.22	0.012	913 ± 47	10.74 ± 1.13	0.62 ± 0.08
	40	2605 ± 208	14.52 ± 1.02	0.006	1559 ± 91	8.68 ± 0.96	0.60 ± 0.08
	50	2566 ± 209	14.76 ± 1.03	0.006	1565 ± 126	9.02 ± 1.12	0.61 ± 0.09
	60	2703 ± 217	13.44 ± 0.94	0.005	1696 ± 165	8.41 ± 1.15	0.63 ± 0.10
	100	1753 ± 152	7.98 ± 0.56	0.005	2391 ± 315	10.91 ± 1.80	1.38 ± 0.25

Spring 2009							
ST1	25	1043 ± 106	9.64 ± 0.68	0.009	352 ± 146	3.26 ± 1.40	0.34 ± 0.15
	40	1699 ± 162	10.91 ± 0.76	0.006	601 ± 142	3.86 ± 1.00	0.35 ± 0.09
	50	1710 ± 160	10.52 ± 0.74	0.006	781 ± 177	4.81 ± 1.20	0.46 ± 0.12
	60	1837 ± 172	10.99 ± 0.77	0.006	927 ± 213	5.55 ± 1.41	0.51 ± 0.13
	100	2309 ± 215	11.00 ± 0.77	0.005	1453 ± 362	6.93 ± 1.88	0.63 ± 0.18
BL2	25	2136 ± 186	46.56 ± 3.26	0.022	653 ± 69	14.24 ± 2.08	0.31 ± 0.05
	40	947 ± 94	18.57 ± 1.30	0.020	1109 ± 108	21.76 ± 3.22	1.17 ± 0.19
	50	941 ± 92	17.07 ± 1.20	0.018	1365 ± 138	24.76 ± 3.70	1.45 ± 0.24
	60	1091 ± 105	19.41 ± 1.36	0.018	1578 ± 171	28.08 ± 4.31	1.45 ± 0.24
	100	1948 ± 149	28.55 ± 2.00	0.015	2229 ± 317	32.68 ± 5.52	1.14 ± 0.21
BL15	25	1843 ± 185	66.30 ± 4.64	0.036	809 ± 60	29.08 ± 3.92	0.44 ± 0.07
	40	923 ± 104	42.53 ± 2.98	0.046	1200 ± 104	55.32 ± 8.33	1.30 ± 0.22
	50	999 ± 111	36.46 ± 2.55	0.036	1388 ± 139	50.64 ± 8.00	1.39 ± 0.24
	60	1207 ± 131	26.93 ± 1.89	0.022	1551 ± 176	34.61 ± 5.71	1.28 ± 0.23
	100	1802 ± 171	40.89 ± 2.86	0.023	2335 ± 316	52.97 ± 9.15	1.30 ± 0.24
BL15-1	25	1502 ± 152	60.71 ± 4.25	0.040	809 ± 60	32.68 ± 4.42	0.54 ± 0.08
	40	993 ± 106	34.16 ± 2.39	0.034	1200 ± 104	41.31 ± 6.05	1.21 ± 0.20
	50	752 ± 83	28.74 ± 2.01	0.038	1388 ± 139	53.00 ± 8.34	1.84 ± 0.32
	60	844 ± 92	22.14 ± 1.55	0.026	1551 ± 176	40.69 ± 6.72	1.84 ± 0.33
	100	2138 ± 184	44.22 ± 3.10	0.021	2335 ± 316	48.28 ± 8.12	1.09 ± 0.20
BL21	25	5085 ± 492	272.91 ± 19.10	0.054	816 ± 59	43.81 ± 5.72	0.16 ± 0.02
	40	3830 ± 374	86.18 ± 6.03	0.023	1321 ± 96	29.73 ± 3.91	0.34 ± 0.05
	50	2939 ± 311	77.64 ± 5.44	0.026	1616 ± 125	42.69 ± 5.98	0.55 ± 0.09
	60	3736 ± 372	81.52 ± 5.71	0.022	1884 ± 155	41.11 ± 5.70	0.50 ± 0.08
	100	6905 ± 562	108.15 ± 7.57	0.016	3201 ± 257	50.14 ± 6.26	0.46 ± 0.07
Summer 2009							
CN17	25	414 ± 61	42.10 ± 2.95	0.102	642 ± 74	65.27 ± 12.99	1.55 ± 0.33
	40	677 ± 93	40.27 ± 2.82	0.059	1163 ± 111	69.20 ± 12.52	1.72 ± 0.33
	50	955 ± 125	40.64 ± 2.84	0.043	1370 ± 147	58.32 ± 10.67	1.43 ± 0.28
	60	1091 ± 147	45.31 ± 3.17	0.042	1535 ± 184	63.74 ± 12.31	1.41 ± 0.29
	100	1436 ± 178	38.54 ± 2.70	0.027	2014 ± 341	54.04 ± 11.96	1.40 ± 0.33
NP15	25	596 ± 71	25.31 ± 1.77	0.042	899 ± 56	38.15 ± 5.50	1.51 ± 0.24
	40	1072 ± 132	42.34 ± 2.96	0.039	1324 ± 101	52.31 ± 8.00	1.24 ± 0.21
	50	1186 ± 142	48.12 ± 3.37	0.041	1549 ± 134	62.82 ± 9.78	1.31 ± 0.22
	60	1208 ± 141	39.96 ± 2.80	0.033	1743 ± 170	57.67 ± 9.25	1.44 ± 0.25
	100	1613 ± 193	29.60 ± 2.07	0.018	2171 ± 333	39.86 ± 8.00	1.35 ± 0.29
P14-7	25	610 ± 67	20.58 ± 1.44	0.034	1109 ± 41	37.41 ± 4.72	1.82 ± 0.26
	40	998 ± 104	25.20 ± 1.76	0.025	1660 ± 77	41.93 ± 5.24	1.66 ± 0.24
	50	1111 ± 113	21.89 ± 1.53	0.020	1877 ± 113	36.98 ± 4.75	1.69 ± 0.25
	60	1330 ± 135	16.06 ± 1.12	0.012	2036 ± 152	24.58 ± 3.33	1.53 ± 0.23
	100	2122 ± 201	23.11 ± 1.62	0.011	2646 ± 309	28.82 ± 4.57	1.25 ± 0.22
MN19	25	117 ± 18	26.57 ± 1.86	0.227	532 ± 98	120.91 ± 29.55	4.55 ± 1.16
	40	294 ± 37	32.83 ± 2.30	0.112	740 ± 148	82.63 ± 19.94	2.52 ± 0.63
	50	319 ± 38	12.51 ± 0.88	0.039	848 ± 189	33.29 ± 8.60	2.66 ± 0.71
	60	291 ± 36	11.70 ± 0.82	0.040	1098 ± 220	44.13 ± 10.61	3.77 ± 0.94
	100	1048 ± 106	12.48 ± 0.87	0.012	1656 ± 371	19.73 ± 4.94	1.58 ± 0.41

Spring 2010							
MN19	25	2446 ± 207	73.71 ± 5.16	0.030	1132 ± 35	34.13 ± 3.89	0.46 ± 0.06
	40	3153 ± 254	37.84 ± 2.65	0.012	1731 ± 65	20.77 ± 2.35	0.55 ± 0.07
	50	3270 ± 262	43.50 ± 3.04	0.013	1941 ± 99	25.83 ± 3.04	0.59 ± 0.08
	60	3319 ± 263	30.55 ± 2.14	0.009	2082 ± 136	19.16 ± 2.38	0.63 ± 0.09
	100	3790 ± 295	48.07 ± 2.40	0.013	2551 ± 291	32.35 ± 4.75	0.67 ± 0.10
NZ11.5	25	1308 ± 125	19.35 ± 1.35	0.015	988 ± 46	14.61 ± 1.86	0.76 ± 0.11
	40	1628 ± 149	23.82 ± 1.19	0.015	1479 ± 84	21.64 ± 2.57	0.91 ± 0.12
	50	1479 ± 135	20.29 ± 1.42	0.014	1737 ± 114	24.83 ± 3.16	1.22 ± 0.18
	60	2065 ± 185	14.39 ± 1.01	0.007	1980 ± 145	13.80 ± 1.87	0.96 ± 0.15
	100	2946 ± 250	11.55 ± 0.81	0.004	2688 ± 284	10.54 ± 1.61	0.91 ± 0.15
CN17	25	2699 ± 227	39.47 ± 2.76	0.015	1004 ± 46	14.68 ± 1.74	0.37 ± 0.05
	40	2631 ± 221	29.63 ± 2.07	0.011	1528 ± 83	17.21 ± 2.10	0.58 ± 0.08
	50	2101 ± 183	15.27 ± 1.07	0.007	1991 ± 283	14.47 ± 2.62	0.95 ± 0.18
	60	1933 ± 171	7.88 ± 0.55	0.004	2007 ± 144	8.18 ± 2.62	1.04 ± 0.34
	100	1937 ± 177	2.71 ± 0.19	0.001	2476 ± 302	3.46 ± 1.09	1.28 ± 0.41
MN19-2	25	971 ± 96	15.48 ± 1.08	0.016	832 ± 64	13.27 ± 0.58	0.86 ± 0.07
	40	1103 ± 110	33.49 ± 2.34	0.030	1083 ± 125	32.91 ± 5.52	0.98 ± 0.18
	50	1122 ± 109	15.75 ± 1.10	0.014	1332 ± 158	18.70 ± 3.15	1.19 ± 0.22
	60	998 ± 97	14.96 ± 1.05	0.015	1553 ± 194	23.29 ± 4.02	1.56 ± 0.29
	100	1357 ± 129	13.58 ± 0.95	0.010	2111 ± 344	21.12 ± 4.26	1.56 ± 0.33
NP14	25	2642 ± 231	24.62 ± 1.72	0.009	1135 ± 37	10.58 ± 1.23	0.43 ± 0.06
	40	2012 ± 184	15.71 ± 1.10	0.008	1590 ± 80	12.41 ± 1.56	0.79 ± 0.11
	50	2078 ± 189	2.08 ± 0.10	0.001	1863 ± 111	1.86 ± 0.22	0.90 ± 0.12
	60	2030 ± 178	12.50 ± 0.87	0.006	2107 ± 142	12.97 ± 1.70	1.04 ± 0.15
	100	2478 ± 223	4.71 ± 0.24	0.002	2695 ± 291	5.12 ± 0.76	1.09 ± 0.17
Summer 2010							
CN17	25	403 ± 50	113.45 ± 7.94	0.282	1023 ± 45	288.21 ± 43.03	2.54 ± 0.42
	40	688 ± 75	114.97 ± 8.05	0.167	1679 ± 73	280.66 ± 38.29	2.44 ± 0.37
	50	1020 ± 99	81.04 ± 5.67	0.079	2093 ± 93	166.33 ± 21.25	2.05 ± 0.30
	60	-	-	-	-	-	-
	100	1974 ± 172	69.12 ± 4.84	0.035	3737 ± 219	130.86 ± 16.52	1.89 ± 0.27
NP14	25	809 ± 92	30.64 ± 2.15	0.038	762 ± 63	28.87 ± 4.54	0.94 ± 0.16
	40	874 ± 95	26.02 ± 1.82	0.030	1103 ± 113	32.84 ± 5.42	1.26 ± 0.23
	50	1055 ± 110	30.50 ± 2.14	0.029	1294 ± 149	37.42 ± 6.37	1.23 ± 0.23
	60	1311 ± 128	27.33 ± 1.91	0.021	1456 ± 185	30.34 ± 5.31	1.11 ± 0.21
	100	3730 ± 286	39.58 ± 2.77	0.011	2122 ± 327	22.52 ± 4.19	0.57 ± 0.11
P14N-7	25	498 ± 62	21.72 ± 1.52	0.044	909 ± 53	39.61 ± 6.10	1.82 ± 0.31
	40	807 ± 89	15.03 ± 1.05	0.019	1392 ± 92	25.93 ± 3.79	1.73 ± 0.28
	50	833 ± 89	15.48 ± 1.08	0.019	1717 ± 118	31.9 ± 4.62	2.06 ± 0.33
	60	1019 ± 101	17.08 ± 1.20	0.017	1996 ± 148	33.46 ± 4.75	1.96 ± 0.31
	100	971 ± 101	19.11 ± 1.34	0.020	2652 ± 296	52.18 ± 8.75	2.73 ± 0.50
MN19	25	692 ± 82	24.89 ± 1.74	0.036	766 ± 65	27.55 ± 4.45	1.11 ± 0.19
	40	880 ± 98	15.60 ± 1.09	0.018	1155 ± 111	20.47 ± 3.34	1.31 ± 0.23
	50	1111 ± 116	17.26 ± 1.21	0.016	1405 ± 142	21.83 ± 3.53	1.26 ± 0.22
	60	1352 ± 134	17.78 ± 1.24	0.013	1595 ± 178	20.98 ± 3.46	1.18 ± 0.21
	100	1213 ± 125	11.83 ± 0.83	0.010	2261 ± 327	22.06 ± 4.21	1.86 ± 0.38

Table 2.4. Comparison of steady state (SS) and non-steady state (NSS) ^{234}Th fluxes (dpm m^{-2} d^{-1}) at BL (a in Fig. 8) and MN19 (b) for the upper 75 m.

Station	Δt (d)	SS ^{234}Th Flux (dpm m^{-2} d^{-1})	NSS ^{234}Th Flux (dpm m^{-2} d^{-1})
Bloom Station			
26/2009 20:52		1834 ± 224	
t from 1 to	0.67		-808 *
27/2009 12:59		1783 ± 232	
t from 2 to	2.00		1897 *
29/2009 13:01		1790 ± 231	
t from 3 to	7.07		4772 ± 1638
/6/2009 14:44		2339 ± 196	
l Δt from 1	9.74		3899 ± 1033
	Average	1937 ± 269	
MN19 Revisits			
/19/2010 4:42		2273 ± 194	
t from 1 to	18.94		965 ± 598
5/7/2010 3:14		1644 ± 259	
t from 2 to	27.16		1990 ± 592
7/4/2010 7:07		1833 ± 233	
	Average	1917 ± 323	

*Short Δt results in error larger than flux

Table 2.5. Export ratios determined from ^{14}C-derived NPP (mmol C m^{-2} d^{-1}) and ^{234}Th-derived (*ThE*) and sediment trap (*e*-ratio) POC fluxes. Rates of NPP are from Lomas *et al.* (2012).

NPP Station	Photic Zone (m)	NPP (mmol C m^{-2} d^{-1})	*ThE* *	*e* -ratio†
Spring 2008				
1-NP15	100	16.49	0.34	0.24
93-ZZ14	26	96.77	0.22	0.19
Summer 2008				
21-PIT1	38	67.01	0.36	0.33
Spring 2009				
60-ST	40	21.51	0.18	0.51
69-BL1	46	459.40	0.05	0.04
73-BL4	38	455.96	0.05	0.04
85-BL15	38	537.73	0.10	0.08
115-BL21	33	504.53	0.05	0.17
Summer 2009				
113-MN19	23	231.58	0.46	0.11
Spring 2010				
49-MN19	75	2284.33	0.01	0.01
55-NZ11.5	60	13.30	1.04	1.08
84-CN17	32	226.12	0.08	0.17
163-MN19	52	121.31	0.20	0.13
Summer 2010				
53-TD2	33	15.77	1.80	1.65
63-P14N-7	38	11.25	1.65	1.34
100-TD4	46	14.69	1.39	1.18

* ^{234}Th profiles integrated to the base of the photic zone and multiplied by POC/^{234}Th ratio from the nearest depth sediment trap.

†Sediment trap POC flux from traps closest to the base of the photic zone.

Table 2.6. Summary of POC export and export ratios in high latitude systems.

Location	POC Export Flux	Primary Production	Export Ratio, %	Comments and References
Antarctic Polar Front; Spring Bloom	0.43-0.86 mol m^{-2} *	3.12 mol m^{-2} •	12-24	Total uptake or export over 34 d
SO JGOFS; transects 2,5,11	Upper limit: 1.43 mol m^{-2} *		avg. 46	growth period
October-December 1992				Rutgers van der Loeff *et al.* (1997)
Northeast Water Polynya, Greenland	1992: 12-45 (avg. 25±14) mmol m^{-2} d^{-1} *	40-60 mmol m^{-2} d^{-1} ∀	42-63	Export 0-50 m
July-August, 1992, 1993	1993: 17-45 (avg. 35±10) mmol m^{-2} d^{-1} *			Cochran *et al.* (1995)
				Wallace *et al.* (1995)
Ross Sea; Bloom Conditions				
SO JGOFS/AESOPS; transect along 76.5°S	3.8±0.9 mol m^{-2} †	3.9±1.0 mol m^{-2} #	55±22	Export over growing season at 200 m
Four cruises; 1996, 1997	0.29 mol m^{-2} ‡			Export Ratio: mean±1σ
				Sweeney *et al.* (2000)
North Water Polynya, Western Greenland	July: 27.4±13.4 mmol m^{-2} d^{-1} *	32.6-86.1 (avg. 57.3) mmol m^{-2} d^{-1} •	0.1-0.9	Export 0-100 m
May and July (1998), August (1999)	August: 8.7±1.7 mmol m^{-2} d^{-1} *	(From annual PP rates)		Amiel *et al.* (2002)
				Klein *et al.* (2002)
Barents Sea to North Pole; Summer	N. Barents: 6-18 mmol m^{-2} d^{-1} *	4.2-12.5 (avg. 7.75) mmol m^{-2} d^{-1} •	16-75	Export 0-40 m
Arctic Ocean, 2001 (AO-01)	Interior basins: 2-7 mmol m^{-2} d^{-1} *		avg. 44	Gustafsson *et al.* (2012)
				Olli *et al.* (2007)
Chukchi Sea Shelf Break; Spring & Summer	Spring: 1.8±2.2 mmol m^{-2} d^{-1} *	12.0±6.9 mmol m^{-2} d^{-1} •	15	Export from photic zone
2002 SBI; 3-4 cross shelf transects	Summer: 10.5±9.3 mmol m^{-2} d^{-1} *	32.9±21.9 mmol m^{-2} d^{-1} •	32	Moran *et al.* (2005)
Chukchi Sea Shelf Break; Spring & Summer	Spring: 19.7±24.8 mmol m^{-2} d^{-1} *	124.4±88.1 mmol m^{-2} d^{-1} •	16	Export from photic zone
2004 SBI II; 4 cross shelf transects	Summer: 20.0±14.5 mmol m^{-2} d^{-1} *	89.9±146.9 mmol m^{-2} d^{-1} •	22	Lepore *et al.* (2007)
E. Bering Sea Shelf Break; Spring Summer	Spring: 3.9-86.2 mmol m^{-2} d^{-1} *‡	13.5-2284.3 mmol m^{-2} d^{-1} •	0.01-1.08	Export from photic zone
2008-2010 BEST-BSIERP	Summer: 15.0-26.6 mmol m^{-2} d^{-1} *‡	11.3-231.6 mmol m^{-2} d^{-1} •	0.11-1.80	Present study

*^{234}Th-derived POC export

†Relationship between NCP and surplus TOC

‡Sediment trap collection

•NPP by ^{14}C uptake

∀Nutrient depletion and O_2 increase

NCP by DIC

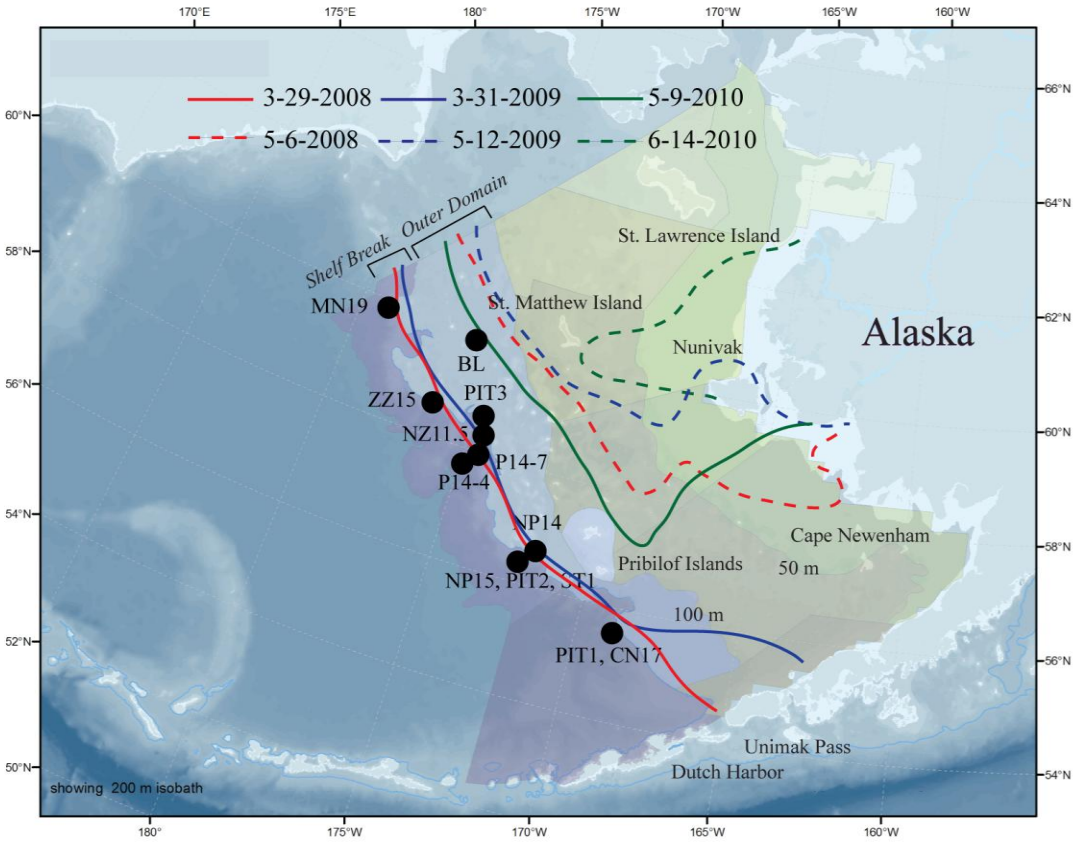

Figure 2.1. Map of the eastern Bering Sea study area. The black circles indicate the stations where drifting sediment traps were deployed. Several locations are stations in which multiple deployments occurred throughout the field program. Solid and dashed lines represent the maximum and minimum ice-edge extent, respectively, during spring sampling periods. Colors: red (2008), blue (2009) and green (2010). Specific dates are listed on the figure.

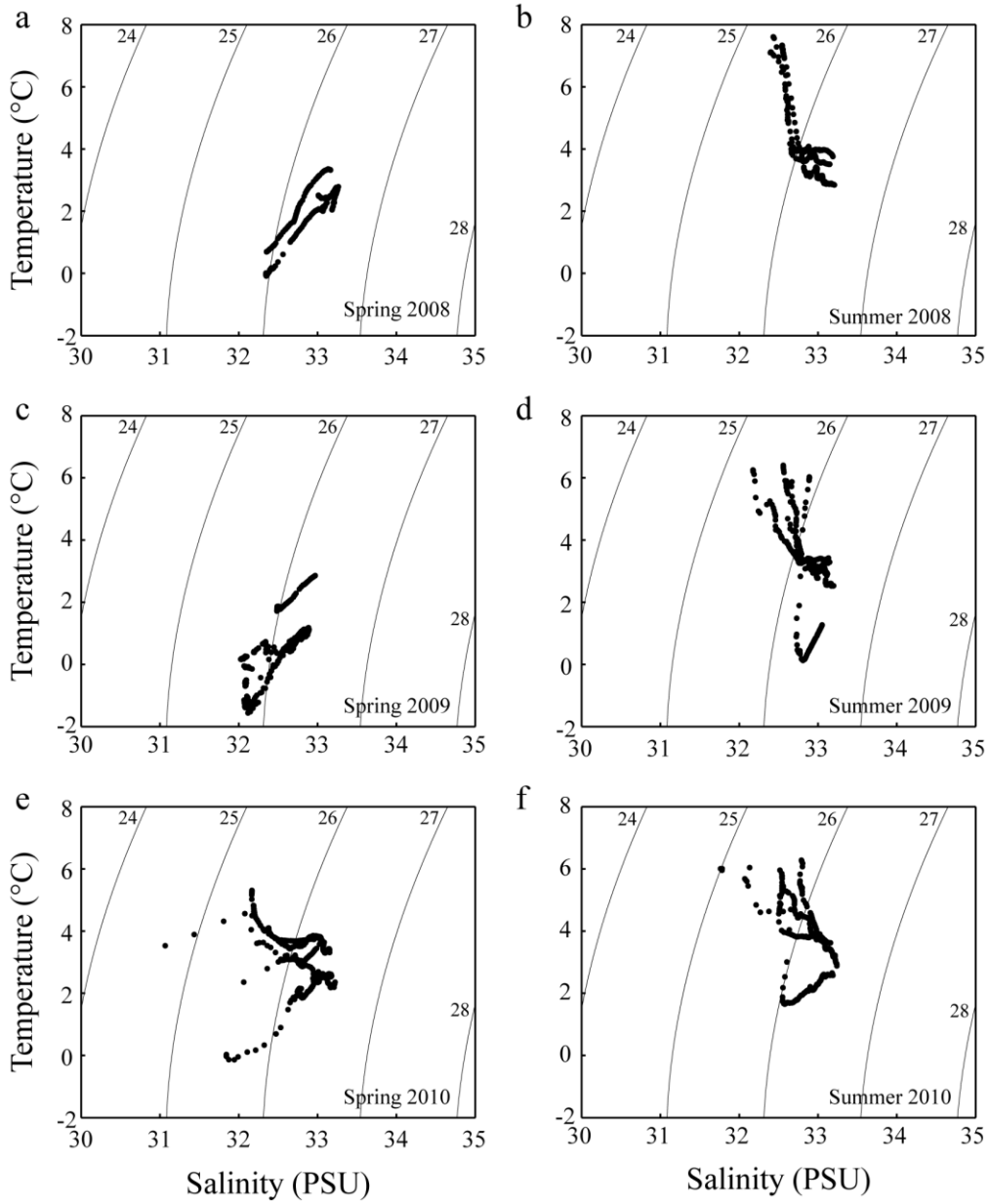

Figure 2.2. Temperature (°C) – salinity (psu) plots at sediment traps stations. Points are 1 m averaged values from the CTD for the upper 150 m (or surface to bottom if shallower than 150 m) of the water column. Panels: spring 2008 (a), summer 2008 (b), spring 2009 (c), summer 2009 (d), spring 20010 (e) and summer 2010 (f). Data from UCAR EOL archive: http://catalog.eol.ucar.edu/best/.

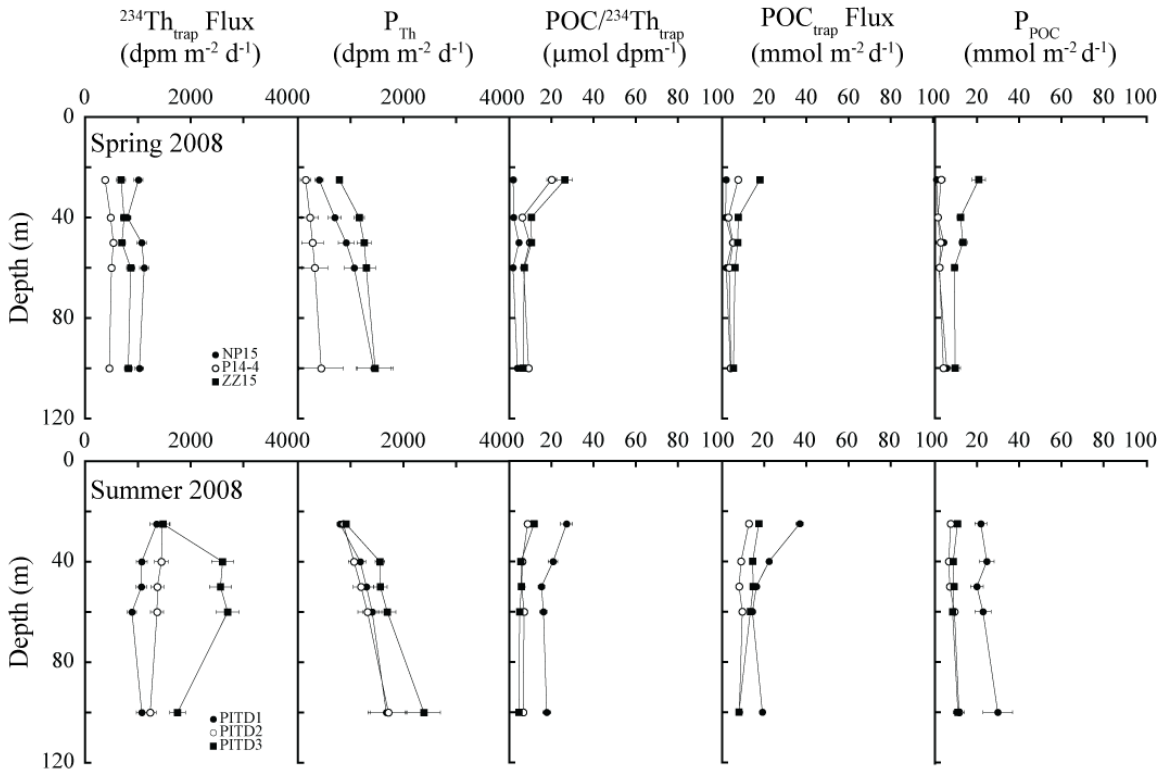

Figure 2.3. Depth profiles of sediment trap ^{234}Th fluxes ($^{234}Th_{trap}$ *Flux*; dpm m^{-2} d^{-1}), POC fluxes (POC_{trap} *Flux*; mmol C m^{-2} d^{-1}), *POC*/^{234}*Th* ratios (*POC*/$^{234}Th_{trap}$; µmol dpm^{-1}), ^{234}Th fluxes calculated from ^{234}Th-^{238}U disequilibrium (P_{Th}), and ^{234}Th-derived POC export (P_{POC}) for spring (top) and summer (bottom) of 2008.

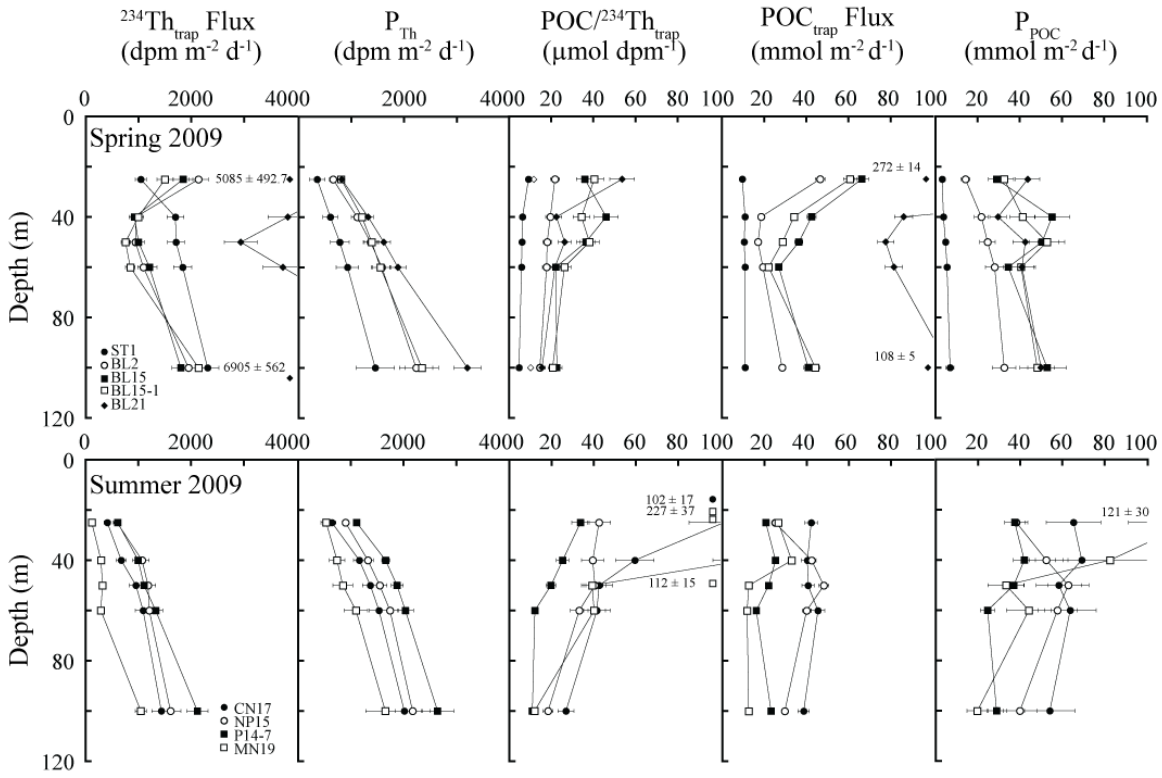

Figure 2.4. Depth profiles of sediment trap ^{234}Th flux (*$^{234}Th_{trap}$ Flux*; dpm m^{-2} d^{-1}), POC flux (*POC_{trap} Flux*; mmol C m^{-2} d^{-1}), *POC/^{234}Th* ratios (*POC/$^{234}Th_{trap}$*; µmol dpm^{-1}), ^{234}Th fluxes calculated from ^{234}Th-^{238}U disequilibrium (P_{Th}), and ^{234}Th-derived POC export (P_{POC}) for spring (top) and summer (bottom) of 2009.

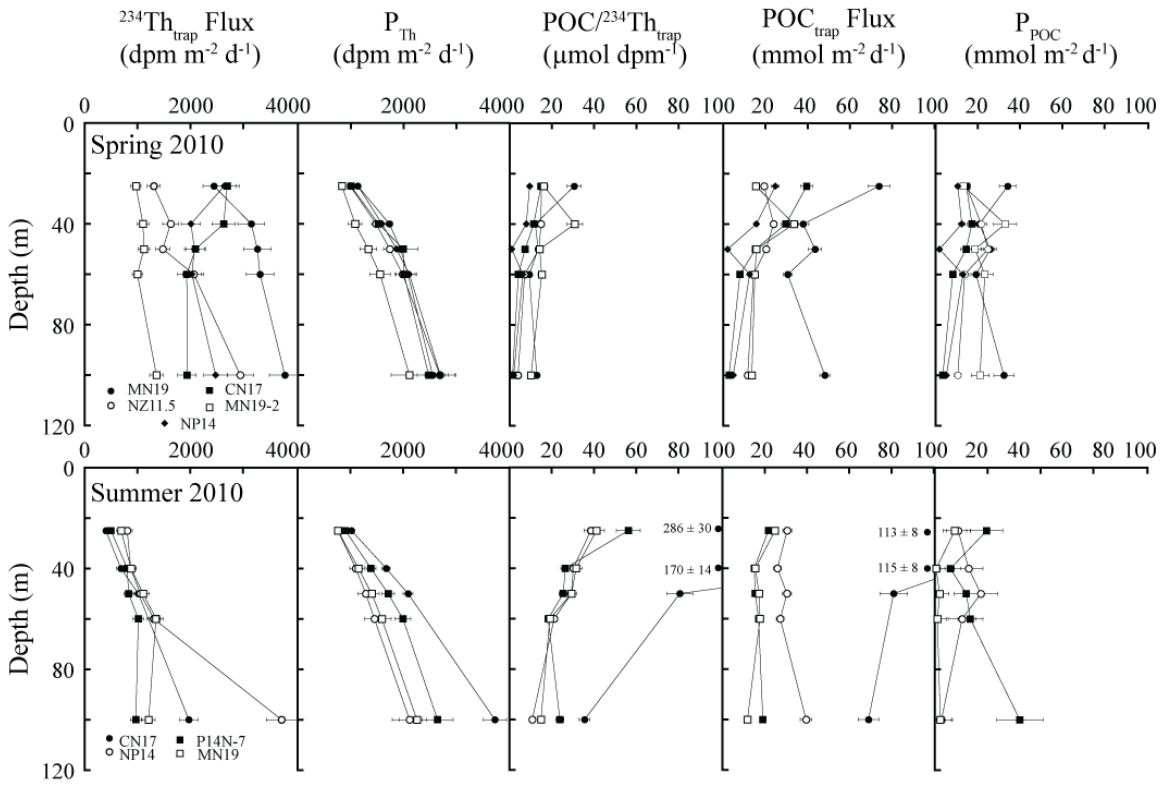

Figure 2.5. Depth profiles of sediment trap ^{234}Th flux (*$^{234}Th_{trap}$ Flux*; dpm m^{-2} d^{-1}), POC flux (*POC_{trap} Flux*; mmol C m^{-2} d^{-1}), *POC/^{234}Th* ratios (*POC/$^{234}Th_{trap}$*; µmol dpm^{-1}), and ^{234}Th fluxes calculated from ^{234}Th-^{238}U disequilibrium (P_{Th}), and ^{234}Th-derived POC export (P_{POC}) for spring (top) and summer (bottom) of 2010.

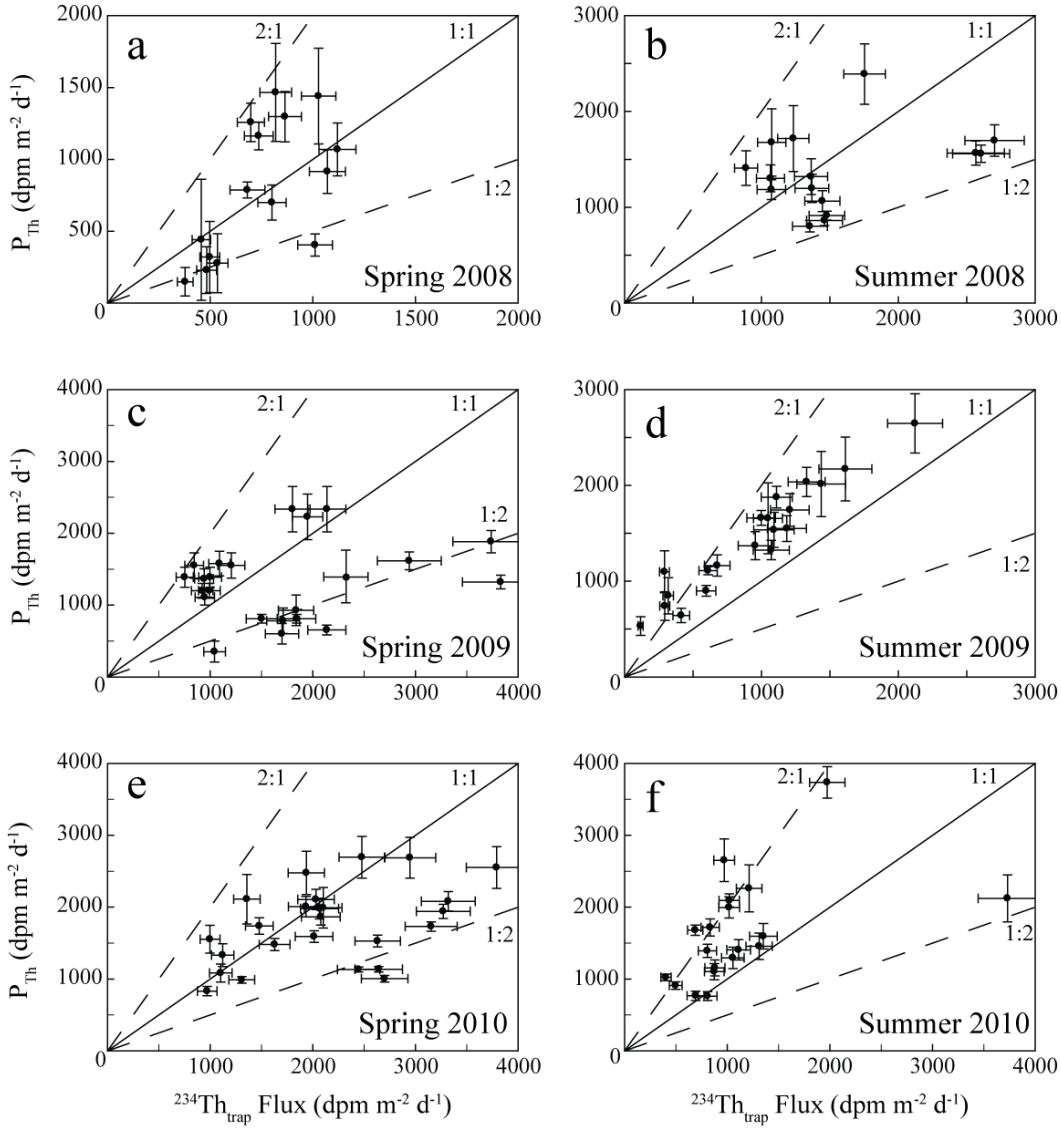

Figure 2.6. Seasonal comparison of ^{234}Th fluxes (dpm m^{-2} d^{-1}) at sediment trap stations determined by ^{234}Th-^{238}U disequilibrium (P_{Th}) and by sinking particles collected in sediment traps ($^{234}Th_{trap}$ *Flux*). Water column profiles integrated to depth of corresponding sediment traps (25, 40, 50, 60 and 100 m). Panels: spring 2008 (a), summer 2008 (b), spring 2009 (c), summer 2009 (d), spring 20010 (e) and summer 2010 (f). Note that the scale varies from season to season. Two points from spring 2009 (c) are off-scale (listed in Table 1.3).

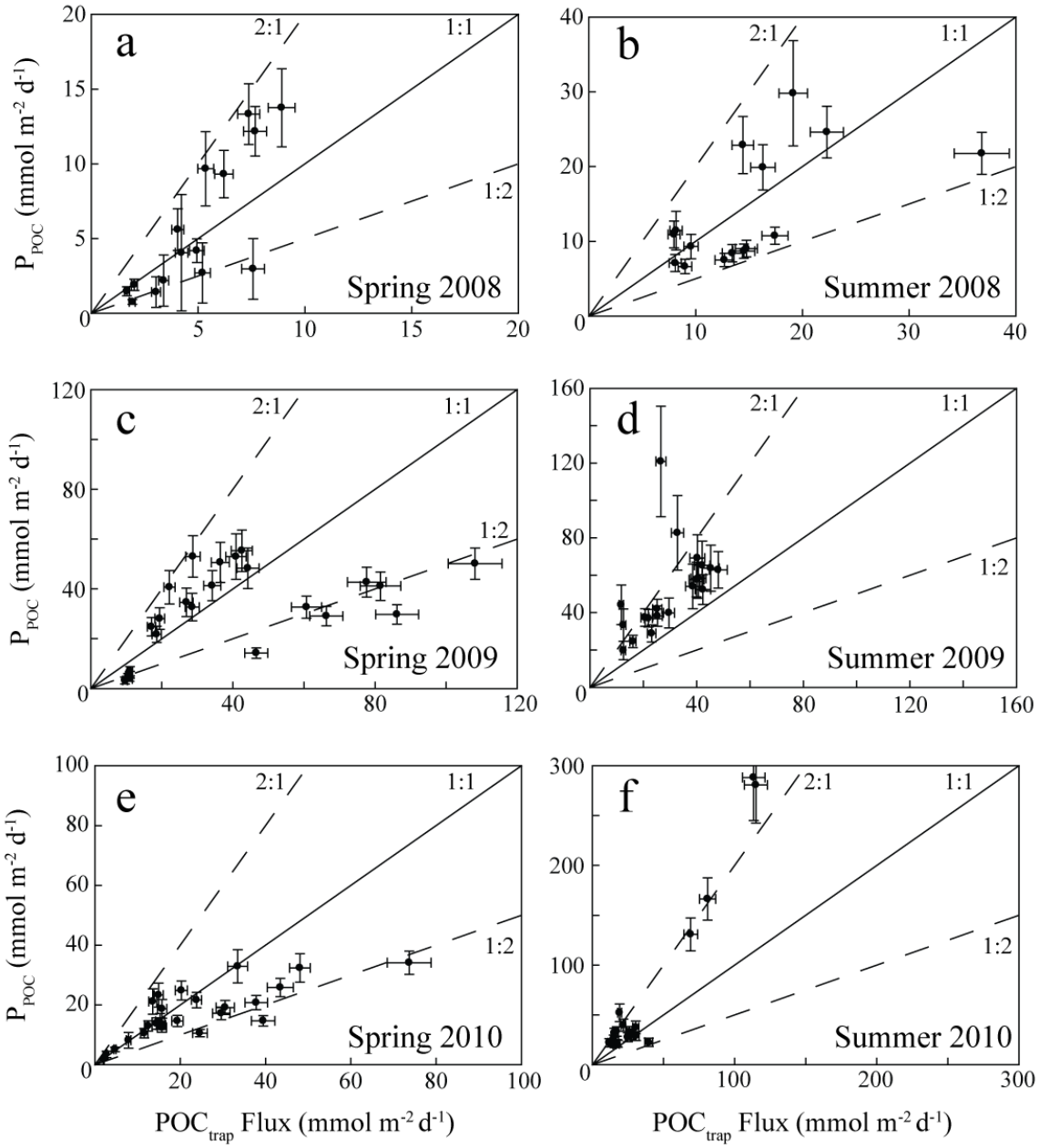

Figure 2.7. Seasonal comparison of POC export (mmol C m^{-2} d^{-1}) determined by the ^{234}Th method (P_{POC}) and sediment traps (POC_{trap} *Flux*). Panels: spring 2008 (a), summer 2008 (b), spring 2009 (c), summer 2009 (d), spring 20010 (e) and summer 2010 (f). Note that the scale varies from season to season. One point from spring 2009 (c) is off scale (listed in Table 1.3).

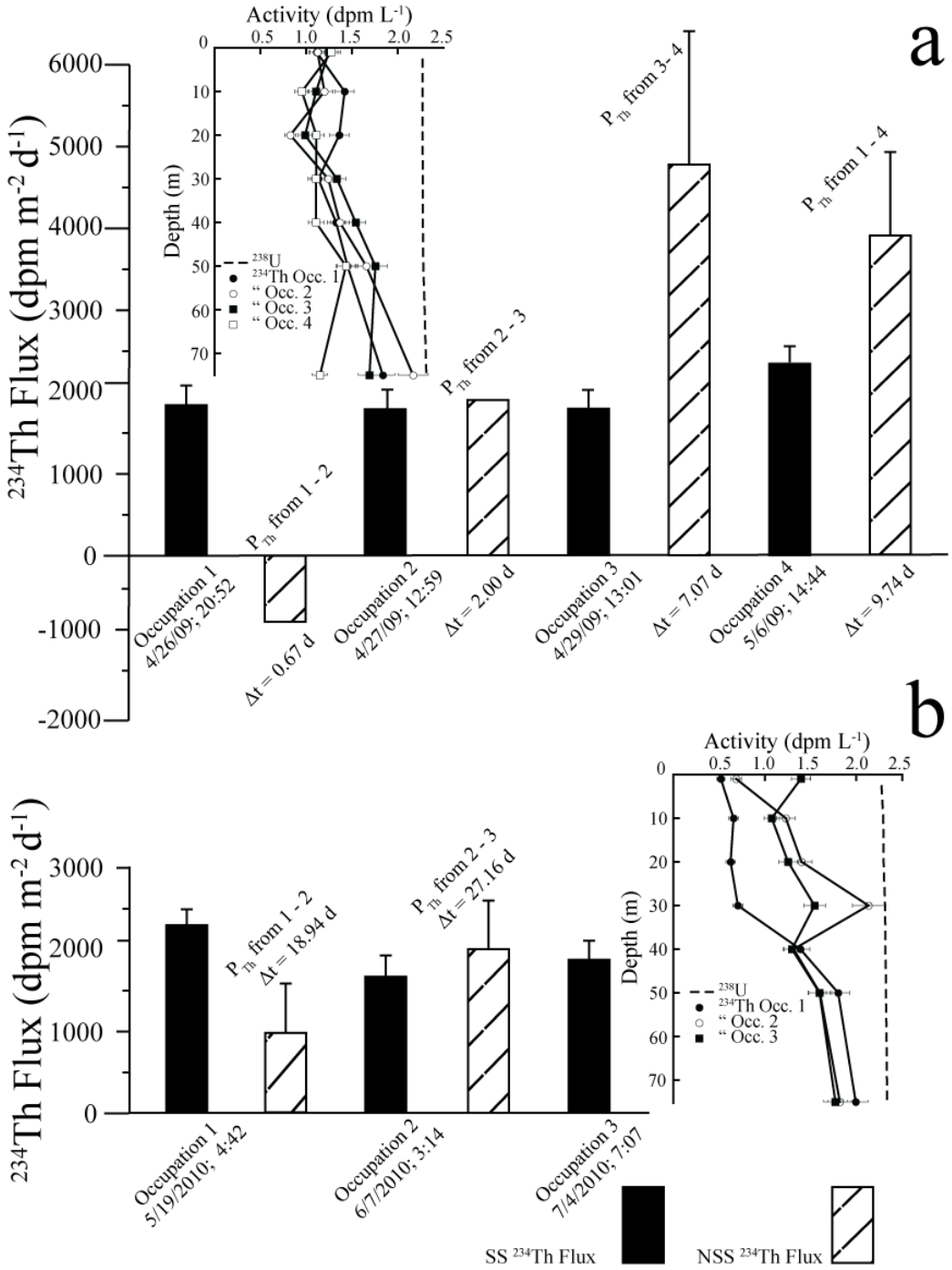

Figure 2.8. Comparison of steady state (SS; $\partial A_{Th}/\partial t = 0$) and non-steady state (NSS; $\partial A_{Th}/\partial t \neq 0$) ^{234}Th fluxes at two locations: Bloom station (BL) in 2009 (a) and MN19 in 2010 (b). Profiles were integrated to 75 m in both cases. Water column depths were ~125 and ~160 m at BL and MN19, respectively.

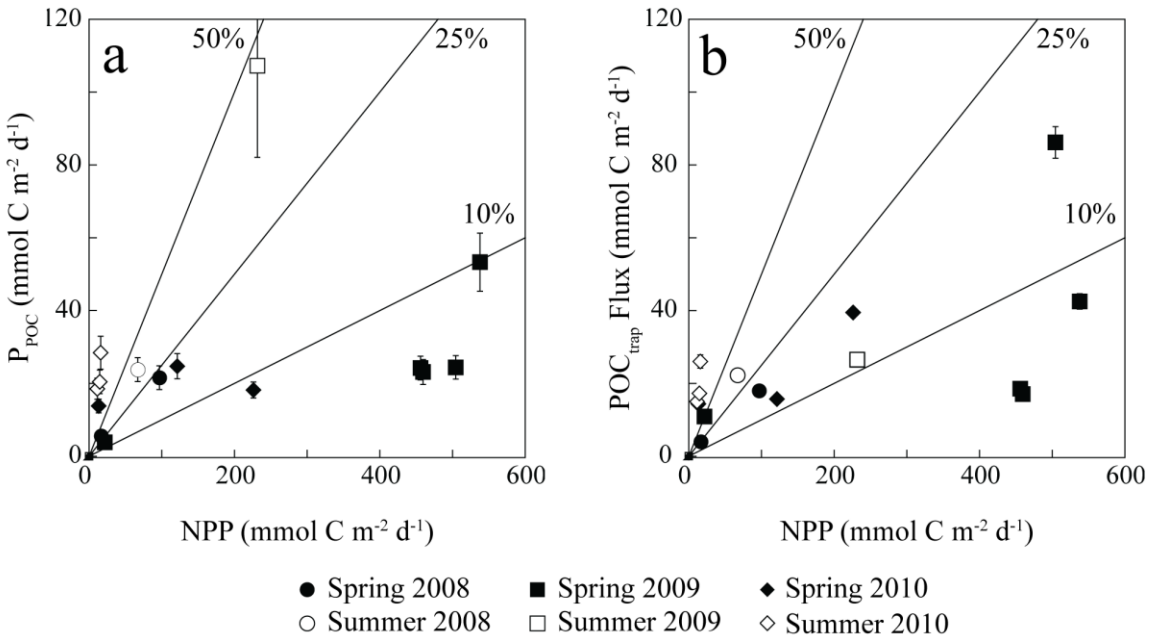

Figure 2.9. Photic zone integrated rate of net primary production (NPP; mmol C m^{-2} d^{-1}) from ^{14}C incubations versus POC fluxes derived from the ^{234}Th approach (a; *ThE*) and sediment traps (b; *e*-ratio). ^{234}Th integrations extend to the base of the photic zone and sediment trap POC fluxes and $POC/^{234}Th$ are from the nearest in depth array. Lines of 50, 25 and 10% have been drawn for comparison of the data.

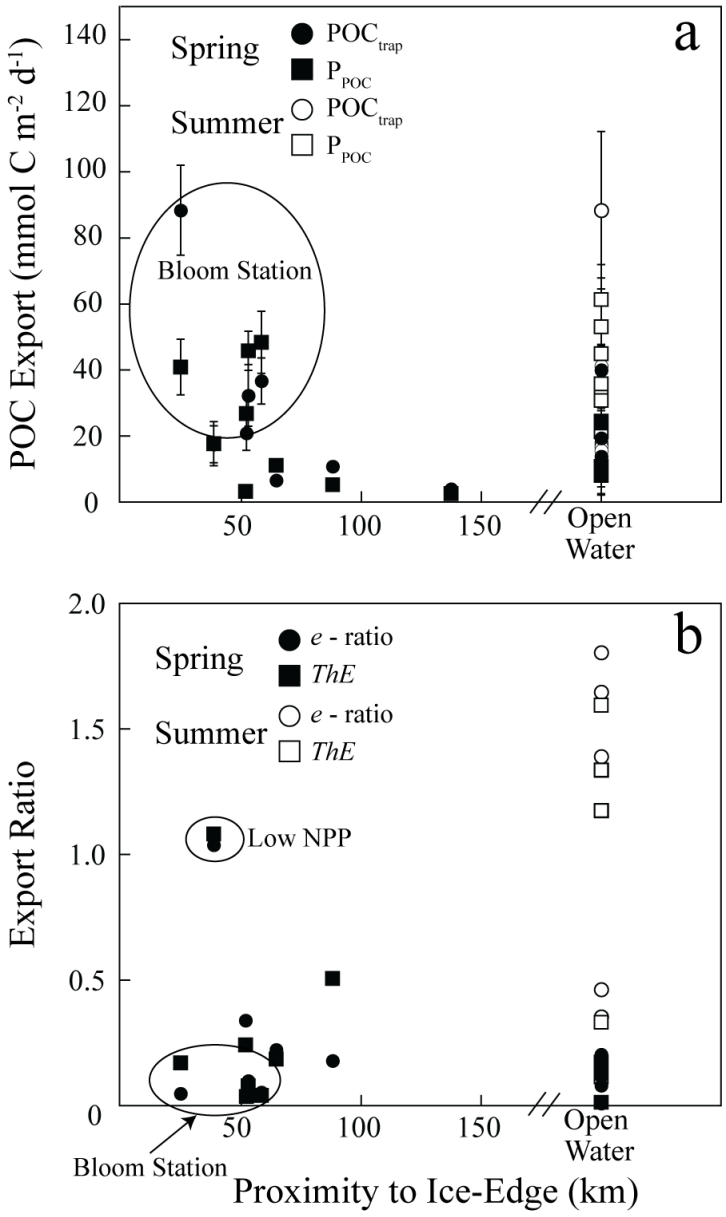

Figure 2.10. (a) Average POC fluxes from 40–100 m for individual sediment trap deployments in relation to the distance from the ice-edge (<8/10ths ice cover). The break separates near-ice stations from open water stations, which are grouped together. Dark/open circles and squares represent spring/summer POC_{trap} and P_{POC} average fluxes (± 1σ), respectively. (b) Same as (a) but for export ratios calculated according to Eq. (2.7). Dark/open circles and squares represent spring/summer *e*-ratio and *ThE*, respectively.

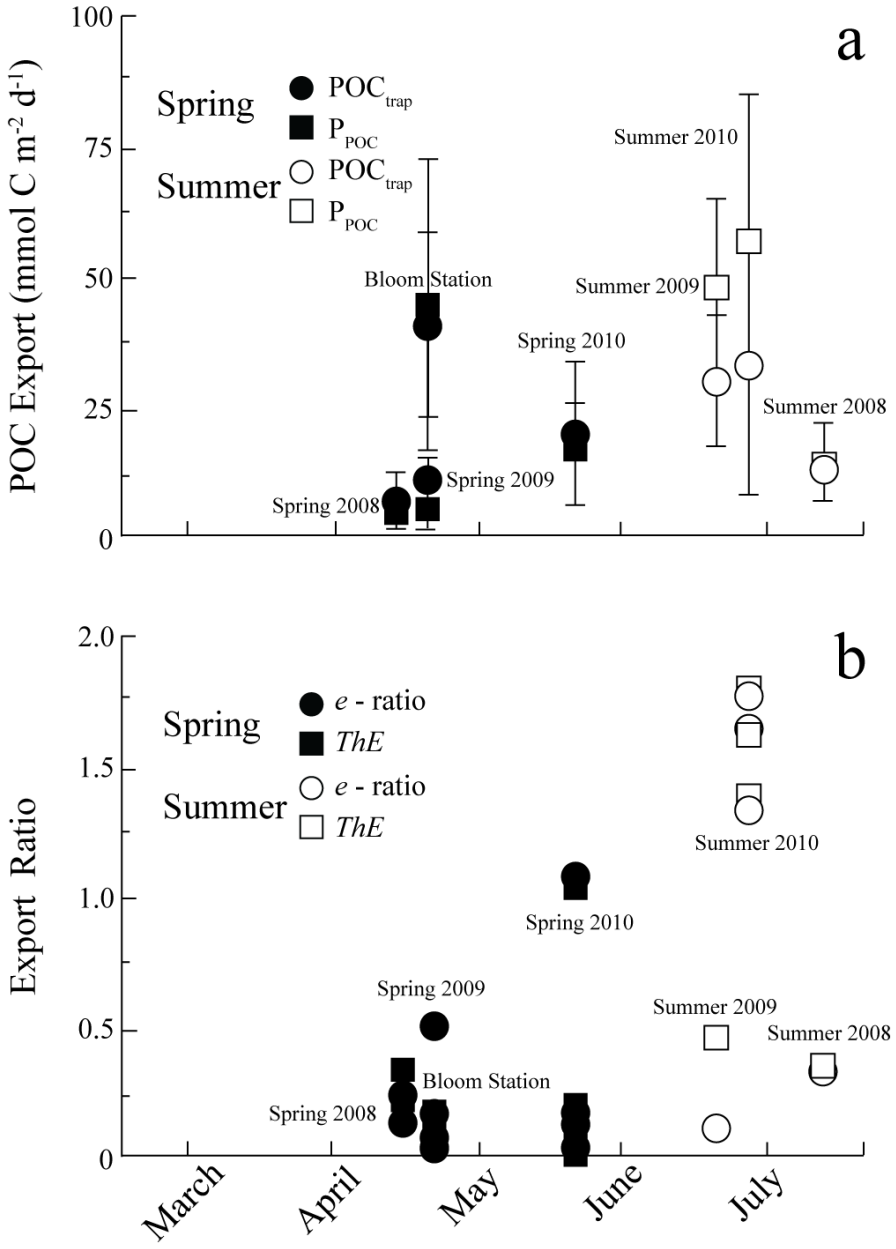

Figure 2.11. (a) POC fluxes below 40 m average by cruise and plotted at the ~mid-point of the expedition. Dark/open circles and squares represent spring/summer POC_{trap} and P_{POC} average fluxes (± 1σ), respectively. (b) Individual export ratios plotted by cruise at the ~mid-point of the expedition. Dark/open circles and squares represent spring/summer *e*-ratio and *ThE*, respectively.

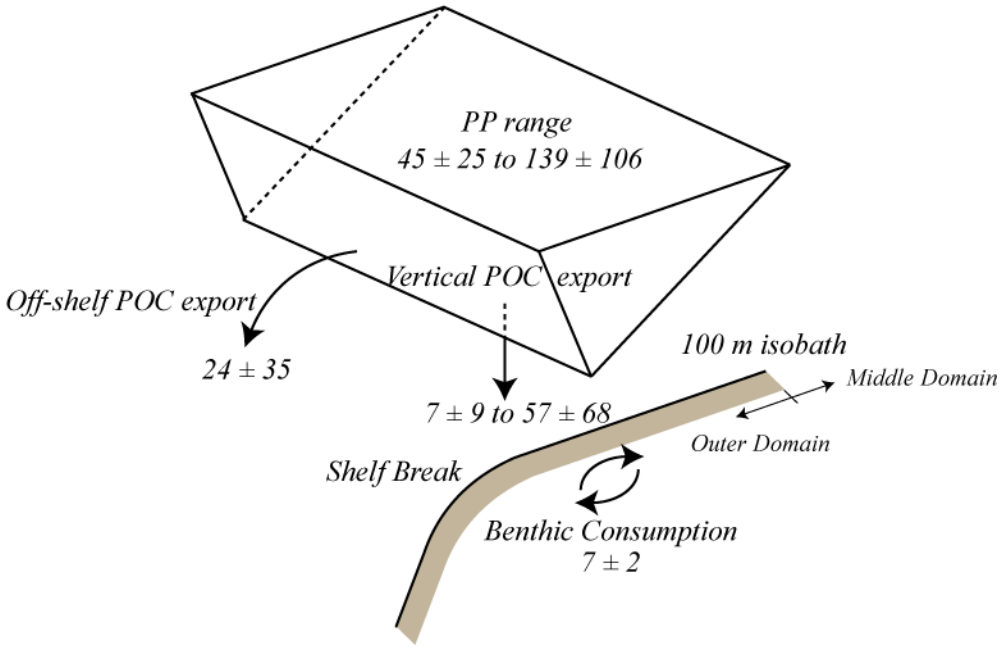

Figure 2.12. Average spring-summer POC export based on a ^{234}Th budget for the Outer Domain of the eastern Bering Sea adapted from Baumann et al. (2013) The off-shelf export flux of ^{234}Th was converted to POC using a *POC/^{234}Th* ratio of 11 ± 9 µmol dpm^{-1}. POC export units are mmol C m^{-2} d^{-1}. The vertical arrow represents minimum and maximum averages of P_{POC} for late spring and early summer. Primary production values are from Rho and Whitledge (2007).

Publication Status

Manuscript III, titled “Diatom control of the autotrophic community and particle export in the eastern Bering Sea during the recent cold years (2008-2010)” is in preparation for submission to *Journal of Marine Research*. The co-authors of this manuscript are S. B Moran, M. W. Lomas, R. P. Kelly, D. W. Bell, and J. W. Krause.

MANUSCRIPT III

DIATOM CONTROL OF THE AUTOTROPHIC COMMUNITY AND PARTICLE EXPORT IN THE EASTERN BERING SEA DURING THE RECENT COLD YEARS (2008-2010)

Abstract

During the recent cold years (2008-2010) in the eastern Bering Sea, a total of 79 water column and 24 sediment trap profiles were collected over the shelf and shelf break and analyzed for autotrophic pigment concentrations and elemental (carbon, nitrogen, phosphorus) concentrations in suspended and exported organic material. These results are used to establish the seasonal succession of the autotrophic community and the control that both phytoplankton and zooplankton exert on export production. In spring, total chlorophyll a concentrations are generally low; however, localized phytoplankton blooms near the marginal ice zone (MIZ) lead to elevated spring average chlorophyll *a* concentrations, relative to summer, over the shelf and at the shelf break. Diatoms represent the greatest contribution to total chlorophyll *a* in spring and summer of cold years. This algal class also represents the majority of total chlorophyll *a* in particles sinking through the water column. Further, the relatively high proportion of pheophorbide *a* in sediment trap material indicates that sinking of zooplankton fecal pellets facilitates the export of particles through the water column. In cold years, the emergence of large diatom blooms in the spring MIZ supports the production of abundant large zooplankton. Large zooplankton are a primary food source for juvenile pelagic fishes of economically important species. Therefore, these cold year specific processes

may be essential for the transfer of POC from the surface waters and the success of the economically important pelagic fishery. A consequence of a warmer Bering Sea in the coming decades is a reduction in seasonal sea-ice extent and duration. A change in sea-ice cover may alter the timing and magnitude of spring primary production and the flow of energy through the lower trophic levels.

3.1. Introduction

The eastern Bering Sea is characterized by some of the highest annual rates of primary production (PP) in the world ocean (Springer *et al.*, 1996). Such high levels of primary production over the broad (~500 km wide) and vast (~10,000 km^2) shelf support one of the largest fisheries in the United States in terms of fish catch revenue (National Marine Fisheries Service). The seasonal extent and duration of sea-ice represents the most important constraint on the location, timing, and magnitude of spring primary production (Alexander and Niebauer, 1981; Stabeno *et al.*, 2010) and the composition of the autotrophic community (Schandelmeier and Alexander, 1981). The lowest trophic levels of the ecosystem exhibits marked variability in distribution and abundance in response to changes in sea-ice in this region (e.g., Napp and Hunt, 2001; Stabeno *et al.*, 2012a; Stabeno *et al.*, 2012b). Because the physical regime exerts a strong control on the spring bloom and carbon flow through phytoplankton and zooplankton (Lovvorn *et al.*, 2005), changes in seasonal sea-ice extent and duration are predicted to affect the distribution and abundance of higher trophic level and economically important organisms in both the southeastern and northern regions of the shelf (Cooper *et al.*, 2013; Grebmeier *et al.*, 2006b; Hunt *et al.*, 2002).

During cold years characterized by late sea-ice retreat in the eastern Bering Sea, spring phytoplankton production is often dominated by intense diatom blooms (Schandelmeier and Alexander, 1981). These diatom blooms are initiated by increasing stability of the upper water column that is induced by stratification from melt water released from the retreating ice edge in the adjacent waters, which is more commonly known as the marginal ice zone (MIZ) (Alexander and Niebauer, 1981; Schandelmeier and Alexander, 1981). More than half of the annual primary production occurs between May and July in this region, a seasonal pulse that is largely controlled by the annual retreat of sea-ice (Brown *et al.*, 2011). Ice-edge blooms are terminated by nutrient limitation (Niebauer *et al.*, 1995), with the phytoplankton community shifting from diatoms to smaller cells, including flagellates, dinoflagellates, and haptophytes (namely *Phaeocystis pouchetti*) (Fujiki *et al.*, 2009; Lomas *et al.*, 2012; Moran *et al.*, 2012; Suzuki *et al.*, 2002b). Important questions relate to how newly formed organic carbon from primary production is removed from the surface waters, and whether exported phytoplankton material reflects the actively growing population in the photic zone. Both of these questions bear on carbon linkages between the lower trophic levels and the pelagic and benthic ecosystems, and the control that the physical regime may have on economically significant animals.

The presence of the intense MIZ spring bloom during mid-spring, a characteristic of cold years and late sea-ice retreat, largely supports the production of abundant large copepods and euphausiids that are less prevalent during warm years (Hunt *et al.*, 2011). Large zooplankton constitute a lipid rich prey source for young age classes of walleye pollock (*Theragra chalcogramma*), and the presence of these secondary producers is

necessary for the success of the age-0 year class (Heintz *et al.*, 2013; Hunt *et al.*, 2011; Siddon *et al.*, 2013) and other pelagic consumers. Primary production may be exported to deeper waters, to the benthos as particulate organic carbon by the sinking of intact algal cells (Cooper *et al.*, 2012; Grebmeier *et al.*, 2006a), or subject to heterotrophic grazing and fecal pellet production by zooplankton (Juul-Pedersen *et al.*, 2006; Wassmann *et al.*, 2006). The sinking flux of fecal pellets represents an important pathway for the transfer of POC from the surface waters in high-latitude shelf systems (Gleiber *et al.*, 2012; Juul-Pedersen *et al.*, 2010). Therefore, in cold years abundant large zooplankton not only support young age classes of economically important animals, they exert an important control on the export flux of particulate organic carbon (POC) from the upper water column.

This study investigates the seasonal succession of the autotrophic community and the controls that both phytoplankton and zooplankton have on the export of particulate organic matter (POM) during the recent cold years (2008-2010) in the eastern Bering Sea. The specific objectives of this study are to (1) characterize the seasonal evolution of the autotrophic community over the shelf and shelf break using total chlorophyll *a* (TChl *a*) concentrations and algal class specific indicator pigment ratios (pigment:TChl *a*), and (2) determine the essential nutrient composition of the POM sinking from the photic zone along the shelf break and the influence that zooplankton exert on particle export using degraded chlorophyll *a* (Σpheopigments) and C:N:P flux ratios. These objectives address two central hypotheses. First, particulate matter export is composed primarily of diatoms in spring and summer, despite the autotrophic community shifting from a diatom dominant system in spring to a more heterogeneous phytoplankton assemblage in

summer. Second, during such cold years, the presence of zooplankton fecal pellets in exported material implies that large secondary producers are an important component of the particle export flux.

3.2. Methods

Sediment trap and water column samples were collected in the eastern Bering Sea during spring and summer cruises from 2008-2010 as part of the BEST-BSIERP (Bering Ecosystem Study-Bering Sea Integrated Ecosystem Research Project) field program (Table 3.1). For the purpose of this study, the regions of the Bering Sea Exclusive Economic Zone of the United States (marine regions of the Bering Sea; http://bsierp.nprb.org/) are grouped into seven geographically larger Regions (Fig. 3.1; Table 3.2). Additionally, data were further binned into spring (HLY0802, HLY0902, and TN249) and summer (HLY0803, KN195-10, and TN250) seasons.

a. Upper water column POC, PON, POP, bSi, and autotrophic pigments

Concentrations of suspended POC, particulate organic nitrogen (PON) and particulate organic phosphorus (POP) in the water column were measured in 0.2 L samples collected from the CTD-rosette. Samples were vacuum filtered onto pre-combusted (4 h at 450°C) 25 mm glass fiber filters (GF/F; 0.7 µm nominal pore size). Biogenic silica (bSi) concentrations were measured in 0.25 L samples and vacuum filtered onto 47 mm, 0.4 µm polycarbonate membrane filters. Total (>0.7µm) water column pigments were measured in 1 L samples and vacuum filtered onto a 47 mm GF/F. All samples were frozen prior to analysis. POC, PON, POP, and bSi samples were frozen at -20°C until analysis and pigment samples were stored at -80°C.

b. Sediment trap sampling

Surface tethered, floating particle trap arrays (*KC Denmark*, Silkeborg, Denmark) were deployed near the shelf break (Fig. 3.1; z = >150 m; *n* = 3 in spring and *n*= 3 in summer of 2008; *n* = 5 in spring and *n* = 4 in summer of 2009 and 2010). Trap deployments were ~24 h in duration at trap depths of 25, 40, 50, 60, and 100 m (4 trap tubes per depth; 72 mm mouth diameter x 450 mm tube length). Sediment traps were filled with non-poisoned, 0.4 μm filtered brine (S = ~85 ‰) prior to deployment to isolate swimmers and suspended particulate matter from passively sinking material. After recovery, the upper seawater layer was siphoned down to the seawater-brine interface, which was indicated by the discontinuity between the layers. Two trap tubes were vacuum filtered onto a pre-combusted 25 mm GF/F. A stainless steel arc-punch was used to generate a 10 mm diameter subsample from each GF/F, which was then frozen at -20°C. The subsample was used for analysis of POC and PON, with the remaining filter material analyzed for ^{234}Th (Moran *et al.*, 2012). One full sediment trap per depth was used for HPLC pigment analysis of sinking material. For both 2010 cruises, a single trap was split into subsamples for POP and bSi analysis.

c. Analysis of POC, PON, POP, and bSi

The subsamples for POC and PON were dried at 60°C in a drying oven, fumed in a desiccator containing concentrated hydrochloric acid for 24 h to oxidize inorganic carbon, and dried again for 24h at 60°C. POC and PON were measured using a Carlo Erba-440 Elemental Analyzer (*Exeter Analytical, Inc*., North Chelmsford, MA, USA) (Pike and Moran, 1997). Field blanks were prepared for each set of samples by filtering

200 mL of filtered brine. An average blank for each cruise was subtracted from the gross POC and PON concentrations.

Concentrations of POP in both sediment trap and water column samples were measured using the ash-hydrolysis method, followed by orthophosphate measurement using the molybdate technique (Lomas *et al.*, 2013; Lomas *et al.*, 2010; Solorzano and Sharp, 1980).

Biogenic silica samples were analyzed by NaOH digestion (Brzezinski and Nelson, 1995; Paasche, 1973); Teflon tubes were used for these analyses to achieve low and consistent blanks (Krause *et al.*, 2009). The optical absorption of each sample was measured at 810 nm following the procedure of Strickland and Parsons (1968). Lithogenic silica (e.g., mineral dust, clays and sands) was not measured.

d. Pigment analysis by HPLC

Autotrophic pigment analysis of sediment trap and water column samples was conducted at the University of Maryland Horn Point Laboratory by HPLC analysis (Van Heukelem and Thomas, 2001). Briefly, samples were extracted using HPLC grade (90-100%) acetone and chilled while sonicated (model 450, *Branson Ultrasonics*, Danbury, CT, USA). The extracts were clarified using a 0.45 µm, PTFE HPLC syringe cartridge filter fitted with a GF/F pre-filter (*Scientific Resources Inc.*, Eatontown, NJ, USA). Samples were analyzed using a Hewlett-Packard (*HP*, Waldbronn, Germany) series 1100 HPLC equipped with a 900 µL syringe head autoinjector. Pigments were identified based on retention times of pure pigment standards or pigments isolated from algal monocultures.

e. Pigment analysis by CHEMTAX

The abundance of specific phytoplankton groups was estimated from indicator pigment concentrations relative to total chlorophyll *a* (TChl *a*) using the CHEMTAX program (Mackey *et al.*, 1996). The initial matrix was adapted from two previous studies that characterized relative phytoplankton abundance in the subarctic North Pacific (Fujiki *et al.*, 2009; Suzuki *et al.*, 2002a). They determined pigment:TChl *a* ratios for the seed matrix by averaging minimum and maximum values listed in Mackey et al., (1996), except for diatoms in which they applied a fucoxanthin:TChl *a* ratio of 0.75 based on observations from a previous study (Obayashi *et al.*, 2001). In this study, the same initial matrix was used for all water column data collected within the photic zone and for pigment fluxes. Based on a limited number of previous studies that relate accessory pigments to algal functional group in the eastern Bering Sea (Fujiki *et al.*, 2009; Suzuki *et al.*, 2002a), this study focuses on three phytoplankton groups (diatoms, chlorophytes and prymnesiophytes). However, the CHEMTAX program provides relative abundances for eight algal classes (pelagophytes, prasinophytes, cryptophytes, dinoflagellates, and cyanobacteria).

For most algal classes, the pigment:chlorophyll *a* ratios used in the initial matrix generally agree to within a factor of ~2 with those calculated in the final matrix for both the water column and trap CHEMTAX analyses (Appendix A.1). By comparison, the final matrix ratios for the water column and sediment trap data fall within range of values reported by Mackey et al., (1996) for the Southern Ocean. A sensitivity analysis was conducted using fucoxanthin to chlorophyll *a* ratios of 0.35 and 1.1 for diatoms as a means to evaluate the consistency of both the final matrix and the autotrophic

percentages of total chlorophyll *a* for the water column samples (Appendix A.2). For the major pigments and autotrophic groups, the final matrix pigment ratios for the three analyses (diatom fuco:TChl *a* ratios of 0.35, 0.75, and 1.1) are generally ~99% similar. The final autotrophic percentages for the individual samples are also ~99% for the three analyses with varying fuco:TChl *a* ratios for diatoms.

3.3. Results

a. Mixed layer hydrography

For the geographic regions assigned in this study, the average mixed layer depth (MLD) is greatest in spring (Table 3.3). The mixed layer is also consistently colder during spring, while average salinity values are indistinguishable between spring and summer (Table 3.3). The warmer surface water temperatures lead to a more buoyant upper water column in summer. Dissolved oxygen (DO) average concentrations in the mixed layer are also greater in spring. The northern and coastal Regions (1, 3 and 4) are undersaturated with respect to dissolved oxygen in spring, most likely due to the recent ice cover. Region 2, encompassing the northern outer shelf and St. Matthew Island, is slightly oversaturated (Table 3.3), which may be attributed to the enhanced primary production observed during HLY0902 in this area. Average percent ice cover at a given station is estimated as the seven day mean ice cover for the period of time preceding the sampling day. For the shelf Regions (1-5), percent ice cover, averaged by cruise, ranges from open water conditions (no ice) to 69±48% ice cover. For the spring cruises, many of the ice covered stations were occupied during HLY0802 (2008) and HLY0902 (2009), while most were ice free during TN249 (2010) as this cruise occurred in late spring.

b. Water column pigment and POM concentrations

Average concentrations of total chlorophyll a (TChl *a*) are greater in spring for all Regions. The exception is Region 3, which may be the result of limited sampling and ~98% ice cover during the collection of one of the two profiles in this Region (Tables 3.3, 3.4). The highest TChl *a* concentrations were consistently observed in Region 2 during the spring, where an intense marginal ice zone (MIZ) bloom occurred in 2009 (HLY0902) (Lomas *et al.*, 2012).

Approximately 35% of all TChl *a* measurements exceed a concentration of 1 µg L^{-1}, and more than 90% of those occurred during spring. At only four stations during this field program does the depth averaged concentration of TChl *a* exceed 5 µg L^{-1} (Fig. 3.2a), which signifies a bloom condition. These stations are BL (Region 2), which was sampled multiple times during HLY0902, MN19 (Region 6), NP14 (Region 5), and HBR1 (Region 4) during TN249. These bloom stations are responsible for the overall high TChl *a* averages in these regions (Table 3.4). The most abundant indicator pigment associated with the chlorophyll *a* measurements is fucoxanthin, which is a primary marker of diatoms. As with TChl *a* concentrations, the spatial distribution of fucoxanthin demonstrates substantial variability, ranging from negligible to greater than 15 µg L^{-1}. Fucoxanthin concentrations that exceed 1 µg L^{-1} are generally associated with the spring bloom stations (Fig. 3.2b). Fucoxanthin concentrations are highly correlated with TChl *a* concentrations ($m = 0.401x$; $r^2 = 0.978$; $p<0.001$, Fig. 3.3a). There is greater variability in the relationship at stations exhibiting lower TChl *a* concentrations, particularly in summer. No relationship exists between TChl *a* and either total chlorophyll *b* (TChl *b*, marker of chlorophytes), or 19'-Hexanoyloxyfucoxanthin (19'-Hex, marker of

prymnesiophytes); however, both of these accessory pigments are present at relatively higher concentrations when TChl *a* is low. Total pheopigment (Σpheopigments) concentrations for particles in the upper water column are low, typically present at levels an order of magnitude less than TChl *a*.

On a station by station basis, average upper water column POC and PON range from less than 7 to greater than 120 µmol C L^{-1} and 1 to 11 µmol N L^{-1} during spring (Table 3.5). During summer, depth averaged POC and PON concentrations are considerably lower ranging from 6 to 17 µmol C L^{-1} and 1 to 3 µmol N L^{-1} (Table 3.5). In both spring and summer of 2010, average POP concentrations are less than 0.7 µmol L^{-1} at all stations. Included with data from 2010, average bSi concentrations from the bloom station (BL) in 2009 are compared with the 2010 values (Table 3.5). Highest average bSi concentrations are consistently observed at stations with bloom condition levels of TChl *a* and elevated POC and PON concentrations.

c. Pigment and particulate organic matter fluxes

The geographic patterns observed in the magnitude of the TChl *a* flux (mg m^{-2} d^{-1}) are similar to that of pigments in the overlying water column (Table 3.6). Specifically, the highest TChl *a* fluxes are associated with geographic areas of the highest chlorophyll *a* standing stock in the spring, such as those observed at station BL during HLY0902 and MN19 during TN249. While fluxes of TChl *a* at times exceed 120 mg m^{-2} d^{-1} at bloom stations, vertical fluxes over the upper 100 m are generally less than 2 mg m^{-2} d^{-1} at non-bloom stations in both spring and summer. As with water column accessory pigments, fucoxanthin is the most abundant indicator pigment in vertically exported particulate

material, and this export flux is greatest at stations exhibiting elevated water column concentrations and vertical fluxes of TChl *a* (Table 3.6). The linear regression of fucoxanthin and TChl *a* in sinking particles ($m = 0.259x$; $r^2 = 0.863$; $p<0.001$, Fig. 3.3b) demonstrates a lower slope than the water column suspended particles. However, the mean ratios (mean: 0.31 for water column particles; 0.35 for sinking particles) are statistically similar, which suggests that material sinking from the photic zone is similar in composition to the autotrophic community with respect to fucoxanthin containing POM (Fig. 3.3b). The presence of TChl *b* and 19'Hex is occasionally detected in settling material, though typically to a lesser extent relative to the overlying water column (Table 3.6). The ratio of Σpheopigments to TChl *a* in sinking particles is usually greater than one, indicating that material sinking through the water column is at least partly degraded due to the presence of senescent cells or zooplankton fecal pellets (Table 3.6).

Sediment trap POC fluxes determined during this field campaign have been presented elsewhere (Baumann *et al.*, in press; Moran *et al.*, 2012). A subset of values used for the present analysis is listed in Table 3.6. Briefly, POC fluxes along the shelf break and in open water in the MIZ during early spring (HLY0802 and NP15 during HLY0902) are relatively low, while those over the outer shelf at station BL represent some of the highest fluxes measured in this study. POC fluxes increase in late spring (TN249) and early summer (KN195-10 and TN250), and decrease by mid-summer (HLY0803). The seasonal succession of the PON flux shows a similar temporal progression as POC export, with low early spring fluxes that increase throughout the growing season (Table 3.6). POP fluxes are typically <1 mmol m^{-2} d^{-1}, with the higher fluxes associated with the higher rates of POC and PON export (Table 3.6). No

correlation exists between the flux of bSi with either POC or TChl *a* export; however, the highest bSi fluxes occur at bloom stations BL (HLY0902) and MN19 (TN249).

3.4. Discussion

a. Characterization of the autotrophic community and vertical export

The observation of a predominantly diatom autotrophic community in the spring and in the MIZ is consistent with previous studies of the ice-edge population (Moran *et al.*, 2012; Schandelmeier and Alexander, 1981) and the presence of abundant resting stage cells in the underlying sediment in this region (Tsukazaki *et al.*, 2013). In particular, in spring, diatoms consistently represent the greatest contribution to TChl *a* over the shelf and along the shelf break. Over the shelf, diatoms represent a range of 71.5±10.8 % to 95.7±2.1% (regional mean ± 1σ) of the total chlorophyll *a* concentration for Regions 1-5. The contribution of diatoms in the northern (Region 6) and southern (Region 7) regions of the shelf break are on average 80.0±18.6% and 65.8±26.5% of the TChl *a* concentration, respectively (Table 3.7). Throughout the shelf and shelf break, other algal classes, namely prymnesiophytes, chlorophytes and cryptophytes, are present, but to a much lesser degree relative to diatoms in spring (Table 3.7). Smaller cells, such as cyanobacteria, also contribute minimally to the autotrophic community in this subarctic shelf system.

A seasonal shift in the autotrophic community is also apparent from the water column pigment distribution.. In spring, the autotrophic community is dominated by diatoms and characterized by localized blooms and high levels of standing stock chlorophyll *a*, whereas in summer the shelf and shelf break exhibit lower TChl *a* levels

and a heterogeneous phytoplankton assemblage. Specifically, as the concentration of TChl *a* markedly decreases in the upper water column in summer, the contribution of diatoms to total chlorophyll *a* also decreases throughout the system. Algal classes present in relatively smaller proportions during spring are key contributors to total chlorophyll *a* in early summer (Table 3.7). In particular, prymnesiophytes emerge along the shelf break comprising 54.5±32.3% and 27.1±23.2% of the total chlorophyll *a* in Regions 6 and 7, respectively. Together with prymnesiophytes, chlorophytes and cryptophytes also become important contributors to the total chlorophyll *a* in the shelf break regions and over the shelf as well (Table 3.7).

Diatoms are primarily responsible for the elevated levels of total chlorophyll *a* (e.g., >5 μg L^{-1}) in the spring and particularly at the bloom stations (Fig. 3.4a), while chlorophytes and prymnesiophytes are typically not present during this period (Fig. 3.4b,c). Interestingly, at lower concentrations of TChl *a* (e.g., <1 μg L^{-1}), in both spring and summer, diatoms frequently still represent the major autotrophic contribution (Figs. 3.4a, 3.5a,b, 3.6). However, when the relative contribution of diatoms is low during the summer, chlorophytes and prymnesiophytes dominate the autotrophic community (Figs. 3.4b,c, 3.5a,b). Key differences with respect to the autotrophic community are evident in the early summer autotrophic communities between 2009 (KN195-10) and 2010 (TN250). In particular, a number of stations in 2009, especially in Regions 6 and 7, are primarily characterized by high contributions of prymnesiophytes to the total chlorophyll *a* (Figs. 3.5b, 3.6; Table 3.7). By contrast in 2010, the autotrophic community is primarily composed of diatoms and chlorophytes, while there is little contribution from prymnesiophytes at these same stations along the shelf break (Fig. 3.5c). It is not known

what factors may be responsible for the differences in the phytoplankton community structure between 2009 and 2010 because sampling dates, average mixed layer depths, dissolved oxygen concentrations, upper water column temperature, and TChl *a* concentrations show little interannual variability.

As with the geographic distribution of the phytoplankton assemblage in the water column, diatoms are also typically the dominant algal class exported in sinking particles from the photic zone along the shelf break (Figs. 3.6, 3.7). On a station by station basis, there is little vertical variability in the percent composition of the major algal classes. However, both TChl *a* and POC fluxes vary substantially over the upper 100 m (Table 3.8), suggesting non-preferential consumption and remineralization of sinking particles. At three locations, all of which are in Region 6 (PIT1-HLY0803) or the southern reach of Region 7 (T1-HLY0802 and NP15-HLY0902), the average composition of the vertical flux is less than 50% diatoms. The relatively low diatom contribution at stations T1 and NP15 are associated with low TChl *a* and POC fluxes (Table 3.8). Interestingly, the average POC flux at PIT1 is the highest observed in summer 2008, whereas the average TChl *a* flux at that station is the lowest observed during the entire field program. At these stations, other algal classes, namely chlorophytes, pelagophytes, and dinoflagellates, represent the largest fraction of the sinking phytoplankton assemblage. Apart from these few stations, the observed shift in the autotrophic community in the water column is not reflected in the phytoplankton composition of exported particles (Fig. 3.7; Tables 3.7, 3.8). For all other stations in Regions 2 (BL), 6 and 7, diatoms represent at least 70% of the vertical flux of TChl *a*. This indicates that, regardless of the

total chlorophyll *a* and POC flux from the photic zone, diatoms are the primary algal class exported from the photic zone (Fig. 3.7).

The magnitude and seasonal progression of POC export flux, combined with differences in the ratio of pheopigments to TChl *a* between the upper water column and in sinking particles, provides important insights into the mechanisms controlling the export of diatoms from the photic zone. With regard to the export flux of POC along the shelf break, this region exhibits a progressive increase in the magnitude of particle flux from early spring to late spring and early summer, as noted above (Table 3.6). Based on the observation that the POC flux increases from spring to summer, and that the export population is primarily diatoms (Fig. 3.7), it has been suggested that export in early summer may be characterized by the sinking of spring and MIZ primary production in this system (Baumann *et al.*, in press). A temporal lag in the export of spring primary production as POC in summer has also been observed in other high-latitude systems (Asper and Smith, 1999; Dunbar *et al.*, 1998; Rutgers van der Loeff *et al.*, 1997; Thibault *et al.*, 1999). The average ratio of the sum of pheopigments to total chlorophyll *a* (Σpheo:TChl *a*) is >1 in material exported below the photic zone in late spring and early summer (Table 3.6; 50 m sediment traps). In contrast, the Σpheo:TChl *a* ratio in phytoplankton derived from integrated pheopigment and total chlorophyll *a* stocks in the photic zone averages ~0.1. The low ratio of the autotrophic population indicates an actively growing phytoplankton community (Bianchi *et al.*, 2002). In comparison to phytoplankton in the photic zone, the Σpheo:TChl *a* ratio in sinking particles at 50 m is ~8-75 times greater than in the overlying water column on a station by station basis (Tables 3.4, 3.6). That the Σpheo:TChl *a* ratio in sinking particles is much greater than

those in the upper water column indicates that sinking POM is composed of substantially degraded chlorophyll *a* and consists of a combination of senescent cells and zooplankton fecal pellets.

Pheophorbide *a*, the degradation pigment resulting from metazoan digestion, represents ~80% of the total pheopigment concentration in sinking particles (Table 3.6). This observation suggests that zooplankton grazing of spring primary production and subsequent sinking of fecal pellets is an important control on the vertical export of POC along the shelf break in this region. While microzooplankton abundance and grazing pressure has been reported to be largely unaffected by climate variability (Sherr *et al.*, 2013; Stabeno *et al.*, 2012b), cold years in the eastern Bering Sea, such as during this study, favor the production of abundant large crustacean zooplankton and euphausiids (Hunt *et al.*, 2011). Therefore, the export of fecal pellets produced by abundant large zooplankton may be an important mechanism controlling the vertical flux of POC from the photic zone along the shelf break in late spring and early summer during cold years.

Assuming that pheopigment fluxes are attributed to zooplankton fecal pellets, and that fucoxanthin fluxes are representative of sinking diatoms, inferences in preferential export of zooplankton fecal pellets and diatoms can be made from the differential loss rates of these pigments compared to those for POC and TChl *a*. Sinking loss rates for these exported constituents are estimated as the ratio of the measured flux at 50 m compared to the standing stock in the water column (Thibault *et al.*, 1999). At all trap locations, the loss of fucoxanthin and Σpheopigments from the photic zone represents a larger fraction of the standing stock than for either POC for TChl *a* (Table 3.9). Specifically, fucoxanthin and Σpheopigment loss rates range from 14-83% and 5-100%

per day, respectively. By comparison, loss rates of TChl *a* and POC are less than ~7% d^{-1} (Table 3.9). Because fucoxanthin and pheopigment loss rates greatly exceed those for POC and TChl *a*, it follows that diatoms are preferentially transported to depth via zooplankton grazing and subsequent sinking of fecal pellets. It must be noted that because the autotrophic community is actively growing, pheopigment concentrations are low, relative to chlorophyll *a*, which leads to relatively large pheopigment loss rates. However, the implication of the high loss rates is that almost all degraded chlorophyll *a* is being rapidly removed by the sinking of zooplankton fecal pellets.

The POC associated with TChl *a* and pheopigment export can be estimated using generalized POC:TChl *a* and POC:pheopigment ratios of 50:1 and 15:1 (Thibault *et al.*, 1999). A POC:pheopigment ratio of 15:1 assumes a 70% carbon assimilation efficiency by zooplankton (Thibault *et al.*, 1999). POC fluxes associated with TChl *a* and pheopigment export range from 5-100% and 1.6-44% of the total POC flux at 50 m, respectively (Table 3.9). The total carbon export by zooplankton is likely underestimated because respiration and excretion below the photic zone during daily vertical migration by mesozooplankton represents a significant component of the total C flux (Hannides *et al.*, 2009). In addition, ~20% of the POC associated with fecal pellets is likely released below the photic zone or below the deepest sediment trap in this study (Durbin *et al.*, 1995). These results support the hypothesis that the export of zooplankton fecal pellets represents an important component of POC export along the shelf break in this region.

b. Elemental composition of phytoplankton and zooplankton controlled export

As described above, autotrophic biomass in the eastern Bering Sea during this study is composed predominantly of diatoms, and export of this algal group is largely controlled by sinking zooplankton fecal pellets in spring and early summer. A quantitative understanding of the C:P and N:P ratio of phytoplankton in the photic zone and in sinking particles can be used to make further inferences into the degree of zooplankton assimilation of these macronutrients, the efficiency of zooplankton controlled particle export, and the potential stoichiometric ratios resulting from respiration and inorganic and organic excretion by zooplankton (e.g., Martiny *et al*., 2013).

On average, phytoplankton in the photic zone are rich in phosphorus relative to both carbon and nitrogen (Fig. 3.8; Table 3.5). For the eastern Bering Sea in 2010, the average particulate C:P and N:P ratio in the upper water column was 87±44 and 12±5.1, respectively, both of which are less than the Redfield stochiometric relationship of 106:16:1 for C:N:P. Collectively, 86% and 92% of all measurements from 2010 exhibit ratios lower than Redfield for C:P and N:P, respectively (Fig. 3.8); note that C:P and N:P ratios of phytoplankton are plotted against absolute and relative fucoxanthin (i.e., fuco:TChl *a*) concentrations. While stoichiometric ratios of phytoplankton cannot be differentiated between spring and summer, the C:P and N:P ratio of suspended particles is invariant with the concentration of fucoxanthin and the fuco:TChl *a* ratio, suggesting that C:P and N:P do not vary with changing diatom biomass or autotrophic community composition (Fig. 3.8). In addition, the collective average ratios of C:P and N:P for spring-early summer phytoplankton are below the global mean and consistent with fast growing cells in nutrient-rich, high-latitude systems (Martiny *et al.*, 2013). Moreover,

suspended particles in the Bering Sea are enriched in phosphorus by a factor of ~2, relative to POC compared to phytoplankton in warm, nutrient depleted oligotrophic systems (Hannides *et al.*, 2009).

The limited number of elevated N:P ratios at relatively low fucoxanthin concentrations (Fig. 8a). Each of these elevated N:P ratios are greater than 20 and observed in different profiles collected during TN250. These few values are not consistent with other ratios from the same profiles and may not be representative of the water column at those locations. However, elevated C:P ratios are present at higher fucoxanthin concentrations and fuco:TChl *a* ratios (Fig. 3.8c,d). These high C:P ratios are found consistently at three stations (TN249; NZ4.5, HBR1 and 70M26), all of which are in Region 4, near the ice-edge, and have low surface dissolved PO_4^{3-} concentrations (EOL data archive: http://catalog.eol.ucar.edu/best_tn249/). The relatively high biomass at these stations is characterized by an autotrophic composition consisting of >90% diatoms and high concentrations of TChl *a* and bSi, similar to the range values measured at the bloom station (BL) in spring 2009. Thus, the diatom community at these stations may be attributed to a post-bloom population growing under phosphorus limitation (Arrigo, 2005).

Elemental ratios in sinking particles are substantially higher than those of water column suspended particles, suggesting either carbon enrichment or phosphorus depletion of sinking zooplankton fecal pellets, relative to suspended particles. Sinking particles (40-100 m traps) exhibit average C:P ratios of 107±71 (TN249) and 156±67 (TN250) and average N:P ratios of 24±14 (TN249) and 14±8 (TN250) for spring and summer in 2010 (Fig. 3.9; Table 3.6). By comparison, fuco:TChl *a* ratios are similar in both

phytoplankton and trap fluxes. For all six cruises, the average C:N of sinking particles was 7.3±2.8 (Table 3.6). The average C:N ratio is consistent with the Redfield ratio of 7.8, which indicates that phosphorus depletion is likely responsible for the high C:P and N:P values of sinking particles along the shelf break. An alternative explanation for the elevated C:P and N:P ratios is that the processes of inorganic and organic excretion by zooplankton may release relatively high proportions of phosphorus relative to carbon and nitrogen.

Zooplankton in this region demonstrate elemental stoichiometric homeostasis, meaning that their C:N:P stoichiometry does not vary as a function of food source. Weighted average C:P and N:P ratios of three subarctic copepods (*Calanus glacialis*, *Eucalanus* sp., and *Metridia pacifica*) and an euphausiid (*Thysanoessa raschii*) are slightly higher (C:P of 176 ±52 and N:P of 35±9; Lomas *et al*. unpublished data) than in the passively sinking particles these organisms produce. Though the standard deviations of these data sets are large, that the average C:P and N:P of these consumers is greater than the averages of both passively sinking particles and the phytoplankton in the water column suggests that the processes of excretion and respiration by zooplankton are likely enriched in phosphorus relative to carbon and nitrogen.

The C:P and N:P stoichiometry of the combined processes of respiration and inorganic/organic excretion by zooplankton may be important for both nutrient regeneration in the photic zone and export of carbon and nutrients to depth by vertical migration. These ratios may be estimated using a mass balance of the C:P and N:P of four pools: phytoplankton food source (*P*), zooplankton (*Z*), particle flux (*F*), and the combined processes of respiration and inorganic/organic excretion (*A*). The C:P and N:P

ratios of respiration and excretion are calculated independently because carbon must be assimilated at a higher rate than nitrogen based on the high C:P of zooplankton in this region. Also, the C:P and N:P ratios of these pools are inversed (i.e., 1/C:P = P:C and 1/N:P = P:N) because *A* is calculated with respect to carbon and nitrogen, respectively. The mass balance equation for these nutrient pools is:

$$P = (Z * ae) + (F * f_1) + (A * f_2) \quad (3.1)$$

where *P*, *Z*, *F*, and *A* are the P:C or P:N ratios of the four pools listed above, *ae* is the carbon or nitrogen assimilation efficiency by zooplankton, and f_1 and f_2 are the fractions of carbon or nitrogen available (not assimilated) for particle export or for the combined processes of respiration and inorganic/organic excretion by zooplankton, respectively. Values of *P*, *Z* and *F* are 87±44, 175±52, and 129±72 for C:P, respectively, and 12±5, 35±9, and 21±14 for N:P, respectively (Tables 3.5, 3.6). With regard to estimating the C:P ratio for *A*, a range of zooplankton assimilation efficiencies (*ae* = 0.6 to 0.8; Hannides *et al.*, 2009) and f_1 values (f_1 = 0.1 to 0.3) are used, while the relationship $1\text{-}ae\text{-}f_1$ is substituted for f_2. For cases in which ae, f_1, f_2 sum to 1, the average C:P ratio of *A* is 21±9.7 (*n* = 89). The same approach is used for estimating the N:P ratio of A; however, a range of lower assimilation efficiencies are used because a large fraction of the ingested nitrogen is likely excreted immediately (E. Durbin, pers. comm.). For the estimation of the N:P ratio, assimilation efficiencies range from 0.3 to 0.5 and f_1 ranges from 0.1 to 0.3. These ranges of *ae* and f_1 result in f_2 values that are generally larger than those used for the C:P ratio estimation, consistent with a larger fraction of excreted nitrogen. Solving equation 1 using these parameters yields an average N:P ratio of 6.3±1.1 (*n* = 121) for *A*. Notwithstanding that the average C:P and N:P ratios calculated for *A* have large

associated uncertainties that include large standard deviations of the *P*, *Z*, and *F* pools, and that the *ae*, f_1, and f_2 values are estimates from literature, these relatively low imputed ratios for *A* suggest that the processes of respiration and excretion are important components of both nutrient cycles in the upper water column and export of carbon and nutrients to depth.

3.5. Conclusions

During cold years in the eastern Bering Sea, the autotrophic community is dominated by diatoms in the spring and in the MIZ. Associated with a high percent composition of diatoms in spring is a greater frequency of elevated rates of net primary production and high levels of TChl *a* and POC in the photic zone. Despite a wide range in the magnitude of particle flux along the shelf break, the diatom algal class represents the majority of the exported total chlorophyll *a*. Because pheophorbide *a* is present in large abundance in sinking particulate matter, often at levels much greater than TChl *a*, the vertical transfer of diatoms is likely mediated by enhanced zooplankton grazing of MIZ primary production and subsequent export of fecal pellets in late spring and early summer. Daily loss rates of fucoxanthin and pheopigments from the photic zone exceed those for both TChl *a* and POC, supporting the notion that sinking of zooplankton fecal pellets exerts an important control on particle export from the surface waters along the shelf break.

This study provides new evidence of the relationship between the phytoplankton community and zooplankton mediated export during cold years in the eastern Bering Sea. This region is predicted to warm in the coming decades (Overland and Wang, 2007;

Wang *et al.*, 2012), resulting in a reduction in maximum sea-ice extent and earlier retreat in spring. As a consequence, a warmer physical regime may restructure the spring autotrophic community to a population consisting of fewer diatoms, similar to summer conditions in this region. Total annual primary production may be greater in years characterized by early sea-ice retreat (Brown and Arrigo, 2013; Brown *et al.*, 2011); however, warm years are unfavorable for large zooplankton (Hunt *et al.*, 2011). A reduction in large zooplankton may threaten the success of economically important animals. Associated with this climate driven shift of the autotrophic and zooplankton community may be a reduction in POC transfer to deeper waters and greater organic carbon retention within the water column. A further implication of a warming Bering Sea is the magnitude to which this subarctic shelf system sequesters carbon to the deep ocean, which may decrease in the future (Bauman *et al*., in press).

Acknowledgments- We thank the Chief Scientists, officers, and crew of the *USCGC Healy*, *R/V Knorr*, and *R/V Thompson* for their efforts. We thank John Karavias of Walt Whitman High School (Queens, NY) and Jason Pavlich of Red Hook High School (Red Hook, NY) for their assistance as part of the ARMADA Project. We also thank the hydrographic team from NOAA-PMEL, especially Sigrid A. Salo and Edward D. Cokelet, for providing hydrographic data and assisting in sample collection, accessible through the EOL data archive supported by NSF and NOAA. We thank Emily Goldman for assistance with the CHEMTAX analysis. This research was supported by awards ARC-0732680 and NPRB-B56 to SBM and ARC-0732359 to MWL.

References

Alexander, V. and Niebauer, H. J. 1981. Oceanography of the Eastern Bering Sea Ice-Edge Zone in Spring. Limnol. Oceanogr. 26(6), 1111-1125.

Arrigo, K. R. 2005. Marine microorganisms and global nutrient cycles. Nature. 437(7057), 349-355.

Asper, V. L. and Smith, W. O., Jr. 1999. Particle fluxes during austral spring and summer in the southern Ross Sea, Antarctica. J. Geophys. Res. 104(C3), 5345-5359.

Baumann, M. S., Moran, S. B., Kelly, R. P., Lomas, M. W., Shull, D. H. 2013. ^{234}Th balance and implications for seasonal particle retention in the eastern Bering Sea. Deep-Sea Res. Pt. II. 94, 7-21.

Baumann, M. S., Moran, S. B., Lomas, M. W., Kelly, R. P., Bell, D. W. in press. Seasonal decoupling of particulate organic carbon export and net primary production in relation to sea-ice at the shelf break of the eastern Bering Sea: implications for off-shelf carbon export Submitted to Journal of Geophysical Research Oceans.

Benitez-Nelson, C. R., Bidigare, R. R., Dickey, T. D., Landry, M. R., Leonard, C. L., Brown, S. L., Nencioli, F., Rii, Y. M., Maiti, K., Becker, J. W., Bibby, T. S., Black, W., Cai, W. J., Carlson, C. A., Chen, F. Z., Kuwahara, V. S., Mahaffey, C.,

McAndrew, P. M., Quay, P. D., Rappe, M. S., Selph, K. E., Simmons, M. P., Yang, E. J. 2007. Mesoscale eddies drive increased silica export in the subtropical Pacific Ocean. Science. 316(5827), 1017-1021.

Bianchi, T. S., Rolff, C., Widbom, B., Elmgren, R. 2002. Phytoplankton Pigments in Baltic Sea Seston and Sediments: Seasonal Variability, Fluxes, and Transformations. Estuar. Coast. Shelf Sci. 55(3), 369-383.

Brown, Z. W. and Arrigo, K. R. 2013. Sea ice impacts on spring bloom dynamics and net primary production in the Eastern Bering Sea. Journal of Geophysical Research: Oceans. 118, 1-20, DOI: 10.1029/2012JC008034.

Brown, Z. W., van Dijken, G. L., Arrigo, K. R. 2011. A reassessment of primary production and environmental change in the Bering Sea. J Geophys Res-Oceans. 116(C8), C08014 DOI:10.1029/2010JC006766.

Brzezinski, M. A. and Nelson, D. M. 1995. The annual silica cycle in the Sargasso Sea near Bermuda. Deep-Sea Res Pt I. 42(7), 1215-1237.

Buesseler, K. O. 1998. The decoupling of production and particulate export in the surface ocean. Global Biogeochem. Cy. 12, 297-310.

Cooper, L. W., Janout, M. A., Frey, K. E., Pirtle-Levy, R., Guarinello, M. L., Grebmeier, J. M., Lovvorn, J. R. 2012. The relationship between sea ice break-up, water mass variation, chlorophyll biomass, and sedimentation in the northern Bering Sea. Deep-Sea Res. Pt. II. 65–70(0), 141-162.

Cooper, L. W., Sexson, M. G., Grebmeier, J. M., Gradinger, R., Mordy, C. W., Lovvorn, J. R. 2013. Linkages between sea-ice coverage, pelagic–benthic coupling, and the distribution of spectacled eiders: Observations in March 2008, 2009 and 2010, northern Bering Sea. Deep-Sea Res. Pt. II. 94, 31-43.

Dunbar, R. B., Leventer, A. R., Mucciarone, D. A. 1998. Water column sediment fluxes in the Ross Sea, Antarctica: Atmospheric and sea ice forcing. J. Geophys. Res. 103(C13), 30741-30759.

Durbin, E. G., Campbell, R. G., Gilman, S. L., Durbin, A. G. 1995. Diel feeding behavior and ingestion rate in the copepod Calanus finmarchicus in the southern Gulf of Maine during late spring. Cont. Shelf Res. 15(4–5), 539-570.

Fujiki, T., Matsumoto, K., Honda, M. C., Kawakami, H., Watanabe, S. 2009. Phytoplankton composition in the subarctic North Pacific during autumn 2005. J Plankton Res. 31(2), 179-191.

Gleiber, M. R., Steinberg, D. K., Ducklow, H. 2012. Time series of vertical flux of zooplankton fecal pellets on the continental shelf of the western Antarctic Peninsula. Mar. Ecol. Prog. Ser. 471, 23-36.

Grebmeier, J. M., Cooper, L. W., Feder, H. M., Sirenko, B. I. 2006a. Ecosystem dynamics of the Pacific-influenced northern Bering and Chukchi seas in the Amerasian Arctic. Prog. Oceanogr. 71, 331-361.

Grebmeier, J. M., Overland, J. E., Moore, S. E., Farley, E. V., Carmack, E. C., Cooper, L. W., Frey, K. E., Helle, J. H., McLaughlin, F. A., McNutt, S. L. 2006b. A major ecosystem shift in the northern Bering Sea. Science. 311, 1461-1464.

Hannides, C. C. S., Landry, M. l. R., Benitez-Nelson, C. R., Styles, R. M., Montoya, J. P., Karl, D. M. 2009. Export stoichiometry and migrant-mediated flux of phosphorus in the North Pacific Subtropical Gyre. Deep-Sea Res. Pt. I. 56(1), 73-88.

Heintz, R. A., Siddon, E. C., Farley Jr, E. V., Napp, J. M. 2013. Correlation between recruitment and fall condition of age-0 pollock (Theragra chalcogramma) from the eastern Bering Sea under varying climate conditions. Deep-Sea Res. Pt. II. 94, 150-156.

Hunt, G. L., Coyle, K. O., Eisner, L. B., Farley, E. V., Heintz, R. A., Mueter, F., Napp, J. M., Overland, J. E., Ressler, P. H., Salo, S. A., Stabeno, P. J. 2011. Climate

impacts on eastern Bering Sea foodwebs: a synthesis of new data and an assessment of the Oscillating Control Hypothesis. ICES Journal of Marine Science: Journal du Conseil. 68(6), 1230-1243.

Hunt, G. L., Stabeno, P., Walters, G., Sinclair, E., Brodeur, R. D., Napp, J. M., Bond, N. A. 2002. Climate change and control of the southeastern Bering Sea pelagic ecosystem. Deep-Sea Res. Pt. II. 49(26), 5821-5853.

Juul-Pedersen, T., Michel, C., Gosselin, M. 2010. Sinking export of particulate organic material from the euphotic zone in the eastern Beaufort Sea. Mar. Ecol. Prog. Ser. 410, 55-70.

Juul-Pedersen, T., Nielsen, T. G., Michel, C., Moller, E. F., Tiselius, P., Thor, P., Olesen, M., Selander, E., Gooding, S. 2006. Sedimentation following the spring bloom in Disko Bay, West Greenland, with special emphasis on the role of copepods. Mar. Ecol. Prog. Ser. 314, 239-255.

Karl, D. M., Christian, J. R., Dore, J. E., Hebel, D. V., Letelier, R. M., Tupas, L. M., Winn, C. D. 1996. Seasonal and interannual variability in primary production and particle flux at Station ALOHA. Deep-Sea Res. Pt. II. 43(2–3), 539-568.

Krause, J. W., Nelson, D. M., Lomas, M. W. 2009. Biogeochemical responses to late-winter storms in the Sargasso Sea, II: Increased rates of biogenic silica production and export. Deep-Sea Res. Pt. I. 56(6), 861-874.

Lomas, M. W., Bates, N. R., Johnson, R. J., Knap, A. H., Steinberg, D. K., Carlson, C. A. 2013. Two decades and counting: 24-years of sustained open ocean biogeochemical measurements in the Sargasso Sea. Deep-Sea Res. Pt. II. 93(0), 16-32.

Lomas, M. W., Burke, A. L., Lomas, D. A., Bell, D. W., Shen, C., Dyhrman, S. T., Ammerman, J. W. 2010. Sargasso Sea phosphorus biogeochemistry: an important role for dissolved organic phosphorus (DOP). Biogeosciences. 7(2), 695-710.

Lomas, M. W., Moran, S. B., Casey, J. R., Bell, D. W., Tiahlo, M., Whitefield, J., Kelly, R. P., Mathis, J. T., Cokelet, E. D. 2012. Spatial and seasonal variability of primary production on the Eastern Bering Sea shelf. Deep-Sea Res. Pt. II. 65–70(0), 126-140.

Lovvorn, J. R., Cooper, L. W., Brooks, M. L., De Ruyck, C. C., Bump, J. K., Grebmeier, J. M. 2005. Organic matter pathways to zooplankton and benthos under pack ice in late winter and open water in late summer in the north-central Bering Sea. Mar. Ecol. Prog. Ser. 291, 135-150.

Mackey, M. D., Mackey, D. J., Higgins, H. W., Wright, S. W. 1996. CHEMTAX - A program for estimating class abundances from chemical markers: Application to HPLC measurements of phytoplankton. Mar. Ecol. Prog. Ser. 144(1-3), 265-283.

Martiny, A. C., Pham, C. T. A., Primeau, F. W., Vrugt, J. A., Moore, J. K., Levin, S. A., Lomas, M. W. 2013. Strong latitudinal patterns in the elemental ratios of marine plankton and organic matter. Nature Geosci. 6(4), 279-283.

Moran, S. B., Lomas, M. W., Kelly, R. P., Gradinger, R., Iken, K., Mathis, J. T. 2012. Seasonal succession of net primary productivity, particulate organic carbon export, and autotrophic community composition in the eastern Bering Sea. Deep-Sea Res. Pt. II. 65–70, 84-97.

Napp, J. M. and Hunt, G. L. 2001. Anomalous conditions in the south-eastern Bering Sea 1997: linkages among climate, weather, ocean, and Biology. Fish. Oceanogr. 10(1), 61-68.

Niebauer, H. J., Alexander, V., Henrichs, S. M. 1995. A time-series study of the spring bloom at the Bering Sea ice edge I. Physical processes, chlorophyll and nutrient chemistry. Cont. Shelf Res. 15, 1859-1877.

Obayashi, Y., Tanoue, E., Suzuki, K., Handa, N., Nojiri, Y., Wong, C. S. 2001. Spatial and temporal variabilities of phytoplankton community structure in the northern

North Pacific as determined by phytoplankton pigments. Deep-Sea Res. Pt. I. 48(2), 439-469.

Ohashi, R., Yamaguchi, A., Matsuno, K., Saito, R., Yamada, N., Iijima, A., Shiga, N., Imai, I. 2013. Interannual changes in the zooplankton community structure on the southeastern Bering Sea shelf during summers of 1994–2009. Deep-Sea Res. Pt. II. 94, 44-56.

Overland, J. E. and Wang, M. Y. 2007. Future regional Arctic sea ice declines. Geophys. Res. Lett. 34(17), L17705, doi:10.1029/2007GL030308.

Paasche, E. 1973. Silicon and the ecology of marine plankton diatoms. I. *Thalassiosira pseudonana* (*Cyclotella nana*) grown in a chemostat with silicate as limiting nutrient. Mar. Biol. 19(2), 117-126.

Pike, S. M. and Moran, S. B. 1997. Use of Poretics® 0.7 μm pore size glass fiber filters for determination of particulate organic carbon and nitrogen in seawater and freshwater. Mar. Chem. 57(3–4), 355-360.

Rutgers van der Loeff, M., Friedrich, J., Bathmann, U. V. 1997. Carbon export during the Spring Bloom at the Antarctic Polar Front, determined with the natural tracer Th-234. Deep-Sea Res. Pt. II. 44(1-2), 457-478.

Schandelmeier, L. and Alexander, V. 1981. An analysis of the influence of ice on spring phytoplankton population structure in the southeast Bering Sea. Limnol. Oceanogr. 26(5), 935-943.

Sherr, E. B., Sherr, B. F., Ross, C. 2013. Microzooplankton grazing impact in the Bering Sea during spring sea ice conditions. Deep-Sea Res. Pt. II. 94, 57-67.

Siddon, E. C., Heintz, R. A., Mueter, F. J. 2013. Conceptual model of energy allocation in walleye pollock (Theragra chalcogramma) from age-0 to age-1 in the southeastern Bering Sea. Deep-Sea Res. Pt. II. 94, 140-149.

Solorzano, L. and Sharp, J. H. 1980. Determination of total dissolved phosphorus and particulate phosphorus in natural-waters. Limnol. Oceanogr. 25(4), 754-757.

Springer, A. M., McRoy, C. P., Flint, M. V. 1996. The Bering Sea Green Belt: Shelf-edge processes and ecosystem production. Fish. Oceanogr. 5(3-4), 205-223.

Stabeno, P., Napp, J., Mordy, C., Whitledge, T. 2010. Factors influencing physical structure and lower trophic levels of the eastern Bering Sea shelf in 2005: Sea ice, tides and winds. Prog. Oceanogr. 85(3–4), 180-196.

Stabeno, P. J., Farley Jr, V., Kachel, N. B., Moore, S., Mordy, C. W., Napp, J. M., Overland, J. E., Pinchuk, A. I., Sigler, M. F. 2012a. A comparison of the physics

of the northern and southern shelves of the eastern Bering Sea and some implications for the ecosystem. Deep-Sea Res. Pt. II. 65–70(0), 14-30.

Stabeno, P. J., Kachel, N. B., Moore, S. E., Napp, J. M., Sigler, M. F., Yamaguchi, A., Zerbini, A. N. 2012b. Comparison of warm and cold years on the southeastern Bering Sea shelf and some implications for the ecosystem. Deep-Sea Res. Pt. II. 65–70(0), 31-45.

Strickland, J. D. H. and Parsons, T. R. 1968. A Practical Handbook of Seawater Analysis, Fisheries Research Board of Canada Ottawa,

Suzuki, K., Minami, C., Liu, H., Saino, T. 2002a. Temporal and spatial patterns of chemotaxonomic algal pigments in the subarctic Pacific and the Bering Sea during theearly summer of 1999. Deep-Sea Res Pt I. 49, 5685-5704.

Suzuki, K., Minami, C., Liu, H., Saino, T. 2002b. Temporal and spatial patterns of chemotaxonomic algal pigments in the subarctic Pacific and the Bering Sea during the early summer of 1999. Deep-Sea Res. Pt. II. 49(24–25), 5685-5704.

Thibault, D., Roy, S., Wong, C. S., Bishop, J. K. 1999. The downward flux of biogenic material in the NE subarctic Pacific: importance of algal sinking and mesozooplankton herbivory. Deep-Sea Res. Pt. II. 46(11–12), 2669-2697.

Tsukazaki, C., Ishii, K.-I., Saito, R., Matsuno, K., Yamaguchi, A., Imai, I. 2013. Distribution of viable diatom resting stage cells in bottom sediments of the eastern Bering Sea shelf. Deep-Sea Res. Pt. II. 94, 22-30.

Van Heukelem, L. and Thomas, C. S. 2001. Computer-assisted high-performance liquid chromatography method development with applications to the isolation and analysis of phytoplankton pigments. J. Chromatogr. A. 910(1), 31-49.

Wang, M., Overland, J. E., Stabeno, P. 2012. Future climate of the Bering and Chukchi Seas projected by global climate models. Deep-Sea Res. Pt. II. 65–70(0), 46-57.

Wassmann, P., Reigstad, M., Haug, T., Rudels, B., Carroll, M. L., Hop, H., Gabrielsen, G. W., Falk-Petersen, S., Denisenko, S. G., Arashkevich, E., Slagstad, D., Pavlova, O. 2006. Food webs and carbon flux in the Barents Sea. Prog. Oceanogr. 71(2–4), 232-287.

Table 3.1. List of cruises and number of sampling profiles collected during the 2008-2010 NSF-NPRB BEST-BSIERP field program.

Cruise	Season	Vessel	Dates	No. Water Col.	No. Traps
HLY0802	Spring 2008	*USCGC Healy*	March 29 - May 6, 2008	10	3
HLY0803	Summer 2008	*USCGC Healy*	July 3 - July 31, 2008	-	3
HLY0902	Spring 2009	*USCGC Healy*	March 31 - May 12, 2009	18	5
KN195-10	Summer 2009	*R/V Knorr*	June 14 - July 13, 2009	18	4
TN249	Spring 2010	*R/V Thompson*	May 9 - June 14, 2010	18	5
TN250	Summer 2010	*R/V Thompson*	June 16 - July 13, 2010	13	4

Table 3.2. BSIERP domains grouped into 7 larger geographic regions as illustrated in Fig. 3.1.

Grouped Region	BSIERP Domain	
1	10	North Middle Shelf
	11	North Inner Shelf
	12	St. Lawrence
2	8	North Outer Shelf
	9	St. Matthews
3	2	South Inner Shelf
	7	Midnorth Inner Shelf
4	5	Pribilofs
	6	Midnorth Middle Shelf
5	1	AK Peninsula
	3	South Middle Shelf
	4	South Outher Shelf
6	15	Off-shelf North
7	16	Off-shelf Southeast

Table 3.3. Regional averages of mixed layer depth (MLD, m), depth of the photic zone (1% PAR, m), and percent ice at stations within each region (% Ice Cover) together with MLD averages of temperature (°C), salinity (‰), density (σ_t, Densit – 1000 kg m^{-3}), dissolved oxygen (DO, µmol kg^{-1}), and dissolved oxygen saturation from equilibrium (ΔDO Saturation, µmol kg^{-1}).

Region	*n*	MLD	1% PAR	% Ice Cover	Temperature	Salinity	σ_t	DO	ΔDO Saturation
		m	m		°C	‰	kg m^{-3}	µmol kg^{-1}	µmol kg^{-1}
Spring									
1	10	36 ± 20	29 ± 8	69 ± 48	-1.32 ± 1.12	32.06 ± 0.44	25.78 ± 0.40	338.85 ± 20.78	-30.02 ± 28.54
2	17	46 ± 19	23 ± 11	43 ± 41	-1.40 ± 0.48	31.99 ± 0.25	25.72 ± 0.21	373.50 ± 39.13	3.77 ± 43.07
3	2	33 ± 8	28 ± 7	49 ± 70	-0.70 ± 1.16	31.16 ± 0.37	25.02 ± 0.34	364.52 ± 16.30	-1.03 ± 26.03
4	9	40 ± 23	26 ± 10	38 ± 47	-1.05 ± 0.93	31.51 ± 0.45	25.32 ± 0.39	366.51 ± 27.46	-1.30 ± 33.15
5	2	38 ± 5	16 ± 0	0	1.14 ± 0.40	31.58 ± 0.02	25.28 ± 0.03	376.87 ± 3.77	29.85 ± 6.67
6	5	23 ± 20	22 ± 18	7 ± 17	-0.51 ± 1.42	32.32 ± 0.41	25.96 ± 0.38	384.42 ± 44.60	24.00 ± 49.42
7	2	43 ± 25	15	0	1.92 ± 1.38	32.44 ± 0.12	25.91 ± 0.18	329.74 ± 10.69	-8.40 ± 20.79
Summer									
1	4	26 ± 13	30 ± 9	0	3.43 ± 1.68	31.17 ± 0.40	24.83 ± 0.23	341.19 ± 26.21	12.06 ± 13.52
2	5	17 ± 7	29 ± 5	0	5.28 ± 0.80	31.61 ± 0.75	25.00 ± 0.57	326.15 ± 10.76	12.82 ± 12.71
3	3	25 ± 14	23 ± 9	0	3.52 ± 0.30	31.27 ± 0.23	24.93 ± 0.18	347.93 ± 33.30	20.29 ± 33.39
4	6	24 ± 6	29 ± 4	0	4.43 ± 1.20	31.54 ± 0.39	25.00 ± 0.25	340.51 ± 9.10	20.40 ± 3.45
5	5	19 ± 6	31 ± 8	0	5.06 ± 1.40	31.64 ± 0.12	25.03 ± 0.09	330.88 ± 12.01	15.80 ± 5.10
6	4	22 ± 5	32 ± 8	0	6.05 ± 0.57	32.75 ± 0.13	25.81 ± 0.15	321.90 ± 13.73	16.85 ± 11.85
7	5	29 ± 25	32 ± 5	0	5.79 ± 0.38	32.60 ± 0.14	25.69 ± 0.11	312.84 ± 7.33	5.69 ± 6.94

Table 3.4. Regional averages of primary pigment concentrations (μg L^{-1}) in the upper water column: total chlorophyll *a* (TChl *a*), fucoxanthin, total chlorophyll *b* (TChl *b*), 19'-Hexanoyloxyfucoxanthin, (19'-Hex), Pheophytin *a*, and Pheophorbide *a*.

Region	TChl *a* μg L^{-1}	Fucoxanthin μg L^{-1}	TChl *b* μg L^{-1}	19'-Hex μg L^{-1}	Pheophytin *a* μg L^{-1}	Pheophorbide *a* μg L^{-1}
Spring						
1	0.7396 ± 1.4725	0.2580 ± 0.5638	0.0188 ± 0.0188	0.0033 ± 0.0047	0.0144 ± 0.0277	0.0292 ± 0.0714
2	8.8680 ± 10.9241	3.5913 ± 4.3042	0.0235 ± 0.0197	0.0030 ± 0.0020	0.1364 ± 0.1325	0.6277 ± 1.3799
3	0.2237 ± 0.1891	0.0774 ± 0.0776	0.0158 ± 0.0061	0.0010 ± 0	0.0158 ± 0.0100	0.0307 ± 0.0283
4	1.7245 ± 2.4198	0.7268 ± 1.2023	0.0313 ± 0.0354	0.0029 ± 0.0025	0.0587 ± 0.1434	0.4247 ± 1.2078
5	5.2613 ± 3.7644	2.1002 ± 1.8099	0.0500 ± 0.0197	0.0043 ± 0.0039	0.0743 ± 0.0600	0.3592 ± 0.0755
6	4.7214 ± 6.3560	2.0296 ± 2.8384	0.0256 ± 0.0182	0.0188 ± 0.0201	0.1422 ± 0.1899	0.4339 ± 0.5948
7	1.7345 ± 1.5323	0.6828 ± 0.6302	0.0962 ± 0.0672	0.0226 ± 0.0181	0.0185 ± 0.0138	0.4185 ± 0.4121
Summer						
1	0.4012 ± 0.9705	0.1519 ± 0.4134	0.0182 ± 0.0170	0.0029 ± 0.0033	0.0035 ± 0.0092	0.0163 ± 0.0423
2	0.8783 ± 1.1486	0.1635 ± 0.2112	0.0743 ± 0.0555	0.1766 ± 0.3692	0.0115 ± 0.0212	0.0299 ± 0.0766
3	0.5295 ± 0.2130	0.1593 ± 0.0859	0.0322 ± 0.0211	0.0056 ± 0.0026	0.0115 ± 0.0094	0.0431 ± 0.0506
4	0.5699 ± 0.3684	0.1265 ± 0.0981	0.0598 ± 0.0424	0.0254 ± 0.0613	0.0124 ± 0.0147	0.0384 ± 0.0630
5	0.4446 ± 0.3836	0.1284 ± 0.1503	0.0238 ± 0.0193	0.0078 ± 0.0086	0.0066 ± 0.0072	0.0534 ± 0.0747
6	0.5807 ± 0.3318	0.0842 ± 0.0612	0.0320 ± 0.0220	0.1625 ± 0.1401	0.0088 ± 0.0101	0.0069 ± 0.0106
7	0.5379 ± 0.3096	0.1158 ± 0.0694	0.0400 ± 0.0500	0.0412 ± 0.0318	0.0143 ± 0.0121	0.0272 ± 0.0203

Table 3.5. Station averages of upper water column particulate organic carbon (POC), particulate organic nitrogen (PON), particulate organic phosphorus (POP), and biogenic silica (bSi). All units in μmol L^{-1}.

Station No.	Station ID	*n*	POC	PON	POP	bSi
			μmol L^{-1}	μmol L^{-1}	μmol L^{-1}	μmol L^{-1}
HLY0902						
85	BL15	7				8.20 ± 3.30
90	BL20	7				11.75 ± 1.51
115	BL21	7				18.47 ± 6.83
TN249						
7	NP12	3				1.96 ± 0.37
24	Z15	3	70.06 ± 18.53	5.88 ± 2.53		10.85 ± 3.30
39	IE1	3	39.40 ± 13.40	3.74 ± 1.45		6.79 ± 4.72
49	MN19	4	62.05 ± 60.89	5.35 ± 4.67		16.03 ± 4.79
50	MN19	3	126.60 ± 7.15	10.89 ± 0.47		
55	NZ11.5	7	6.58 ± 2.86	1.09 ± 0.42	0.08 ± 0.02	1.27 ± 0.38
66	NZ4.5	3	56.40 ± 6.44	3.19 ± 0.54	0.34 ± 0.03	9.02 ± 0.68
71	HBR1	3	100.32 ± 56.58	7.27 ± 3.57	0.69 ± 0.14	16.03 ± 3.61
81	70M26	3	21.93 ± 2.16	1.25 ± 0.19	0.17 ± 0.03	5.48 ± 0.91
87	CN17	7	20.84 ± 10.17	1.43 ± 5.29	0.35 ± 0.12	2.93 ± 1.37
99	70M4	3	46.11 ± 33.62	5.81 ± 4.10		6.49 ± 0.51
124	70M29	3	9.97 ± 4.45	1.75 ± 0.32	0.13 ± 0.01	1.89 ± 0.92
147	70M52	3	15.17 ± 14.70	2.63 ± 2.42	0.20 ± 0.14	2.95 ± 2.72
156	SL12	3	10.96 ± 11.61	1.31 ± 1.56	0.17 ± 0.12	1.82 ± 1.50
163	MN19	7	29.38 ± 14.83	3.16 ± 2.30	0.24 ± 0.17	1.80 ± 0.80
175	MN8	3	11.15 ± 2.00	1.54 ± 0.23	0.21 ± 0.13	1.49 ± 0.73
179	NP3	7	11.43 ± 3.04	1.96 ± 0.45	0.16 ± 0.06	1.58 ± 0.95
TN250						
8	UAP5	4	12.93 ± 1.62	1.82 ± 0.20	0.22 ± 0.05	1.55 ± 0.06
20	CN8	3	12.05 ± 5.24	2.55 ± 1.08	0.14 ± 0.05	2.07 ± 1.91
25	CN17	7	11.57 ± 1.43	2.39 ± 0.23	0.26 ± 0.10	1.02 ± 0.14
32	CNN4	3	15.26 ± 1.88	2.36 ± 0.76	0.21 ± 0.03	1.69 ± 1.16
47	NP9	3	16.94 ± 5.41	1.79 ± 1.58	0.14 ± 0.01	1.79 ± 1.76
53	TD2	6	13.60 ± 4.18	1.82 ± 0.67	0.19 ± 0.05	0.90 ± 0.28
67	TR3	7	11.20 ± 3.17	1.12 ± 0.28	0.11 ± 0.02	0.33 ± 0.06
82	MN1	3	14.57 ± 0.57	1.98 ± 0.20	0.27 ± 0.04	5.55 ± 0.99
97	MN16	3	14.24 ± 10.70	2.02 ± 1.79	0.26 ± 0.31	1.22 ± 1.73
103	TR4	6	11.65 ± 4.13	2.08 ± 1.06	0.17 ± 0.08	1.11 ± 0.33
122	ML3	3	5.52 ± 13.72	1.94 ± 1.46	0.14 ± 0.08	1.68 ± 2.15
145	BN3	4	6.82 ± 2.39	1.33 ± 0.80	0.08 ± 0.01	0.29 ± 0.06
167	70M39	3	8.52 ± 0.93	1.16 ± 0.24	0.07 ± 0.02	0.88 ± 1.05
197	70M9	3	12.27 ± 2.45	2.16 ± 0.90	0.17 ± 0.09	1.25 ± 1.53

Table 3.6. Sediment trap profiles of primary pigment (mg m^{-2} d^{-1}) and particulate fluxes (mmol m^{-2} d^{-1}): total chlorophyll *a* (TChl *a*), fucoxanthin , Pheophytin *a*, Pheophorbide *a*, particulate organic carbon (POC), particulate organic nitrogen (PON), particulate organic phosphorus (POP), and biogenic silica (bSi).

Station/Depth m	TChl *a* mg m^{-2} d^{-1}	Fucoxanthin mg m^{-2} d^{-1}	Pheophytin *a* mg m^{-2} d^{-1}	Pheophorbide *a* mg m^{-2} d^{-1}	POC mmol m^{-2} d^{-1}	PON mmol m^{-2} d^{-1}	POP mmol m^{-2} d^{-1}	bSi mmol m^{-2} d^{-1}
HLY0802								
T1-25	0.194	0.038	0.006	0.026	1.92	0.49		
40	0.226	0.053	0.007	0.039	1.67	0.43		
50	0.224	0.059	0.009	0.047	4.94	0.72		
60	0.227	0.071	0.011	0.052	2.02	0.49		
100	0.138	0.045	0.007	0.039	4.05	0.72		
T2-25	0.221	0.034	0.005	0.020	7.58	1.35		
40	0.097	0.062	0.002	0.014	3.03	0.69		
50	0.227	0.024	0.007	0.030	5.20	1.01		
60	0.128	0.033	0.002	0.014	3.39	0.69		
100	0.151	0.052	0.012	0.025	4.22	0.75		
T3-25	2.832	1.007	0.369	3.997	8.91	0.60		
40	1.980	1.042	0.155	2.583	7.67	1.35		
50	3.145	0.671	0.390	6.086	7.37	1.29		
60	1.150	0.388	0.105	1.489	6.21	1.18		
100	1.436	0.509	0.099	2.988	5.36	1.15		
HLY0803								
PIT1-40	0.015	0.009	0.153	0.194	22.30	3.04		
60	0.019	0.009	0.134	0.172	14.43	2.07		
100	0.015	0.009	0.102	0.173	19.14	2.48		
PIT2-40	0.039	0.010	0.010	0.091	9.00	1.27		
60	0.027	0.012	0.009	0.084	9.57	1.21		
100	0.021	0.011	0.010	0.065	8.17	0.95		
PIT3-40	0.079	0.033	0.026	0.592	14.52	2.02		
60	0.047	0.026	0.030	0.458	13.44	1.93		
100	0.031	0.019	0.018	0.183	7.98	0.96		
HLY0902								
NP15-25	0.165	0.041	0.009	0.058	9.64	1.47		
50	0.182	0.074	0.014	0.099	10.52	1.52		
100	0.163	0.110	0.020	0.105	11.00	1.19		
BL2-25	36.886	13.205	0.723	3.911	46.56	7.91		
50	7.570	2.795	0.247	1.788	17.07	2.55		
100	4.275	1.671	0.152	1.149	28.55	3.65		
BL15-25	113.536	22.407	1.532	7.405	66.30	10.92		9.58
50	17.558	4.182	0.255	1.548	36.46	5.19		6.86
100	24.258	5.242	0.354	1.833	40.89	5.46		10.27
BL15-1-25	44.857	8.589	0.912	6.026	60.71	10.85		26.03
50	16.382	3.262	0.324	2.374	28.74	4.93		7.32
100	10.536	2.217	0.185	1.475	44.22	6.19		45.35
B:21-25	72.354	30.664	1.071	13.837	272.91	40.32		
50	7.761	3.214	0.202	1.778	77.64	9.64		
100	5.954	2.513	0.214	1.656	108.15	13.92		

KN195-10								
CN17-25	0.543	0.086	0.067	0.343	42.10	4.32		
50	0.623	0.104	0.103	0.858	40.64	4.19		
100	0.383	0.059	0.062	0.564	38.54	3.74		
NP15-25	0.147	0.063	0.052	0.714	25.31	3.75		
50	0.200		0.142	0.992	48.12	5.00		
100	0.229	0.065	0.132	1.071	29.60	2.45		
P14-7-25	0.326	0.101	0.155	0.939	20.58	2.97		
50	0.314	0.103	0.283	1.332	21.89	2.57		
100	0.295	0.136	0.224	2.140	23.11	2.65		
TN249								
MN19-25	3.024	2.169	1.576	9.565	73.71	8.97		46.21
50	4.512	1.886	1.929	7.941	43.50	6.16		34.27
100	3.052	1.239	1.561	4.933	48.07	5.91		42.18
NZ11.5-25	0.525	0.175	0.171	0.607	19.35	3.76	0.12	18.81
50	0.529	0.157	0.283	0.714	20.29	3.96	0.12	17.72
100	0.518	0.186	0.309	0.583	11.55	2.74	0.11	24.36
CN17-25	1.951	0.729	0.156	7.360	39.47	6.48	0.22	18.53
50	0.566	0.183	0.077	5.251	15.27	2.79	0.23	11.81
100	0.464	0.162	0.073	3.067	2.71	1.17	0.24	9.95
MN19-2-25	0.704	0.289	0.143	1.243	15.48	2.49	0.36	10.55
50	0.669	0.208	0.200	1.578	15.75	2.95	0.11	8.49
100	0.416	0.119	0.158	1.187	13.58	2.61	0.07	8.28
NP14-25	1.403	0.522	0.146	16.700	24.62	5.40	0.11	42.41
50	0.917	0.326	0.090	10.941	2.08	1.62	0.16	26.07
100	0.466	0.184	0.063	7.844	4.71	3.03	0.06	21.17
TN250								
CN17-25	0.524	0.112	0.065	0.210	113.45	14.15	0.54	7.14
50	1.158	0.166	0.275	0.785	81.04	8.98	0.43	11.36
100	1.713	0.287	0.426	1.810	69.12	7.38	0.42	18.40
NP14-25	0.283	0.084	0.066	0.182	30.64	3.01	0.19	6.25
50	0.365	0.095	0.089	0.488	30.50	2.22	0.22	6.75
100	0.707	0.189	0.217	1.784	39.58	3.12	0.07	21.56
P14-7-25	0.099	0.031	0.020	0.075	21.72	2.47	0.04	1.69
50	0.066	0.021	0.041	0.166	15.48	1.41	0.15	3.65
100	0.141	0.032	0.055	0.176	19.11	1.09	0.10	1.82
MN19-25	0.167	0.070	0.088	0.065	24.89	2.89	0.15	4.38
50	0.209	0.174	0.394	0.002	17.26	1.83	0.03	5.04
100	0.250	0.150	0.889	0.001	11.83	1.00	0.23	5.98

Table 3.7. Regional averages of percent contribution by algal group to total chlorophyll *a*.

Region	Diatoms	Prymnesiophytes	Pelagophytes	Chlorophytes	Prasinophytes	Cryptophytes	Dinoflagellates	Cyanobacteria
Spring								
1	77.57 ± 17.67	2.91 ± 3.31	1.91 ± 2.11	9.96 ± 10.74	1.36 ± 1.58	4.07 ± 3.15	1.70 ± 1.89	0.52 ± 0.64
2	88.01 ± 18.43	1.61 ± 2.78	1.16 ± 2.10	4.35 ± 6.67	1.06 ± 2.10	2.34 ± 3.55	1.12 ± 1.85	0.34 ± 0.74
3	71.45 ± 10.77	1.23 ± 0.53	2.41 ± 1.20	12.44 ± 3.55	0.84 ± 0.41	7.18 ± 3.56	2.92 ± 3.25	1.53 ± 1.16
4	85.38 ± 14.17	1.83 ± 2.76	0.95 ± 0.83	7.22 ± 7.51	0.83 ± 1.04	2.69 ± 2.36	0.83 ± 0.85	0.28 ± 0.44
5	95.67 ± 2.08	0.29 ± 0.03	0.18 ± 0.28	1.96 ± 0.97	0.20 ± 0.06	1.47 ± 0.90	0.17 ± 0.05	0.06 ± 0.06
6	79.95 ± 18.63	7.77 ± 8.86	2.11 ± 2.45	4.94 ± 4.42	0.62 ± 0.90	3.02 ± 3.45	1.47 ± 1.91	0.12 ± 0.17
7	65.79 ± 26.53	5.58 ± 3.85	1.96 ± 1.43	19.11 ± 16.61	1.03 ± 1.41	4.08 ± 2.51	2.17 ± 1.40	0.28 ± 0.41
Summer								
1	50.21 ± 34.72	6.66 ± 6.10	2.73 ± 2.39	27.11 ± 23.77	2.35 ± 2.43	6.51 ± 7.65	2.34 ± 1.85	2.10 ± 2.16
2	37.83 ± 24.10	18.52 ± 28.38	1.61 ± 1.70	34.94 ± 26.32	1.99 ± 2.64	3.14 ± 2.26	1.55 ± 2.60	0.42 ± 0.55
3	74.44 ± 10.48	4.31 ± 4.62	4.06 ± 4.13	9.10 ± 3.48	2.73 ± 1.61	3.70 ± 2.32	1.10 ± 1.46	0.56 ± 0.77
4	54.38 ± 26.01	12.87 ± 25.73	2.01 ± 1.99	22.30 ± 16.81	3.25 ± 4.07	3.31 ± 3.73	1.40 ± 1.65	0.47 ± 0.88
5	63.44 ± 23.73	5.47 ± 6.32	1.46 ± 1.81	17.95 ± 17.69	2.12 ± 3.29	6.92 ± 7.27	2.42 ± 3.66	0.23 ± 0.25
6	24.43 ± 20.62	54.48 ± 31.09	3.02 ± 1.09	13.53 ± 18.08	0.68 ± 0.85	3.04 ± 3.71	0.57 ± 0.55	0.25 ± 0.29
7	49.46 ± 28.58	27.11 ± 23.23	3.01 ± 2.10	9.18 ± 10.95	1.66 ± 1.89	8.39 ± 8.16	0.71 ± 0.49	0.49 ± 0.49

Table 3.8. Algal group percent contribution to the flux of total chlorophyll *a* through the water column.

Station/Depth m	Diatoms	Prymnesiophytes	Pelagophytes	Chlorophytes	Prasinophytes	Cryptophytes	Dinoflagellates	Cyanobacteria
HLY0802								
T1-25	57.17	1.66	8.40	22.48	5.58	0.23	4.48	0
40	51.94	1.87	8.83	28.19	1.00	0.19	7.97	0
50	43.37	1.97	9.12	28.01	8.85	0.16	8.52	0
60	44.04	2.35	10.95	28.89	1.70	0.15	11.91	0
100	45.89	2.42	10.60	26.68	1.95	0.17	12.28	0
T2-25	72.03	1.68	4.01	13.24	0.93	0.22	7.61	0.29
40	74.32	1.14	2.06	8.15	1.09	0.07	12.44	0.73
50	75.26	1.60	3.56	8.46	0.50	0.14	10.49	0
60	75.07	1.59	3.40	8.67	0.74	0.15	10.38	0
100	72.90	1.50	4.30	9.05	0.59	0.07	11.59	0
T3-25	97.02	0.05	0.29	1.61	0.36	0.03	0.51	0.13
40	97.13	0.04	0.63	0.60	0.48	0.02	0.82	0.27
50	97.70	0.07	0.00	1.63	0.38	0.02	0.10	0.10
60	97.39	0.07	0.02	1.63	0.43	0.02	0.19	0.24
100	97.66	0.09	0.02	1.52	0.37	0.02	0.14	0.17
HLY0803								
PIT1-40	39.98	4.84	1.58	45.31	3.23	0.44	2.84	1.78
60	38.21	3.81	1.35	50.86	2.10	0.45	2.40	0.83
100	44.52	5.80	1.65	37.76	4.08	0.51	3.09	2.60
PIT2-40	70.44	1.36	0.67	24.23	0.99	0.90	1.12	0.29
60	72.35	2.14	0.88	19.84	2.61	1.10	0.97	0.12
100	72.51	2.59	1.10	19.35	1.80	0.61	1.35	0.70
PIT3-40	81.53	2.48	0.31	13.76	0	1.91	0	0
60	83.47	2.27	0.47	11.69	0	2.09	0	0
100	82.18	4.04	0.71	8.74	0	1.17	0.06	3.10
HLY0902								
NP15-25	53.60	1.90	7.66	24.83	0.73	0.20	11.08	0
50	27.27	4.21	13.81	26.64	1.09	0.30	26.67	0
100	0	6.33	20.07	26.43	1.42	0.26	45.50	0
BL2-25	98.67	0	0.01	0.07	0.42	0.00	0.44	0.40
50	98.91	0	0.01	0.06	0.42	0.01	0.14	0.45
100	98.44	0	0.02	0.04	0.34	0.02	0.09	1.05
BL15-25	98.84	0	0.02	0.07	0.39	0	0.39	0.29
50	98.44	0	0.02	0.09	0.49	0	0.49	0.47
100	98.23	0	0.02	0.09	0.54	0.01	0.51	0.60
BL15-1-25	98.60	0	0.01	0.07	0.40	0	0.49	0.42
50	98.65	0	0.02	0.06	0.41	0	0.47	0.38
100	98.80	0	0.03	0.04	0.34	0.01	0.35	0.43
B:21-25	99.54	0	0.03	0.01	0.17	0	0.13	0.12
50	99.51	0	0.03	0.01	0.15	0	0.21	0.09
100	98.98	0	0.03	0	0.46	0	0.22	0.30

KN195-10								
CN17-25	92.55	0.48	0.52	3.20	0.68	0.03	0.48	2.07
50	95.48	0.37	0.00	0.21	0.74	0.01	0.43	2.78
100	94.69	0.36	0.00	0.20	0.71	0.03	0.40	3.60
NP15-25	89.43	1.81	0.21	0.17	0.55	0.07	0.28	7.47
50	83.89	1.51	2.87	0	4.18	0.09	0.32	7.13
100	82.13	1.83	3.77	0	4.98	0.01	0.11	7.17
P14-7-25	83.37	4.59	2.77	1.90	0.77	0.05	1.28	5.26
50	84.87	3.25	3.29	0	0	0.06	0	8.53
100	76.44	2.50	6.53	1.08	0	0.07	0	13.39
TN249								
MN19-25	99.51	0.00	0.12	0.04	0.14	0.00	0.07	0.11
50	99.60	0.00	0.03	0.01	0.17	0.00	0.01	0.19
100	99.96	0.02	0.02	0.00	0.00	0.00	0.00	0
NZ11.5-25	91.06	1.30	0.03	3.61	0.67	0.05	2.02	1.25
50	93.10	0.71	0.02	4.08	0.50	0.05	1.36	0.19
100	95.51	0.48	0.04	1.99	0.36	0.03	1.38	0.21
CN17-25	97.64	0.11	0.01	2.18	0	0.05	0	0
50	95.88	0.24	0.01	3.73	0.03	0.11	0	0
100	95.79	0.24	0.02	3.74	0.09	0.11	0	0
MN19-2-25	97.21	0.11	0.04	2.06	0.23	0.03	0.15	0.16
50	96.59	0.24	0.00	2.15	0.20	0.04	0.65	0.12
100	96.45	0.53	0.00	2.95	0.00	0.07	0	0
NP14-25	99.76	0.17	0	0	0	0.07	0	0
50	98.80	0.20	0.00	0.96	0	0.05	0	0
100	99.23	0.18	0.01	0.52	0	0.06	0	0
TN250								
CN17-25	97.37	0.10	0	0.17	0.70	0.02	0.93	0.70
50	91.28	0.19	0	0.17	0.62	0.00	0.81	6.94
100	98.40	0.29	0	0.12	0.44	0.00	0.26	0.49
NP14-25	92.22	0.40	1.01	3.58	0.28	0.09	1.10	1.33
50	86.20	0.60	2.01	6.92	0.16	0.15	1.34	2.63
100	92.93	0.84	5.32	0	0.72	0.11	0.03	0.05
P14-7-25	67.17	4.55	6.62	13.72	0.89	0.24	4.23	2.58
50	47.74	4.11	6.26	20.21	0	0.67	3.83	17.19
100	68.43	7.23	7.33	9.91	0.67	0.19	0.37	5.86
MN19-25	84.07	0.66	1.17	6.97	1.08	0.09	2.66	3.30
50	89.78	0.73	1.82	3.50	0.26	0.08	0.98	2.86
100	92.89	0.49	1.29	2.72	0.22	0.05	0.09	2.24

Table 3.9. Photic zone stock of particulate organic carbon (POC, mmol m^{-2}), total chlorophyll *a* (TChl *a*, mg m^{-2}), pheopigment sum (Σpheopigment, Pheophytin *a* + Pheophorbide *a*, mg m^{-2}), and fucoxanthin (mg m^{-2}) together with daily loss rates and fraction of total POC flux associated with TChl *a* (F Chl *a* (C)) and pheopigments (F pheo (C)).

Cruise	Station	1% PAR	Photic zone stock				Loss due to flux					
			POC	TChl *a*	Σpheopigment	Fucoxanthin	POC	TChl *a*	Σpheopigment	Fucoxanthin	F Chl *a* (C)	F pheo (C)
		m	mmol m^{-2}	mg m-2	mg m-2	mg m-2	% d^{-1}	% d^{-1}	% d^{-1}	% d^{-1}	% of C Flux	% of C Flux
HLY0802	NP15	100		13.7		1.8		1.6		26.2		
	ZZ15	26		28.2	6.5	8.1		11.2	99.7	21.3		
HLY0902	BL2	38		557.4	12.5	200.2		1.4	16.3	36.9	49.6	14.9
	BL15	38		535.1	10.4	200.2		3.3	17.3	23.8	20.6	6.2
	BL15-1	38		535.1	10.4	200.2		3.1	25.9	19.9	39.1	11.7
	BL21	33		1051.3	39.6	432.0		0.7	5.0	41.4	10.6	3.2
KN195-10	NP15	20		4.4	0.5	1.4		4.5			9.8	2.9
	MN19	23	917.3	17.3		2.7						
TN249	MN19	75	3641.6	905.8	109.2	395.1	1.2	0.5	9.0	41.8	94.5	28.3
	NZ11.5	60	385.0	20.8	4.1	6.5	5.3	2.5	24.5	29.7	20.4	6.1
	CN17	32	623.0	74.3	18.3	29.9	2.5	0.8	29.1	32.3	145.3	43.6
	MN19-2	40	1496.5	47.0	7.1	19.1	1.1	1.4	25.1	31.0	47.0	14.1
TN250	CN17	23	255.4	18.0	1.9	4.2	31.7	6.5	55.6	14.3	5.4	1.6
	NP14	33	450.5	21.8	1.3	4.9	6.8	1.7	44.5	25.9	7.9	2.4
	P14-7	38	425.0	20.3	0.9	3.1	3.6	0.3	24.3	32.1	5.6	1.7
	MN19	46	501.0	16.9	1.0	5.7	3.4	1.2	37.8	83.6	9.5	2.9

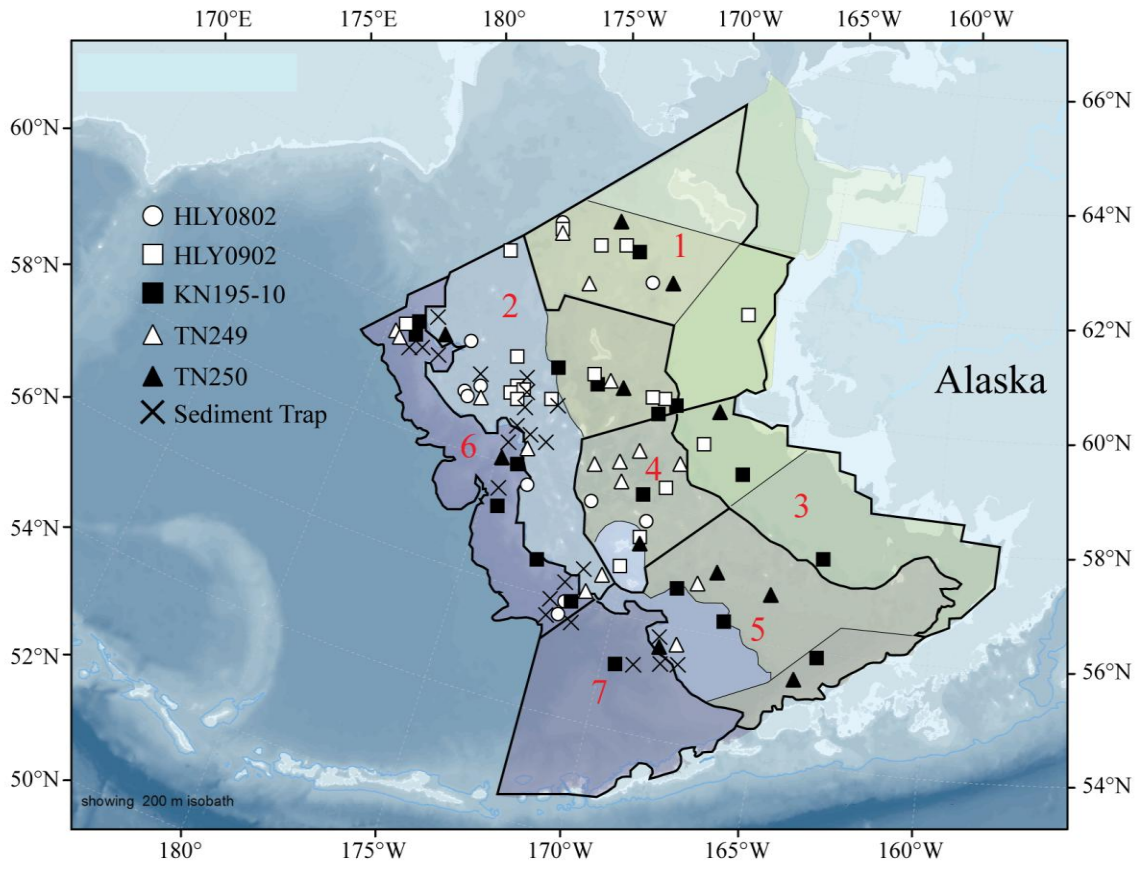

Figure 3.1. Map of the eastern Bering Sea study area. Thin lines delineate the regions designated during the BEST-BSIERP program. Bold lines represent the seven larger geographic regions used for data interpretation in this study. Listed in Table 2 are the BEST-BSIERP regions grouped in this study. White (spring) and black (summer) symbols represent water column sampling locations during the field study (see Table 1 for cruise information). Cross symbols are sediment trap deployment locations.

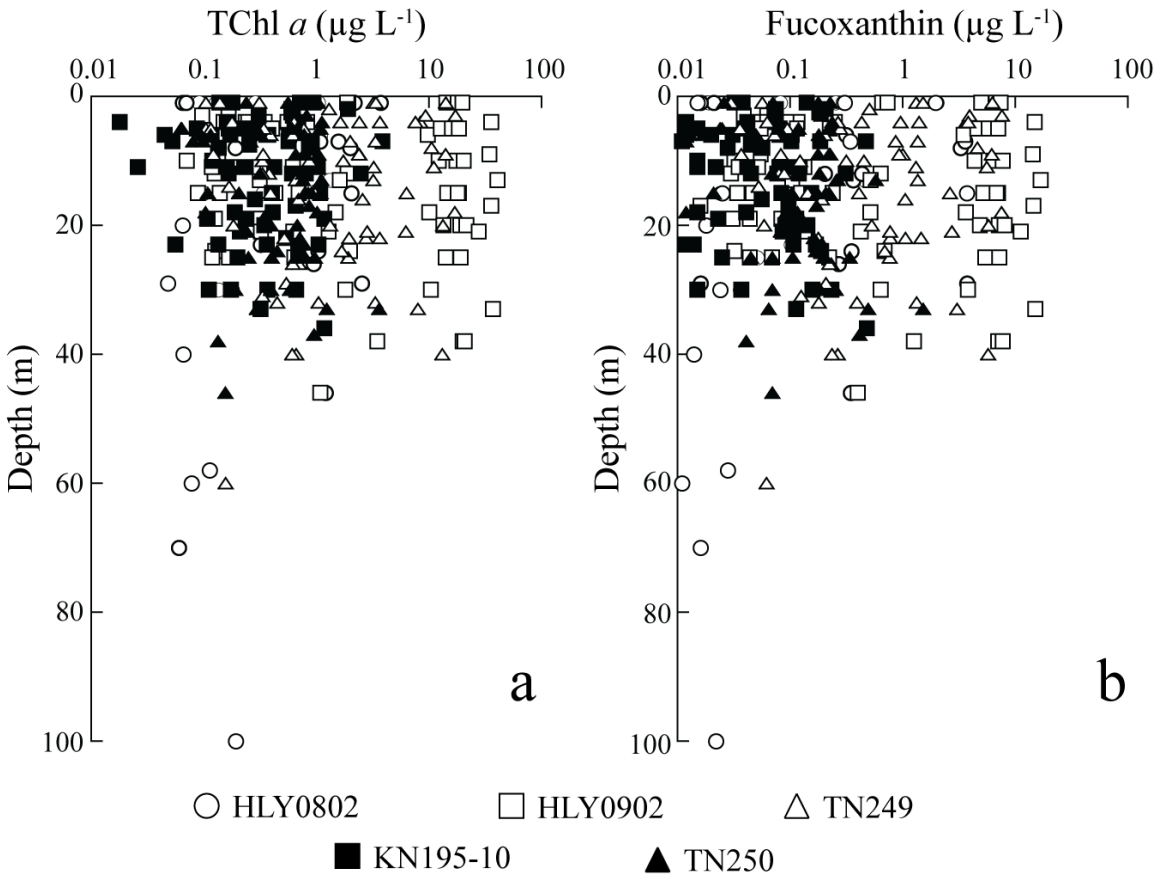

Figure 3.2. Depth profiles of total chlorophyll *a* and fucoxanthin (µg L^{-1}). Open (spring) and shaded (summer) symbols correspond to specific cruises listed on the figure.

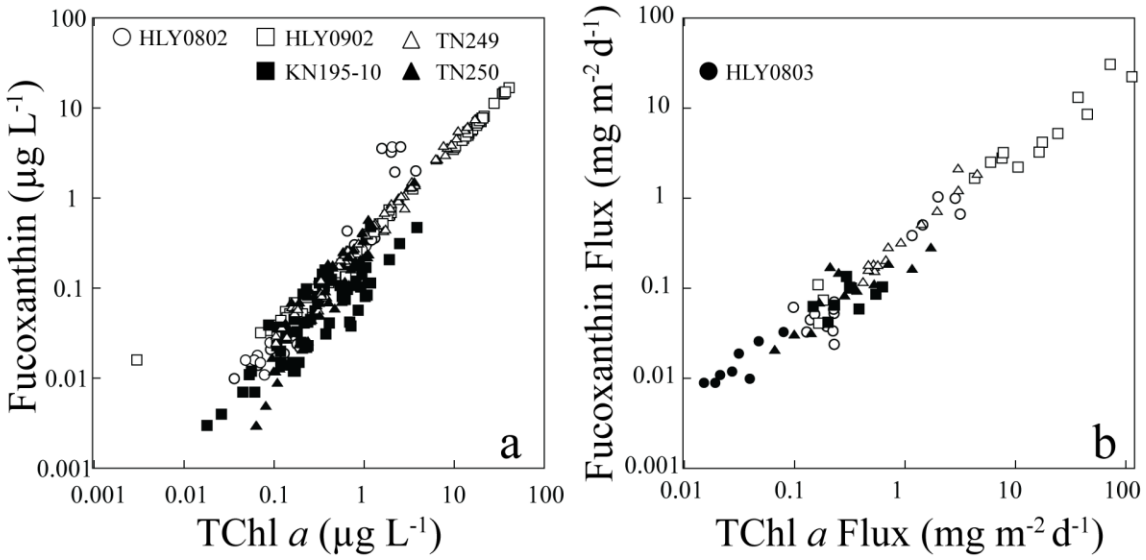

Figure 3.3. Relationship between water column concentrations (a) and sediment trap fluxes (b) of total chlorophyll *a* and fucoxanthin (a: µg L^{-1}, b: mg m^{-2} d^{-1}).

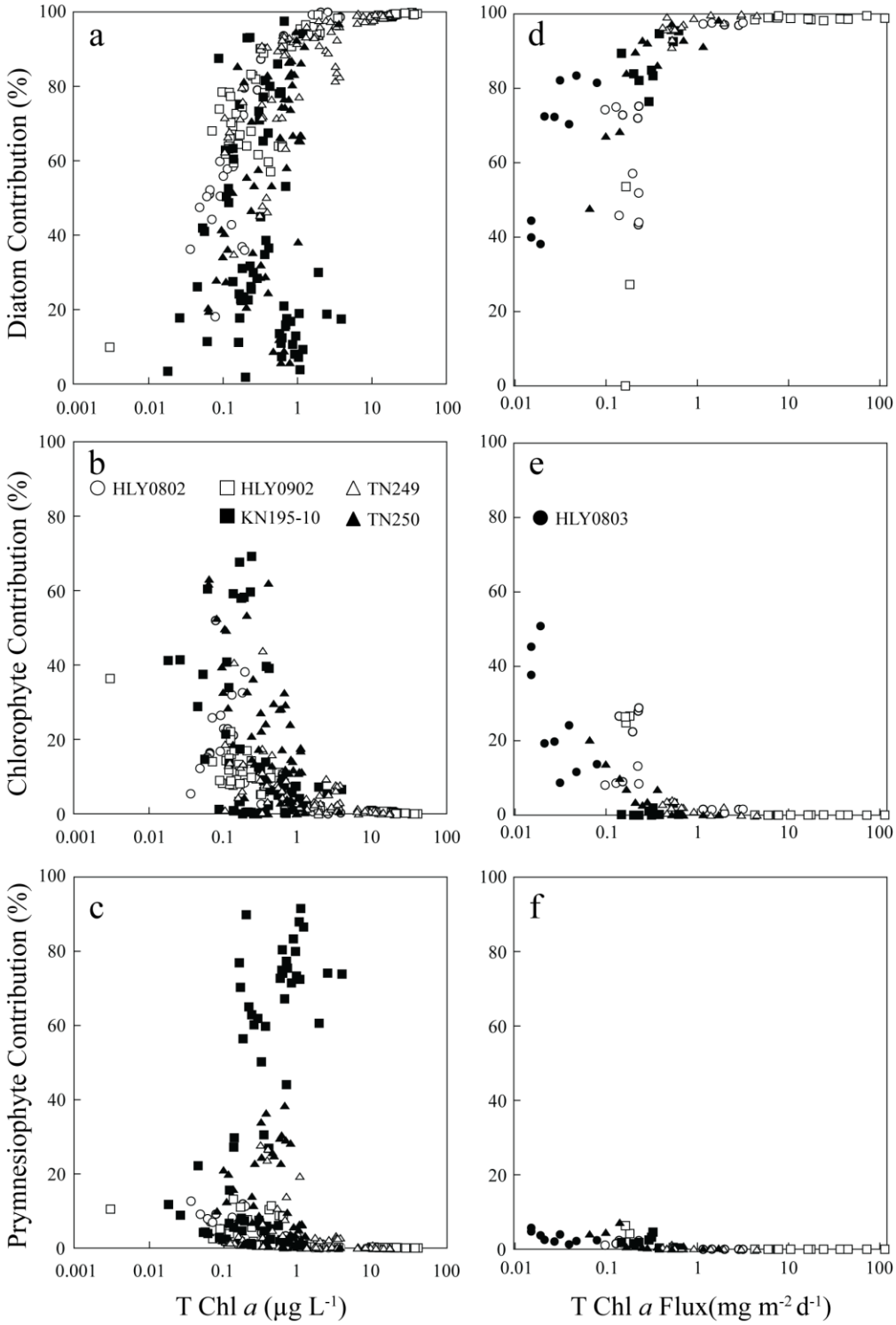

Figure 3.4. Percent contribution to total ambient chlorophyll *a* (a-c) and total chlorophyll *a* flux (d-f) for diatoms (a and d), chlorophytes (b and e), and prymnesiophytes (c and f).

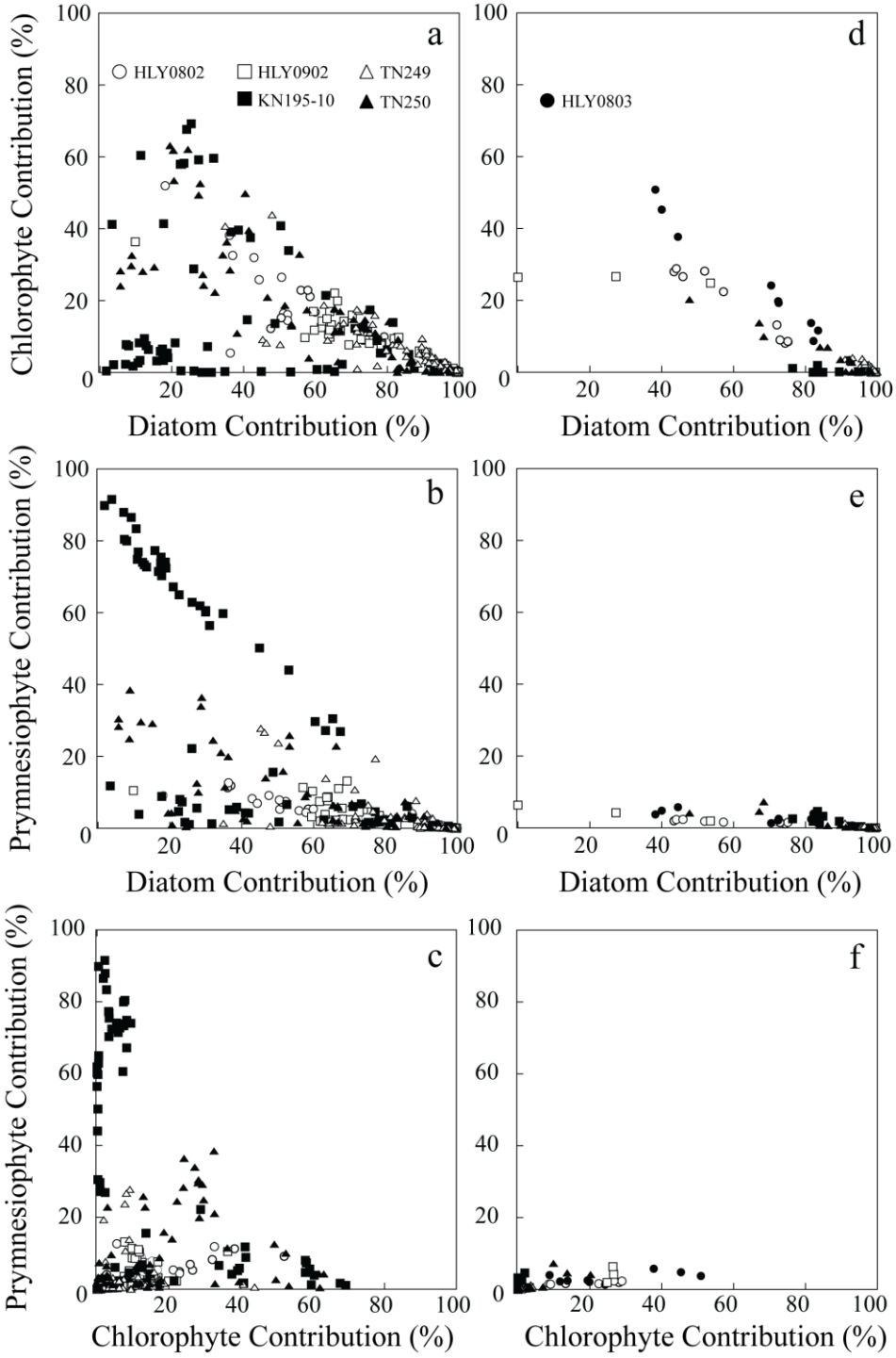

Figure 3.5. Chlorophyte and prymnesiophyte contribution versus diatom contribution to total chlorophyll *a* (a: chlorophytes, b: prymnesiophytes) and total chlorophyll a flux (d: chlorophytes, e: prymnesiophytes). Prymnesiophyte contribution versus chlorophyte contribution for water column total chlorophyll *a* (c) and total chlorophyll *a* flux (f).

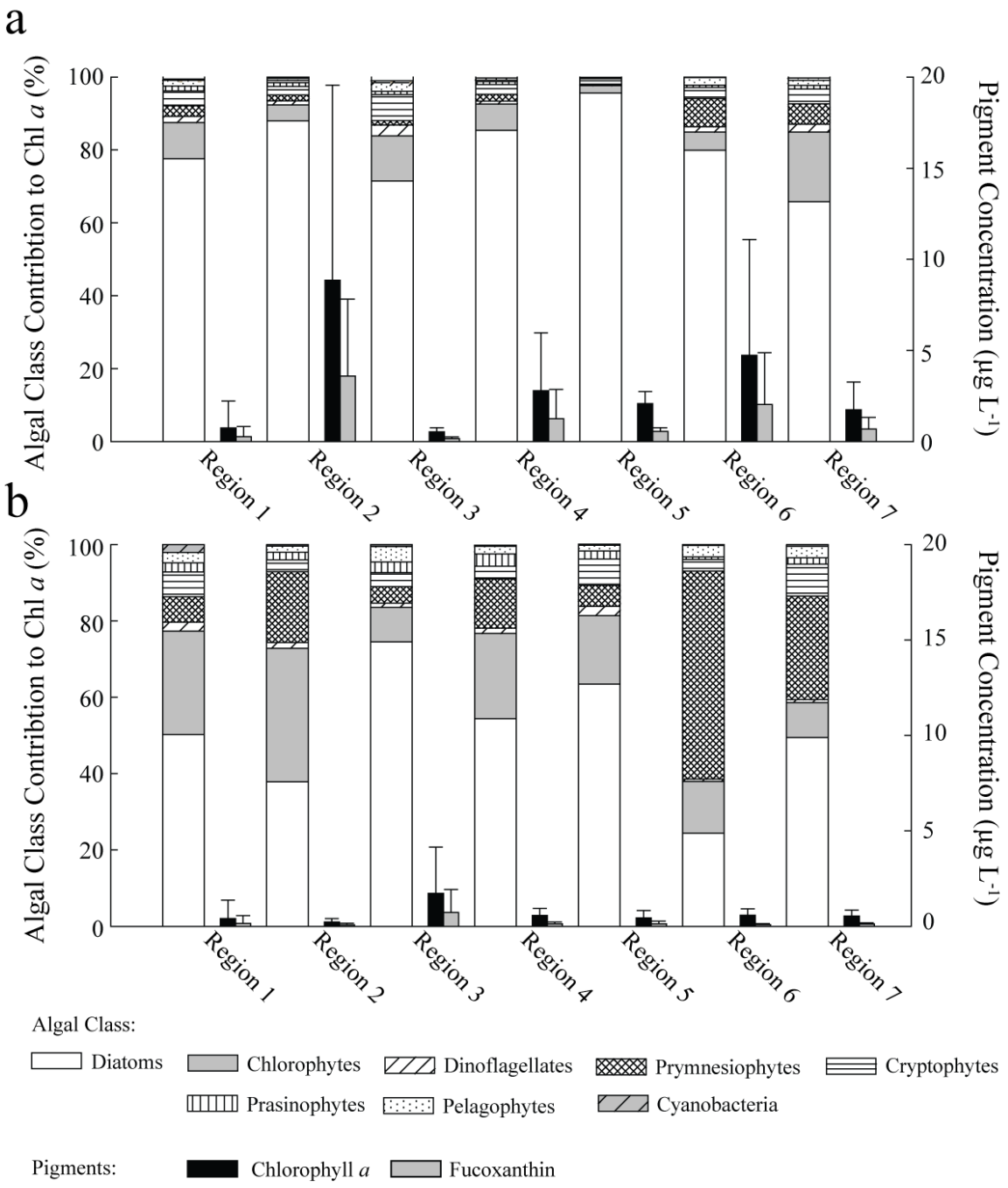

Figure 3.6. Average algal class contribution to autotrophic community (%) by region for spring (a) and summer (b). Thin bars represent average total chlorophyll a (black) and fucoxanthin (grey) concentrations, and correspond to the right vertical axes.

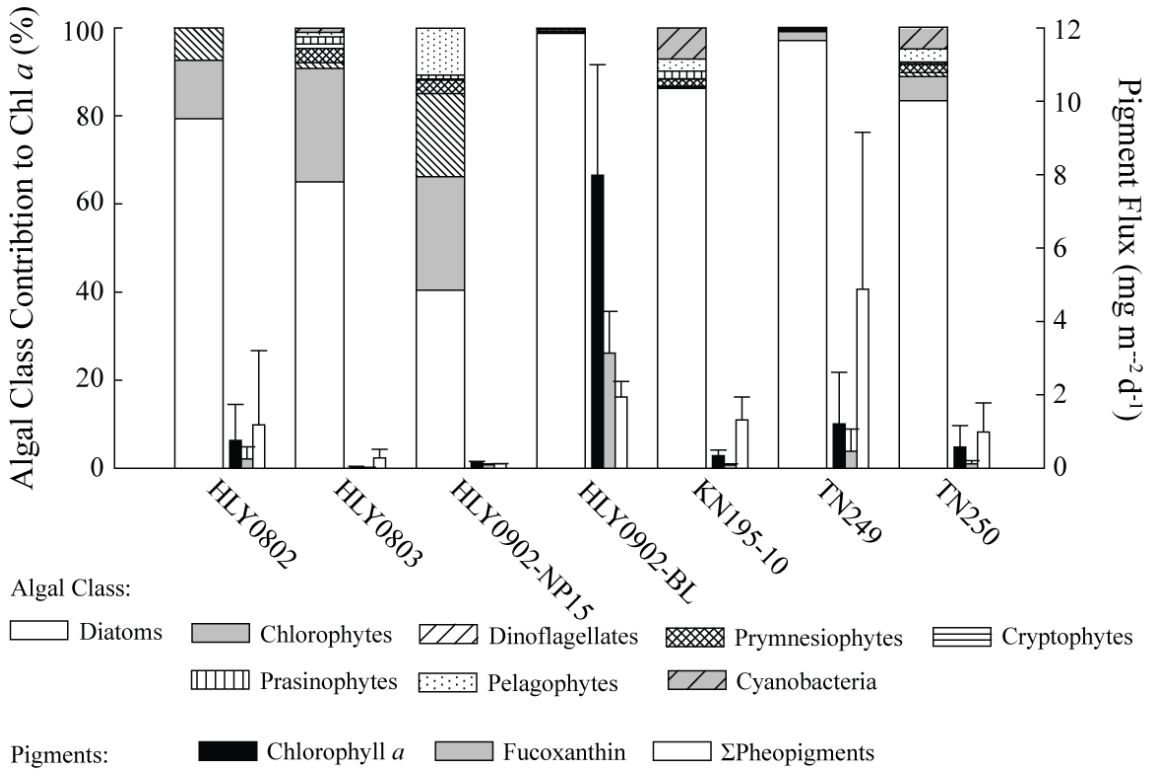

Figure 3.7. Phytoplankton composition (%) of the vertical flux of POM by cruise. Thin bars represent average total chlorophyll a (black), fucoxanthin (grey), and Σpheopigments, and correspond to the right vertical axes.

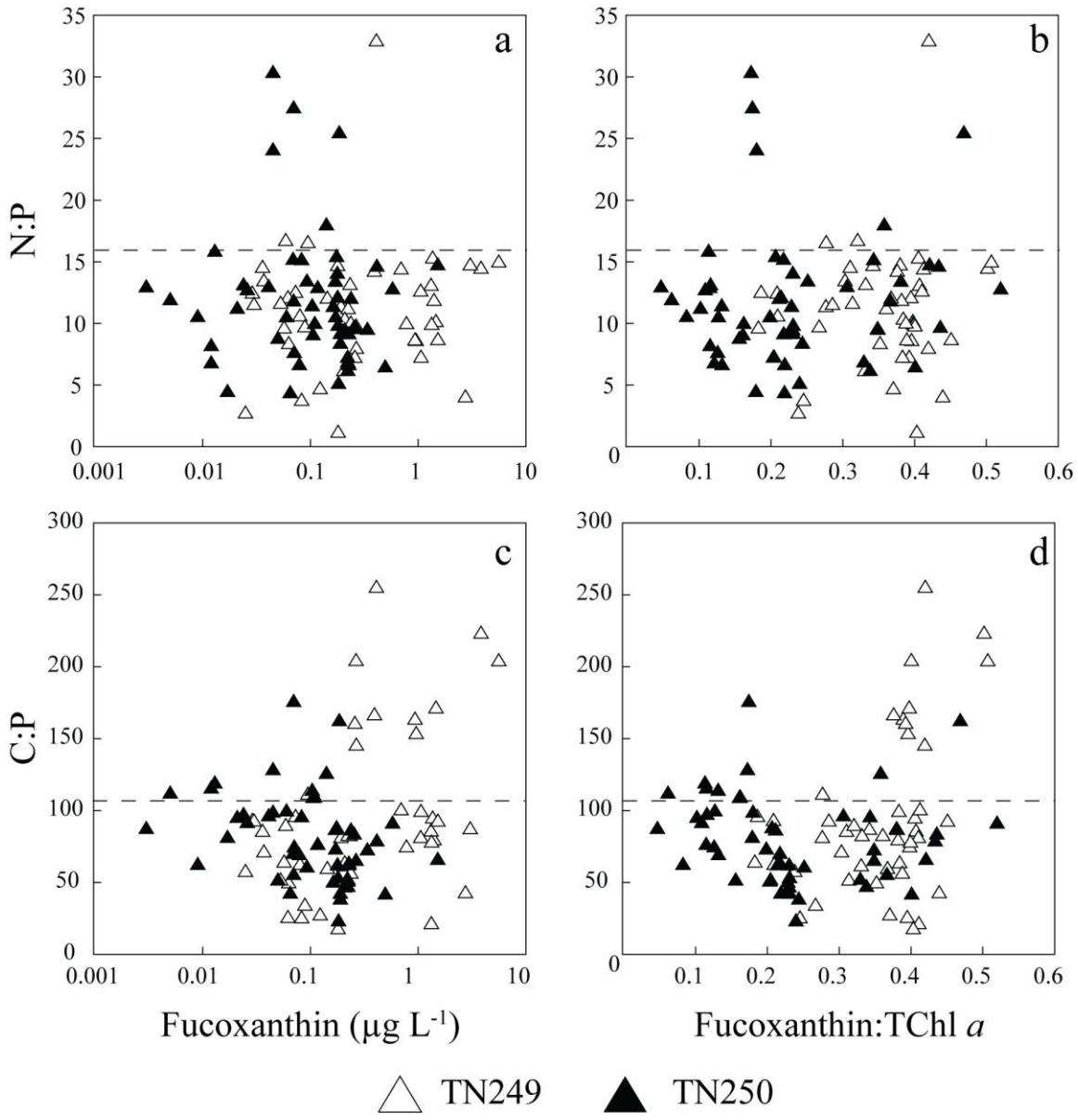

Figure 3.8. N:P (a and b) and C:P (c and d) of suspended POM plotted against fucoxanthin concentration (µg L^{-1}; a and c) and the ratio of fucoxanthin to total chlorophyll *a* (b and d). Reference lines of 16:1 and 106:1 are drawn for N:P and C:P, respectively, for comparison of the data.

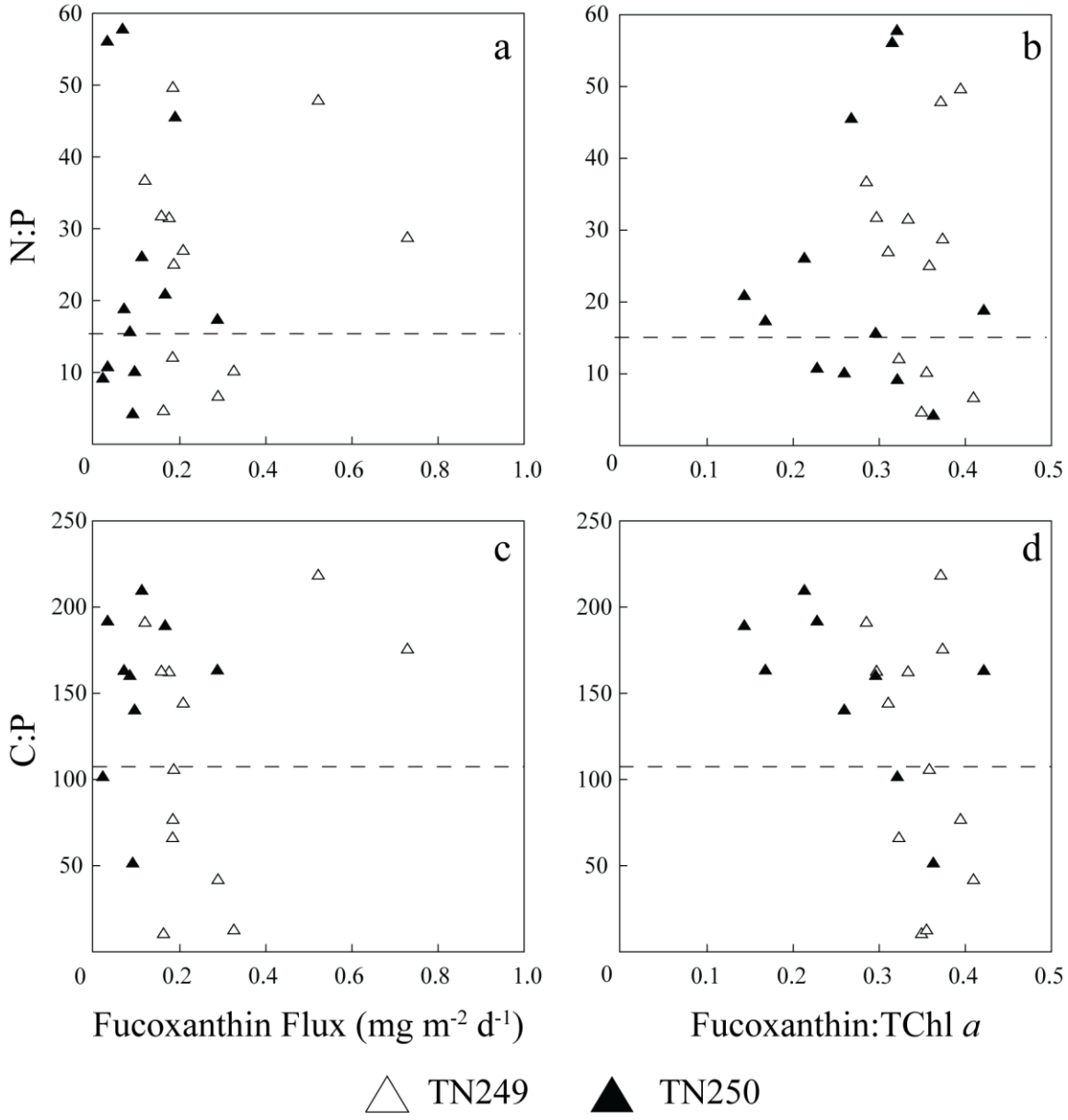

Figure 3.9. N:P (a and b) and C:P (c and d) of the vertical flux of POM plotted against fucoxanthin flux (mg m^{-2} d^{-1}; a and c) and the flux ratio of fucoxanthin to total chlorophyll *a* (b and d). Reference lines of 16:1 and 106:1 are drawn for N:P and C:P, respectively, for comparison of the data.

APPENDIX

A: SUPPORTING TABLES FOR THE CHEMTAX ANALYSIS PRESENTED IN MANUSCRIPT III

Appendix A includes two tables, which present the output matrices of the CHEMTAX analysis used for the identification of algal group percent contribution to total chlorophyll *a* in Manuscript III. In Table A.1, the initial input matrix used for the analysis (a) is listed together with the final matrices for the analysis of water column pigments (b) and pigments in settling particles collected by sediment traps (c). In Table A.2, the final matrices of the CHEMTAX analysis performed using varying input ratios of fucoxanthin to total chlorophyll *a* on the water column pigment data. The fucoxanthin:total chlorophyll *a* input ratios were: 0.75 (a), 0.35 (b), and 1.1 (c). Abbreviations in Tables A.1 and A.2 are as follows: Peri; Peridinin, 19'-But; 19'-Butanoyloxyfucoxanthin, Fuco; Fucoxanthin, 19'-Hex; 19'-Hexanoyloxyfucoxanthin, Neo; Neoxanthin, Violax; Violaxanthin, Diadinox; Diadinoxanthin, Allox; Alloxanthin, Prasinox; Prasinoxanthin, Zeax; Zeaxanthin, Chl *b*; Total Chlorophyll *b*, and Chl *a*; Total Chlorophyll *a*.

Appendix A.1. Initial pigment:chlorophyl a matrix (a) used for the CHEMTAX analysis together with final matrices for the water column (b) and sediment trap (c) analyses.

	Peri	19'-But	Fuco	19'-Hex	Neo	Violax	Diadinox	Allox	Prasinox	Zeax	Chl *b*	Chl *a*
a.	Initial Matrix											
Diatoms	0	0	0.377	0	0	0	0.121	0	0	0	0	0.503
Prymnesiophytes	0	0	0	0.547	0	0	0.063	0	0	0	0	0.391
Pelagophytes	0	0.311	0.207	0	0	0	0.147	0	0	0	0	0.334
Chlorophytes	0	0	0	0	0.028	0.021	0	0	0	0.043	0.199	0.709
Parasinophytes	0	0	0	0	0.045	0.045	0	0	0.146	0	0.360	0.405
Cryptophytes	0	0	0	0	0	0	0	0.123	0	0	0	0.877
Dinoflagellates	0.346	0	0	0	0	0	0	0	0	0	0	0.654
Cyanobacteria	0	0	0	0	0	0	0	0	0	0.248	0	0.752
b.	Final Matrix - Water Column											
Diatoms	0	0	0.287	0	0	0	0.021	0	0	0	0	0.692
Prymnesiophytes	0	0	0	0.287	0	0	0.001	0	0	0	0	0.712
Pelagophytes	0	0.269	0.221	0	0	0	0.195	0	0	0	0	0.315
Chlorophytes	0	0	0	0	0.024	0.017	0	0	0	0.010	0.383	0.566
Parasinophytes	0	0	0	0	0.077	0.085	0	0	0.302	0	0.080	0.457
Cryptophytes	0	0	0	0	0	0	0	0.238	0	0	0	0.762
Dinoflagellates	0.421	0	0	0	0	0	0	0	0	0	0	0.579
Cyanobacteria	0	0	0	0	0	0	0	0	0	0.567	0	0.433
c.	Final Matrix - Sediment Trap											
Diatoms	0	0	0.255	0	0	0	0.030	0	0	0	0	0.714
Prymnesiophytes	0	0	0	0.692	0	0	0.123	0	0	0	0	0.185
Pelagophytes	0	0.285	0.379	0	0	0	0.029	0	0	0	0	0.307
Chlorophytes	0	0	0	0	0.026	0.017	0	0	0	0.011	0.370	0.576
Parasinophytes	0	0	0	0	0.066	0.066	0	0	0.216	0	0.053	0.599
Cryptophytes	0	0	0	0	0	0	0	0.939	0	0	0	0.061
Dinoflagellates	0.346	0	0	0	0	0	0	0	0	0	0	0.654
Cyanobacteria	0	0	0	0	0	0	0	0	0	0.268	0	0.732

Appendix A.2. Final matrices in the CHEMTAX analysis of the water column samples using fucoxanthin:chlorophyl a ratios of 0.75 (a), 0.35 (b), and 1.1 (c).

	Peri	19'-But	Fuco	19'-Hex	Neo	Violax	Diadinox	Allox	Prasinox	Zeax	Chl *b*	Chl *a*
a.	Fuco:Chl *a* : 0.75											
Diatoms	0	0	0.287	0	0	0	0.021	0	0	0	0	0.692
Prymnesiophytes	0	0	0	0.287	0	0	0.001	0	0	0	0	0.712
Pelagophytes	0	0.269	0.221	0	0	0	0.195	0	0	0	0	0.315
Chlorophytes	0	0	0	0	0.024	0.017	0	0	0	0.010	0.383	0.566
Parasinophytes	0	0	0	0	0.077	0.085	0	0	0.302	0	0.080	0.457
Cryptophytes	0	0	0	0	0	0	0	0.238	0	0	0	0.762
Dinoflagellates	0.421	0	0	0	0	0	0	0	0	0	0	0.579
Cyanobacteria	0	0	0	0	0	0	0	0	0	0.567	0	0.433
b.	Fuco:Chl *a* : 0.35											
Diatoms	0	0	0.288	0	0	0	0.021	0	0	0	0	0.691
Prymnesiophytes	0	0	0	0.287	0	0	0.002	0	0	0	0	0.711
Pelagophytes	0	0.283	0.197	0	0	0	0.203	0	0	0	0	0.317
Chlorophytes	0	0	0	0	0.025	0.017	0	0	0	0.011	0.387	0.561
Parasinophytes	0	0	0	0	0.074	0.081	0	0	0.296	0	0.075	0.474
Cryptophytes	0	0	0	0	0	0	0	0.238	0	0	0	0.762
Dinoflagellates	0.422	0	0	0	0	0	0	0	0	0	0	0.578
Cyanobacteria	0	0	0	0	0	0	0	0	0	0.545	0	0.455
c.	Fuco:Chl *a* : 1.1											
Diatoms	0	0	0.287	0	0	0	0.021	0	0	0	0	0.692
Prymnesiophytes	0	0	0	0.288	0	0	0.001	0	0	0	0	0.711
Pelagophytes	0	0.272	0.219	0	0	0	0.196	0	0	0	0	0.313
Chlorophytes	0	0	0	0	0.024	0.016	0	0	0	0.010	0.382	0.568
Parasinophytes	0	0	0	0	0.079	0.088	0	0	0.311	0	0.078	0.444
Cryptophytes	0	0	0	0	0	0	0	0.236	0	0	0	0.764
Dinoflagellates	0.435	0	0	0	0	0	0	0	0	0	0	0.565
Cyanobacteria	0	0	0	0	0	0	0	0	0	0.575	0	0.425

BIBLIOGRAPHY

Aagaard, K., Weingartner, T. J., Danielson, S. L., Woodgate, R. A., Johnson, G. C., Whitledge, T. E. 2006. Some controls on flow and salinity in Bering Strait. Geophys. Res. Lett. 33(19), L19602.10.1029/2006gl026612.

Alexander, V. and Niebauer, H. J. 1981. Oceanography of the Eastern Bering Sea Ice-Edge Zone in Spring. Limnol. Oceanogr. 26(6), 1111-1125.

Amiel, D. and Cochran, J. K. 2008. Terrestrial and marine POC fluxes derived from ^{234}Th distributions and δ^{13}C measurements on the Mackenzie Shelf. J. Geophys. Res. 113(C3), DOI: 10.1029/2007JC004260.

Amiel, D., Cochran, J. K., Hirschberg, D. J. 2002. ^{234}Th/^{238}U disequilibrium as an indicator of the seasonal export flux of particulate organic carbon in the North Water. Deep-Sea Res. Pt. II. 49, 5191-5209.

Anderson, R. F., Fleisher, M. Q., Biscaye, P. E., Kumar, N., Ditrich, B., Kubik, P., Suter, M. 1994. Anomalous boundary scavenging in the Middle Atlantic Bight: evidence from Th-230, Pa-231, Be-1O and Pb-210. Deep-Sea Res. Pt. II. 41(2-3), 537-561.

Arrigo, K. R. 2005. Marine microorganisms and global nutrient cycles. Nature. 437(7057), 349-355.

Arrigo, K. R., van Dijken, G., Pabi, S. 2008. Impact of a shrinking Arctic ice cover on marine primary production. Geophys. Res. Lett. 35(19), DOI: 10.1029/2008GL035028.

Asper, V. L. and Smith, W. O., Jr. 1999. Particle fluxes during austral spring and summer in the southern Ross Sea, Antarctica. J. Geophys. Res. 104(C3), 5345-5359.

Bacon, M. P., Belastock, R. A., Bothner, M. H. 1994. Pb-210 balance and implications for particle-transport on the continental-shelf, US Middle Atlantic Bight. Deep-Sea Res. Pt. II. 41(2-3), 511-535.

Baumann, M. S., Moran, S. B., Kelly, R. P., Lomas, M. W., Shull, D. H. 2013. ^{234}Th balance and implications for seasonal particle retention in the eastern Bering Sea. Deep-Sea Res. Pt. II. 94, 7-21.

Baumann, M. S., Moran, S. B., Lomas, M. W., Kelly, R. P., Bell, D. W. 2012. Seasonal decoupling of primary production and POC export in relation to sea-ice extent at the shelf break of the eastern Bering Sea (Abstract). 2013 Aquatic Sciences Meeting

Baumann, M. S., Moran, S. B., Lomas, M. W., Kelly, R. P., Bell, D. W. in press. Seasonal decoupling of particulate organic carbon export and net primary production in relation to sea-ice at the shelf break of the eastern Bering Sea:

implications for off-shelf carbon export Submitted to Journal of Geophysical Research Oceans.

Benitez-Nelson, C., Buesseler, K. O., Karl, D. M., Andrews, J. 2001a. A time-series study of particulate matter export in the North Pacific Subtropical Gyre based on ^{234}Th:^{238}U disequilibrium. Deep-Sea Res. Pt. I. 48(12), 2595-2611.

Benitez-Nelson, C., Buesseler, K. O., Rutgers van der Loeff, M., Andrews, J., Ball, L., Crossin, G., Charette, M. 2001b. Testing a new small-volume technique for determining ^{234}Th in seawater. J. Radioanal. Nucl. Ch. 248(3), 795-799.

Benitez-Nelson, C. R., Bidigare, R. R., Dickey, T. D., Landry, M. R., Leonard, C. L., Brown, S. L., Nencioli, F., Rii, Y. M., Maiti, K., Becker, J. W., Bibby, T. S., Black, W., Cai, W. J., Carlson, C. A., Chen, F. Z., Kuwahara, V. S., Mahaffey, C., McAndrew, P. M., Quay, P. D., Rappe, M. S., Selph, K. E., Simmons, M. P., Yang, E. J. 2007. Mesoscale eddies drive increased silica export in the subtropical Pacific Ocean. Science. 316(5827), 1017-1021.

Berelson, W. M. 2002. Particle settling rates increase with depth in the ocean. Deep-Sea Res. Pt. II. 49(1-3), 237-251.

Bianchi, T. S., Rolff, C., Widbom, B., Elmgren, R. 2002. Phytoplankton Pigments in Baltic Sea Seston and Sediments: Seasonal Variability, Fluxes, and Transformations. Estuar. Coast. Shelf Sci. 55(3), 369-383.

Brown, Z. W. and Arrigo, K. R. 2013. Sea ice impacts on spring bloom dynamics and net primary production in the Eastern Bering Sea. Journal of Geophysical Research: Oceans. 118, 1-20, DOI: 10.1029/2012JC008034.

Brown, Z. W., van Dijken, G. L., Arrigo, K. R. 2011. A reassessment of primary production and environmental change in the Bering Sea. J Geophys Res-Oceans. 116(C8), C08014 DOI:10.1029/2010JC006766.

Brzezinski, M. A. and Nelson, D. M. 1995. The annual silica cycle in the Sargasso Sea near Bermuda. Deep-Sea Res Pt I. 42(7), 1215-1237.

Buesseler, K. O. 1991. Do upper-ocean sediment traps provide an accurate record of particle-flux. Nature. 353(6343), 420-423.

Buesseler, K. O. 1998. The decoupling of production and particulate export in the surface ocean. Global Biogeochem. Cy. 12, 297-310.

Buesseler, K. O., Andrews, J. A., Hartman, M. C., Belastock, R., Chai, F. 1995. Regional estimates of the export flux of particulate organic carbon derived from thorium-234 during the JGOFS EqPac program. Deep-Sea Res. Pt. II. 42(2–3), 777-804.

Buesseler, K. O., Bacon, M. P., Cochran, J. K., Livingston, H. D. 1992. Carbon and nitrogen export during the JGOFS North Atlantic Bloom experiment estimated from ^{234}Th: ^{238}U disequilibria. Deep-Sea Res. 39(7–8), 1115-1137.

Buesseler, K. O., Ball, L., Andrews, J., Benitez-Nelson, C., Belastock, R., Chai, F., Chao, Y. 1998. Upper ocean export of particulate organic carbon in the Arabian Sea derived from thorium-234. Deep-Sea Res. Pt. II. 45, 2461-2487.

Buesseler, K. O., Benitez-Nelson, C., Rutgers van der Loeff, M., Andrews, J., Ball, L., Crossin, G., Charette, M. A. 2001. An intercomparison of small-and large-volume technqiues for thorium-234 in seawater. Mar. Chem. 74, 15-28.

Burd, A. B., Moran, S. B., Jackson, G. A. 2000. A coupled adsorption–aggregation model of the POC/234Th ratio of marine particles. Deep-Sea Res. Pt. I. 47(1), 103-120.

Burdige, D. J. 2006. Geochemistry of Marine Sediments, Princeton University Press Princeton, NJ.

Cai, P., Rutgers van der Loeff, M., Stimac, I., Nöthig, E. M., Lepore, K., Moran, S. B. 2010. Low export flux of particulate organic carbon in the central Arctic Ocean as revealed by 234Th:238U disequilibrium. J. Geophys. Res. 115(C10), C10037, 10.1029/2009jc005595.

Charette, M. A., Moran, S. B., Pike, S. M., Smith, J. N. 2001. Investigating the carbon cycle in the Gulf of Maine using the natural tracer thorium-234. J. Geophys. Res. 106, 11,553-11,579.

Chen, J. H., Edwards, R. L., Wasserburg, G. J. 1986. U-238, U-234 and Th-232 in seawater. Earth Planet. Sc. Lett. 80(3-4), 241-251.

Coachman, L. K. 1982. Flow convergence over a broad, flat continental shelf. Cont. Shelf Res. 1(1), 1-14.

Coachman, L. K. 1986. Circulation, water masses, and fluxes on the southeastern Bering Sea shelf. Cont. Shelf Res. 5(1-2), 23-108.

Coale, K. H. and Bruland, K. W. 1985. ^{234}Th:^{238}U disequilibria within the California Current. Limnol. Oceanogr. 30(1), 22-33.

Coale, K. H. and Bruland, K. W. 1987. Oceanic stratified euphotic zone as elucidated by ^{234}Th:^{238}U disequilibria. Limnol. Oceanogr. 32(1), 189-200.

Cochran, J. K., Barnes, C., Achman, D., Hirschberg, D. J. 1995. Thorium-234/Uranium-238 disequilibrium as an indicator of scavenging rates and particulate organic carbon fluxes in the Northeast Water Polynya, Greenland. J. Geophys. Res. 100, 4399-4410.

Cochran, J. K., Mckibbin-Vaughan, T., Dornblaser, M. M., Hirschberg, D., Livingston, H. D., Buesseler, K. O. 1990. Pb-210 scavenging in the North-Atlantic and North Pacific oceans. Earth Planet. Sc. Lett. 97(3-4), 332-352.

Cooper, L. W., Janout, M. A., Frey, K. E., Pirtle-Levy, R., Guarinello, M. L., Grebmeier, J. M., Lovvorn, J. R. 2012. The relationship between sea ice break-up, water mass variation, chlorophyll biomass, and sedimentation in the northern Bering Sea. Deep-Sea Res. Pt. II. 65–70(0), 141-162.

Cooper, L. W., Sexson, M. G., Grebmeier, J. M., Gradinger, R., Mordy, C. W., Lovvorn, J. R. 2013. Linkages between sea-ice coverage, pelagic–benthic coupling, and the distribution of spectacled eiders: Observations in March 2008, 2009 and 2010, northern Bering Sea. Deep-Sea Res. Pt. II. 94, 31-43.

Cutshall, N. H., Larsen, I. L., Olsen, C. R. 1983. Direct analysis of ^{210}Pb in sediment samples: Self-absorption corrections. Nucl. Instrum. Methods. 206(1–2), 309-312.

Danielson, S., Hedstrom, K., Aagaard, K., Weingartner, T., Curchitser, E. 2012. Wind-induced reorganization of the Bering shelf circulation. Geophys. Res. Lett. 39(8), L08601, doi:10.1029/2012GL051231.

Dunbar, R. B., Leventer, A. R., Mucciarone, D. A. 1998. Water column sediment fluxes in the Ross Sea, Antarctica: Atmospheric and sea ice forcing. J. Geophys. Res. 103(C13), 30741-30759.

Durbin, E. G., Campbell, R. G., Gilman, S. L., Durbin, A. G. 1995. Diel feeding behavior and ingestion rate in the copepod Calanus finmarchicus in the southern Gulf of Maine during late spring. Cont. Shelf Res. 15(4–5), 539-570.

Fujiki, T., Matsumoto, K., Honda, M. C., Kawakami, H., Watanabe, S. 2009. Phytoplankton composition in the subarctic North Pacific during autumn 2005. J Plankton Res. 31(2), 179-191.

Gleiber, M. R., Steinberg, D. K., Ducklow, H. 2012. Time series of vertical flux of zooplankton fecal pellets on the continental shelf of the western Antarctic Peninsula. Mar. Ecol. Prog. Ser. 471, 23-36.

Grebmeier, J. M., Cooper, L. W., Feder, H. M., Sirenko, B. I. 2006a. Ecosystem dynamics of the Pacific-influenced northern Bering and Chukchi seas in the Amerasian Arctic. Prog. Oceanogr. 71, 331-361.

Grebmeier, J. M., Overland, J. E., Moore, S. E., Farley, E. V., Carmack, E. C., Cooper, L. W., Frey, K. E., Helle, J. H., McLaughlin, F. A., McNutt, S. L. 2006b. A major ecosystem shift in the northern Bering Sea. Science. 311, 1461-1464.

Gustafsson, Ö. and Andersson, P. S. 2012. ^{234}Th-derived surface export fluxes of POC from the Northern Barents Sea and the Eurasian sector of the Central Arctic Ocean. Deep-Sea Res. Pt. I. 68(0), 1-11.

Hannides, C. C. S., Landry, M. l. R., Benitez-Nelson, C. R., Styles, R. M., Montoya, J. P., Karl, D. M. 2009. Export stoichiometry and migrant-mediated flux of phosphorus in the North Pacific Subtropical Gyre. Deep-Sea Res. Pt. I. 56(1), 73-88.

Heintz, R. A., Siddon, E. C., Farley Jr, E. V., Napp, J. M. 2013. Correlation between recruitment and fall condition of age-0 pollock (Theragra chalcogramma) from the eastern Bering Sea under varying climate conditions. Deep-Sea Res. Pt. II. 94, 150-156.

Hunt, G. L., Coyle, K. O., Eisner, L. B., Farley, E. V., Heintz, R. A., Mueter, F., Napp, J. M., Overland, J. E., Ressler, P. H., Salo, S. A., Stabeno, P. J. 2011. Climate impacts on eastern Bering Sea foodwebs: a synthesis of new data and an assessment of the Oscillating Control Hypothesis. ICES Journal of Marine Science: Journal du Conseil. 68(6), 1230-1243.

Hunt, G. L., Stabeno, P., Walters, G., Sinclair, E., Brodeur, R. D., Napp, J. M., Bond, N. A. 2002. Climate change and control of the southeastern Bering Sea pelagic ecosystem. Deep-Sea Res. Pt. II. 49(26), 5821-5853.

Juul-Pedersen, T., Michel, C., Gosselin, M. 2010. Sinking export of particulate organic material from the euphotic zone in the eastern Beaufort Sea. Mar. Ecol. Prog. Ser. 410, 55-70.

Juul-Pedersen, T., Nielsen, T. G., Michel, C., Moller, E. F., Tiselius, P., Thor, P., Olesen, M., Selander, E., Gooding, S. 2006. Sedimentation following the spring bloom in Disko Bay, West Greenland, with special emphasis on the role of copepods. Mar. Ecol. Prog. Ser. 314, 239-255.

Kachel, N. B., Hunt, G. L., Salo, S. A., Schumacher, J. D., Stabeno, P. J., Whitledge, T. E. 2002. Characteristics and variability of the inner front of the southeastern Bering Sea. Deep-Sea Res. Pt. II. 49, 5889-5909.

Karl, D. M., Christian, J. R., Dore, J. E., Hebel, D. V., Letelier, R. M., Tupas, L. M., Winn, C. D. 1996. Seasonal and interannual variability in primary production and particle flux at Station ALOHA. Deep-Sea Res. Pt. II. 43(2–3), 539-568.

Klein, B., LeBlanc, B., Mei, Z.-P., Beret, R., Michaud, J., Mundy, C. J., von Quillfeldt, C. H., Garneau, M.-È., Roy, S., Gratton, Y., Cochran, J. K., Bélanger, S., Larouche, P., Pakulski, J. D., Rivkin, R. B., Legendre, L. 2002. Phytoplankton biomass, production and potential export in the North Water. Deep-Sea Res. Pt. II. 49(22–23), 4983-5002.

Krause, J. W., Nelson, D. M., Lomas, M. W. 2009. Biogeochemical responses to late-winter storms in the Sargasso Sea, II: Increased rates of biogenic silica production and export. Deep-Sea Res. Pt. I. 56(6), 861-874.

Lalande, C., Lepore, K., Cooper, L. W., Grebmeier, J. M., Moran, S. B. 2007. Export fluxes of particulate organic carbon in the Chukchi Sea: A comparative study using ^{234}Th/^{238}U disequilibria and drifting sediment traps. Mar. Chem. 103, 185-196.

Lalande, C., Moran, S. B., Wassmann, P., Grebmeier, J. M., Cooper, L. W. 2008. ^{234}Th-derived particulate organic carbon fluxes in the northern Barents Sea with comparison to drifting sediment trap fluxes. J. Mar. Syst. 73(1–2), 103-113.

Lepore, K. and Moran, S. B. 2007. Seasonal changes in thorium scavenging and particle aggregation in the western Arctic Ocean. Deep-Sea Res Pt I. 54(6), 919-938.

Lepore, K., Moran, S. B., Grebmeier, J. M., Cooper, L. W., Lalande, C., Maslowski, W., Hill, V., Bates, N. R., Hansell, D. A., Mathis, J. T., Kelly, R. P. 2007. Seasonal and interannual changes in particulate organic carbon export and deposition in the Chukchi Sea. J. Geophys. Res. 112(C10), C10024 DOI: 10.1029/2006JC003555.

Lomas, M. W., Bates, N. R., Johnson, R. J., Knap, A. H., Steinberg, D. K., Carlson, C. A. 2013. Two decades and counting: 24-years of sustained open ocean biogeochemical measurements in the Sargasso Sea. Deep-Sea Res. Pt. II. 93(0), 16-32.

Lomas, M. W., Burke, A. L., Lomas, D. A., Bell, D. W., Shen, C., Dyhrman, S. T., Ammerman, J. W. 2010. Sargasso Sea phosphorus biogeochemistry: an important role for dissolved organic phosphorus (DOP). Biogeosciences. 7(2), 695-710.

Lomas, M. W., Moran, S. B., Casey, J. R., Bell, D. W., Tiahlo, M., Whitefield, J., Kelly, R. P., Mathis, J. T., Cokelet, E. D. 2012. Spatial and seasonal variability of primary production on the Eastern Bering Sea shelf. Deep-Sea Res. Pt. II. 65–70(0), 126-140.

Lovvorn, J. R., Cooper, L. W., Brooks, M. L., De Ruyck, C. C., Bump, J. K., Grebmeier, J. M. 2005. Organic matter pathways to zooplankton and benthos under pack ice in late winter and open water in late summer in the north-central Bering Sea. Mar. Ecol. Prog. Ser. 291, 135-150.

Mackey, M. D., Mackey, D. J., Higgins, H. W., Wright, S. W. 1996. CHEMTAX - A program for estimating class abundances from chemical markers: Application to HPLC measurements of phytoplankton. Mar. Ecol. Prog. Ser. 144(1-3), 265-283.

Maiti, K., Charette, M. A., Buesseler, K. O., Kahru, M. 2013. An inverse relationship between production and export efficiency in the Southern Ocean. Geophys. Res. Lett. 40(8), 1557-1561.

Martiny, A. C., Pham, C. T. A., Primeau, F. W., Vrugt, J. A., Moore, J. K., Levin, S. A., Lomas, M. W. 2013. Strong latitudinal patterns in the elemental ratios of marine plankton and organic matter. Nature Geosci. 6(4), 279-283.

Mathis, J. T., Cross, J. N., Bates, N. R., Moran, S. B., Lomas, M. W., Mordy, C. W., Stabeno, P. J. 2010. Seasonal distribution of dissolved inorganic carbon and net community production on the Bering Sea shelf. Biogeosciences. 7(5), 1769-1787.

McRoy, C. P., Hood, D. W., Coachman, L. K., Walsh, J. J., Goering, J. J. 1986. Processes and Resources of the Bering Sea Shelf (PROBES) - the development and accomplishments of the project. Cont. Shelf Res. 5(1-2), 5-21.

Moran, S. B. and Buesseler, K. O. 1993. Size-fractionated ^{234}Th in continental shelf waters off New England: Implications for the role of colloids in oceanic trace metal scavenging J. Mar. Res. 51, 893-922.

Moran, S. B., Ellis, K. M., Smith, J. N. 1997. Th-234/U-238 disequilibrium in the central Arctic Ocean: implications for particulate organic carbon export. Deep-Sea Res. Pt. II. 44(8), 1593-1606.

Moran, S. B., Kelly, R. P., Hagstrom, K., Smith, J. N., Grebmeier, J. M., Cooper, L. W., Cota, G. F., Walsh, J. J., Bates, N. R., Hansell, D. A., Maslowski, W., Nelson, R. P., Mulsow, S. 2005. Seasonal changes in POC export flux in the Chukchi Sea and implications for water column-benthic coupling in Arctic shelves. Deep-Sea Res. Pt. II. 52(24–26), 3427-3451.

Moran, S. B., Lomas, M. W., Kelly, R. P., Gradinger, R., Iken, K., Mathis, J. T. 2012. Seasonal succession of net primary productivity, particulate organic carbon export, and autotrophic community composition in the eastern Bering Sea. Deep-Sea Res. Pt. II. 65–70, 84-97.

Moran, S. B. and Smith, J. N. 2000. ^{234}Th as a tracer of scavenging and particle export in the Beaufort Sea. Cont. Shelf Res. 20(2), 153-167.

Moran, S. B., Weinstein, S. E., Edmonds, H. N., Smith, J. N., Kelly, R. P., Pilson, M. E. Q., Harrison, W. G. 2003. Does ^{234}Th/^{238}U disequilibrium provide an accurate record of the export flux of particulate organic carbon from the upper ocean? Limnol. Oceanogr. 48(3), 1018-1029.

Napp, J. M. and Hunt, G. L. 2001. Anomalous conditions in the south-eastern Bering Sea 1997: linkages among climate, weather, ocean, and Biology. Fish. Oceanogr. 10(1), 61-68.

Niebauer, H. J., Alexander, V., Henrichs, S. M. 1995. A time-series study of the spring bloom at the Bering Sea ice edge I. Physical processes, chlorophyll and nutrient chemistry. Cont. Shelf Res. 15, 1859-1877.

Nozaki, Y., Zhang, J., Takeda, A. 1997. Pb-210 and Po-210 in the equatorial Pacific and the Bering Sea: the effects of biological productivity and boundary scavenging. Deep-Sea Res. Pt. II. 44(9-10), 2203-2220.

Obayashi, Y., Tanoue, E., Suzuki, K., Handa, N., Nojiri, Y., Wong, C. S. 2001. Spatial and temporal variabilities of phytoplankton community structure in the northern North Pacific as determined by phytoplankton pigments. Deep-Sea Res. Pt. I. 48(2), 439-469.

Ohashi, R., Yamaguchi, A., Matsuno, K., Saito, R., Yamada, N., Iijima, A., Shiga, N., Imai, I. 2013. Interannual changes in the zooplankton community structure on the southeastern Bering Sea shelf during summers of 1994–2009. Deep-Sea Res. Pt. II. 94, 44-56.

Olli, K., Wassmann, P., Reigstad, M., Ratkova, T. N., Arashkevich, E., Pasternak, A., Matrai, P. A., Knulst, J., Tranvik, L., Klais, R., Jacobsen, A. 2007. The fate of production in the central Arctic Ocean – top–down regulation by zooplankton expatriates? Prog. Oceanogr. 72(1), 84-113.

Overland, J. E. and Wang, M. Y. 2007. Future regional Arctic sea ice declines. Geophys. Res. Lett. 34(17), L17705, doi:10.1029/2007GL030308.

Paasche, E. 1973. Silicon and the ecology of marine plankton diatoms. I. *Thalassiosira pseudonana* (*Cyclotella nana*) grown in a chemostat with silicate as limiting nutrient. Mar. Biol. 19(2), 117-126.

Pike, S. M. and Moran, S. B. 1997. Use of Poretics® 0.7 μm pore size glass fiber filters for determination of particulate organic carbon and nitrogen in seawater and freshwater. Mar. Chem. 57(3–4), 355-360.

Rho, T. and Whitledge, T. 2007. Characteristics of seasonal and spatial variations of primary production over the southeastern Bering Sea shelf. Cont. Shelf Res. 27, 2556-2569.

Roy-Barman, M. 2009. Modelling the effect of boundary scavenging on thorium and protactinium profiles in the ocean. Biogeosciences. 6(12), 3091-3107.

Rutgers van der Loeff, M., Friedrich, J., Bathmann, U. V. 1997. Carbon export during the Spring Bloom at the Antarctic Polar Front, determined with the natural tracer Th-234. Deep-Sea Res. Pt. II. 44(1-2), 457-478.

Sakshaug, E. Primary and seconday production in the Arctic Sea. in: The Organic Carbon Cycle in the Arctic Ocean. R. Stein and R. W. MacDonald (Eds.). pp Springer. Berlin. 2004.

Savoye, N., Benitez-Nelson, C., Burd, A. B., Cochran, J. K., Charette, M., Buesseler, K. O., Jackson, G. A., Roy-Barman, M., Schmidt, S., Elskens, M. 2006. ^{234}Th sorption and export models in the water column: A review. Mar. Chem. 100, 234-249.

Savoye, N., Buesseler, K. O., Cardinal, D., Dehairs, F. 2004. ^{234}Th deficit and excess in the Southern Ocean during spring 2001: Particle export and remineralization. Geophys. Res. Lett. 31(12), L12301.

Schandelmeier, L. and Alexander, V. 1981. An analysis of the influence of ice on spring phytoplankton population structure in the southeast Bering Sea. Limnol. Oceanogr. 26(5), 935-943.

Schumacher, J. D. and Kinder, T. H. 1983. Low-frequency current regimes over the Bering Sea shelf. J. Phys. Oceanogr. 13, 607-623.

Sherr, E. B., Sherr, B. F., Ross, C. 2013. Microzooplankton grazing impact in the Bering Sea during spring sea ice conditions. Deep-Sea Res. Pt. II. 94, 57-67.

Siddon, E. C., Heintz, R. A., Mueter, F. J. 2013. Conceptual model of energy allocation in walleye pollock (Theragra chalcogramma) from age-0 to age-1 in the southeastern Bering Sea. Deep-Sea Res. Pt. II. 94, 140-149.

Smith, J. N., Moran, S. B., Macdonald, R. W. 2003. Shelf–basin interactions in the Arctic Ocean based on ^{210}Pb and Ra isotope tracer distributions. Deep-Sea Res Pt I. 50, 397-416.

Solorzano, L. and Sharp, J. H. 1980. Determination of total dissolved phosphorus and particulate phosphorus in natural-waters. Limnol. Oceanogr. 25(4), 754-757.

Speicher, E. A., Moran, S. B., Burd, A. B., Delfanti, R., Kaberi, H., Kelly, R. P., Papucci, C., Smith, J. N., Stavrakakis, S., Torricelli, L., Zervakis, V. 2006. Particulate organic carbon export fluxes and size-fractionated POC/^{234}Th ratios in the Ligurian, Tyrrhenian and Aegean Seas. Deep-Sea Res. Pt. I. 53(11), 1810-1830.

Springer, A. M., McRoy, C. P., Flint, M. V. 1996. The Bering Sea Green Belt: Shelf-edge processes and ecosystem production. Fish. Oceanogr. 5(3-4), 205-223.

Stabeno, P., Napp, J., Mordy, C., Whitledge, T. 2010. Factors influencing physical structure and lower trophic levels of the eastern Bering Sea shelf in 2005: Sea ice, tides and winds. Prog. Oceanogr. 85(3–4), 180-196.

Stabeno, P. J., Farley Jr, V., Kachel, N. B., Moore, S., Mordy, C. W., Napp, J. M., Overland, J. E., Pinchuk, A. I., Sigler, M. F. 2012a. A comparison of the physics of the northern and southern shelves of the eastern Bering Sea and some implications for the ecosystem. Deep-Sea Res. Pt. II. 65–70(0), 14-30.

Stabeno, P. J., Kachel, N. B., Moore, S. E., Napp, J. M., Sigler, M. F., Yamaguchi, A., Zerbini, A. N. 2012b. Comparison of warm and cold years on the southeastern Bering Sea shelf and some implications for the ecosystem. Deep-Sea Res. Pt. II. 65–70(0), 31-45.

Stabeno, P. J., Kachel, N. B., Sullivan, M., Whitledge, T. E. 2002. Variability of physical and chemical characteristics along the 70-m isobath of the southeastern Bering Sea. Deep-Sea Res. Pt. II. 49, 5931-5943.

Stabeno, P. J., Schumacher, J. D., Ohtani, K. The physical oceanography of the Bering Sea. in: A Summary of Physical, Chemical, and Biological Characteristics, and a Synopsis of Research on the Bering Sea. T. R. Loughlin and K. Ohtani (Eds.). pp 1-28. North Pacific Marine Science Organization (PICES), Univ. of Alaska Sea Grant, AK-SG-99-03. 1999.

Strickland, J. D. H. and Parsons, T. R. 1968. A Practical Handbook of Seawater Analysis, Fisheries Research Board of Canada Ottawa.

Suzuki, K., Minami, C., Liu, H., Saino, T. 2002a. Temporal and spatial patterns of chemotaxonomic algal pigments in the subarctic Pacific and the Bering Sea during the early summer of 1999. Deep-Sea Res. Pt. II. 49(24–25), 5685-5704.

Suzuki, K., Minami, C., Liu, H., Saino, T. 2002b. Temporal and spatial patterns of chemotaxonomic algal pigments in the subarctic Pacific and the Bering Sea during theearly summer of 1999. Deep-Sea Res Pt I. 49, 5685-5704.

Sweeney, C., Smith, W. O., Hales, B., Bidigare, R. R., Carlson, C. A., Codispoti, L. A., Gordon, L. I., Hansell, D. A., Millero, F. J., Park, M. O. K., Takahashi, T. 2000. Nutrient and carbon removal ratios and fluxes in the Ross Sea, Antarctica. Deep-Sea Res. Pt. II. 47(15–16), 3395-3421.

Thibault, D., Roy, S., Wong, C. S., Bishop, J. K. 1999. The downward flux of biogenic material in the NE subarctic Pacific: importance of algal sinking and mesozooplankton herbivory. Deep-Sea Res. Pt. II. 46(11–12), 2669-2697.

Tsukazaki, C., Ishii, K.-I., Saito, R., Matsuno, K., Yamaguchi, A., Imai, I. 2013. Distribution of viable diatom resting stage cells in bottom sediments of the eastern Bering Sea shelf. Deep-Sea Res. Pt. II. 94, 22-30.

Van Heukelem, L. and Thomas, C. S. 2001. Computer-assisted high-performance liquid chromatography method development with applications to the isolation and analysis of phytoplankton pigments. J. Chromatogr. A. 910(1), 31-49.

Wallace, D. W. R., Minnett, P. J., Hopkins, T. S. 1995. Nutrients, oxygen, and inferred new production in the Northeast Water Polynya, 1992. J. Geophys. Res. 100(C3), 4323-4340.

Walsh, J. J. 1988. On the nature of continental shelves, Academic Press

Walsh, J. J., Rowe, G. T., Iverson, R. L., McRoy, C. P. 1981. Biological export of shelf carbon is a sink of the global CO2 cycle. Nature. 291(5812), 196-201.

Wang, M., Overland, J. E., Stabeno, P. 2012. Future climate of the Bering and Chukchi Seas projected by global climate models. Deep-Sea Res. Pt. II. 65–70(0), 46-57.

Wassmann, P., Bauerfeind, E., Fortier, M., Fukuchi, M., Hargrave, B., Moran, S. B., Noji, T., Nöthig, E.-M., Olli, K., Peinert, R., Sasaki, H., Shevchenko, V. Particulate organic carbon flux to the Arctic Ocean sea floor. in: The Organic Carbon Cycle in the Arctic Ocean. R. Stein and R. W. MacDonald (Eds.). pp Springer. Berlin. 2004.

Wassmann, P., Reigstad, M., Haug, T., Rudels, B., Carroll, M. L., Hop, H., Gabrielsen, G. W., Falk-Petersen, S., Denisenko, S. G., Arashkevich, E., Slagstad, D., Pavlova, O. 2006. Food webs and carbon flux in the Barents Sea. Prog. Oceanogr. 71(2–4), 232-287.

Wei, C.-L. and Murray, J. W. 1992. Temporal variations of ^{234}Th activity in the water column of Dabob Bay: particle scavenging. Limnol. Oceanogr. 37(2), 296-314.